The Pennsylvania State University

The Graduate School

Energy and Mineral Engineering

DEVELOPMENT OF AN ARTIFICIAL NEURAL NETWORK FOR CYCLIC STEAM STIMULATION METHOD IN NATURALLY FRACTURED RESERVOIRS

A Thesis in

Energy and Mineral Engineering

by

Buket Arpaci

Submitted in Partial Fulfillment
of the Requirements
for the Degree of

Master of Science

May 2014

The thesis of Buket Arpaci was reviewed and approved* by the following:

Turgay Ertekin

Head, John and Willie Leone Family Department of Energy and Mineral Engineering
Professor of Petroleum and Natural Gas Engineering
George E. Trimble Chair in Earth and Mineral Sciences
Thesis Advisor

Zuleima T. Karpyn

Associate Professor of Petroleum and Natural Gas Engineering;
Quentin E. and Louise L. Wood Faculty Fellow in Petroleum and Natural Gas Engineering;
Interim Director, EMS Energy Institute

John Yilin Wang

Assistant Professor of Petroleum and Natural Gas Engineering

Luis F. Ayala H.

Associate Professor of Petroleum and Natural Gas Engineering;
Associate Department Head for Graduate Education

*Signatures are on file in the Graduate School

Abstract

In recent years, increased demand of energy requires improvement in recovery factor by implementing enhanced oil recovery (EOR) method that can be applied efficiently into the naturally fractured reservoirs. Cyclic steam stimulation (CSS) is one of the thermal EOR techniques in which reduction of oil viscosity is achieved by increasing the reservoir temperature. A single well is applied in the CSS process. The well is used for both injection and production, sequentially. The implementation of CSS into the naturally fractured reservoirs can be considered more appropriate because fractures provide a large area in where injected steam diffused. In the petroleum industry, commercial simulators are applied for forecasting of production profile; however, their algorithms are considerably complex and time-consuming. Usage of artificial neural network (ANN) is getting attention in recent years owing to its ability to provide a solution for non-linear relationship.

In this study, an elliptical inner zone that is more fractured than corresponding naturally fractured reservoir is designed to increase the performance of CSS process. A variable number of cycles is studied and production period of each cycle is controlled by specified abandonment oil flow rate. The goal of this study is to provide an accurate estimation for the performance of cyclic steam injection process in relatively short period by developing artificial neural network models. Design parameters of both fractured inner zone and cyclic steam injection are used as variables of ANN models, besides reservoir properties. Production profiles of the first ten cycles of each case are evaluated during the network training. Six ANN models are developed and a total of 555 case samples are generated in order to train the networks. Two of them are assigned to forward-looking problem. Forward ANN-1 is designed as a predictor of oil flow rate and number of cycle whereas Forward-ANN-2 is constructed as a predictor of cumulative oil production of project, cumulative oil production and cycle duration of each cycle. Two of the six ANN models are generated for

estimation of design parameters by using performance indicators and properties of corresponding reservoir. Inverse ANN-1A is able to predict fractured inner zone and cyclic steam injection design parameters at the same time. Inverse ANN-1B is developed to improve the capability of design parameters prediction by focusing on only cyclic steam injection design. The last two networks are assigned to prediction of reservoir properties by applying desired production profile and design parameters. Inverse ANN-2A is created for estimation of reservoir properties after fractured inner zone was created, in case performance indicators and CSI design parameters are provided. Inverse ANN-2B is trained as a predictor of only fractured inner zone properties. Significant improvement is observed in terms of accuracy by developing Inverse ANN-1B and Inverse ANN-2B additionally.

Table of Contents

List of Figures

List of Tables

Nomenclature

ANN Artificial Neural Network

CMG Computer Modeling Group

CSI Cyclic Steam Injection

CSS Cyclic Steam Stimulation

EOR Enhanced Oil Recovery

GUI Graphical User Interface

LMS Least Mean Squared Rule

WOC Water/Oil Contact

Acknowledgments

First and foremost, I would like to express sincere appreciations to my thesis advisor, Dr. Turgay Ertekin, for his generous guidance, support and patience from the beginning of my master degree until the completion of my studies. This work would not have been successful without his wide knowledge andlogical approach. I am grateful to him for his help during my studies.

I would like to give my special thanks to my family, my father Kadir Arpaci, my mother Hatice Arpaci, my brother Bilal Arpaci and my nephew Ruzgar Burak Arpaci as their love, and encouragement helped me to complete this thesis successfully.

I want to thank all my friends from Turkey and the US for their support and friendship. I would like to give my sincere gratitude to Turkish Petroleum Corporation for providing financial support to my studies.

Buket ARPACI
University Park, Pennsylvania
May, 2014

Chapter 1

Introduction

In recent years, increased demand of energy requires improvement in recovery factor by applying enhanced oil recovery (EOR) method that is the tertiary oil recovery. Many types of EOR process can be applied for reservoirs within different characterized. Effectiveness of the process depends on choosing the most appropriate type of chemical and thermal oil recovery method and operating under the most suitable conditions for existing reservoir properties. Thermal enhanced oil recovery is usually considered for relatively shallow reservoirs and heavy crude oil that is very viscous under reservoir temperature. Cyclic steam stimulation is one of the thermal EOR methods, of which main mechanism is injecting steam to enhance oil displacement and increase reservoir pressure. In addition, injected steam reduces oil viscosity by increasing the reservoir temperature.

In cyclic steam stimulation, a single well is used for both steam injection and oil production; hence, heat chamber is created around the well bore by injected energy. In order to increase efficiency of this recovery technique, horizontal wells are implemented. Horizontal wells improve sweep efficiency by higher injection rates and provide comparatively larger heated zone around the well by its ability to access larger volume than vertical wells. Furthermore, cyclic steam stimulation process can be determined as the most appropriate thermal recovery technique especially for fractured reservoirs. Fractures provide a more efficient area to injected heat for the diffusion and penetration into the matrix that has relatively low permeability. The main benefit of this process is having shorter payback period than steam flooding since giving production response in short period and requiring relatively low initial investment cost. This thesis is organized having 8 chapters as follows:

Chapter 2 includes a survey of literature on naturally fractured reservoirs, summary of the previous studies on cyclic steam stimulation process and explanations of artificial neural networks. Chapter 3 contains the statement of problem and workflows propose. Chapter 4 describes the reservoir modeling and explains the methodology of data generation for training of the networks. Chapter 5 includes the development of ANN models and discussion of results. Chapter 6 describes a graphical user interface (GUI) and visualizes the performance of the networks. Chapter 7 contains a brief summary and concludes the observations. Chapter 8 provides potential research that can be further improved the current study. Appendix A displays the uniformly parameter distributions in the search space. Appendix B contains an example input file, which is built in the commercial simulator for cyclic steam injection process. Appendix C provides MATLAB code used for training of the network (Forward ANN-1).

In this research, CMG[1] STARS[2] (version 2011.10) thermal simulator is applied for numerical reservoir simulation. The artificial neural network is developed by using toolbox of MATLAB [3] (version R2009b).

[1] CMG: Computer Modeling Group

[2] STARS: Steam Thermal & Advanced Processes Reservoir Simulator

[3] MATLAB: MATrix LABoratory

Chapter 2

Literature Review

There are several investigations have been reported about effectiveness of the cyclic steam stimulation process since the first application of it in late 1950's. In this chapter, suitability of naturally fractured reservoirs, mechanism of cyclic steam injection and description of artificial neural network (ANN) are summarized. In addition, results of some studies that are especially focused on the field applications and numerical modeling of this process are given from petroleum engineering literature.

2.1 Naturally Fractured Reservoirs

Naturally fractured reservoirs have different geometrical characteristics from homogenous reservoirs due to their alteration in porous media properties occurred during the deposition of the reservoirs. These kinds of reservoirs require extra attention for modeling in case of overweighting to control sweep efficiency and having significant effect on productivity or injectivity of wells. In many naturally fractured reservoir characterization models, it is idealized that these kinds of reservoirs have network consisting of fracture and matrix. The fracture systems having lower storability provide higher flow capacity due to the flow paths that have lower tortuosity whereas, the matrix systems have high storability but low fluid flow capacity. Therefore, formation fluids flow from matrix to the highly fluid conductive fracture media.

There are papers that represent different models to characterize the reservoir properties and fluid flow mechanisms in naturally fractured reservoirs. Warren-Root and Kazemi lead to the most common theoretical model for naturally fractured reservoirs. In these two models, it is stated that naturally fractured reservoirs contain two distinct porous regions as matrix (Figure 2.1) where fluids are stored under low permeability and fracture from where fluids are carried into wellbore region within low porosity. Both models assumed that there is a finite reservoir with centrally located well. Single-phase flow is taking place in both vertical and radial directions (Kazemi, 1969). While Warren-Root motivated analytical model that is concluded S-shape curve owing to the inflection point, Kazemi proposed numerical model that yields linear curve results (Mohammadi, 2012).

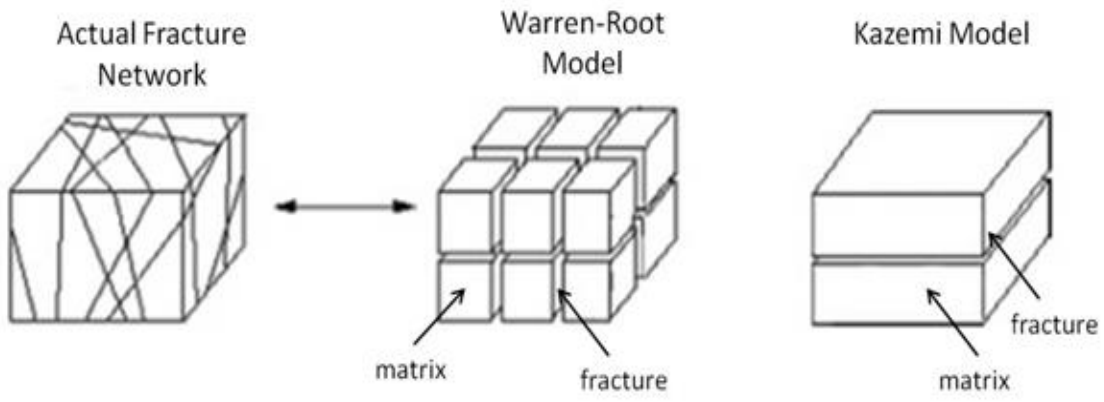

Figure 2.1 Simplified models of Warren-Root and Kazemi reproduced from Bahrami et. al (2012)

In naturally fractured reservoir models, reservoir is exhibited by a set of grid blocks and space between blocks represents fracture. In these models, fracture network is categorized as dual porosity and dual permeability.

Dual Porosity: Dual porosity model is based on the assumption of matrix feeds fracture system as fluid storage and fracture provides flow path to the well column. This model is sub-divided into three more models as following:

- ***Standard Dual-Porosity Model***: The simplest model in which matrix and fracture interchange information through a single exchange term. In other words, the heat or the fluid in the matrix can be transferred only to fracture.
- ***Multiple Interacting Continua Model***: In this model, the matrix is divided into several nested volume domains that provide a transient interaction between fracture and matrix.
- ***Vertical Refinement Model***: The vertical direction of matrix due to gravitational effect is considered. Vertical Refinement model considers transient flow.

Dual Permeability: Unlike dual porosity model, both matrix and fracture systems contribute to fluid flow and heat distribution in dual permeability model. The most significant difference is that matrix blocks are connected to not only fracture but also neighboring grid blocks (CMG STARS User's Guide, 2007). The simplest representation of the standard dual porosity and dual permeability are shown in Figure 2.2.

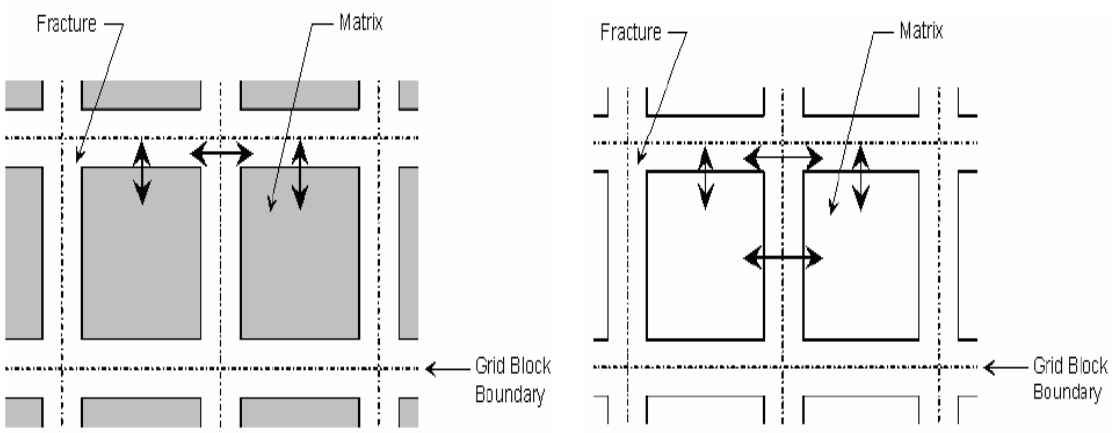

Figure 2.2 Standard dual porosity model (on left) and dual permeability model (on right) (CMG STARS User's Guide, 2007)

2.2 Cyclic Steam Stimulation

Cyclic steam stimulation provides thermal energy around the well bore by using a single well. In each cycle of this process, three distinct periods follow each other sequentially as shown in Figure 2.3.

***Injection Period*:** Steam is injected into the reservoir for a short period. Length of this period usually varies from 3 to 4 weeks in field experiences.

Soaking Period: After steam injection, well is shut in to allow steam interaction with reservoir fluids and reduce the oil viscosity. Length of this period that is generally defined as 2-4 weeks in literature is a very important operating parameter. It should be long enough for injected steam to heat formation around the wellbore, however; it should not be too long causing to heat loss.

Production Period: In this stage, well is put on production until termination oil flow rate that is determined based on the cost efficiency of process is reached. The initial oil production rate reaches peak rate that is generally higher than the primary oil recovery rate.

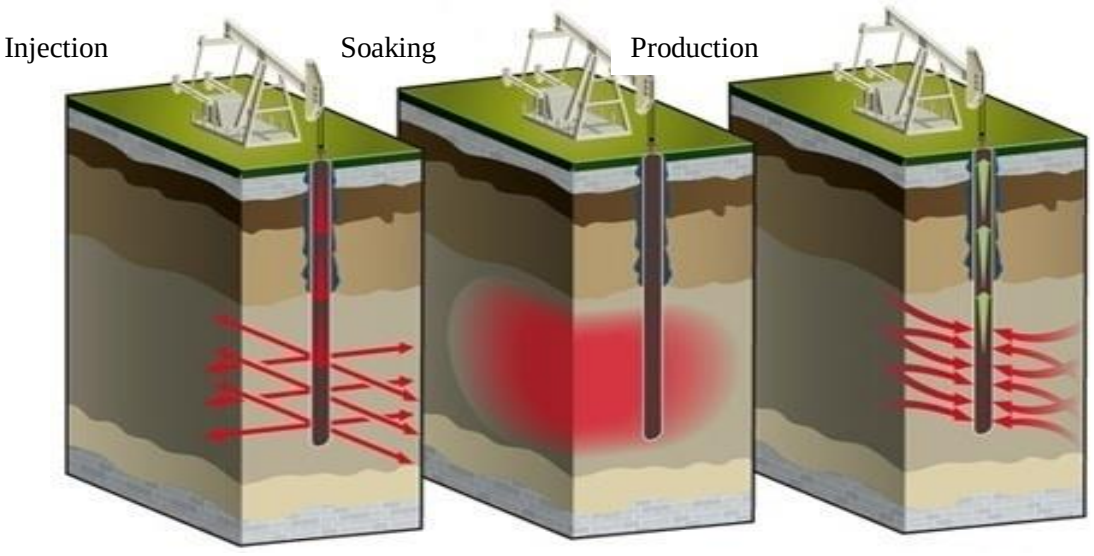

Figure 2.3 Cyclic steam stimulation process (TOTAL Oil and Gas Company, 2012)

Aziz *et al.* (1987) presented a comparative solution to cyclic steam injection problems that were resulted from six organizations: Arco Oil and Gas Co., Chevron Oil Field Research Co., Computer Modeling Group (CMG), Mobil R&D Corp., Societe Nationale Elf Aquitaine, Scientific Software-Intercomp., respectively. In this comparison study, commercial model of cyclic steam injection in a non-distillable oil reservoir with two-dimensional (2D) radial cross-sectional grid was used. A complete problem statement was provided to participants with the option of using their own simulator in order to exercise the features of different thermal models. However, all six organizations were offered same problem in which basic flow equations and fluid properties were fixed. They compared model results from simulators based on oil flow rate cumulative oil production, cumulative water production and heat loss. Moreover, some of the participants indicated computational works in the purpose of decreasing time steps, number of iteration and especially computing time. The results were in good agreements even if they observed some significant differences because participants applied different treatment of wells, convergence criteria of iterations, selection of operating constraints and time step size.

Razavi *et al.*(2009) conducted a numerical simulation of cyclic steam injection in K-field which is one of the fractured heavy oil reservoirs in Iran. They applied available measured data to simulation that was constructed as thermal dual porosity model by using CMG's STARS thermal simulator. They performed comprehensive sensitivity analysis in order to investigate an optimum scenario for oil recovery from this reservoir, based on design factors that were well numbers and directions, steam injection rates, oil production rates, soaking period and steam quality. They considered all these parameters simultaneously. Best scenario was defined as having higher oil recovery factor with water oil ratio, and steam oil ratio less than 10. They stated that oil recovery factor was higher when well was drilled in Y-direction than it was drilled in X or XY-direction with 45 degree slopes. The higher cumulative oil production was achieved with increased number

of wells, however; cost efficiency was considered and 20 wells were applied as the best case owing to the fact that it produced not much less than case having the highest well numbers. They arranged cycle periods in two different ways. One of them is known as “conventional”, in which all wells behave as injectors at the same time and they are shifted to producers, simultaneously. Another arrangement is called as “periodic cycles”, have one injector, one producer and, in next cycle they behaves reversely. Razavi et al. observed that there was no significant difference in results of both arrangement and they preferred to use conventional cycles. They proposed that the higher steam quality improved the oil recovery factor by increased heated zone volume, however; they also considered being cost-efficient. In this purpose, they compared the cost of higher qualified steam and revenue gained from incremental oil recovery. They observed that longer soaking period caused to lower temperature at heated zone owing to the fact that heat dissipated in longer interval of soaking. This study was concluded by defining the best case of having 20 wells in Y-direction with production and injection rate of 2000 bbl/day and steam quality of 0.8. They concluded the best conventional cycle design with injection, soaking and production periods of 20, 5, 95 days, respectively.

Al-Hadrami *et al.* (1997) presented the results of simulation study for the Midway Sunset field located in Kern County, Southern California. They showed a model of reservoir section containing a single horizontal infill well was more productive than vertical well recompletion strategy. They aimed to determine optimal design conditions for horizontal well production by obtaining the simulation results of oil and water production rates. In this purpose, they studied the effects of horizontal well placement at different height above the water/oil contact (WOC), steam injection rate and cycle period on productivity based on cumulative water and oil production results. They placed horizontal well in different layers in each runs to observe the effect of well distance to water oil contact depth. Placing the well too close to WOC caused to increased water production

and heat loss at boundary of reservoir. When they place the well in layer that was the furthest to water/oil contact depth, both water production and oil production decreased since injected steam was not sufficient to heat oil from that distance. Therefore, they concluded that the most efficient heating was achieved with the well located around the water oil contact referred depth. They compared cases under different injection rates, and investigated that lower injection rates yielded less cumulative production. However, application of doubled injection rate after some point was not effective to increase oil rate. Furthermore, they examined three cases by varying injection and soaking interval time and obtained the best performance by applying the shortest period of injection and soaking since the reduction in heat loss between well and water oil contact depth.

Rodriguez *et al.* (2008) presented a history matching and prediction of simulation model that was the first thermal compositional model in Colombia by using commercial simulator (CMG, SATRS). They conducted this simulation in two steps. In the first step, they achieved history matching for primary production of all existed wells in the field for 17 years. Then they implemented cyclic steam injection process to improve recovery factor. They especially focused on injection period of this process to improve recovery factor by optimizing the pressure and temperature of injected steam, rate of injection, injected heat, soaking period, steam quality and number of injection cycles. They investigated that injection at high pressure led to better injectivity by decreasing the amount of steam necessity for flooding. Even if soaking period was determined as parameter had less impact on cumulative recovery, the longer period of soaking led to the best production. They stated that oil production rate increased slightly with the higher quality of injected steam although there was no significant difference on cumulative production. They concluded this study by scheduling three injection cycles based on the sensitivity analysis.

Alvarez *et al.* (2013) summarized the development of cyclic steam injection by comparing past and current status of it based on commercial cases. They stated that in early time, numbers of cycles, number of wells and their orientation, operating constraints, were needed to optimize by performing trial-and-error field experiences. They noticed that recovery factor increased up to 40% by combining the cyclic steam injection with chemical addition, drilling horizontal wells and, introducing hydraulic fracturing. They proposed that there was a dilemma about application of horizontal well. It decreased drilling cost and improved sweep efficiency even though operating cost was considerably high since great amount of heat loss. They concluded that all these unconventional additions to conventional cyclic steam injection process require more investigations for different reservoirs and fluid properties.

2.3 Overview of Artificial Neural Networks

Artificial neural network (ANN) was developed by inspiration from neurons in the biological nervous system. In artificial neural network, functions are associated with three major parts of typical nervous neuron that are cell body, dendrites, and an axon.

The first model of neural networks was introduced by McCulloch and Pitts in 1943 and it was improved by Zuse with application of the first computer precursors (Kriesel, 2011). The next design of neuron called as perceptron was invented by Rosenblatt in 1958. He proposed random interconnection by developing a weight vector. He conducted multi-layers neural network in order to overcome limitations of simple perceptron. Widrow and Hoff (1960) developed an analytical method that solved the weight adaptation problem. This algorithm achieved to minimize the error squared which would lead to Least Mean Squares (LMS). In early 1980, neural network researches gained importance again by Hopfield's effort in the development of new learning algorithms (Mohaghegh, 2000).

2.3.1. Artificial Neural Network Structure

Artificial neural network is defined as information-processing system that simplifies simulation to generalize complex mathematical models with approximations. In this network, there are connecting links that provide signal passing between neurons in which information processing occurs. The simple schematic diagram of a processing element of a neural network is illustrated in Figure 2.4.

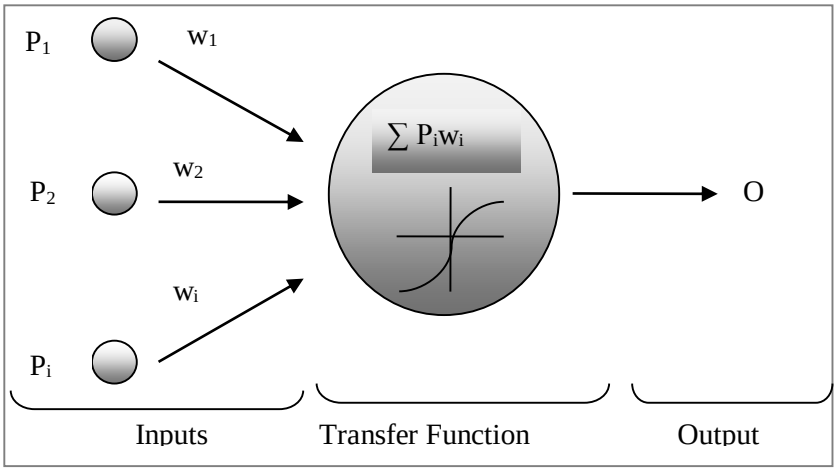

Figure 2.4 Artificial neuron reproduced from Artun (2008)

In the basic mechanism of information processing, inputs (P) are multiplied by their associated weights (w) and summation of them is transmitted in the forward direction by any activation function to determine outputs (Mohaghegh, 2000).

Fausett (1994) proposed that a typical neural network contains three main parts described as following:

- *Architecture* is an arrangement between neurons,
- *Training algorithm,*
- *Transfer function.*

2.3.1.1. Artificial Neural Network Architecture

Number of connecting links and outputs, number of hidden layers that have different connections with neurons are important architecture parameters. There are two main types of network: single layer and multilayer. In single layer structure (Figure 2.5), information are transferred from input layer to the output layer. On the other hand, multilayer network contains an input layer, one or more internal (hidden) layers, and an output layer. Figure 2.5-b shows the structure of multi-layer network with four neurons in single hidden layer.

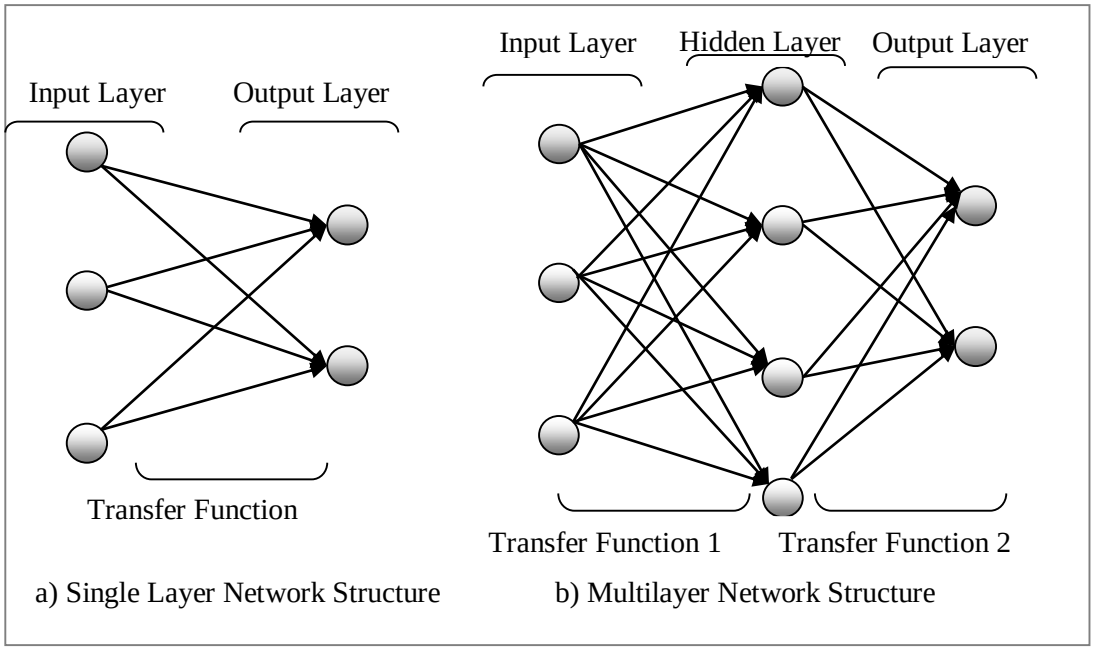

Figure 2.5 Types of artificial network architecture reproduced from Parada (2008)

Determination of number of hidden layers and number of neurons in each hidden layer are main parts of the network design based on the studied problem complexity. *Under-fitting* problems occur if used number of neurons is not enough to detect the signals in complex problem. On the contrary, too many neurons cause *over-fitting* problem that oscillates fitting curve even if it is seen as all training points are well fitted. There are some rule-of-thumb methods have been developed

to prevent over-fitting problem by providing formulation for number of hidden layer and the number of neurons in each hidden layer. In Karsoliya (2012), three of them are summarized as following:

- Successful training can be achieved by the neurons number of hidden layer that should be 70-90 % of the summation of input and output layer neurons.
- The size of hidden layer neurons should not exceed the twice of the neuron numbers in the input layer.
- The number of hidden layer neurons should vary between the number of input and output neurons.

Even if these approximations should not be considered as always true, they can be good start point for the training. Sensitivity of hidden layer neurons depends not only on the input and output layer size but also on the complexity of applied activation function

2.3.1.2. Training/Learning Algorithm and Weights

A connection weight represents an influence of corresponding input on connected neuron based on its sign. Stimulation occurs with positive weight whereas negative weight cause to inhabitation. In some cases, weight is zero, therefore; it is not possible to observe any effect from weight to neuron (Patterson, 1996).

Artificial neural networks are categorized as unsupervised and supervised based on training process and quality of weights that are determined iteratively during this process. Unsupervised neural networks have only input layers and modified weights. They are generally applied for well logs interpretation and lithology identification (Mohaghegh, 2000). On the other hand, in supervised training method, not only neurons in the input layers but also associated output vectors are provided and weights are initialized randomly. The size of weights is fitted iteratively until

satisfactory errors between calculated output and provided target values are achieved. In general, back-propagation neural network, which is known as supervised training algorithm, is applied in oil and gas industry. MATLAB toolbox provides many training algorithm functions, such as Bayesian Regulation (*trainbr*), Scaled Conjugate Gradient (*trainscg*), Conjugate Gradient (*traincgb*), Gradient Descent (*traingd*), Levenberg-Marquardt (*trainlm*).

2.3.1.3 Transfer Functions

Transfer functions provide transmission of information from artificial neurons to output vectors. In general, only one transfer function is used for all neurons in hidden layer, however in some complicated cases more than one different transfer function can be applied for one layer. (Maren et al., 1990). Usually, in multilayer networks, nonlinear transfer functions are used. Sigmoid transfer function is the most common nonlinear function that is classified as log-sigmoid and hyperbolic tangent sigmoid function. These two functions are preferred in back-propagation training algorithm owing to their differentiability. Reduction in computational requirements can be achieved by using differentiable transfer functions.

Log-sigmoid function (logsig) is given in the following expression, activates neurons and gives outputs that are scaled between 0 and 1by using input neurons whose values vary between minus and plus infinity (Figure 2.6).

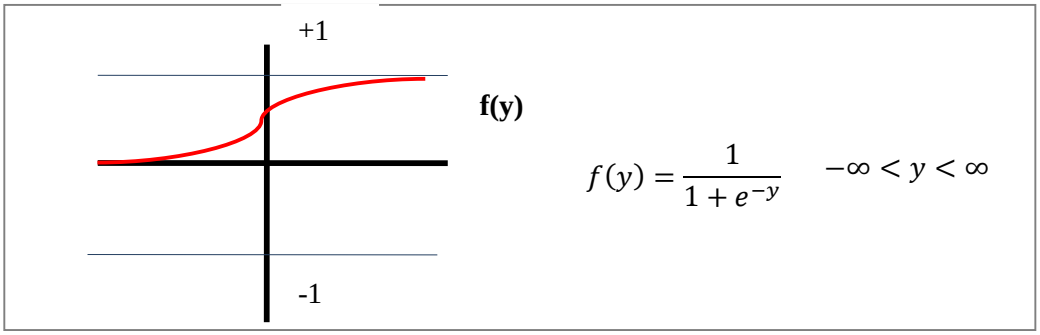

Figure 2.6 Log-sigmoid function *(logsig)* reproduced from Kulga (2010)

Hyperbolic tangent sigmoid (tansig) function presents output changing from -1 to 1. Usage of this transfer function is suggested when reduction of computing time is more important than shape of transfer function (Figure 2.7).

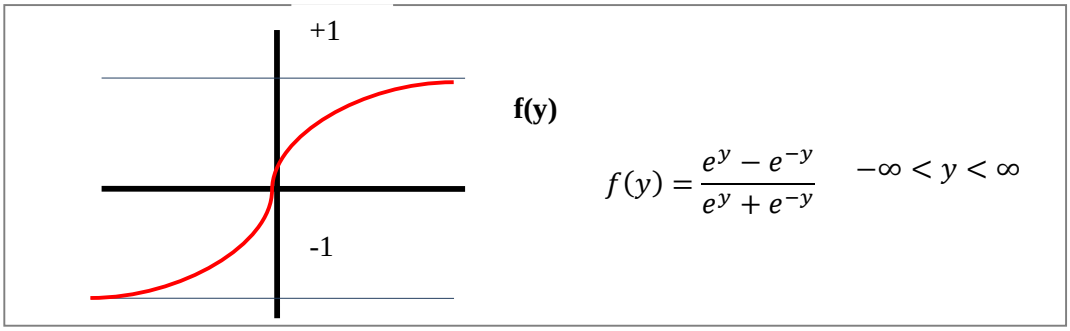

Figure 2.7 Hyperbolic tangent sigmoid function *(tansig)* reproduced from Kulga (2010)

Linear Function (purelin) generates output within the desired limit by multiplication of input with a constant factor.

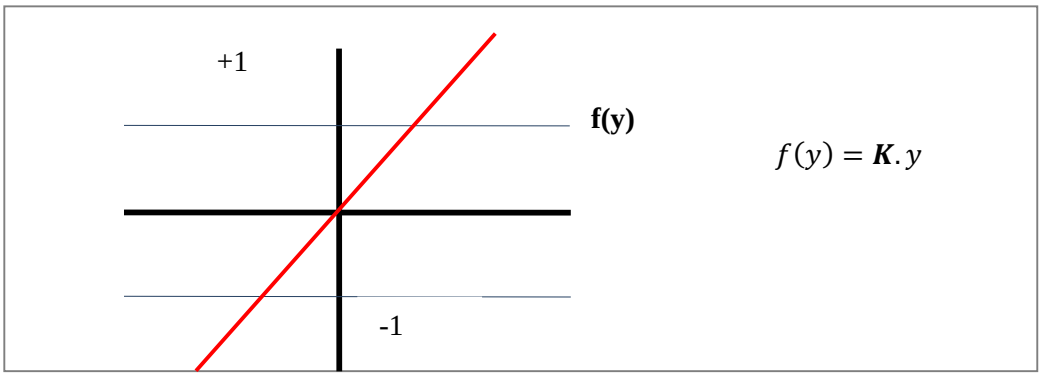

Figure 2.8 Linear function *(purelin)* reproduced from Kulga (2010)

2.3.2. Multilayer Feed Forward Networks with Back Propagation

Back propagation, which is known as gradient descent method is the most widely, used algorithm for feed forward network since its ability in minimization of total error between network outputs and target values. This algorithm technique is applied in the purpose of giving acceptable

response to the input vectors that are generalized covering most of the possible scenarios. Back propagation algorithm is one of the supervised training methods and contains three main stages; feed forward of input units, back propagation of the error and adjustment of the weights.

Feed Forward Stage: In this stage, input neurons are given with randomly initialized weights. Multiplications of input neurons by corresponding weights are summed and transmitted to the next layer in which transfer function is applied. When the activation of each layer is completed, output units can be calculated.

Error Back Propagation Stage: In this stage, calculation of error for each output unit is done by the difference between the network output and actual output that is wanted to achieve.

Weight Adjustment Stage: After getting error information, weights and biases are adjusted based on the *Generalized Delta Rule,* which is developed based on the *Least Mean Squared Rule (LMS)*.

Back propagation algorithm is completed when repetitions of all three stages stopped by reaching pre-specified terminating conditions, such as number of training cycles *(epoch),* performance gradient, and computing time to converge. These stopping conditions vary by selected training function type.

2.3.3. Generalization and Early Stopping

Generalization is the most significant part of the network since getting accurate response for different cases that cover all possibility. The most common problem during network training is over-fitting in which given data are memorized instead of generalized. Network results seem as if training is achieved because of having small value for error. However, error raises to higher value for new data that has not been used during training process. For this reason, early stopping method is implemented and data set is divided into three parts as training, validation and, testing. While training data set is applied to network, error of validation is monitored. At the beginning of training,

both training and validation errors decrease. However, at some point validation error starts to increase even if training error continues to decrease. This behavior of network signs the over-fitting problem and it should be stopped early. Testing data set that has not seen before by network is used to check generalization of it. If available cases are not divided randomly to cover all possible different input patterns, testing error starts to increase before validation error that requires stopping network early. Moreover, addition of functional links that are related to given input units by taking logarithm or square root of them can improve efficiency of training.

Chapter 3

Statement of the Problem and Workflow Propose

Success of cyclic steam injection applications depends on feasibility of process in reservoir under consideration. When suitable reservoir properties are found, important design parameters value should be decided carefully by answering following key questions:

- ✓ What should be the injection rate?
- ✓ What should be the properties of injected steam such as: steam quality and steam temperature?
- ✓ How long should be the production periods of each cycle with pre-specified injection and soaking periods based on terminated oil flow rate?
- ✓ How many cycles should be completed during project length?
- ✓ What should be the area of inner zone that is intensely fractured to increase efficiency of cyclic steam injection process?
- ✓ What should be the characteristics of this fractured inner zone such as: fracture porosity, fracture permeability, fracture spacing?

Reservoir engineers try to accomplish design of the process efficiently and they conduct numerical studies that require long computing time and complex work in order to analyze the production profile. It is complex and time-consuming process to evaluate all possible different scenarios and find the optimum one. This complex problem can be overcame by developing artificial neural network (ANN) that is capable of solving nonlinear relationship between the input and output of complicated systems.

In this study, ANN tools is developed which can provide considerably good estimation for implementation of cyclic steam injection in different naturally fractured reservoirs with a fractured elliptical zone around the horizontal wellbore. The main objective of this research is development of an expert proxy system for cyclic steam injection process. These objectives can be achieved by completing following steps. Figure 3.1 shows the workflow of this research.

- Construct a representative reservoir model in commercial thermal simulation software CMG STARS for cyclic steam injection in a dual porosity system.
- Extend the cyclic steam injection by adding more intensely fractured elliptical inner zone design.
- Run different scenarios by using simulator for combinations of different reservoirs and design parameters that are determined in meaningful ranges.
- Collect the critical production results and generate data sets containing inputs and outputs.
- Feed the artificial neural network with created data sets and train it.
- Compare neural network results with actual results that are obtained from the simulator to evaluate the accuracy of the network structure.

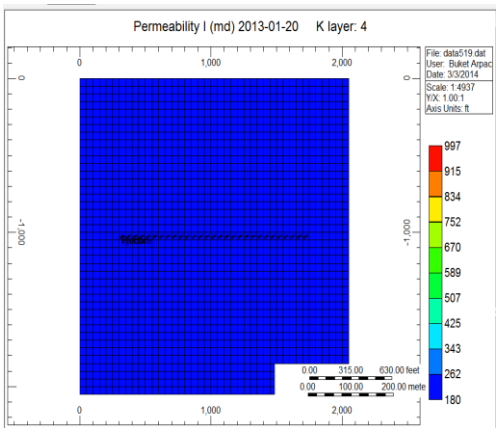

Representative reservoir model for CSI

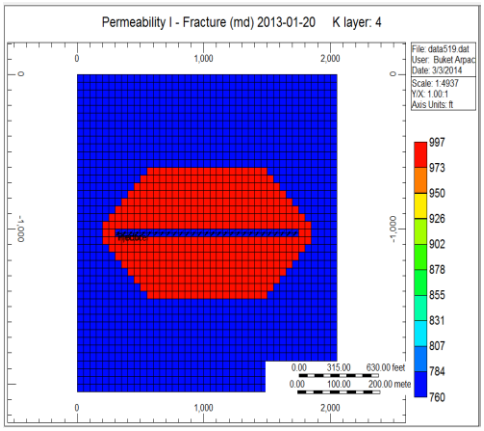

Extend CSI by addition of elliptical fractured zone

	Cumulative Production bbl			Cycle Duration (days)		
	Case 1		Case 555	Case 1		Case 555
Cycle 1	125833		117642	4464	..	3356
Cycle 2	41664	..	17004	652	..	1240
Cycle 3	33550	..	10697	448	..	976
Cycle 4	35953	..	8953	388	..	880
Cycle 5	36388	..	12041	476	..	784
Cycle 6	26133	..	10330	424	..	588
Cycle 7	23745	..	22611	792	..	640
Cycle 8	18183	..	9534	420	..	588
Cycle 9	16213	..	10191	448	..	456
Cycle 10	13168	..	8717	392	..	416

Collection of critical production results

	Case 1	Case 2	Case 3		Case 555
Reservoir Properties					
Thickness (ft)	40	55	164	..	195
Matrix Permeability (mD)	20	120	65	..	157
⋮	⋮	⋮	⋮	..	⋮
Fracture Spacing (ft)	50	20	550	..	200
Design Parameters					
Steam Quality	0.7	0.95	0.78	..	0.82
Steam Temperature (F)	550	620	735	..	475
⋮	⋮	⋮	⋮	..	⋮
Soaking Period (days)	6	21	48	..	32

Different scenarios by combinations of different reservoir and design

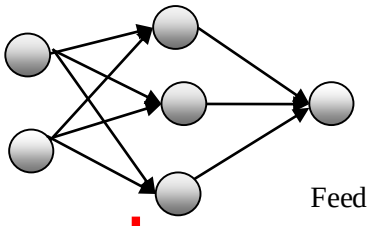

Feed ANN with created data sets.

Comparison of network results with simulator results

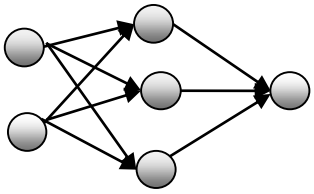

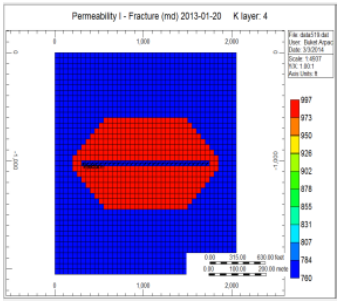

Figure 3.1 Flowchart followed to design proxy model for a given problem

In this research, performance of cyclic steam injection is evaluated based on outputs of the process for the first ten cycles. These performance indicators are cumulative oil production at the end of each cycle, duration of production period of each cycle, cycle oil production rate, total number of cycles and, total cumulative oil production at the end of project. Reservoir properties studied in this thesis are reservoir thickness, matrix porosity, fracture porosity, matrix permeability, fracture permeability, fracture spacing, oil saturation, initial pressure, initial temperature, and reservoir depth. Design parameters are divided in two parts as pertaining to CSI and fractured inner zone. Cyclic steam injection design parameters are well length, layer in where well is located, steam quality, steam temperature, soaking period, injection period, and injection rate. Inner zone design parameters are drainage area, minor and major axes of elliptical inner area, fracture porosity, fracture permeability and fracture spacing of this area.

Two forward-looking and four inverse-looking ANN tools are developed for described reservoir properties, design parameters and performance indicators. In the first forward ANN-1 tool, cycle oil rate and number of cycle can be estimated. In the forward ANN-2, three performance indicators are; total cumulative oil production at the end of project length, total cumulative oil production and production period of each cycle can be predicted for a given data set of reservoir properties and design parameters as it is shown in Figure 3.2.

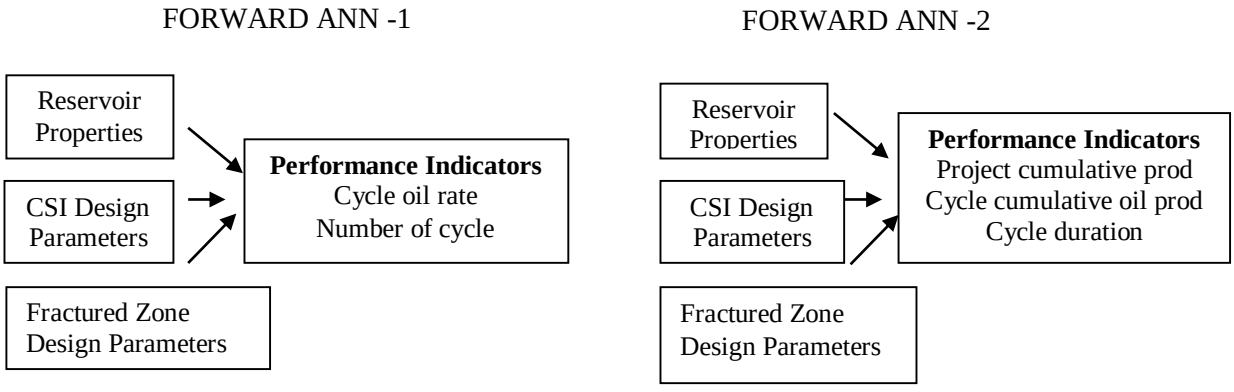

Figure 3.2 Development of forward ANN proxies

In the inverse ANN-1A tool, performance indicators and reservoir properties are fed as inputs in order to predict both cyclic steam stimulation and fractured zone design parameters. In inverse ANN-1B tool, fractured inner zone design parameters are given as input in addition to inverse ANN-1A inputs to estimate only CSI design parameters. Inverse ANN-2A is used if reservoir characteristics after implementation of more intensely fractured inner zone are wanted to predict with known CSI design parameters and performance indicators. The last tool that is named as inverse ANN-2B, determines what kind of fractured elliptical zone should be designed for given reservoir properties with cyclic steam injection design parameters to get desired performance indicators. All these developed inverse proxy models are summarized in Figure 3.3. Graphical user interface (GUI) is designed. It contains all six ANN tools to provide facility to user getting production profiles of reservoirs without using time consuming simulation software.

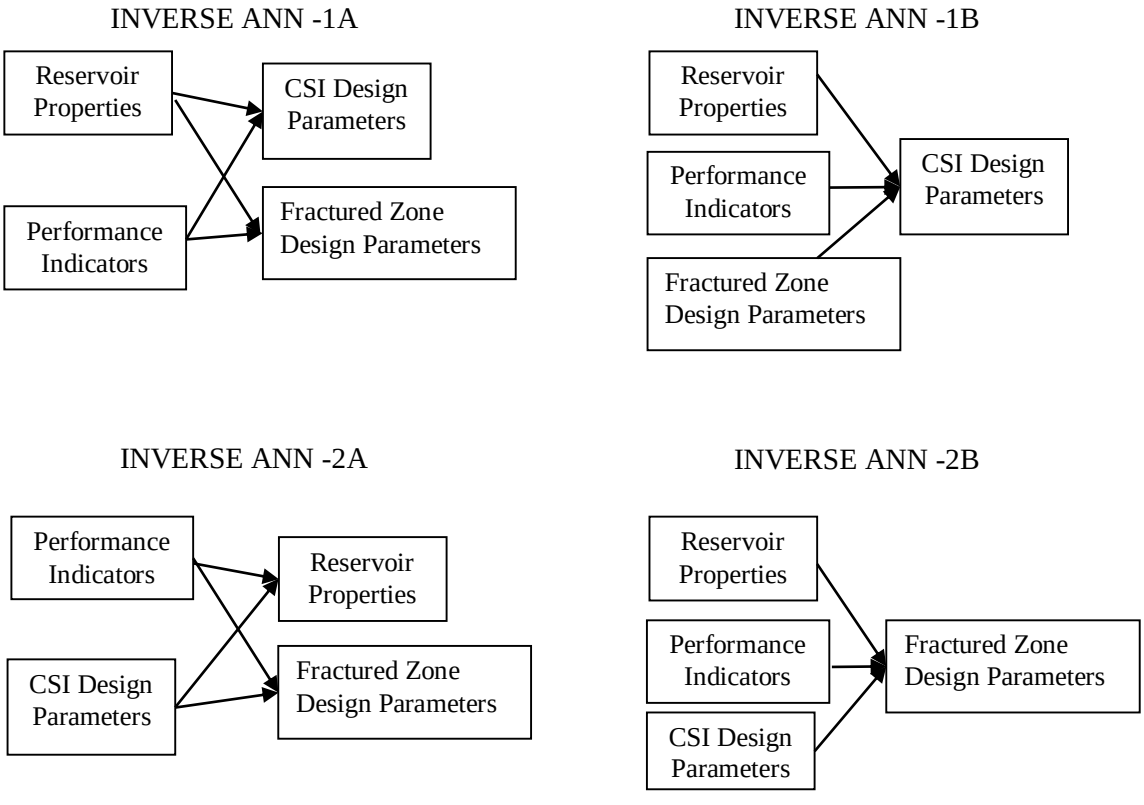

Figure 3.3 Development of inverse ANN proxies

Chapter 4

Reservoir Model and Generation & Collection of Data

4.1 Reservoir Model

The reservoir model developed in this study is built using CMG's Advanced Processes & Thermal Reservoir Simulator (STARS). All followed steps to create this model are explained under reservoir description, component properties, rock-fluid properties, well design description sections in this chapter.

4.1.1 Reservoir Description

Reservoir pattern is defined as three-dimensional Cartesian model. Number of grid blocks is randomly changed with constant grid width 50 (ft) due to the variable reservoir area. Square reservoir model consists 5 grid layers and the layer thickness is equally distributed. Cross-section of the reservoir along the drilling direction is displayed in Figure 4.1.

Dual porosity system is used in naturally fractured reservoir model. Reservoir characteristics: reservoir depth, grid thickness, matrix porosity, fracture porosity, matrix permeability, fracture permeability, fracture spacing, reservoir temperature, reservoir pressure, and oil saturation are specified in the pre-determined range.

More intensely fractured inner zone due to stimulation is created in elliptical-shape around the well bore based on fracture porosity, fracture permeability and fracture spacing that are different from original reservoir properties. Well length should not exceed the elliptical fractured zone hence,

the major axis of this area is determined depending on the well length. The minor axis is changed between 30% and 95% of the reservoir edge. Top view of the reservoir containing inner zone is shown in Figure 4.2.

Rock type of reservoir is determined by providing specified thermal rock properties. Thermal conductivity and heat capacity of the reservoir for both over-burden and under-burden are equal to 24 Btu/(ft*day*F) and 35 Btu/(ft^3* F), respectively.

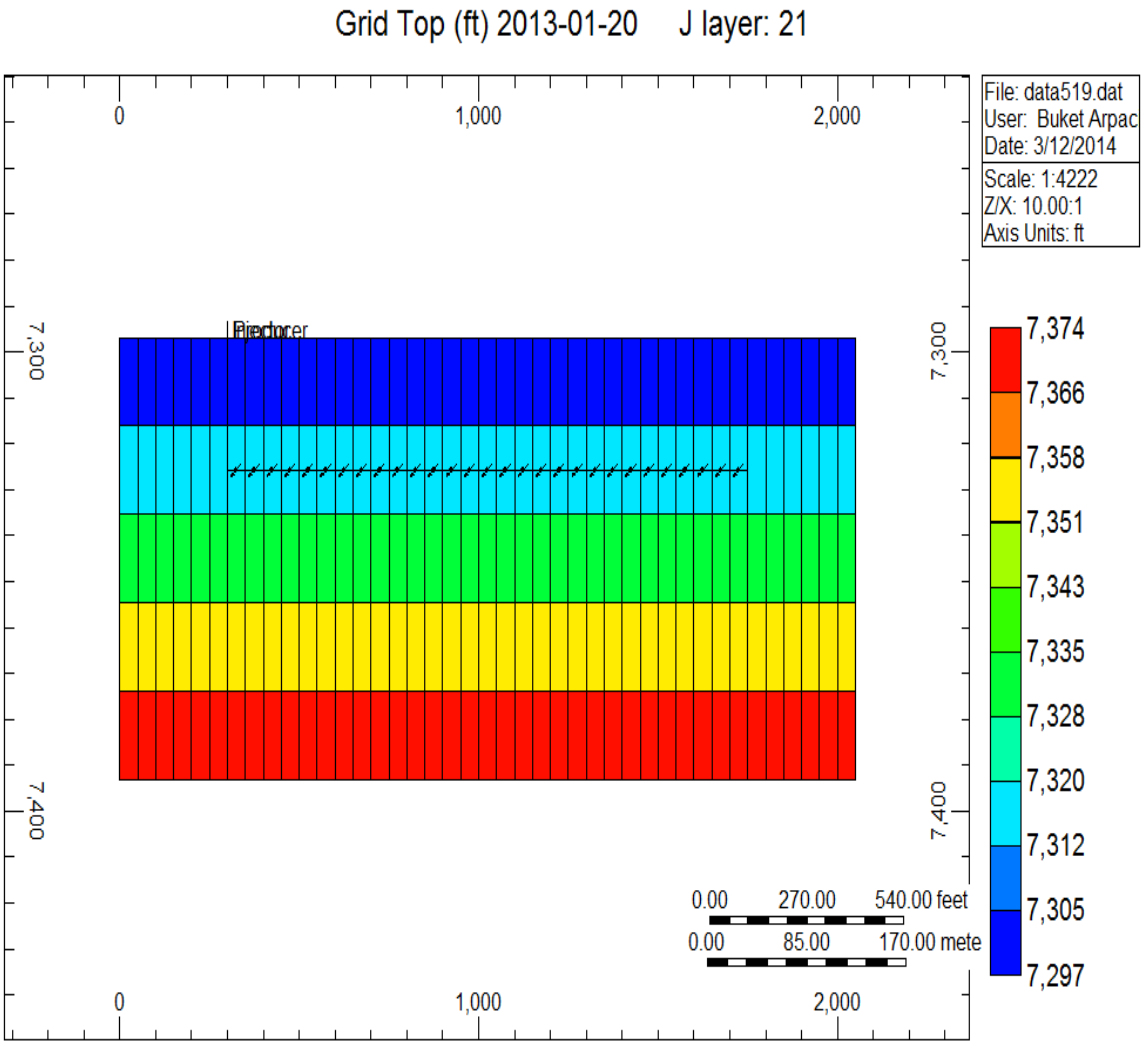

Figure 4.1 Cross-section of the reservoir along the drilling direction

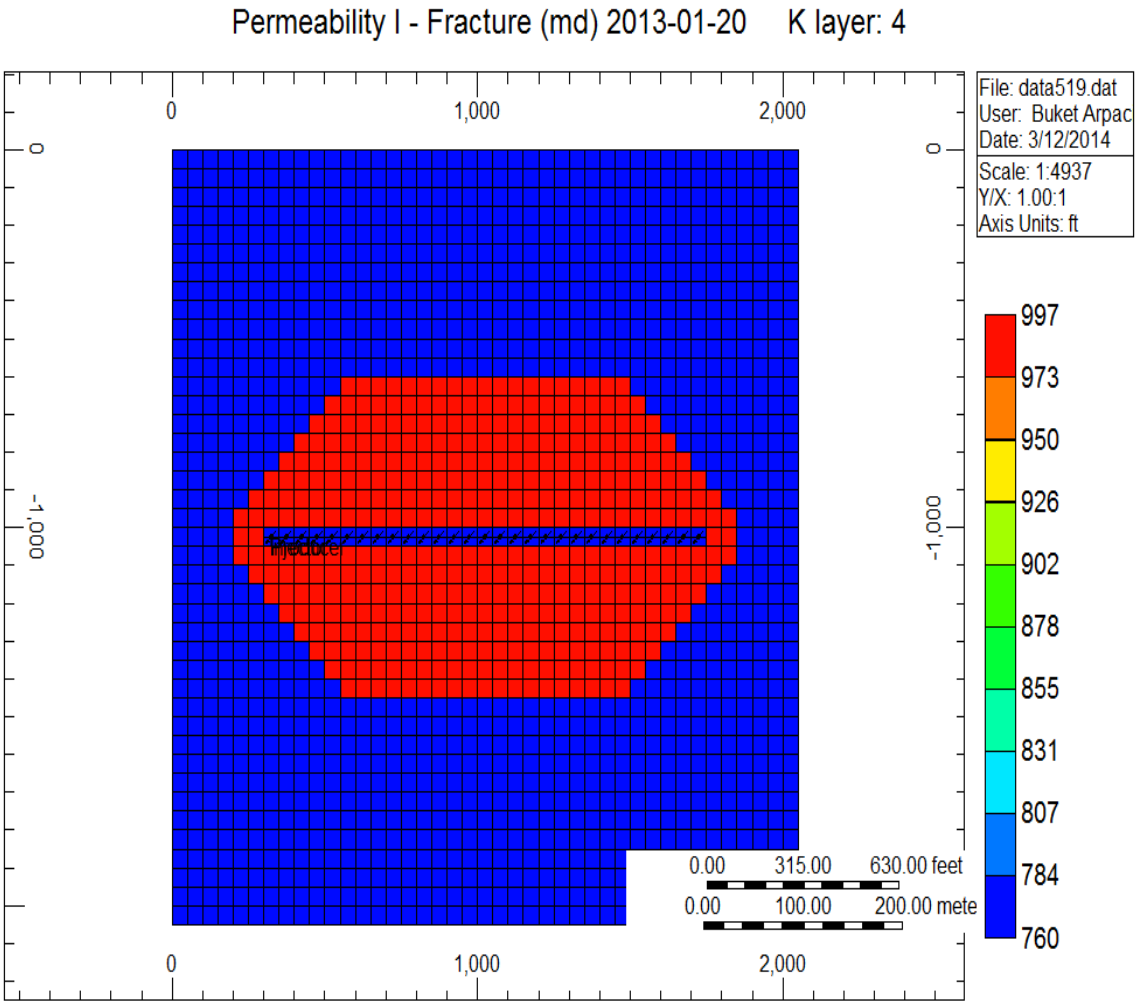

Figure 4.2 Top view of the reservoir which contains inner zone

4.1.2 Component Properties

Component properties of the reservoir are given for both water and oil. Heavy oil is used in this reservoir model. Molecular weight and density of oil are specified as 600 (lb/lbmole) and 60.678 (lb/(ft^3), respectively. The variation of heavy oil viscosity with respect to temperature is given in Table 4.1.

Table 4.1 Variation of the heavy oil viscosity with temperature

Temperature (^{o}F)	Viscosity (cp)
75	5780
100	1380
150	187
200	47
250	17.4
300	8.5
350	5.2
500	2.5
750	2.4

4.1.3 Rock-Fluid Properties

It is assumed that there is no capillary pressure in this model. The connate water saturation S_{wcon} is assumed to be equal to critical water saturation S_{wcrit} ($S_{wcon} = S_{wcrit} = 0.25$). The residual oil saturation for water/oil is $S_{orw} = 0.15$, and the residual oil saturation for gas/oil is $S_{org} = 0.1$ and the critical gas saturation is $S_{gcrit} = 0.06$. Oil relative permeability at connate water is krocw = 0.4, water relative permeability at irreducible oil saturation (water/ oil system) is $k_{rwiro} = 0.1$, and gas relative permeability at connate liquid (gas/oil system) is $k_{rgcl} = 0.2$. Relative permeability table is generated by using following correlations (Aziz et al, 1987). Graphs of relative permeability for water/oil and oil/liquid system are shown in Figure 4.3 and Figure 4.4, respectively.

Water/Oil System;

$$k_{rw} = k_{rwiro}\left(\frac{\left(S_w - S_{wcrit}\right)}{\left(1 - S_{wcrit} - S_{oirw}\right)}\right)^{2.5}$$

$$k_{row} = k_{rocw}\left(\frac{\left(S_o - S_{orw}\right)}{\left(1 - S_{wcon} - S_{orw}\right)}\right)^{2}$$

k_{rw} : relative permeability to water
k_{rwiro} : k_{rw} at irreducible oil saturation
k_{row} : relative permability of oil w.r.t water
k_{rocw} : k_{ro} at connate water saturation

S_w : saturation of water
S_{wcon} : saturation of connate water
S_{wcrit} : saturation of critical water
S_o : saturation of oil
S_{oirw} : irreducible oil saturation for water/oil system
S_{orw} : residual oil saturation for water/oil system

Gas/Oil System;

$$k_{rog} = k_{rogcg}\left(\frac{\left(S_l - S_{org} - S_{wcon}\right)}{\left(1 - S_{gcon} - S_{org} - S_{wcon}\right)}\right)^2$$

$$k_{rg} = k_{rgcl}\left(\frac{\left(S_g - S_{gcrit}\right)}{\left(1 - S_{gcrit} - S_{oirg} - S_{wcon}\right)}\right)^{1.5}$$

k_{rg} : relative permability to gas
k_{rog} : relative permability of oil w.r.t gas
k_{rogcg} : k_{rog} at connate gas
k_{rgcl} : k_{rg} at connate liquid

S_l : saturation of liquid
S_{org} : residual oil saturation for gas/oil system
S_{orig} : irreducible oil saturation for gas/oil system
S_g : saturation of gas
S_{gcon} : saturation of connate gas
S_{gcrit} : saturation of critical gas

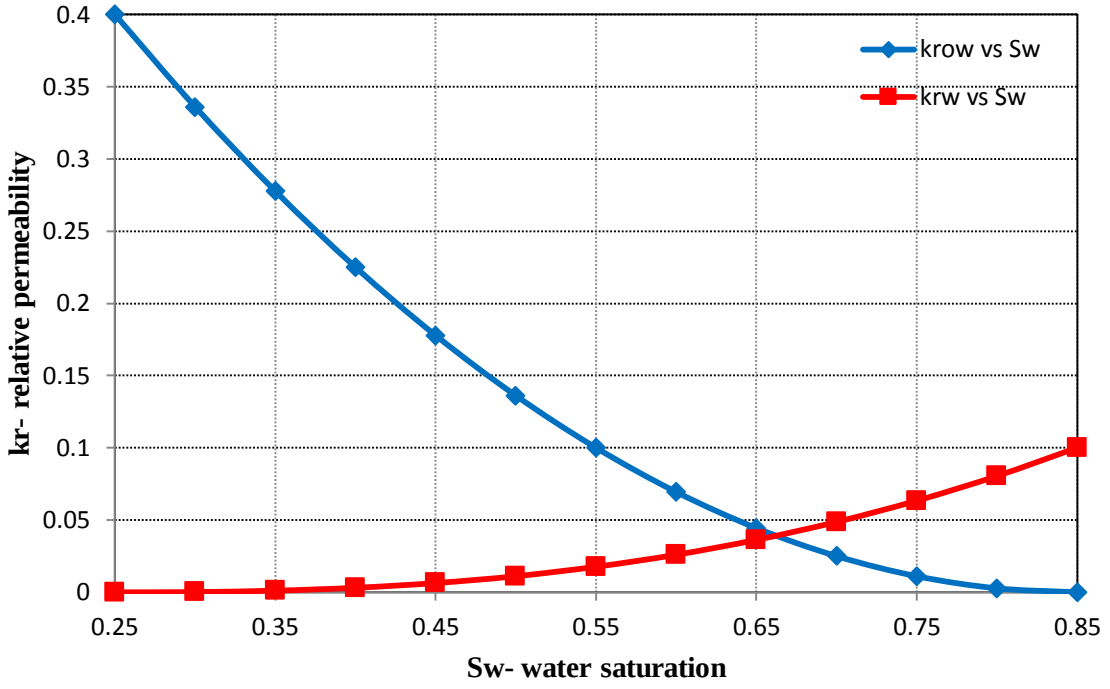

Figure 4.3 Relative permeability of water/oil system

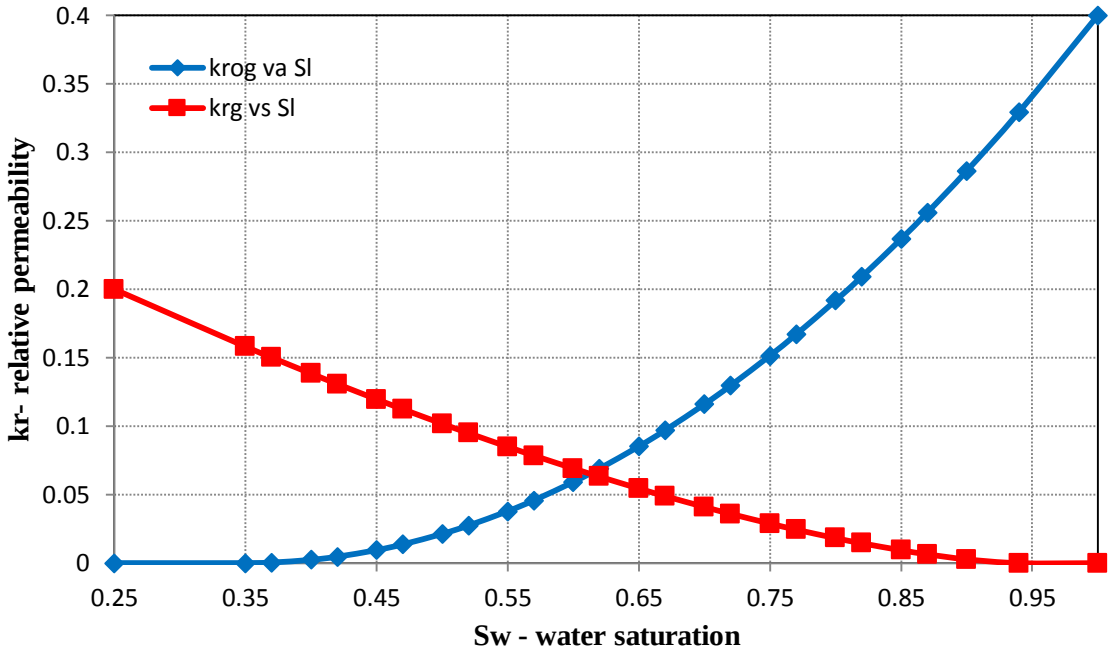

Figure 4.4 Relative permeability of gas/liquid system

4.1.4 Well Design Description

Single well is drilled along the x-direction with a variable length. It is used as an injector and a producer depending on being in which period of cyclic steam injection operation. Drilling of well at the first or the last layer is avoided to prevent heat loss. Hence, the layer where the well is placed is selected randomly between 2^{nd} and 4^{th} layer. Constant well bore radius of 0.3 ft is used.

Trigger method is applied in this reservoir simulation. Before cyclic steam injection implementation, well is put on production until terminated oil flow rate of 30 bbl/day has been reached. This abandonment rate is decided after trial and error method that is applied for 10, 20, 30, 40, and 50 bbl/day of oil flow rate. Production may continue at lower oil flow rate for a long time in some reservoirs when abandonment rate of 10 or 20 bbl/per day is selected. This kind of primary production period makes implementation of cyclic steam injection process is inefficient due to the less amount of remained oil. However, when the well is constrained by production rate of 40 or 50 bbl/day, amount of oil left after primary production might be relatively more. Therefore, more numbers of cycle requires during cyclic steam injection process. Because of all these explained reasons, 30 bbl/day is chosen as an optimum abandonment rate of primary production and when it is reached, the well is shut in. Next, specified volume of steam is injected during injection period that is randomly selected from uniformly distributed design parameters. Soaking period is constant for each cycle of one case, but it is varied case by case. After soaking period is completed, well is put on production until terminated oil flow rate of 20 bbl/day is reached. Thus, production periods are different in each cycle of project. Repetition of injection, soaking and production periods are counted as one cycle. When initial rate of the next cycle is less than abandonment rate, project is terminated. Thus, the number of cycle is going to be different in each reservoir scenario.

4.2 Generation of Data File

In order to observe the performance of cyclic steam injection process, expert proxy system should be trained with more possible scenario. In this case, reservoir model are created for different combinations of reservoir properties and design parameters that are generated by using random number generator function of MATLAB. Upper and lower limits of reservoir properties and design parameters are shown in Table 4.2 and Table 4.3, respectively.

Table 4.2. Range of reservoir properties

Reservoir Properties		Minimum Value	Maximum Value	Unit
Thickness	(*h)*	40	200	ft
Matrix Porosity	(*phi_m)*	15	40	%
Fracture Porosity	(*phi_f)*	1	3	%
Matrix Permeability	(*k_m)*	20	200	mD
Fracture Permeability	(*k_f)*	50	2000	mD
Fracture Spacing	(*fs)*	20	800	ft
Initial Pressure	*(P)*	500	3500	psi
Initial Oil Saturation	*(So)*	40	85	%
Depth	(*d)*	1000	10000	ft
Initial Reservoir Temperature	(*T)*	70	160	°F

While reservoir properties are generated, some constraints are considered in order to prevent the possibility of having physically impossible parameter combinations.

Matrix porosity (phi_m) must be larger than fracture porosity (phi_k) whereas matrix permeability (k_m) must be lower than fracture permeability (k_f) due to the characteristic of naturally fractured reservoirs. Furthermore, reservoir temperature is calculated with regard to reservoir depth based on geothermal gradient. Expression used in temperature determination is,

$$\text{Reservoir temperature (T)} = \frac{1^{\circ}\text{F}}{100\ \text{ft}} \times \text{Depth (d)} + 60$$

Table 4.3 Range of design parameters

Cyclic Steam Injection Design Parameters	**Minimum Value**	**Maximum Value**	**Unit**
Steam Quality (*Qs)*	0.7	1.0	-
Steam Temperature (*Ts)*	450	750	°F
Soaking Period (*ts)*	5	50	days
Injection Period (*ti)*	5	50	days
Steam Injection Rate (*qinj)*	350	5000	bbl/day
Well Length (*L_w*)	250	1550	ft
Layer on Well Located *(layer_w)*	2	4	-
Fractured Inner Zone Design Parameters			
Inner Zone Fracture Porosity *(phi_f_in)*	2	6	%
Inner Zone Fracture Permeability (*k_f_in)*	150	3000	mD
Inner Zone Fracture Spacing (*fs_in)*	10	200	ft
Major Axis of Inner Zone *(a)*	500	1800	ft
Minor Axis of Inner Zone *(b)*	200	1800	ft
Drainage Area *(A)*	5	100	acres

Some criteria should be considered during selection of design parameters with regard to reservoir properties.

In the aim of having more fractured area, fracture permeability of inner zone should be higher than reservoir's original permeability. Furthermore, fracture spacing of inner zone should be less than the outer zone thus, is possible to have more fracture. In addition, major axis of elliptical fractured area should be larger than well length. It is possible to observe some unreasonable cases since physically impossible combinations of parameter. After unreasonable cases were eliminated, a total of 555 reservoir model cases left behind and were simulated by using CMG's Advanced Processes & Thermal Reservoir Simulator (STARS).

4.3 Data Collection for Network Training

Results used in the training of proxy systems are collected as outputs of simulator and summarized in this section. In this study, cyclic steam injection is implemented after primary production; for this reason, results belong to the primary production period are not evaluated. Instead of using fixed number of cycle, a variable cycle number is applied which let the system produce more as it is possible. Therefore, the number of cycles and the production period length of each cycle become outputs of the process as a function of abandonment rate. Thus, both of them are going to change from case to case. In addition, both cumulative oil production at the end of cycles and total cumulative oil production of whole project are collected from simulation results. 29 data points of oil flow rate are taken in the production period of every cycle. All cases are going to have different number of outputs collection owing to the variable cycle number. For example, 1st sample case produces during 11 cycles whereas 2nd case continues to production until 20 cycles depending on the difference on their reservoir characteristic and design parameters. Therefore, 1st case has 11x1 values of cumulative oil production, 11x1 values of production period length and 11x29 oil flow rate data points, while the other one has 20x1, 20x1 and 20x29. However, it is not possible to feed data in different numbers into the artificial neural network. As a result, first 10 cycles of each case are evaluated to predict the behavior of reservoirs regardless of cycle numbers. Design scheme and evaluated perform e indicators are shown in Figure 4.5

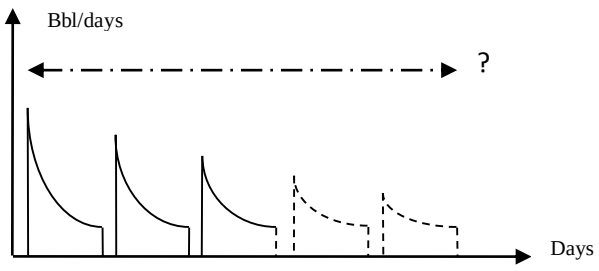

Variable number of cycles scheme

Performance Indicators

- Oil flow rates
- Project cumulative oil production
- Cycle cumulative oil production
- Cycle duration
- Number of cycle

Figure 4.5 Design scheme and performance indicators of CSI process

Chapter 5

ANN Model Development

In this chapter, developments of six different expert systems are presented. Artificial neural network toolbox on MATLAB is applied for training of all six networks. Designed ANN models are categorized as Forward ANN-1, Forward ANN-2, Inverse ANN-1A, Inverse ANN-1B, Inverse ANN-2A and Inverse ANN-2B that are explained deeply in the following section of this chapter. Creating an accurate artificial neural network is a complex problem that requires optimization of components used in the structure of ANN. Following steps are taken into consideration in this study:

- The number of datasets used for training, validation and testing of process is one of the design components. During training, performance of the network can be evaluated by validation datasets that help to prevent under-fitting and over-fitting problem. Thus, division percentage of the datasets is important. In order to prevent gathering similar reservoir properties that causes to limitation of expert system usage, datasets are divided randomly by using *dividerand* function of MATLAB.
- Number of hidden layers and the number of neurons are the most significant part of the ANN model structure. In this study, it was observed that single hidden layer provided more accurate prediction than multi-hidden layer based on trial and error method results. Moreover, different neuron numbers were tried in order to find the most powerful structure. Three thumb rules that were explained in Chapter 2.3 were applied, while the most appropriate number of neurons was decided.

- Other component of ANN model design is functions used in the training, activation and learning algorithms. A cascade feed-forward network *(newcf)* with scaled conjugate gradient back-propagation algorithm function *(trainscg)* was selected after its predictions were compared with different functions' results. In the learning algorithm, gradient descent with momentum weight and bias *(learngdm)* was applied and performance of network was controlled by mean squared error with regularization performance function *(mereg)*.

- Functional links are additional components that provide relationship between inputs and outputs. Addition of functional links improves prediction ability of network; however, using of them as inputs or outputs should be decided by trial and error method. Functional links used in this research will be mentioned for each ANN model separately in the following sections.

The prediction performance of the network is evaluated based on error percentage of each data point used in the neural network. This error percentage is calculated by the following equation:

$$Error\ \% = \left|\frac{Value_{Numerical\ simulator} - Value_{Network}}{Value_{Numerical\ Simulator}}\right| x100$$

Values of numerical simulator are obtained by thermal commercial simulator, CMG's STARS, and these values are wanted to predicted by developed networks. Overall error of performance indicators can be calculated by taking arithmetic average of data points' error percentages as expressed in the following equation:

$$Average\ Error\ \% = \frac{\sum_{i=1}^{n} Error\ \%}{n}$$

where *n* represents the number of data points used in one case. For instance, *n* is equal to 290 for oil flow rate prediction whereas it is equal to 10 for cumulative oil production prediction. In addition, mean error of all testing data sets can be calculated by taking the arithmetic average of case errors.

5.1 Forward ANN Models

The forward problem includes developed neural networks, which can predict the performance indicators accurately by using design parameters with corresponding reservoir properties. At the beginning of forward ANN design, a single forward ANN model was developed as predicting all performance indicators. The error percentages of cumulative oil production and cycle duration were around 30% even if this model was able to provide accurate prediction for oil flow rates and number of cycles. Differences on the structure of data points were considered as a reason of this problem. 29 data points were used whereas only one cumulative oil production and one cycle duration value were taken for each cycle. Hence, cumulative oil production and cycle duration are estimated in another ANN model which have different structure from the model that estimate oil flow rate and number of cycle.

5.1.1 Forward ANN-1

In the forward ANN-1 tool, cycle oil rate and number of cycles can be estimated for a given data set of reservoir properties and design parameters of both cyclic steam injection and intensely fractured inner zone. In the network model, a total of 555 datasets were generated and 79 %, 14 %, 7 % of them were selected randomly for training, validation and testing, respectively. Tan-sigmoid function *(tansig)* was applied for activation function with scaled conjugate gradient *(trainscg)* training function. The optimum structure providing predictions that are more accurate includes a single hidden layer of 275 neurons. Input layer contains a total of 27 neurons; 23 of them belong to reservoir properties and design parameters while 4 of them are functional links called as eigenvalue. Output layer has 291 neurons; 290 of them are oil flow rates and 1 of them is cycle number. The network structure is illustrated in the Figure 5.1.

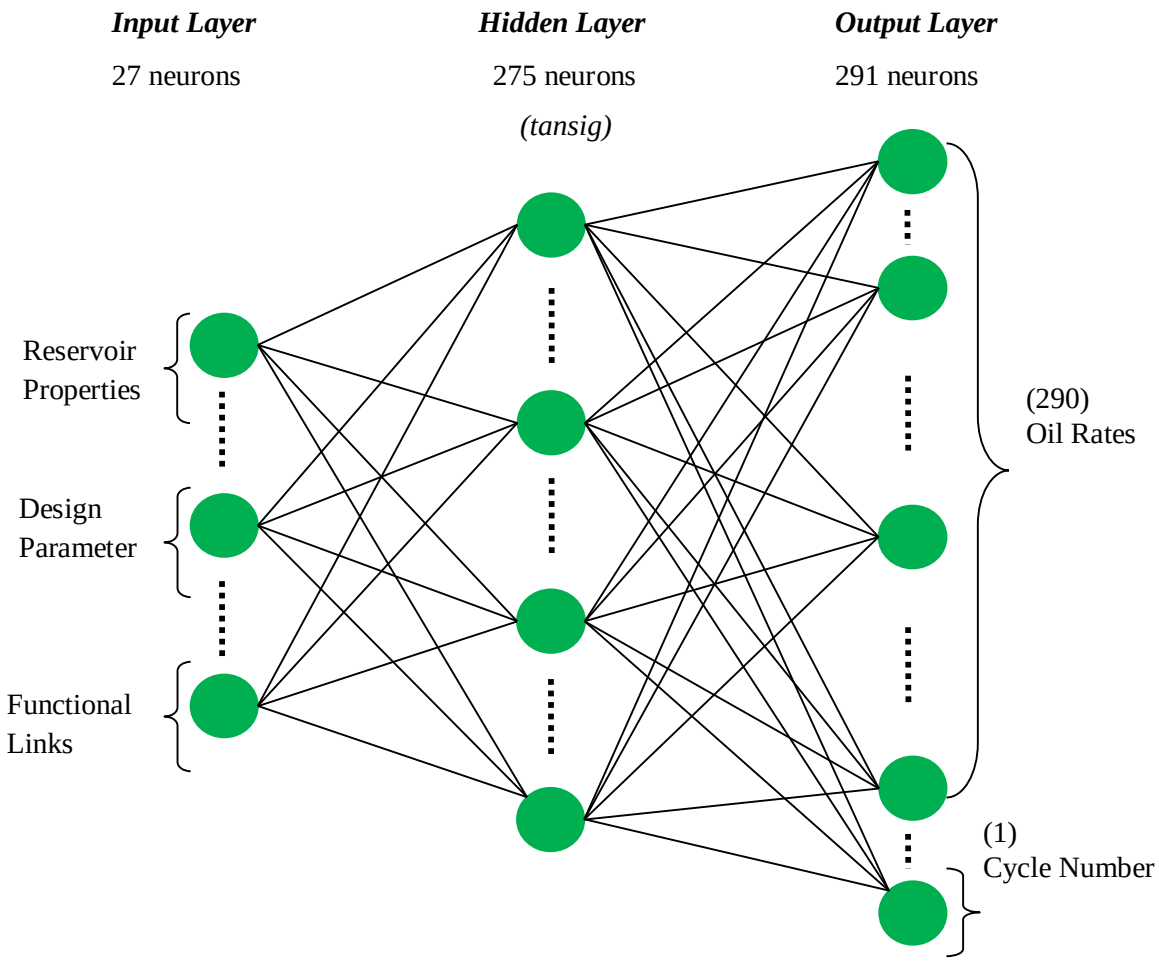

Figure 5.1 Network structure for the forward ANN-1

Functional links used in this model are expressed as follows:

$$\lambda_1 = eig\begin{bmatrix} k\_m & phi\_m \\ k\_f & phi\_f \end{bmatrix} \qquad \lambda_3 = eig\begin{bmatrix} A & A\_inner \\ f\_s & f\_s\_in \end{bmatrix}$$

$$\lambda_5 = eig\begin{bmatrix} A & A\_inner \\ k\_f & k\_f\_in \end{bmatrix} \qquad \lambda_7 = eig\begin{bmatrix} A & h \\ P & qinj \end{bmatrix}$$

Input and output components used in the training of this ANN model are summarized in Table 5.1. It was observed that implementations of logarithmic form for some of the input and all of the output parameters improve the network performance.

Table 5.1 Input and output layer components of Forward ANN-1

INPUT	**Reservoir Properties**	Thickness Matrix Porosity Fracture Porosity Matrix Permeability Fracture Permeability Fracture Spacing Initial Pressure Initial Oil Saturation Depth Initial Reservoir Temperature
	Cyclic Steam Injection Design Parameters	Steam Quality Steam Temperature Soaking Period Injection Period Steam Injection Rate Well Length Layer on Well Located
	Fractured Inner Zone Design Parameters	Inner Zone Fracture Porosity Inner Zone Fracture Permeability Inner Zone Fracture Spacing Major Axis of Inner Zone Minor Axis of Inner Zone Drainage Area
	Functional Links	λ_1 λ_3 λ_5 λ_7
OUTPUT	**Oil Flow Rate**	290 data points (29 values / each cycle)*10 cycles
	Cycle Number	Total number of cycle completed during project length

5.1.2 Forward ANN-2

Forward ANN-2 model was developed in order to predict three performance indicators that are total cumulative oil production at the end of project length, cumulative oil production and production period of each cycle for a given data set of reservoir properties and design parameters. A total of 555 datasets were used and 79 %, 14 %, 7 % of them were chosen randomly for training, validation and testing, respectively. Scaled conjugate gradient function *(trainscg)* was used in the output layer while tan-sigmoid activation function *(tansig)* was applied for hidden layer. The developed network includes a single hidden layer with 175 neurons. Input layer contains 27 neurons that are same with the input layer components of forward ANN-1. Output layer contains 21 neurons; 1 of them is project cumulative oil production, 10 of them are cumulative oil productions of every cycle, and 10 of them are production periods of each cycle. Figure 5.2 shows the network architecture.

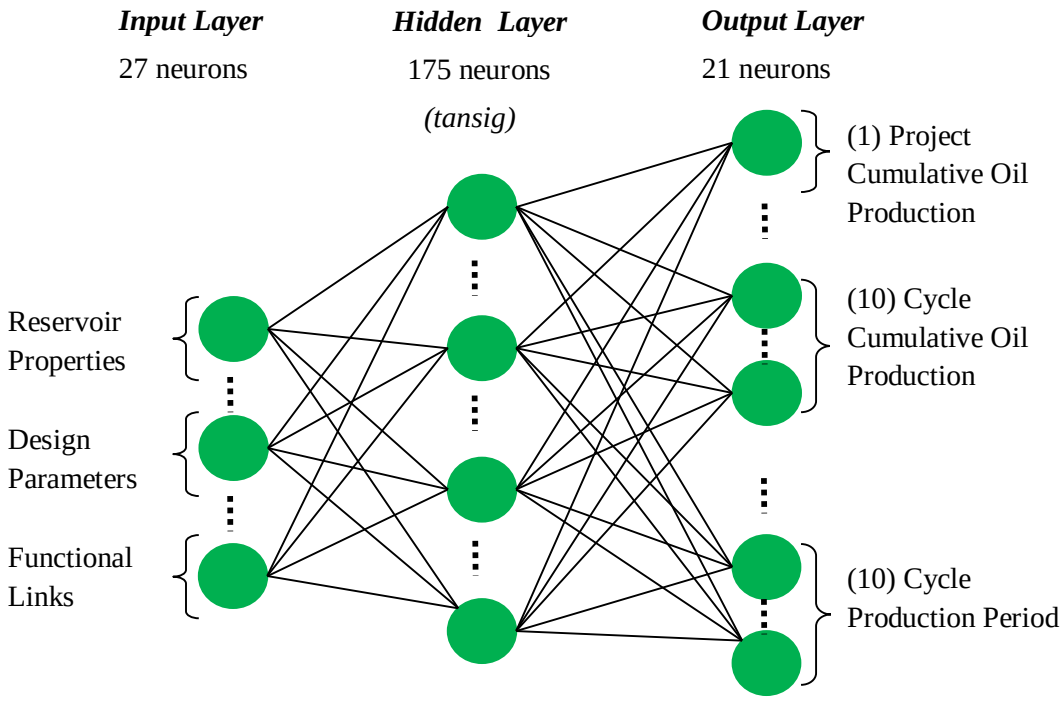

Figure 5.2 Network structure for the forward ANN-2

Table 5.2 summarizes components of input and output layers used in the training of forward ANN-2. It was observed that taking logarithm of all output components increased the accuracy of network by decreasing error percentage of the testing datasets.

Table 5.2 Input and output layer components of Forward ANN-2

INPUT	**Reservoir Properties**	Thickness Matrix Porosity Fracture Porosity Matrix Permeability Fracture Permeability Fracture Spacing Initial Pressure Initial Oil Saturation Depth Initial Reservoir Temperature
	Cyclic Steam Injection Design Parameters	Steam Quality Steam Temperature Soaking Period Injection Period Steam Injection Rate Well Length Layer on Well Located
	Fractured Inner Zone Design Parameters	Inner Zone Fracture Porosity Inner Zone Fracture Permeability Inner Zone Fracture Spacing Major Axis of Inner Zone Minor Axis of Inner Zone Drainage Area
	Functional Links	λ_1 λ_3 λ_5 λ_7
OUTPUT	**Project Cumulative Oil Production**	(1) Cumulative oil production at the end of project
	Cycle Cumulative Oil Production	(10) Cumulative oil production at the end of each cycle (1 value / each cycle)*10 cycles
	Cycle Production Period	(10) Duration of each cycle production period (1 value / each cycle)*10 cycles

Even if two distinct ANN models are developed for forward problem, prediction performance of them is evaluated together. A number of 41 testing data sets is used to compare the results of networks with the actual values in order to qualify the accuracy of structured ANN models. 7 of the testing data sets *(Data-6, Data-9, Data-12, Data-16, Data-20, Data-23, and Data-39)* which represent all possible results are chosen in order to discuss the accuracy of predictions. The results of all performance indicators which are number of cycle, oil flow rates, cumulative oil productions and production periods of each cycle, project cumulative oil production are shown for same seven data sets in order to provide integrity of the forward problem.

Following seven figures (Figure 5.3, Figure 5.4, Figure 5.5, Figure 5.6, Figure 5.7, Figure 5.8, and Figure 5.9) show the comparative results of production period length of each 10 cycles based on the output of numerical simulator and prediction of network. Each cycle is terminated by an abandonment rate and time to reach this rate determines the length of production period. Thus, duration of the production period varies by cycle to cycle for each case. However, it can be generalized that length of the first cycle's production period is usually longer than following cycles as it is clearly seen from following figures. It can be explained by the amount of oil in place that reduces during the cyclic steam injection process. Since, the peak rate of the first cycle is usually higher than the next cycles as it is expected, it requires longer time to produce until reaching the specified abandonment rate of 20 bbl/day. However, it is possible to see different cases such as data-23 that is shown in the Figure 5.8. In this case, production periods of the first and the second cycle are close to each other. Reservoir properties, design parameters and the amount of heat that left behind the previous cycle can be considered as a reason of this situation.

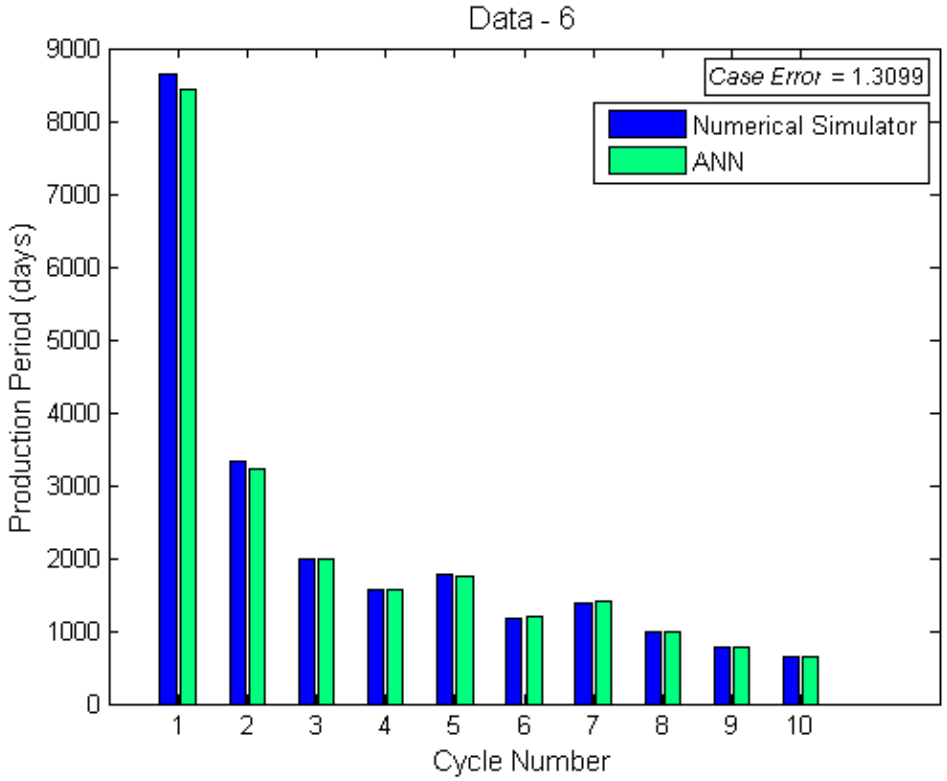

Figure 5.3 Prediction of production period for Data-6

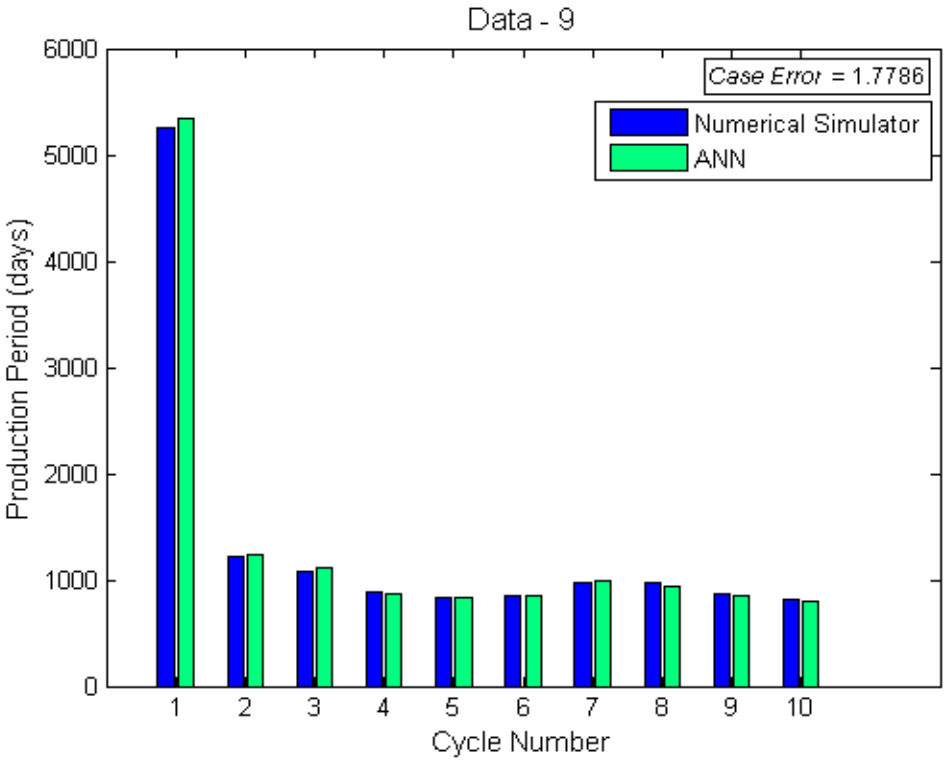

Figure 5.4 Prediction of production period for Data-9

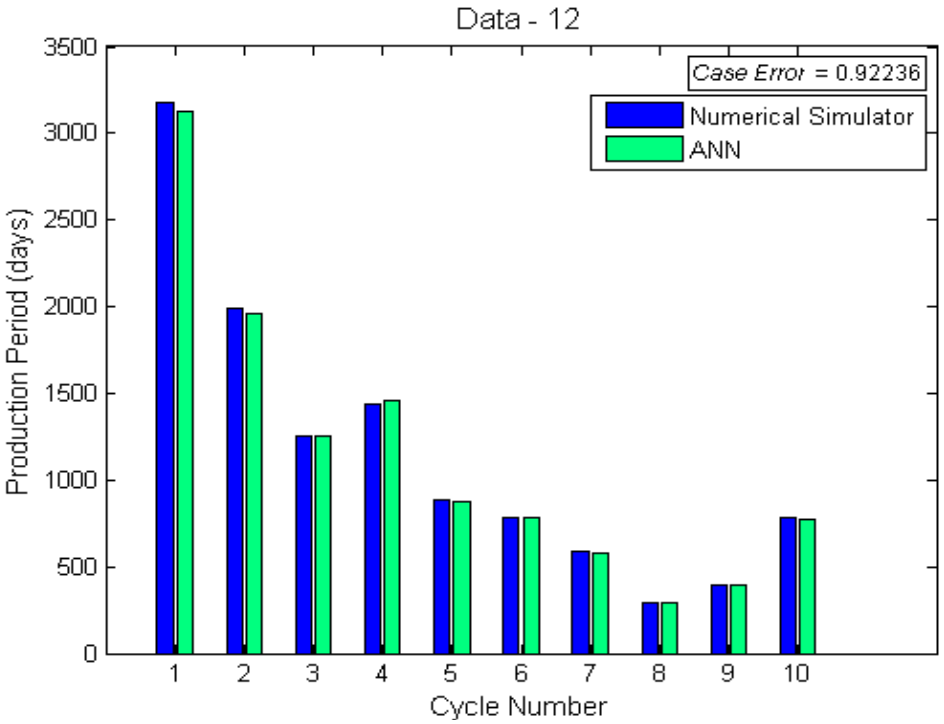

Figure 5.5 Prediction of production period for Data-12

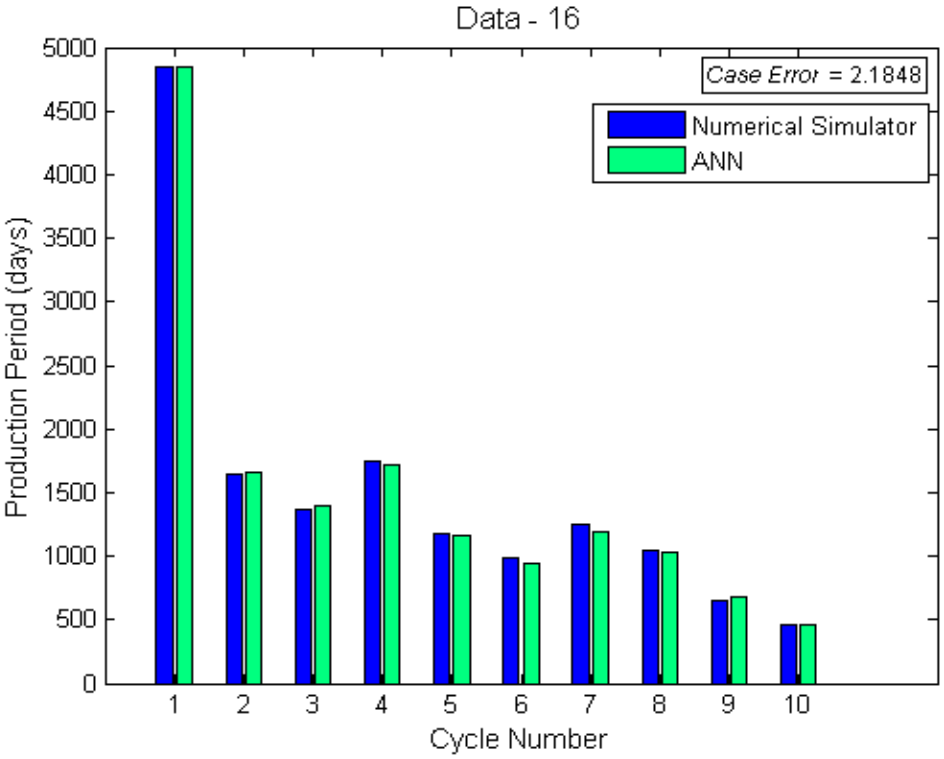

Figure 5.6 Prediction of production period for Data-16

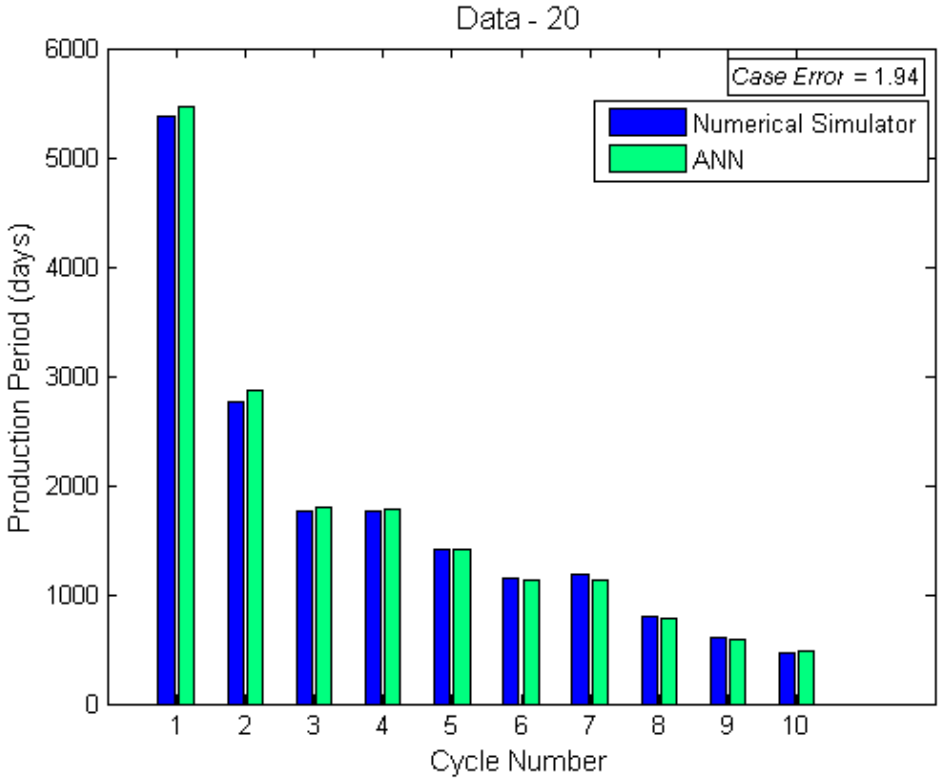

Figure 5.7 Prediction of production period for Data-20

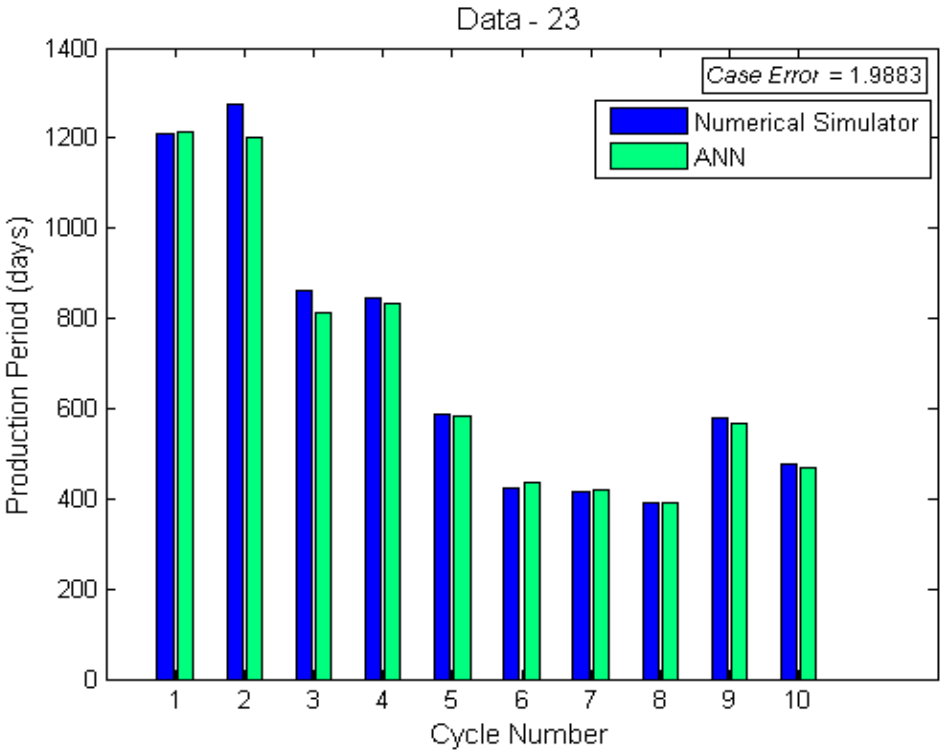

Figure 5.8 Prediction of production period for Data-23

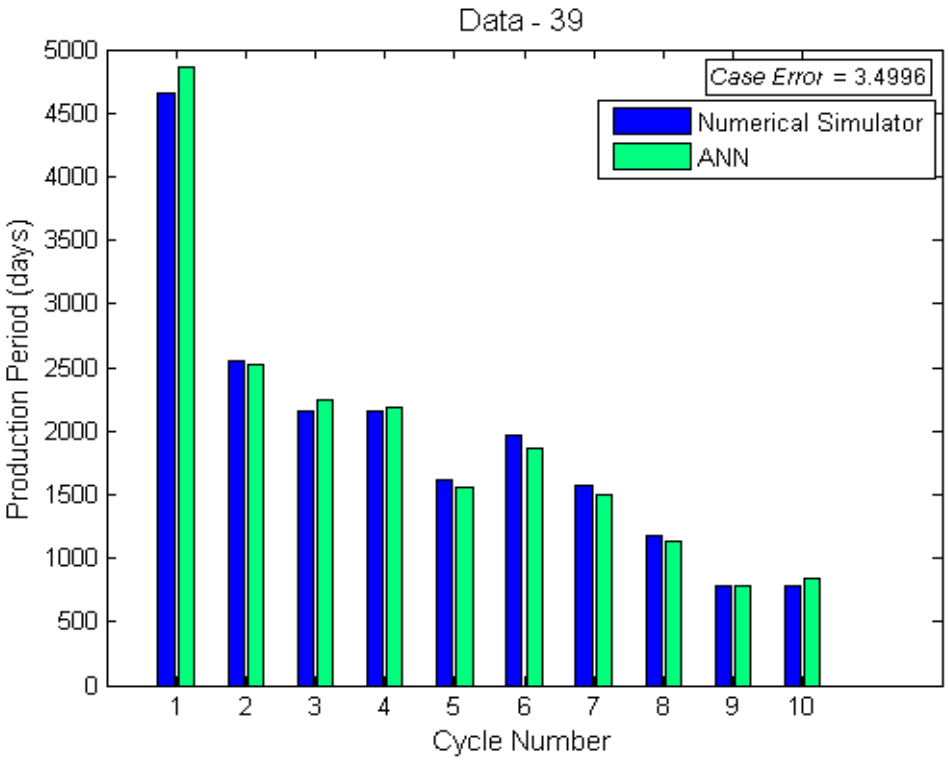

Figure 5.9 Prediction of production period for Data-39

The desired tolerance is specified as 5 % for forward problem and data sets that have error percentage value less than 5 % can be considered as good predictions. The error values shown on the graphs represent the average error percentages of 10 cycles. Difference on the actual production period length and network prediction value is relatively higher on the early cycles of the project. For instance, the maximum error percentage is observed on the second cycle of data-23 illustrated in Figure 5.8. The network predicts the production period as 1200 days whereas the actual value is equal to 1271 days so error percentage of this cycle is calculated as 5.6 %. However, accurate predictions observed on the other cycles of this case. Hence, average error of this case is equal to 1.9883 %. Average error distribution of 41 testing data sets is shown in Figure 5.10.

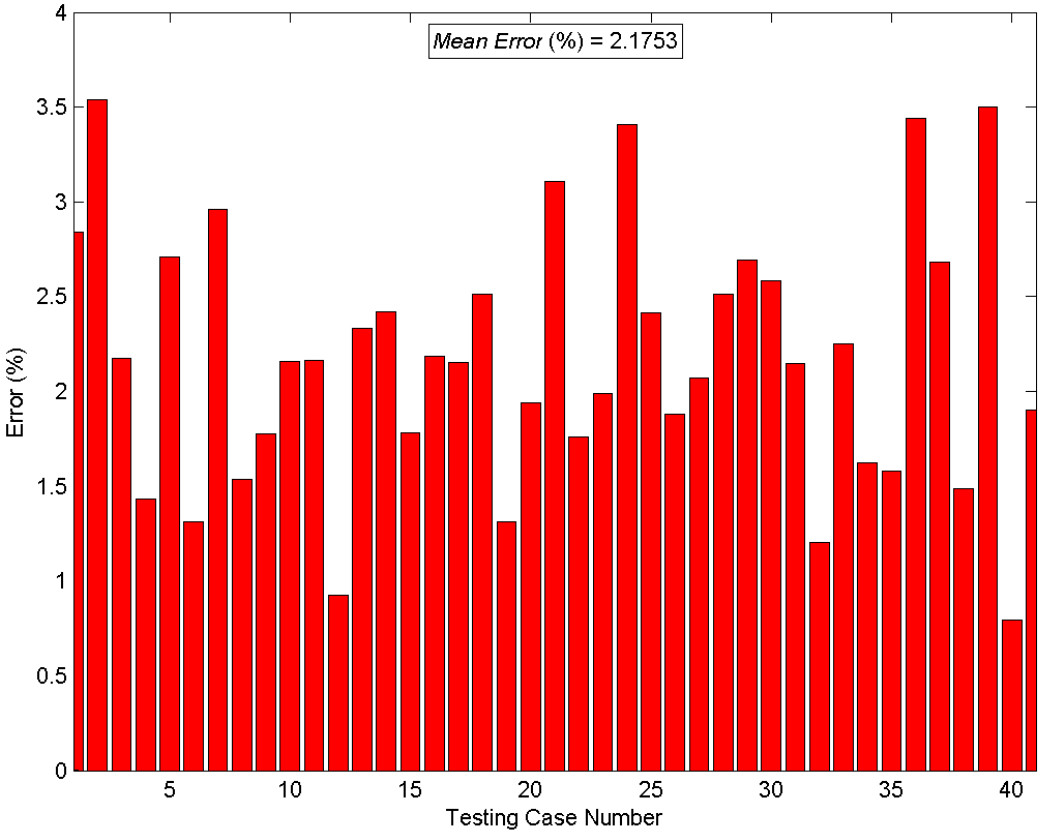

Figure 5.10 Error distribution of production period prediction for testing data sets

It is seen in Figure 5.10 that all testing data sets have error values that are less than desired tolerance. The highest average error of 3.4996 % observed in the data-39. Mean error of all testing cases are equal to 2.1753 % as shown on the top of error distribution graph.

High level of accuracy on production period prediction is also important for evaluation of oil flow rates and cumulative oil production results. Times corresponding to 29 data points of oil flow rate are calculated from the predicted duration of each cycle. Both cumulative oil production and oil flow rate comparison graphs are plotted as a function of these calculated times.

Following seven figures from Figure 5.11 to Figure 5.17 represent the comparative results of oil flow rate of each 10 cycles based on the simulator output and network prediction. Oil flow rates follow a typical declining curve and become zero during soaking and injection period of cyclic steam injection process. Oil flow rate at the end of cycles are same and equal to termination rate of 20 bbl/day. Reservoir properties and design parameters cause data sets to have different peak rates. It is observed that peak rates of early cycles are usually higher than following cycles due to the fact that amount of oil in place decreases during process. However, it is possible to see different cases, for example; peak rate of third cycle is higher than the second cycle in data-9 and data-39 shown in Figure 5.12 and Figure 5.17, respectively. It can be explained by the heat accumulation in the previous cycle. In the second cycles of these cases, abandonment oil flow rate could be reached before consumption of injected heat. Thus, remaining heat provides higher peak rate in the third (next) cycle.

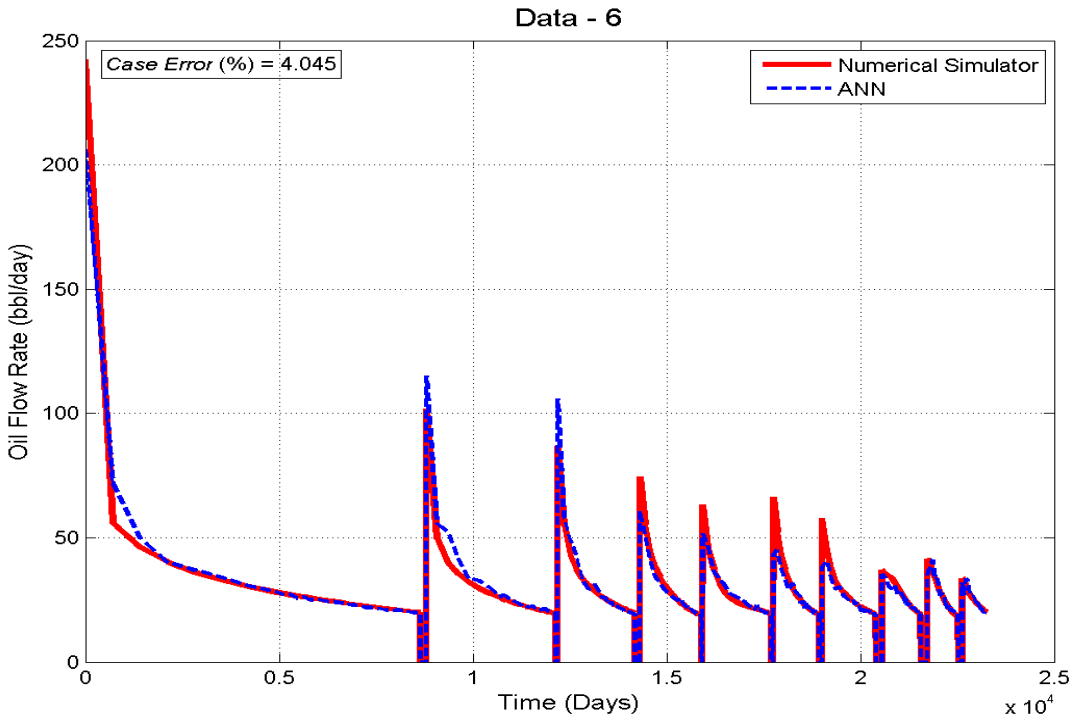

Figure 5.11 Prediction of oil flow rate for Data-6

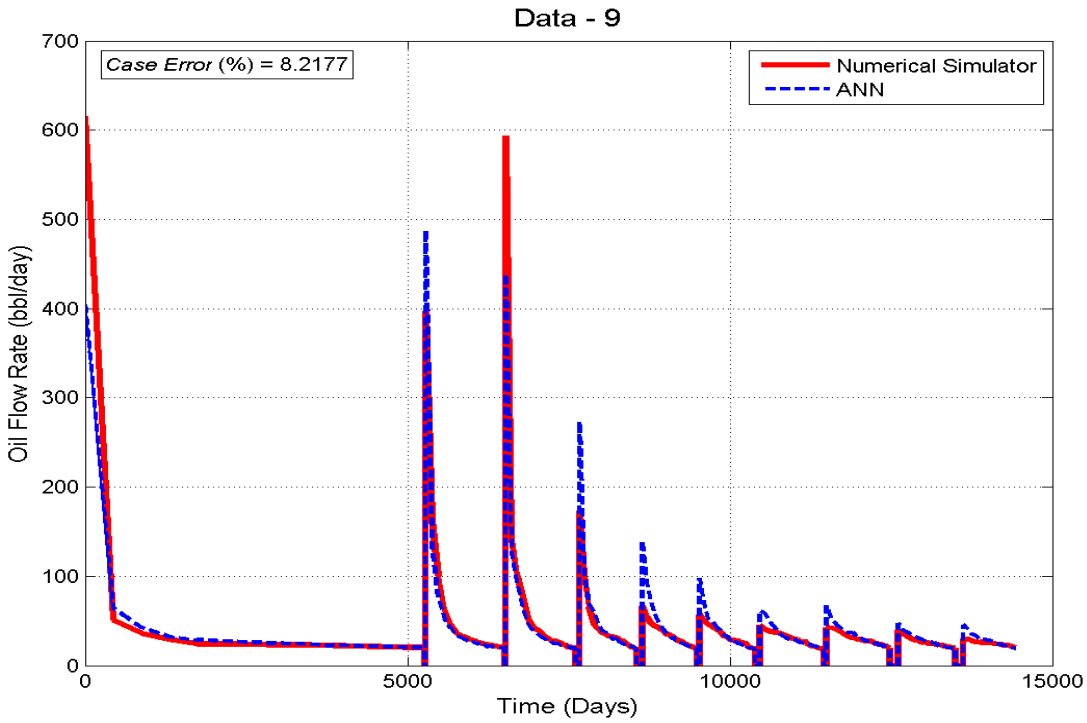

Figure 5.12 Prediction of oil flow rate for Data-9

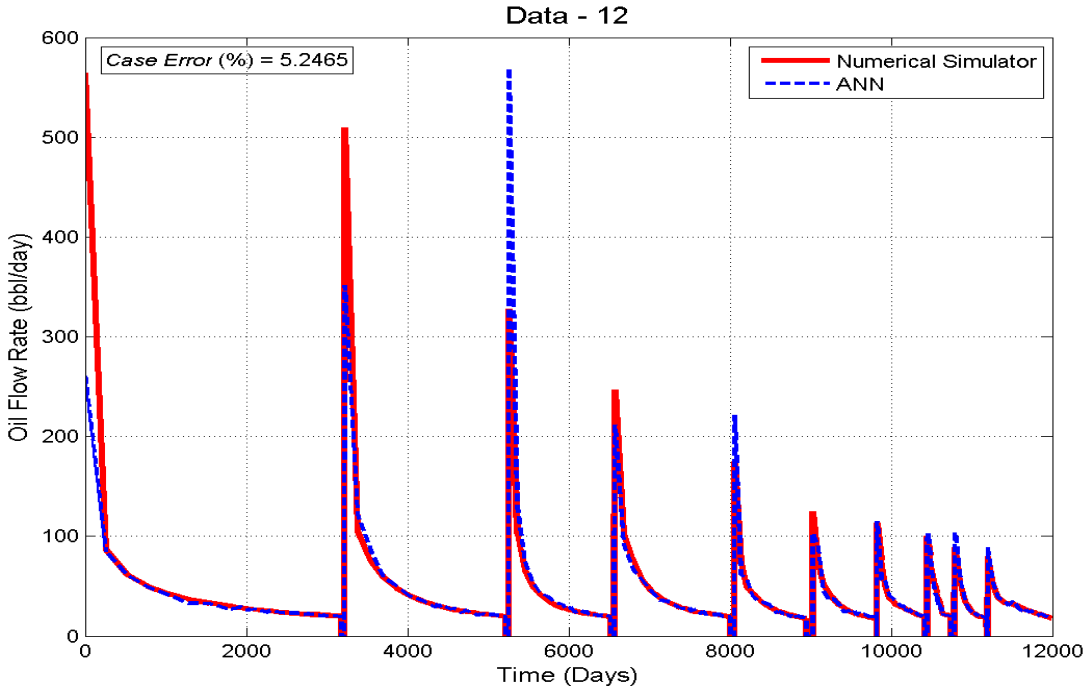

Figure 5.13 Prediction of oil flow rate for Data-12

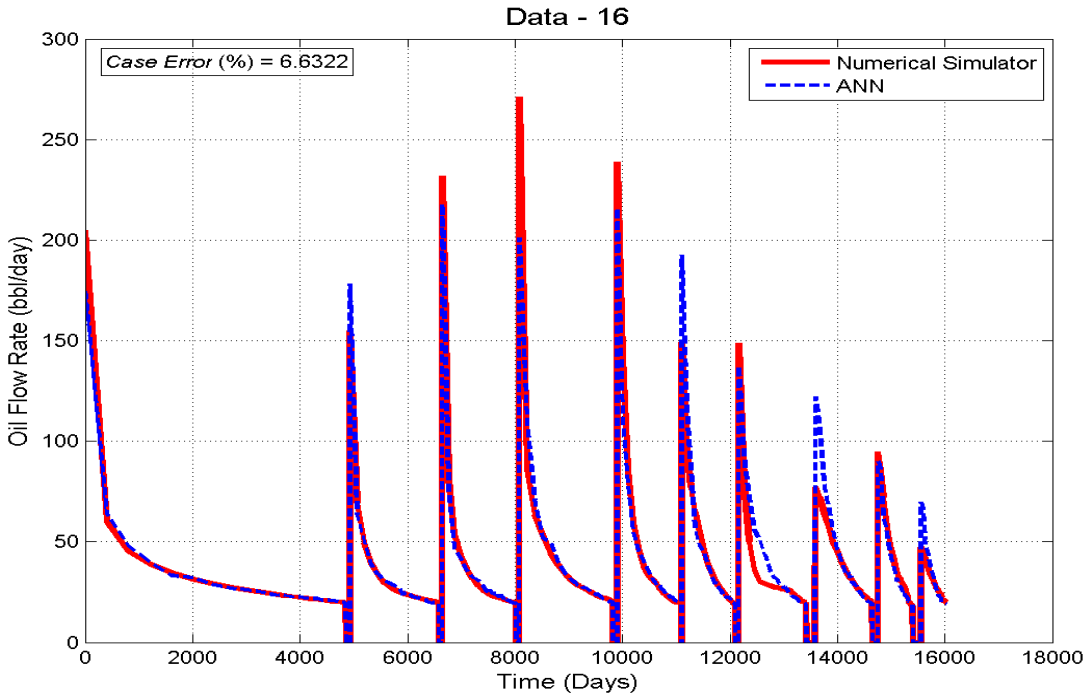

Figure 5.14 Prediction of oil flow rate for Data-16

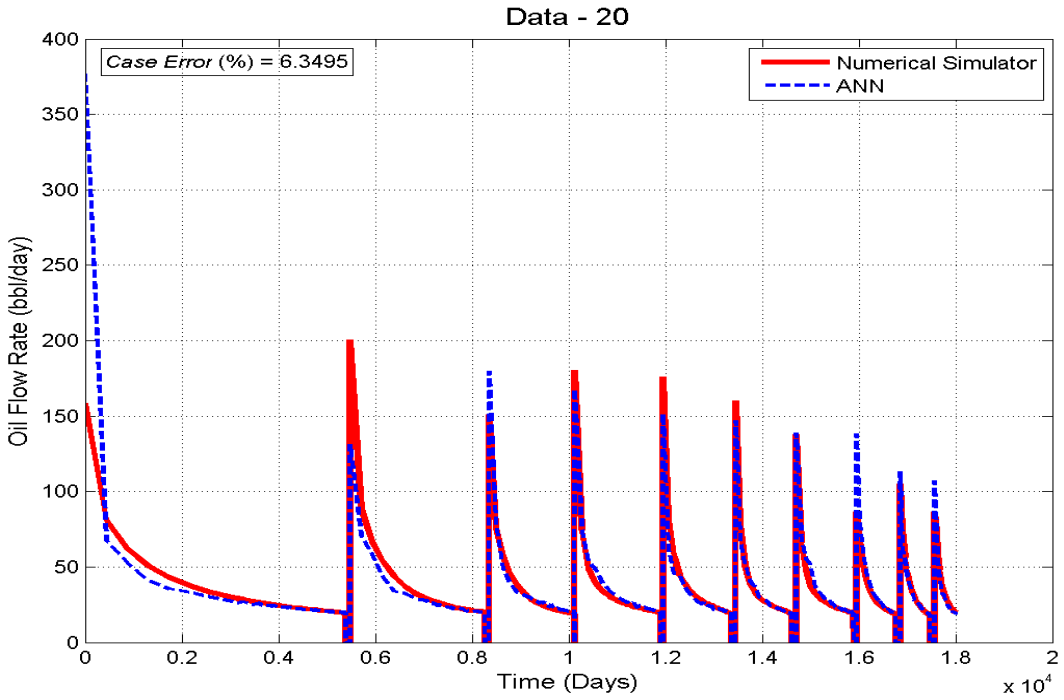

Figure 5.15 Prediction of oil flow rate for Data-20

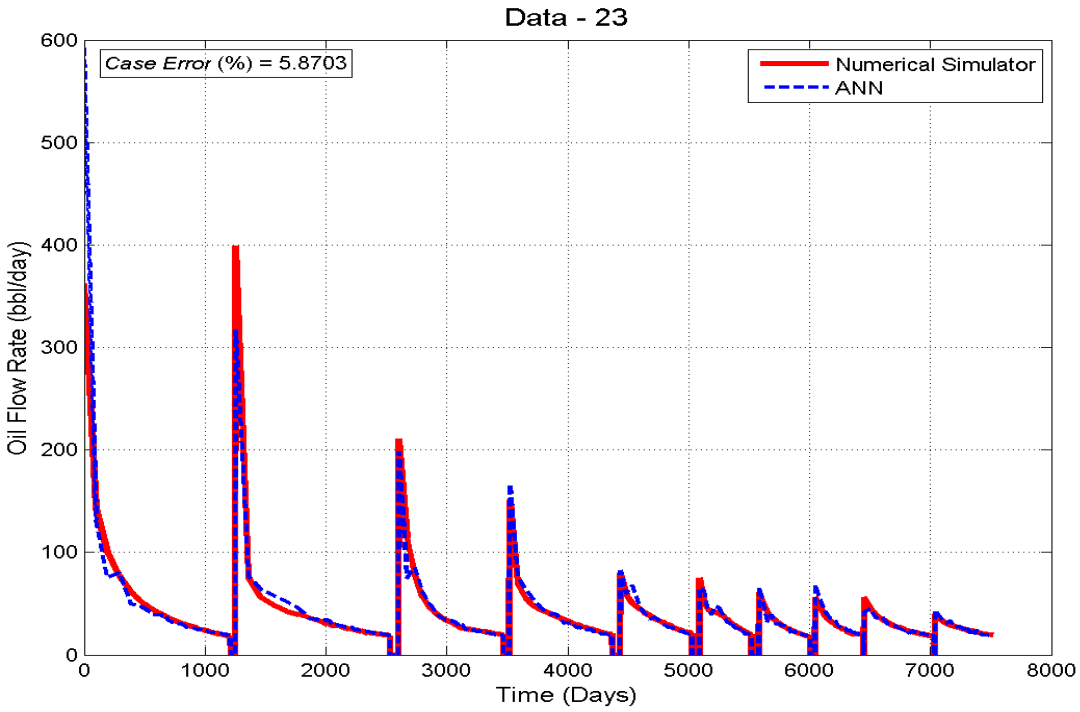

Figure 5.16 Prediction of oil flow rate for Data-23

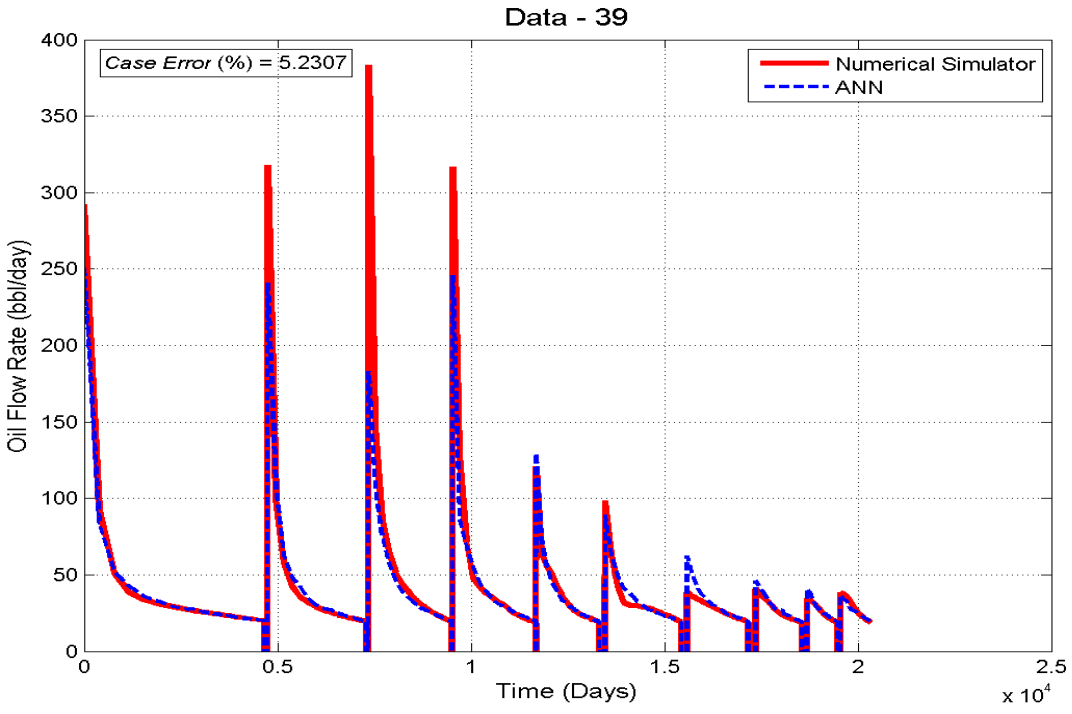

Figure 5.17 Prediction of oil flow rate for Data-39

The desired tolerance is specified as 10 % for oil rate prediction of the forward problem and data sets that have error percentage values less than 10 % can be considered as predicted accurately. The error values shown on the top of the oil rate graphs represent the average error percentage of 290 data points for 10 cycles. Difference on the actual oil flow rate and network prediction value is relatively higher on the peak rates of first a few cycles. After that, the network begins to catch up the cyclic steam injection trend and provides more accurate estimation even in the peak rates of late time cycles. Although some cases have higher errors on peak rates than desired tolerance, average errors of all data points (290 oil rate/case) are below 10 %. Thus, these kinds of cases can be accepted as having reasonable prediction. Average error distribution of oil flow rates for 41 testing data sets is shown in Figure 5.18.

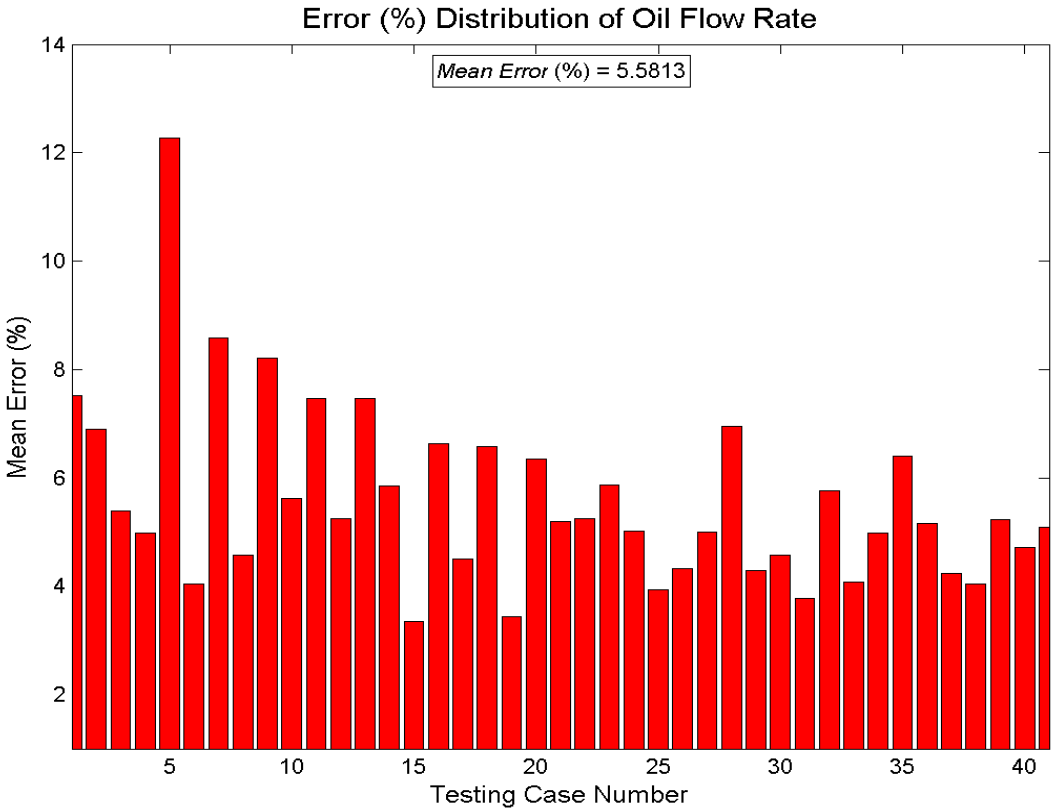

Figure 5.18 Error distribution of oil flow rate prediction for testing data sets

It is seen in Figure 5.18 that most of the testing data sets have error values less than 8 %. Only one case exceeds the desired tolerance having error percentage of 12 %. Mean error of all testing cases are equal to 5.5813 % as it is seen on error distribution graph.

High level of accuracy on estimation of oil flow rate is also significant to examine the consistency of two distinct forward ANN networks. Oil flow rate prediction of the forward ANN-1 and production period prediction of forward ANN-2 are used to calculate cumulative oil production by trapezoidal method. Comparison of cumulative oil productions, obtained from the numerical simulator, forward ANN-2 network (ANN), and trapezoidal calculation (TRAPZ) are shown from Figure 5.19 through Figure 5.25.

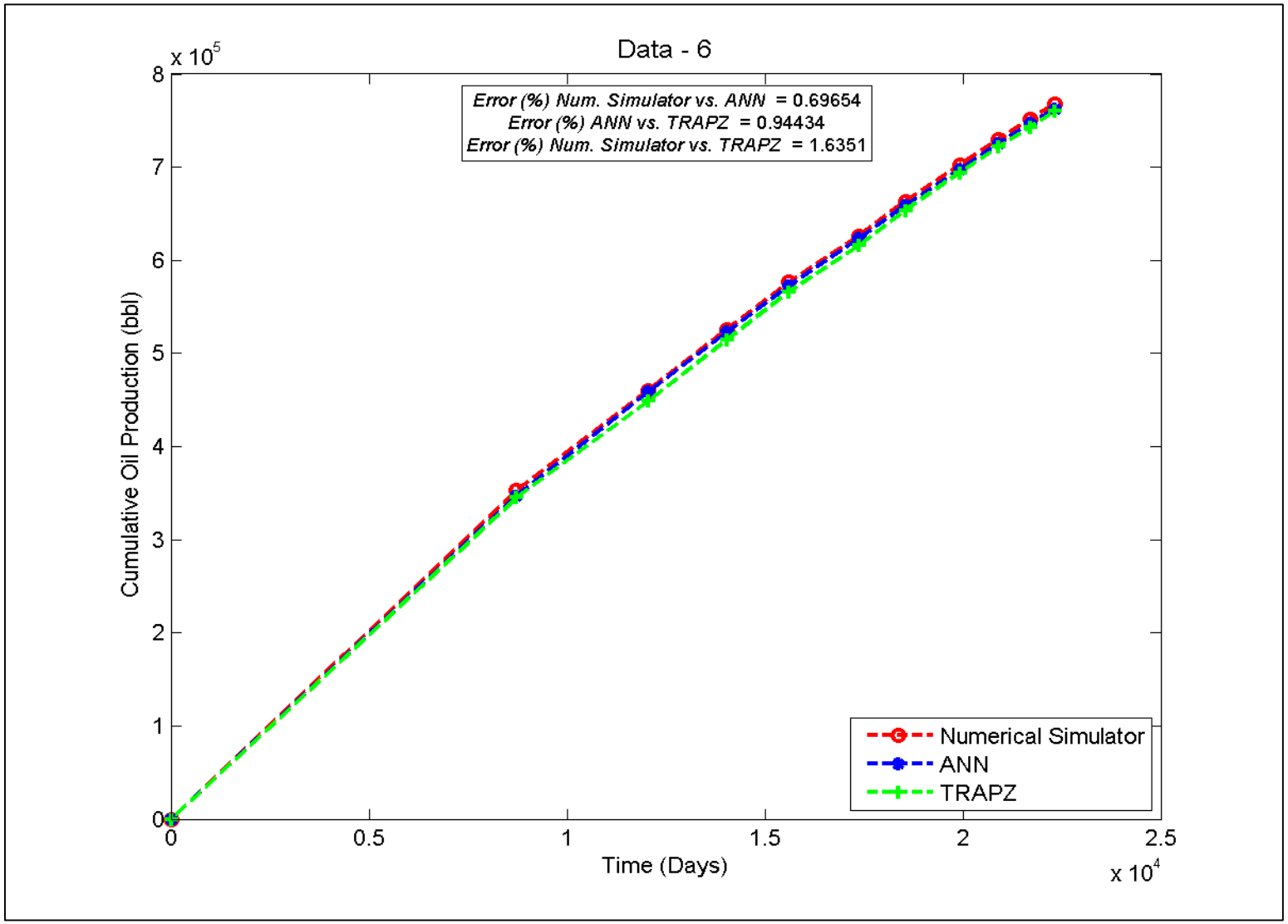

Figure 5.19 Prediction of cumulative oil production for Data-6

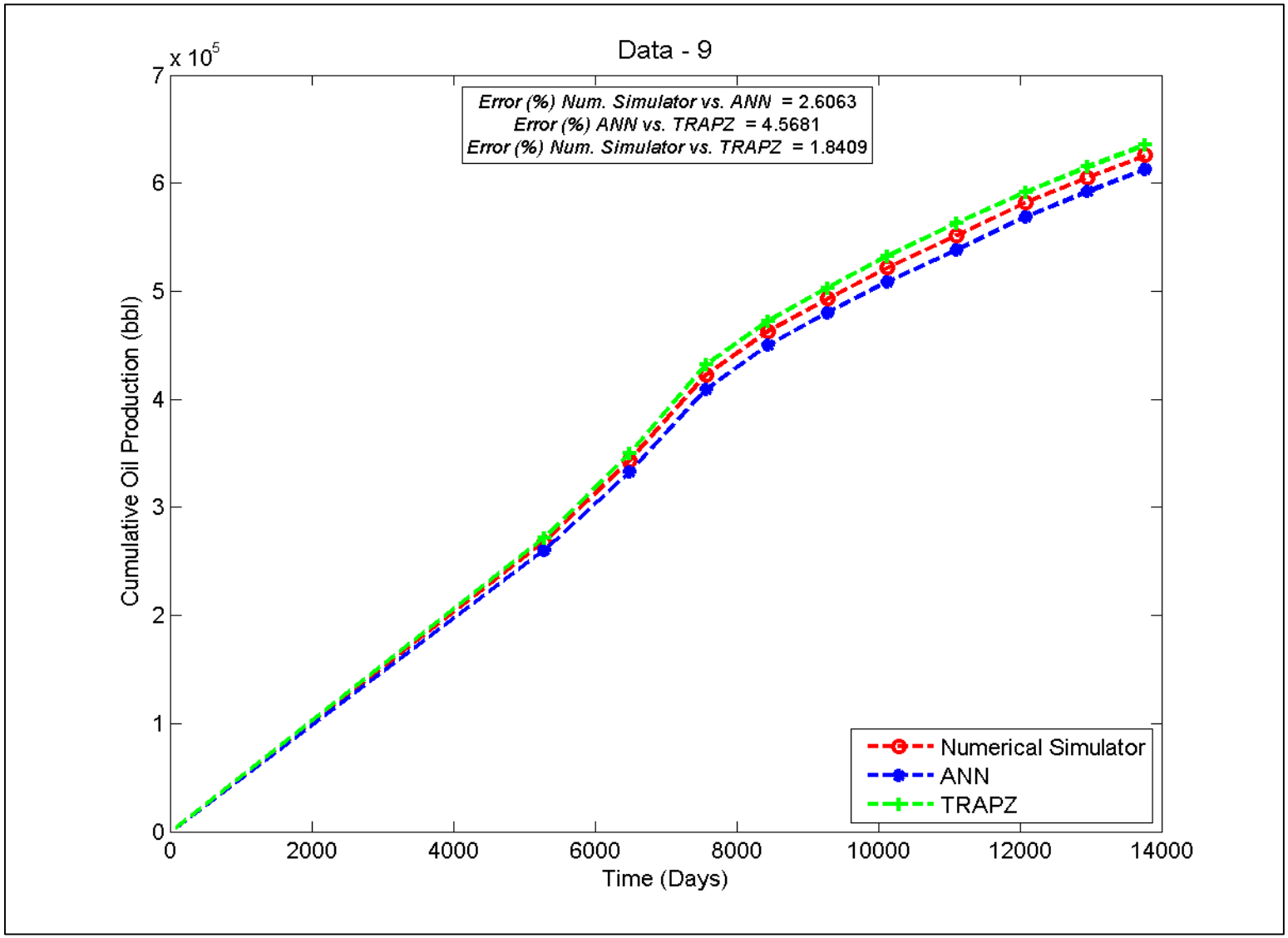

Figure 5.20 Prediction of cumulative oil production for Data-9

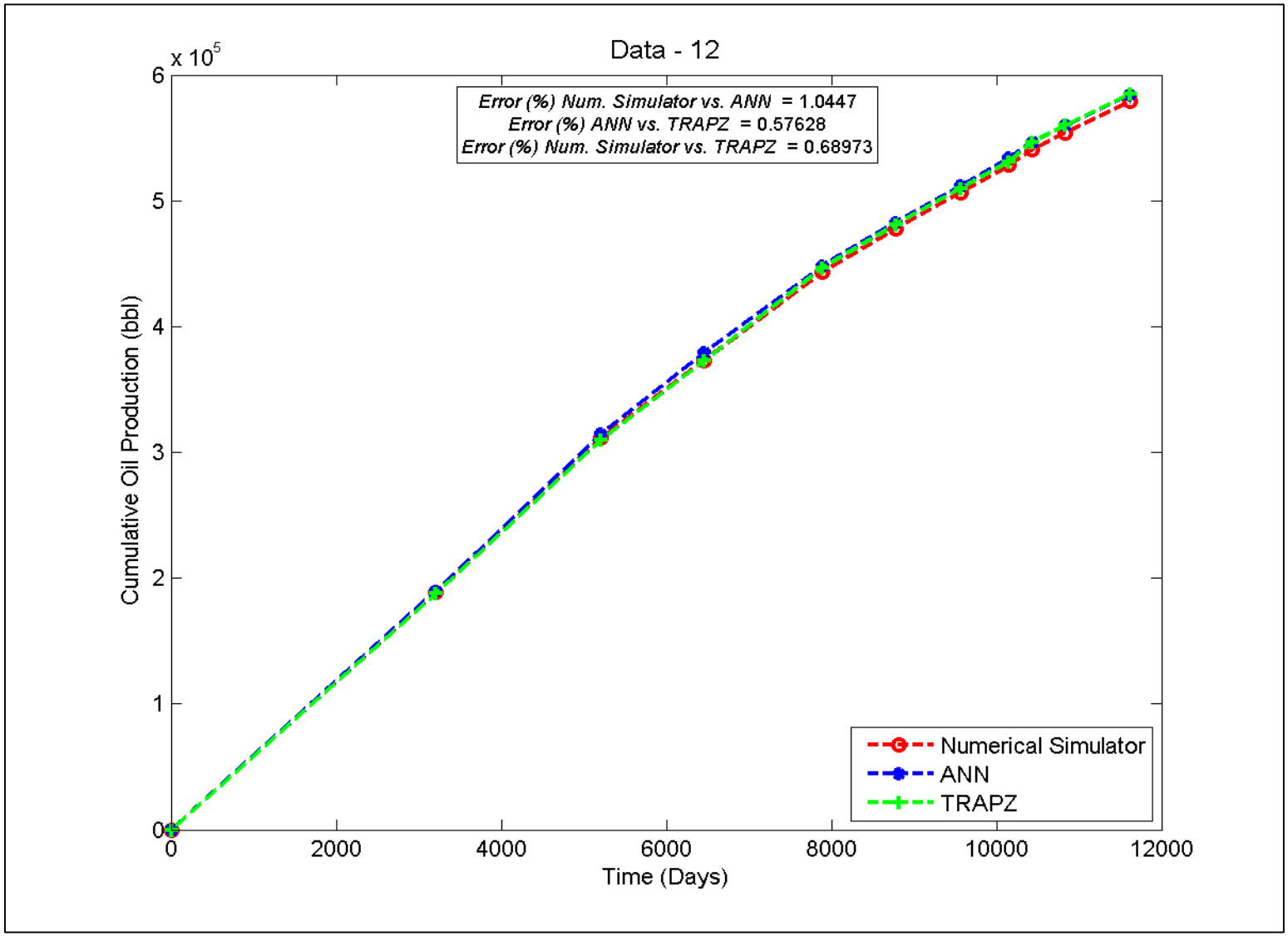

Figure 5.21 Prediction of cumulative oil production for Data-12

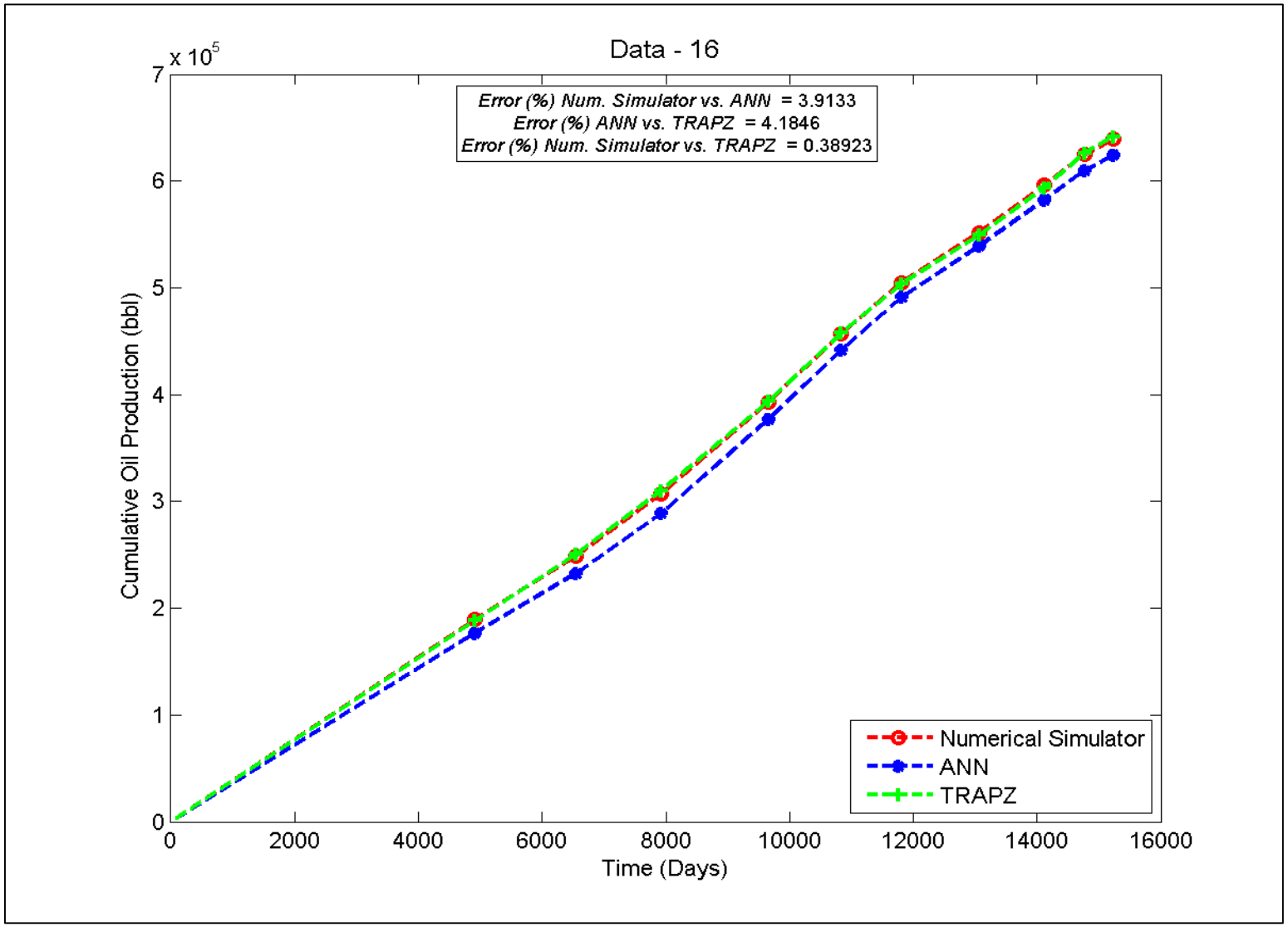

Figure 5.22 Prediction of cumulative oil production for Data-16

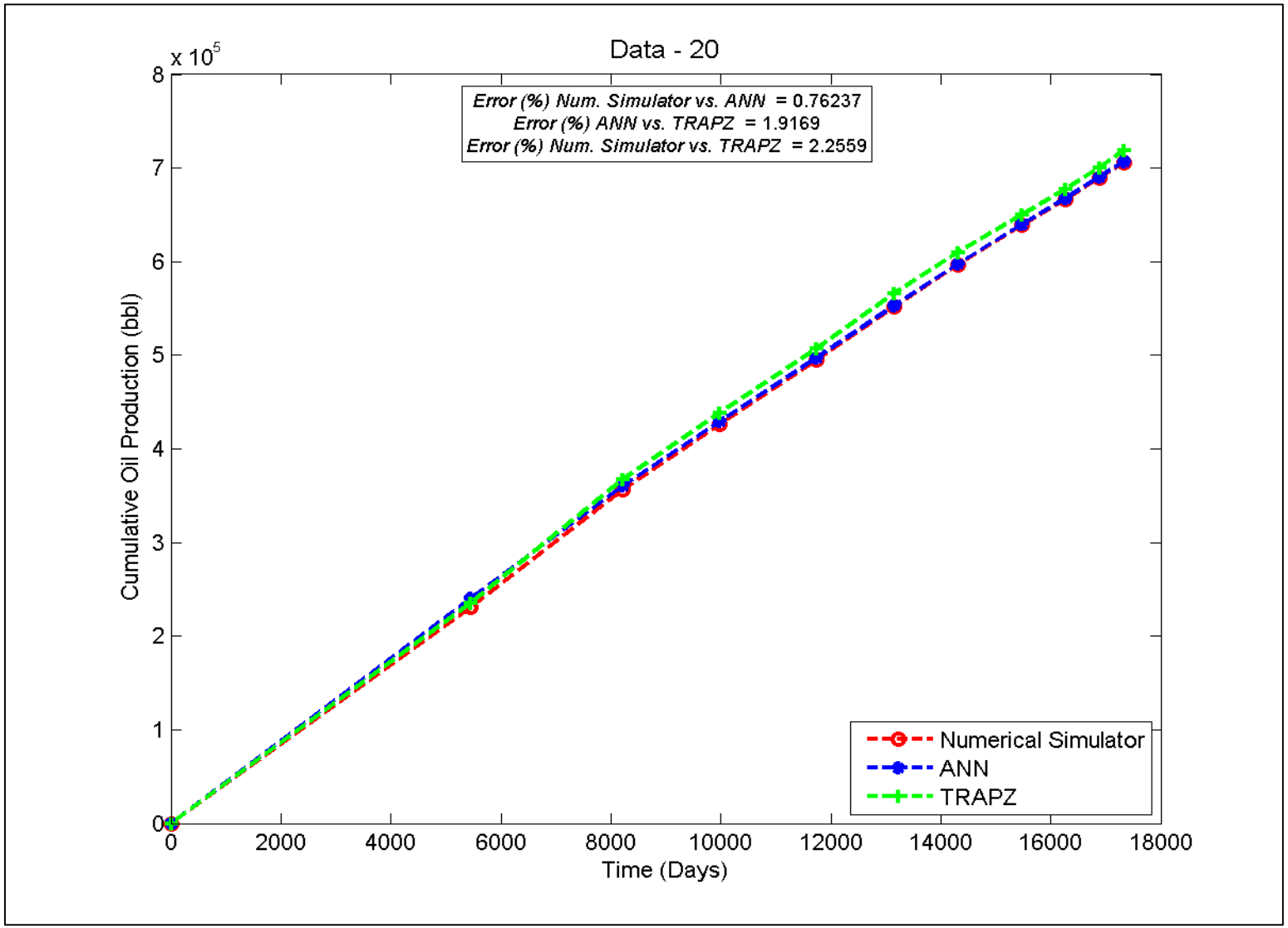

Figure 5.23 Prediction of cumulative oil production for Data-20

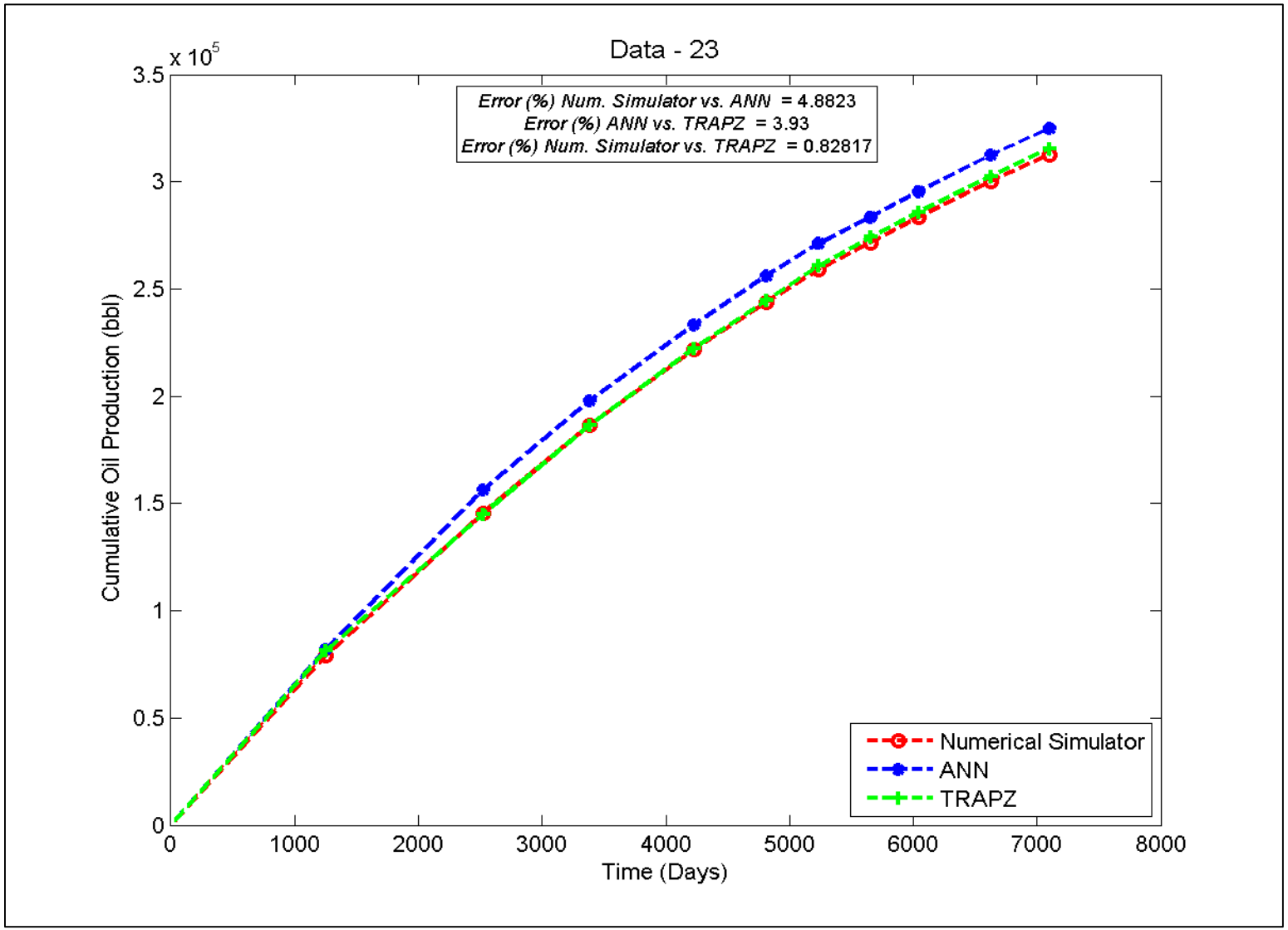

Figure 5.24 Prediction of cumulative oil production for Data-23

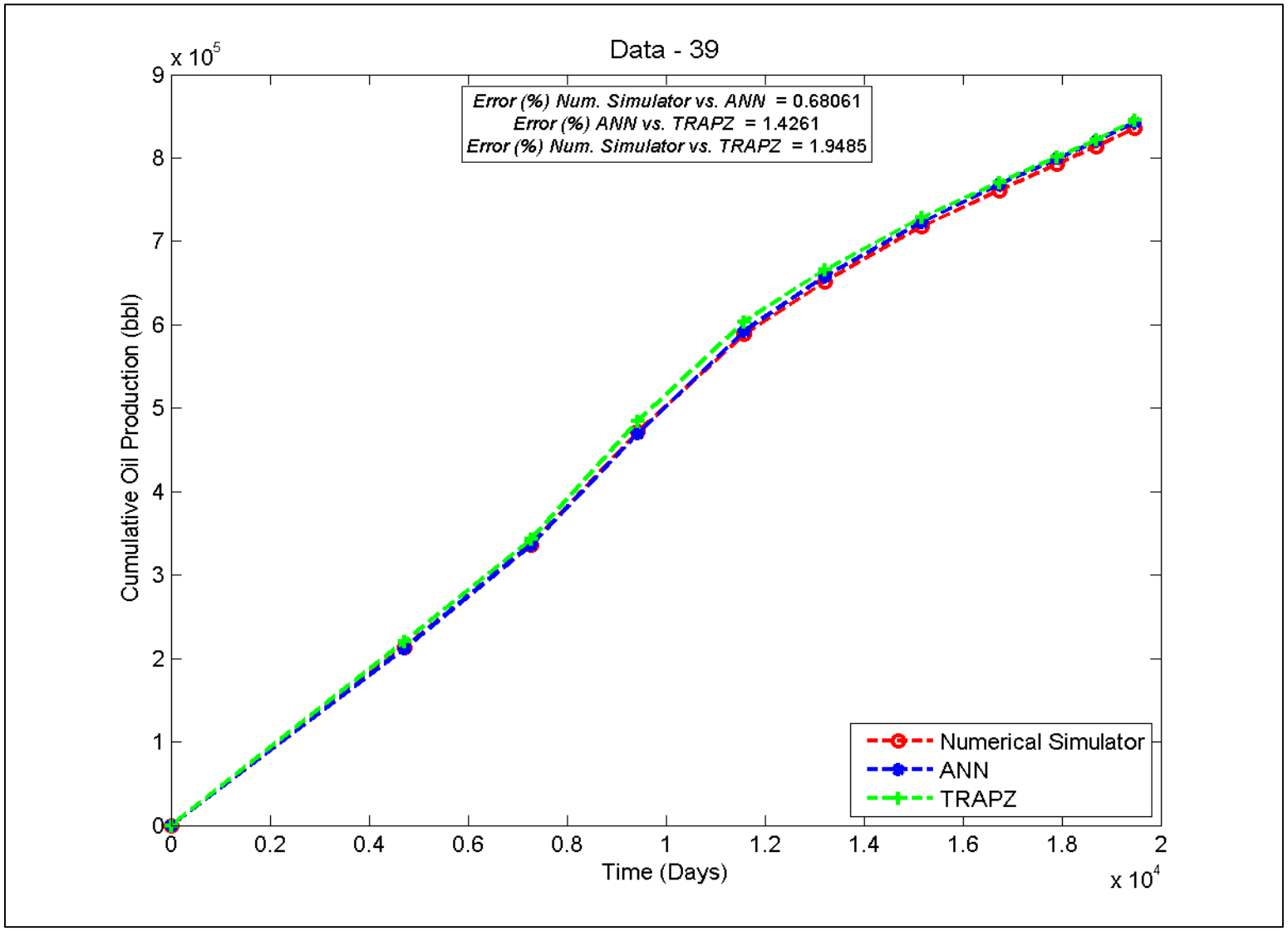

Figure 5.25 Prediction of cumulative oil production for Data-39

The prediction of cumulative oil production is accepted reasonable if its error percentage is lower than desired tolerance of 5 % likewise, production period. Three error values are shown on the top of cumulative oil production graphs. First one represents the error calculated from the difference between the simulator result and network prediction *(Num. Simulator vs. ANN).* Second error value compares the network result with the calculated cumulative oil production *(ANN vs. TRAPZ)*. Third error percentage value that belongs to comparison of simulator result and calculated cumulative oil production (*Num. Simulator vs. TRAPZ*) provides an opportunity to check the accuracy of developed networks. As it is clearly seen from the figures that neural network models present high accuracy with the error percentage values less than tolerance. Although three cumulative oil production plots show good-fitting, in most cases, calculated cumulative oil productions are more close to actual results than the predictions of network (forward -ANN-2). Because it is calculated from the production period prediction of forward-ANN-1 and oil rate prediction of forward-ANN-2. In some cases, while production period is slightly under-predicted, oil rate of same case might be slightly over-predicted. Therefore, positive and negative errors neutralize each other and calculated cumulative oil productions approach to actual results. Hence, there is no disadvantage to develop two distinct neural network models.

The average error distributions of cumulative oil production for 41 testing data sets can be seen in Figure 5.26. Most of the testing data sets have error values less than 4 %. Three of them are around 5 % that is specified as upper limit of the error percentage. Mean error of all testing cases are equal to 2.5579 % as it is seen on the top-right of error distribution graph. This figure summarizes that forward-ANN-2 tool is able to predict cumulative oil production of each cycle accurately.

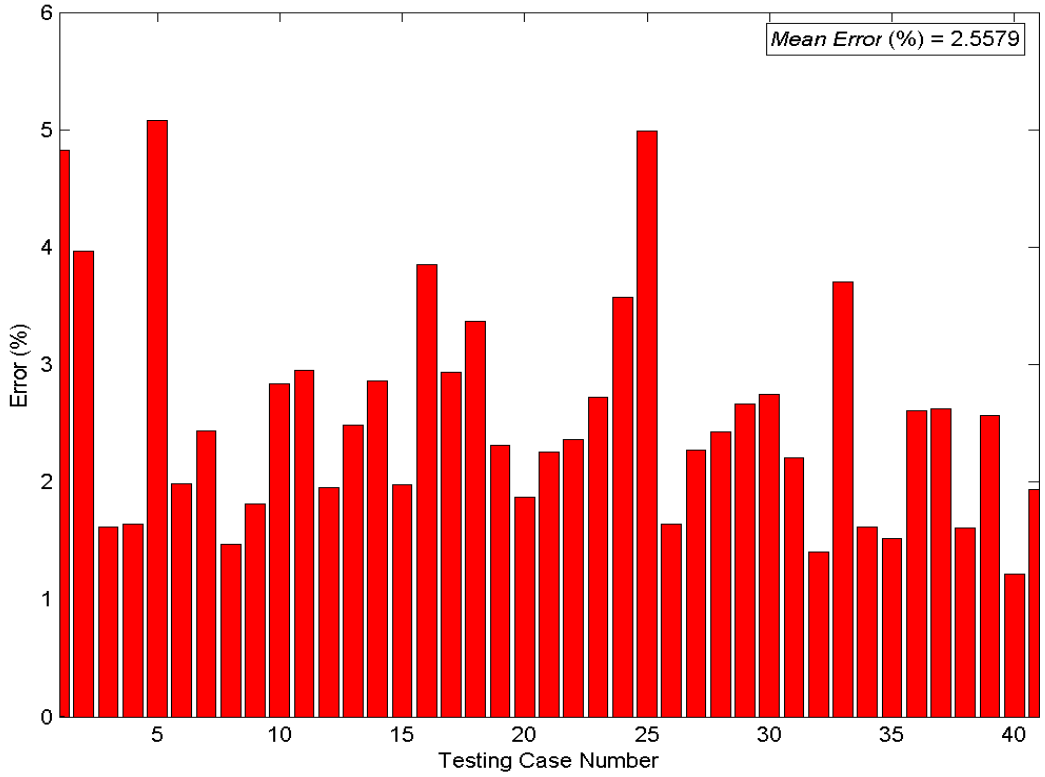

Figure 5.26 Error distribution cumulative oil production prediction for testing data sets

In this study, a variable number of cycles is applied and the first 10 cycles of each data set are evaluated to predict the behavior of reservoirs regardless of cycle numbers as it is explained in the Chapter 4.3. Therefore, cumulative oil production at the end of 10 cycles could be calculated but if data set has more cycles than 10 it would not be possible to estimate total oil production. For this reason, cumulative oil production at the end of project is added to network separately as an extra data point for each case. For example, if data set has 15 cycles, project cumulative oil production represents the total oil production amounts at the end of last cycle that is the 15^{th} cycle. Figure 5.27 shows the comparison of network predictions with the actual project cumulative oil production amounts for 41 testing data sets.

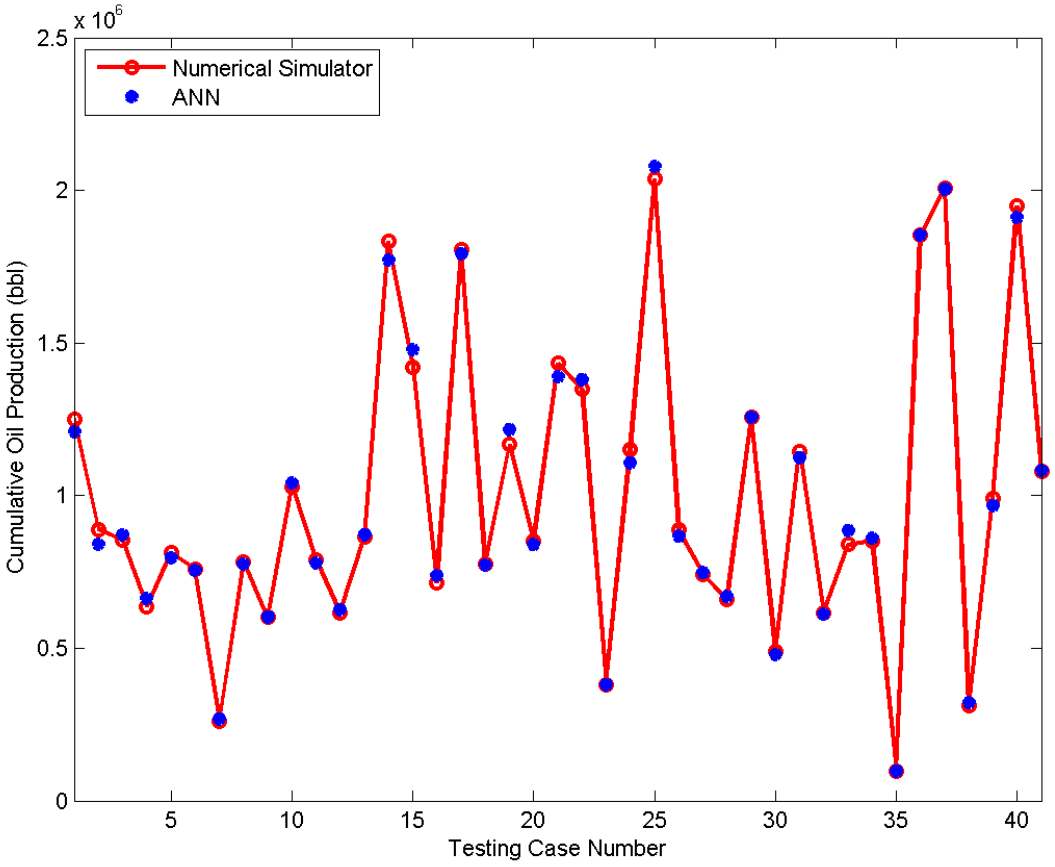

Figure 5.27 Prediction of cumulative oil production at the end of project for testing data sets

The desired tolerance of project cumulative oil production is specified as 5%. Actual value and the prediction of network are very close in many cases, as it is clearly seen in Figure 5.27. Error distribution graph of this performance indicator also supports the ability of network to predict with the errors less than 5%. Mean error of all testing cases is equal to 1.9635% as it is seen on the top of Figure 5.28.

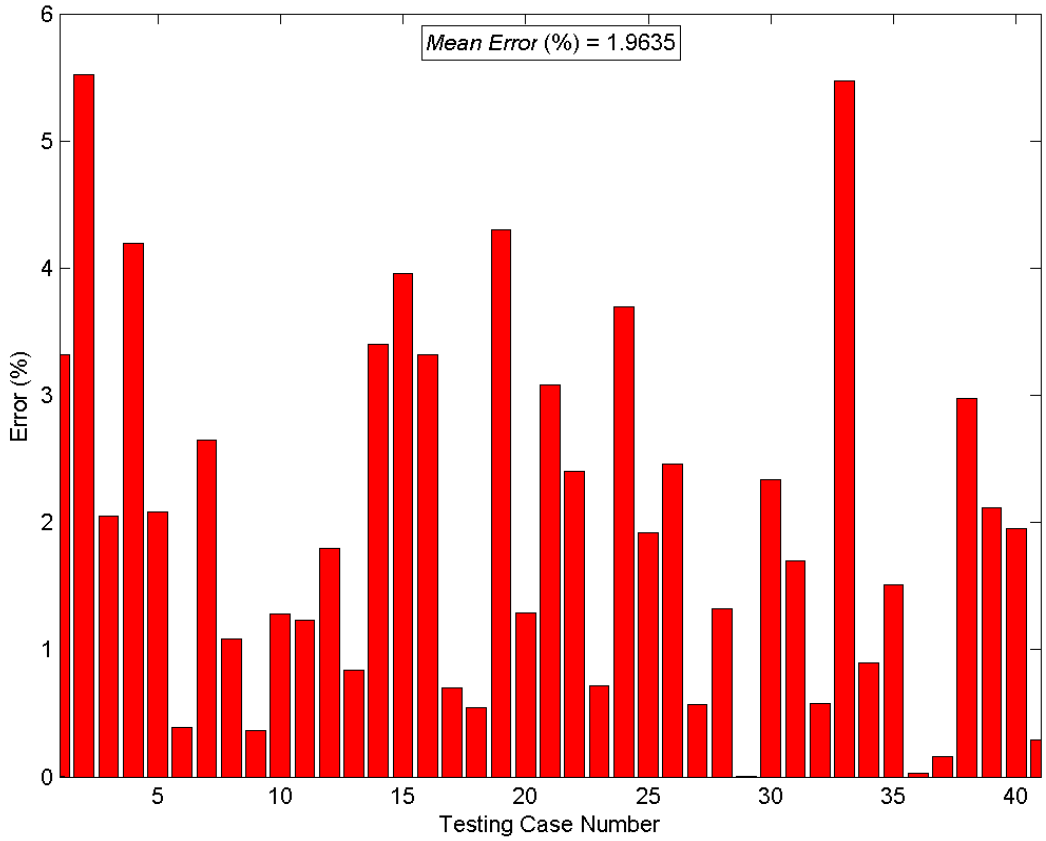

Figure 5.28 Error distribution of cumulative oil production at the end of project for testing data sets

The last one of 5 performance indicators is the number of cycles, which is predicted by forward-ANN-1. Numbers of cycles results of simulator are compared with the network predictions in the bar chart (Figure 5.29). Even if the cycle number differences can be seen clearly in this figure, results of all testing cases are going to be summarized in the histogram chart (Figure 5.30).

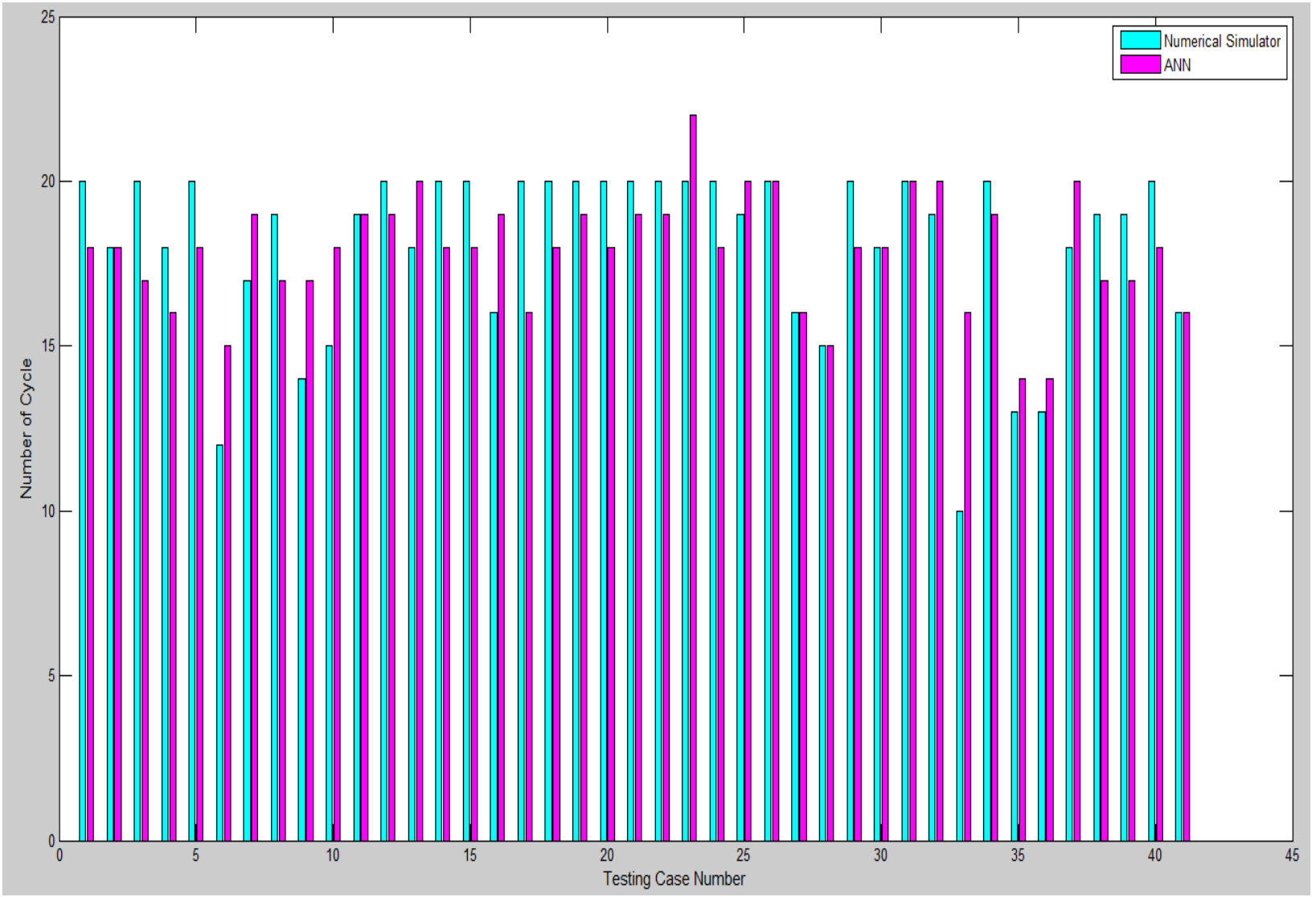

Figure 5.29 Prediction of number of cycles for testing data set

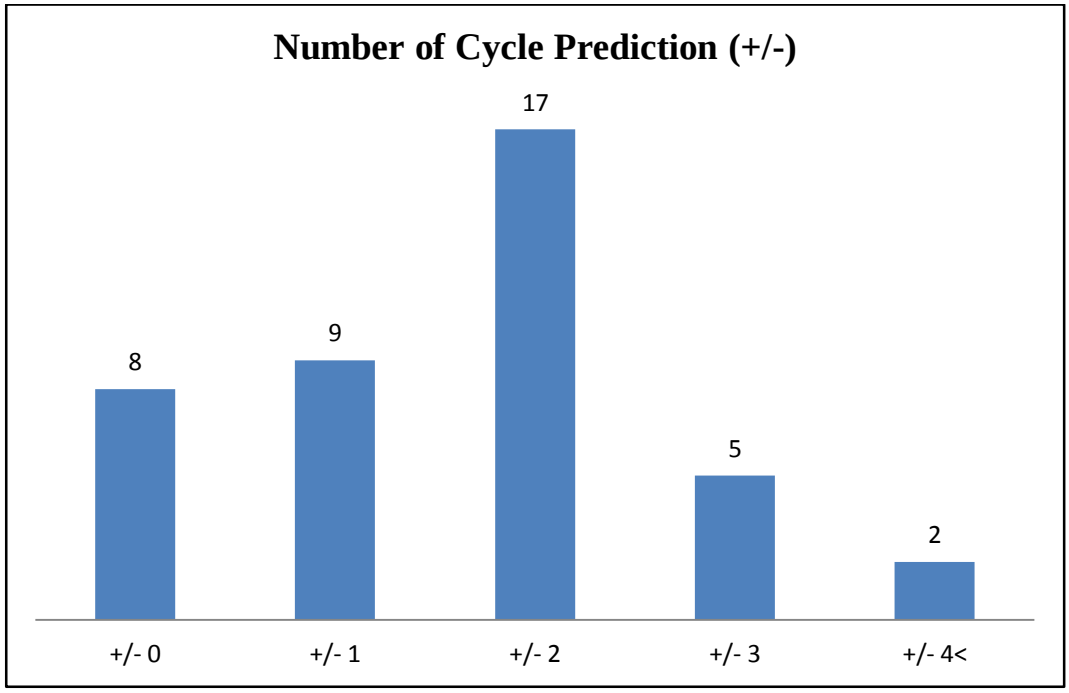

Figure 5.30 Accuracy of number of cycle predictions for testing data sets

Histogram chart for the number of cycle prediction displays the number of cases with ±0, 1, 2, 3, and 4 approximate predictions in Figure 5.30. It also shows that 8 out of 41 data sets have neural network results for number of cycles equal to actual values. 9 of the testing data sets are estimated with ± 1 accuracy whereas 17 of them are predicted with ± 2 accuracy. Only two cases that are equal to approximately 5 % of 41 testing cases are under or over predicted with 4 cycles. If the prediction with difference of maximum ± 2 cycles is considered as reasonable, it can be stated that 34 out of 41 data sets (83 %) are predicted with high accuracy.

5.2 Inverse ANN Models

The inverse-looking neural networks are able to predict design parameters and reservoir properties separately by using performance indicators. The inverse problem is complex because of implementation of two distinct designs (fractured inner zone, cyclic steam injection) in this study. Therefore, four inverse-looking artificial neural networks are developed in order to examine those designs deeply and increase the network accuracy.

At the beginning of this study, first two inverse models called as Inverse ANN-1A and Inverse ANN 1B are assigned for prediction of design parameters. First, Inverse ANN-1A is developed and it is able to predict both fractured inner zone and cyclic steam injection design parameters at the same time. However, combination of all design parameters causes to complexity of the problem. It is assumed that implementation of cyclic steam injection is done after inner zone creation. Thus, Inverse ANN-1B is developed additionally to achieve high-level accuracy on prediction of only cyclic steam injection design parameters. Next tools named as Inverse ANN-2A and Inverse ANN-2B structured to estimate reservoir properties. Inverse ANN-2A is designed in the aim of giving an idea about the condition of reservoir before cyclic steam stimulation process. Hence, reservoir properties that are updated by creating of intensely fractured inner zone can be estimated in this tool. Inverse ANN-2B is considered to estimate only fractured inner zone properties by specifying desired performance indicators with corresponding reservoir properties and design parameters of cyclic steam injection process. Detailed information about structures of four inverse ANN tools and their performances are discussed sequentially in this section.

5.2.1 Inverse ANN-1A

Inverse ANN-1A tool was developed for prediction of both cyclic steam stimulation and fractured zone design parameters for a given data set of reservoir properties and performance indicators. In this ANN tool, 555 datasets were used and 80%, 10%, and 10 % of them were chosen randomly, for training, validation, and testing of network, respectively. Tan-sigmoid function *(tansig)* was applied for activation function with scaled conjugate gradient *(trainscg)* training function. The optimum structure that provides accurate predictions includes a single hidden layer with 42 neurons. The network structure is illustrated in the Figure 5.31.

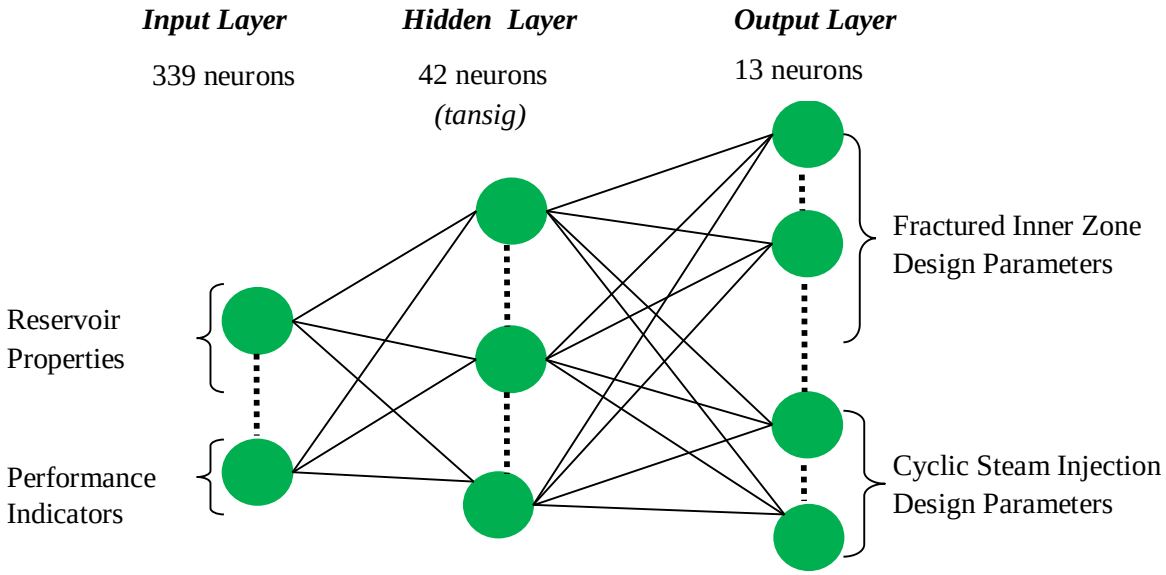

Figure 5.31 Network structure for the inverse ANN-1A

Input layer contains a total of 339 neurons; 10 of them are reservoir properties, 312 of them belong to performance indictors while 17 of them are functional links listed in Table 5.4. Output layer has 13 neurons; 6 of them are fractured inner zone design parameters and 7 of them are cyclic steam injection design parameters. Input and output components used in the training of

this ANN model are summarized in Table 5.3. It was observed that implementation of logarithmic form for some of the input and all of the output parameters enhance the performance of network.

Table 5.3. Input and output layer components of Inverse ANN-1A

INPUT	**Reservoir Properties**	Thickness Matrix Porosity Fracture Porosity Matrix Permeability Fracture Permeability Fracture Spacing Initial Pressure Initial Oil Saturation Depth Initial Reservoir Temperature
	Performance Indicators	Oil Flow Rate (290) Number of Cycle (1) Project Cumulative Oil Production (1) Cumulative Oil Production (10) Production Period (10)
OUTPUT	**Cyclic Steam Injection Design Parameters**	Steam Quality Steam Temperature Soaking Period Injection Period Steam Injection Rate Well Length Layer on Well Located
	Fractured Inner Zone Design Parameters	Inner Zone Fracture Porosity Inner Zone Fracture Permeability Inner Zone Fracture Spacing Major Axis of Inner Zone Minor Axis of Inner Zone Drainage Area

A number of different structures were tried in order to improve accuracy of the predictions. First, input and output neurons were focused by feeding them into ANN in different formats. For example, major and minor axes of inner zone were transformed into grid block numbers instead of length. Grid block width is constant as 50 ft among all reservoir; therefore, length of the major and minor axis were divided by 50 (ft) and grid block numbers corresponding

to them were calculated. It was noticed that this procedure improved the performance of network and it was repeated for well length. Second, functional links such as eigen values were considered. However, it was noticed that addition of these kinds of functional links did not help to progression of the network performance. Therefore, effects of some mathematical functions were tried. It was clear that addition of functional links to both input and output layers at the same time increased the error percentages owing to causing complexity. Then, it was concluded that the network performance progressed when functional links were added to input layer. Hence, numbers of mathematical functions were tried for the reservoir properties. Porosity and permeability of both matrix and fracture systems were more influential reservoir properties based on trial and error method. 17 functional links were added and 12 of them were related to porosity and permeability of the reservoir. All used functional links are listed in Table 5.4.

Table 5.4. Functional links of Inverse ANN-1A

Input Functional Links	Output Functional Links
log((Matrix Porosity)*100) log((Fracture Porosity)*100) log((Matrix Porosity + Fracture Porosity)*100) $(\text{Matrix Porosity})^{0.5}$ $(\text{Fracture Porosity})^{0.5}$ $(\text{Matrix Porosity + Fracture Porosity})^{0.5}$ (Matrix Porosity - Fracture Porosity) (Matrix Porosity) / (Fracture Porosity) $(\text{Matrix Permeability})^{0.5}$ $(\text{Fracture Permeability})^{0.5}$ (Matrix Permeability)-(Fracture Permeability) (Matrix Permeability)/(Fracture Permeability) $(\text{Fracture Spacing})^{0.5}$ $(\text{Initial Pressure})^{0.5}$ $(\text{Depth})^{0.5}$ $(\text{Initial Reservoir Temperature})^{0.5}$ (Oil saturation)*100	There is no functional link used in the output layer

Errors of the predicted outputs are examined to determine whether this model is accurate, or not. While estimating the network efficiency, reasonable error is considered as 5 %. The comparison between the predicted values of design parameters *(ANN)* and result of numerical simulator for the testing data sets are shown from the Figure 5.32 through Figure 5.44.

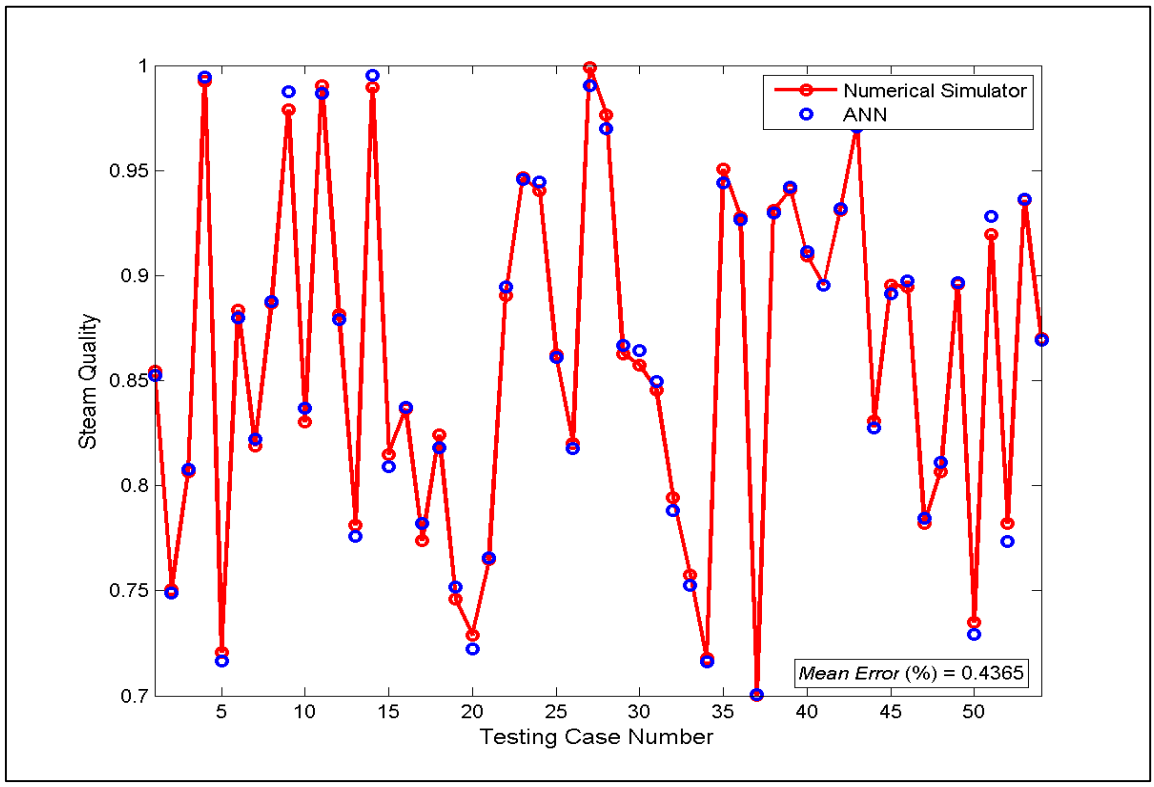

Figure 5.32 Comparison of simulator and predicted steam quality for Inverse ANN-1A

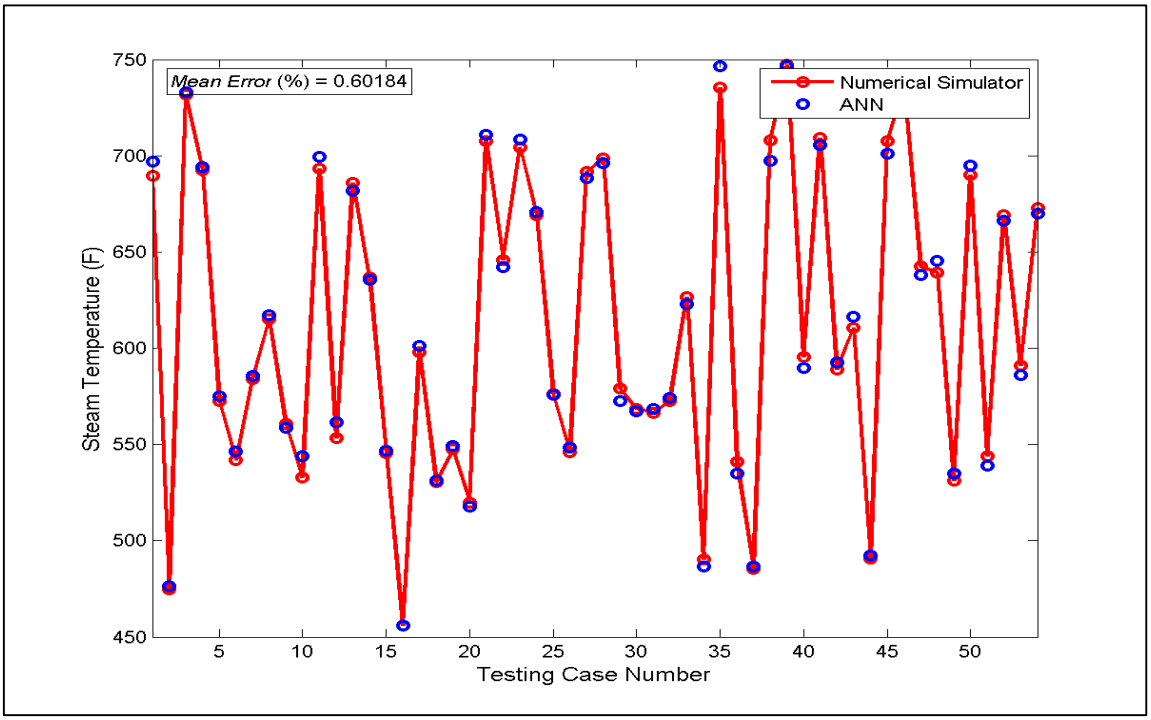

Figure 5.33 Comparison of simulator and predicted steam temperature for Inverse ANN-1A

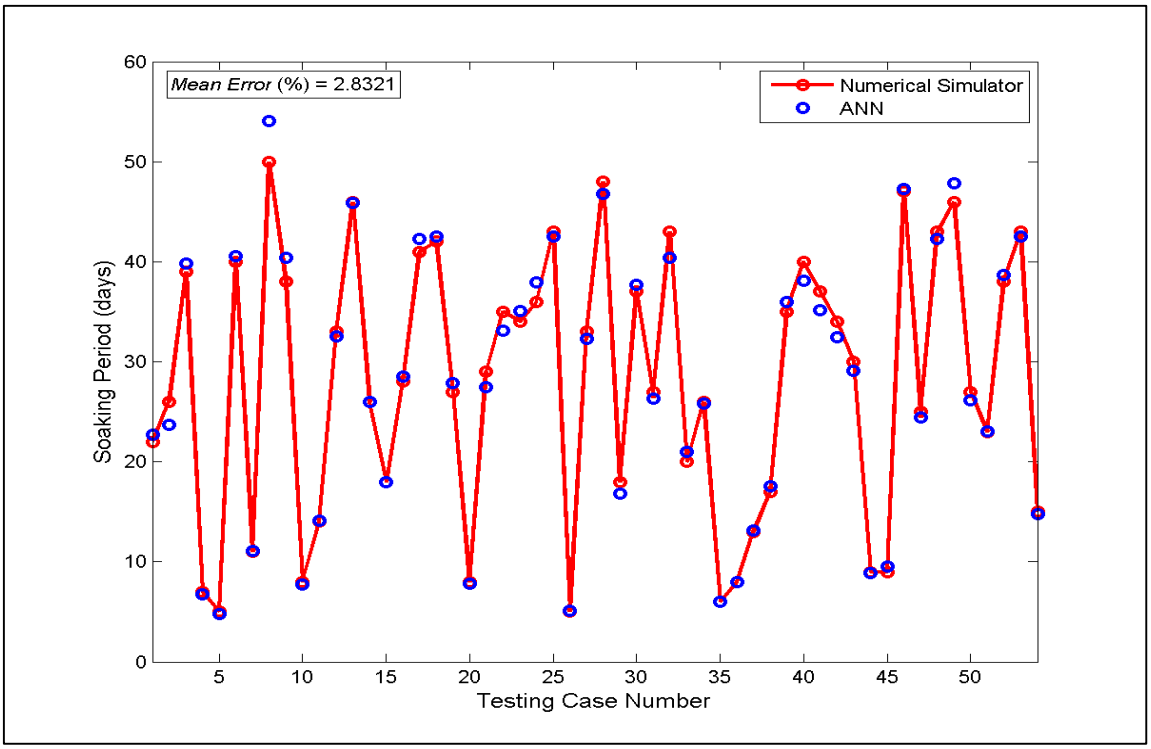

Figure 5.34 Comparison of simulator and predicted soaking period for Inverse ANN-1A

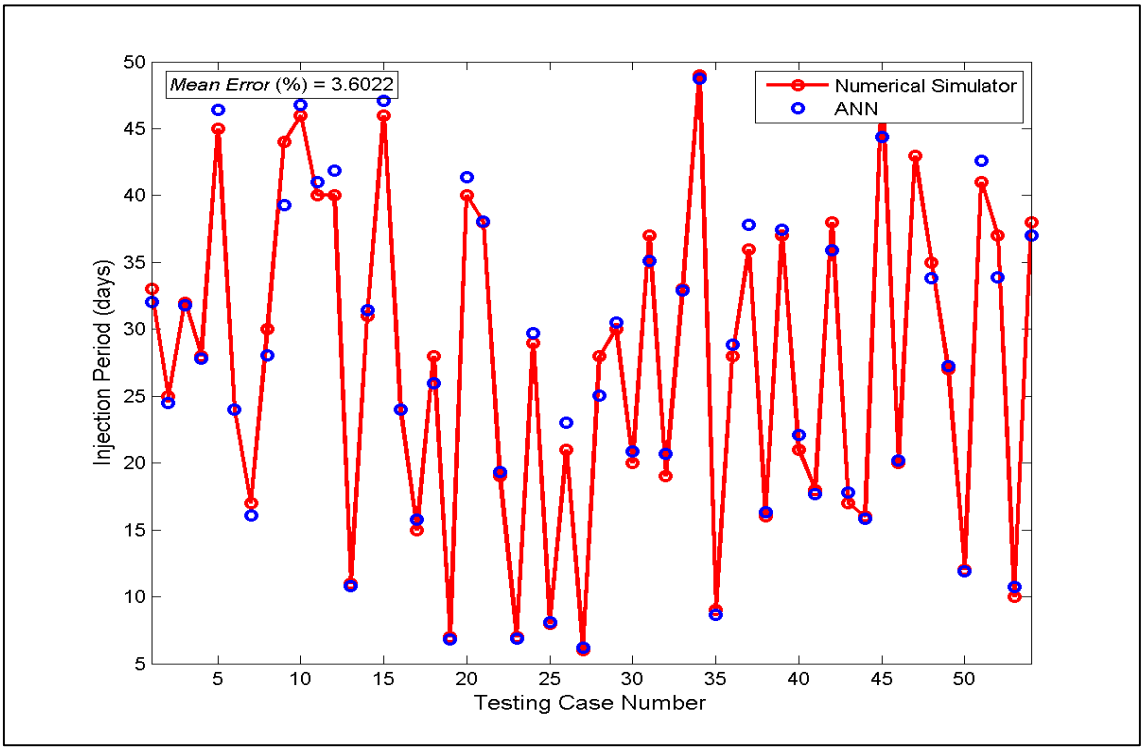

Figure 5.35 Comparison of simulator and predicted injection period for Inverse ANN-1A

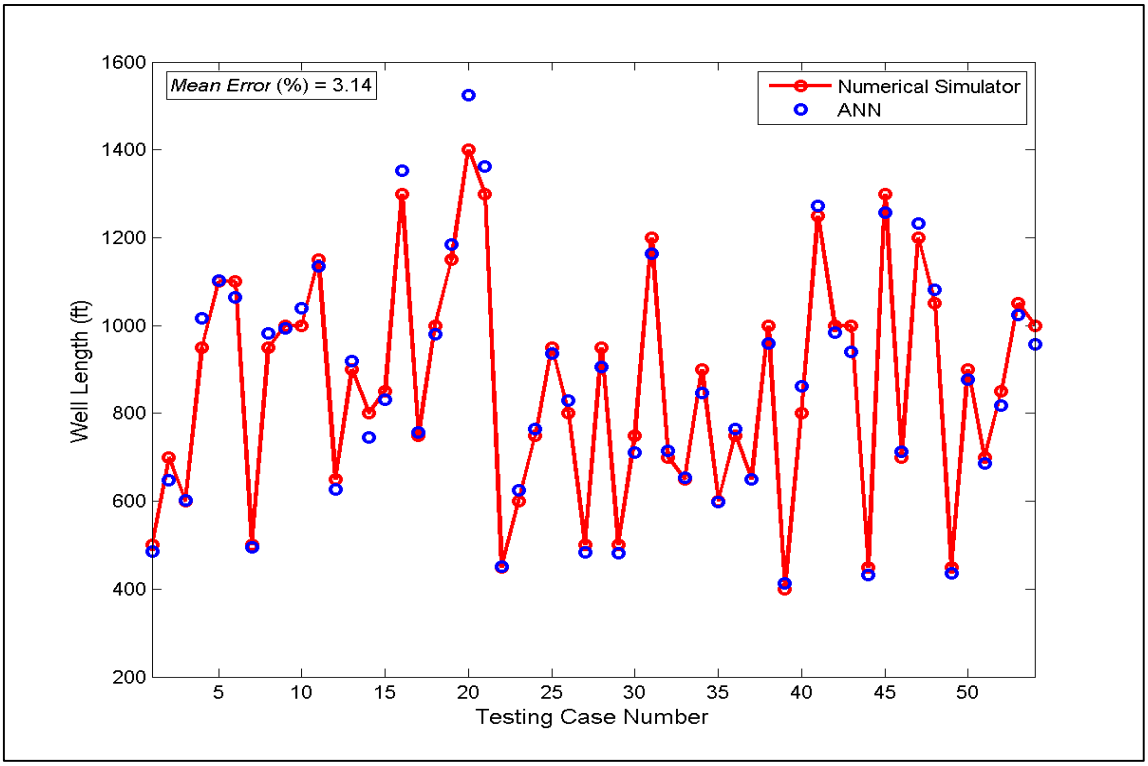

Figure 5.36 Comparison of simulator and predicted well length for Inverse ANN-1A

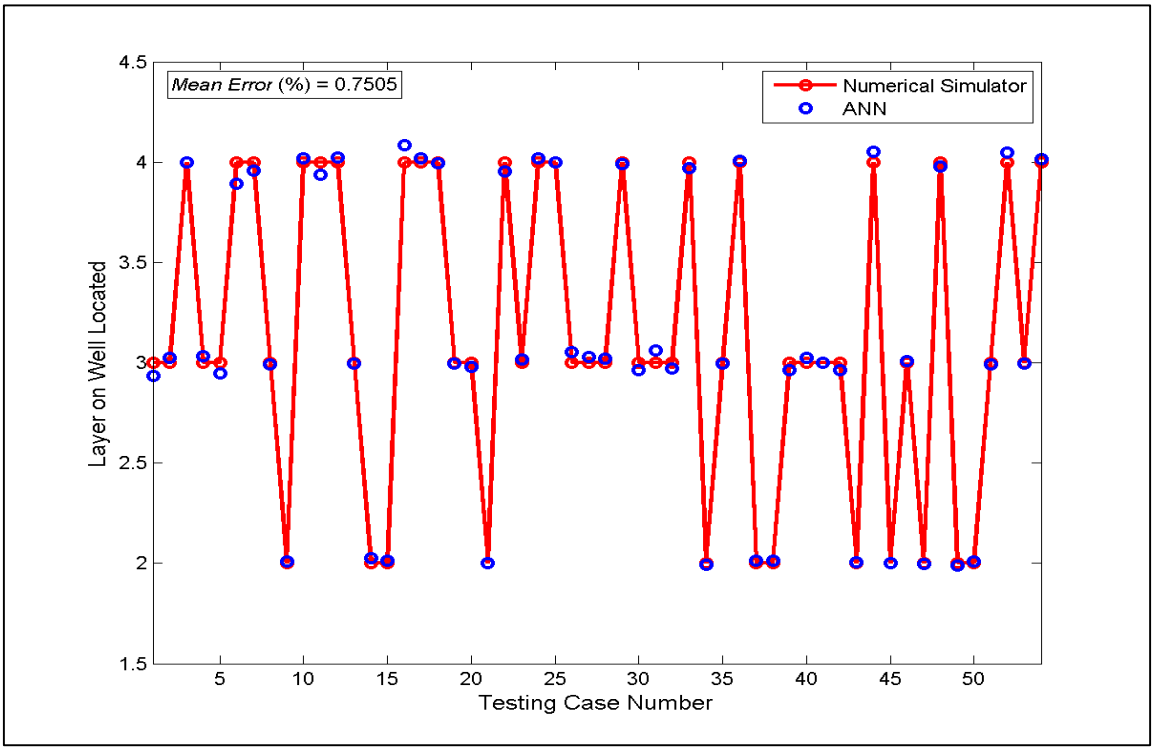

Figure 5.37 Comparison of simulator and predicted layer on well located for Inverse ANN-1A

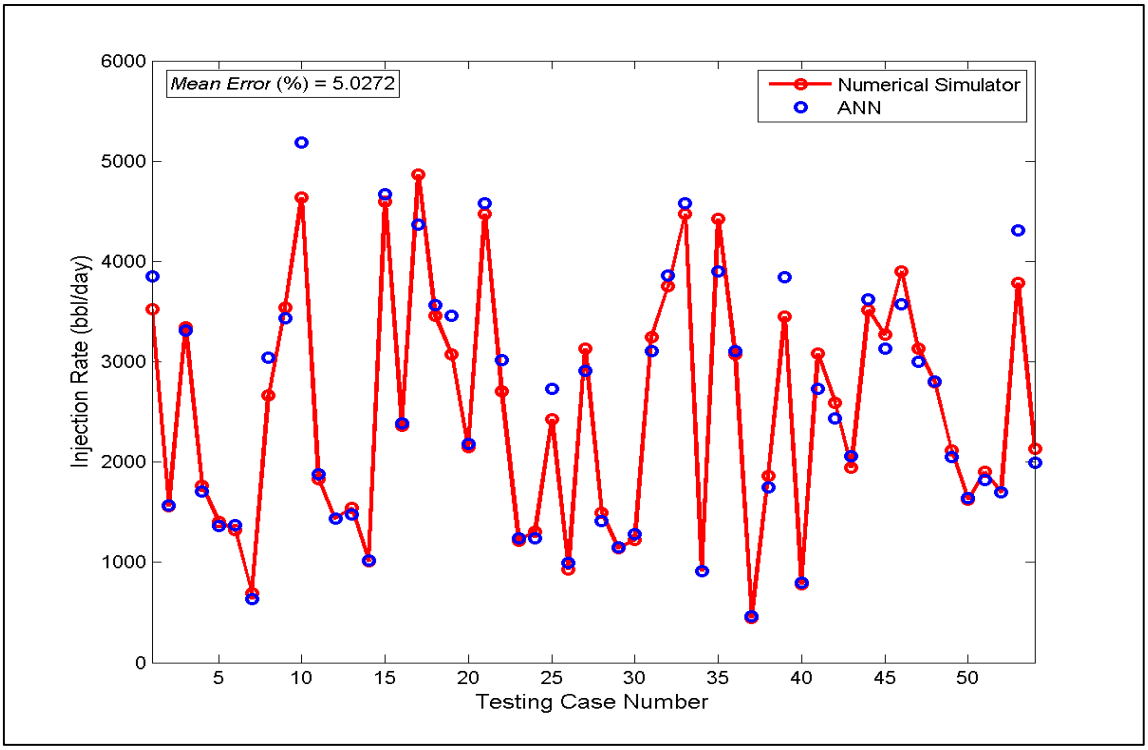

Figure 5.38 Comparison of simulator and predicted injection rate for Inverse ANN-1A

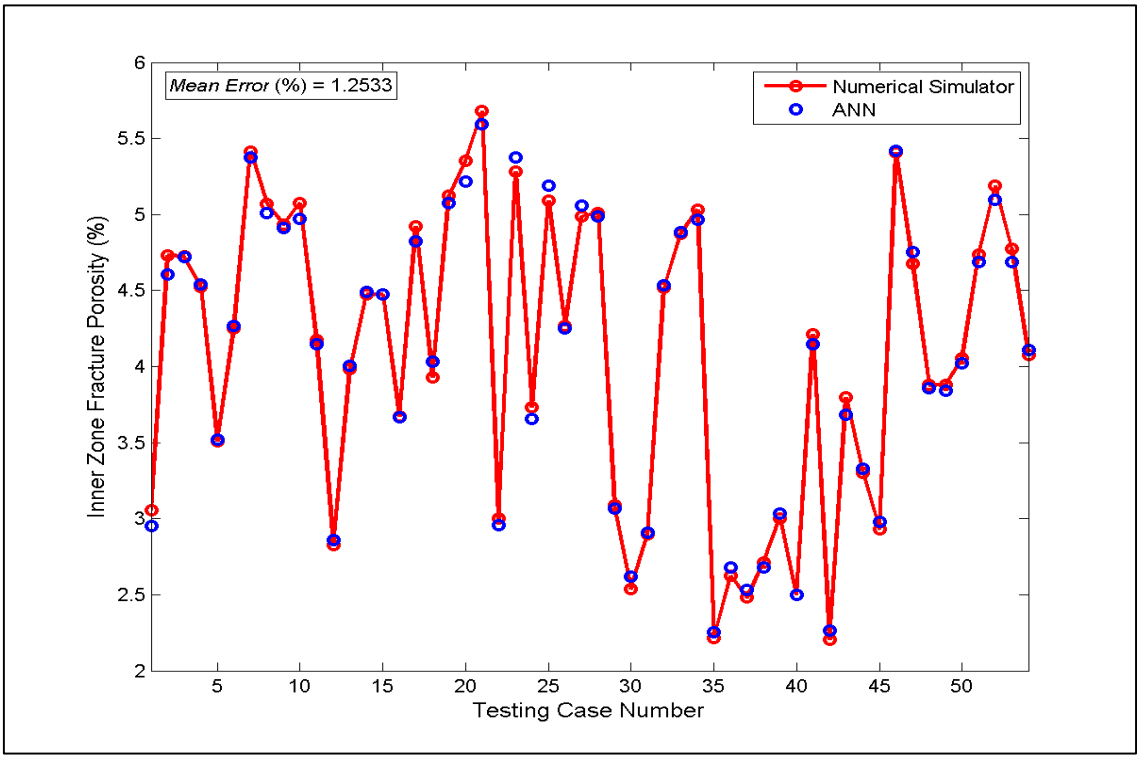

Figure 5.39 Comparison of simulator and predicted inner zone fracture porosity for Inverse ANN-1A

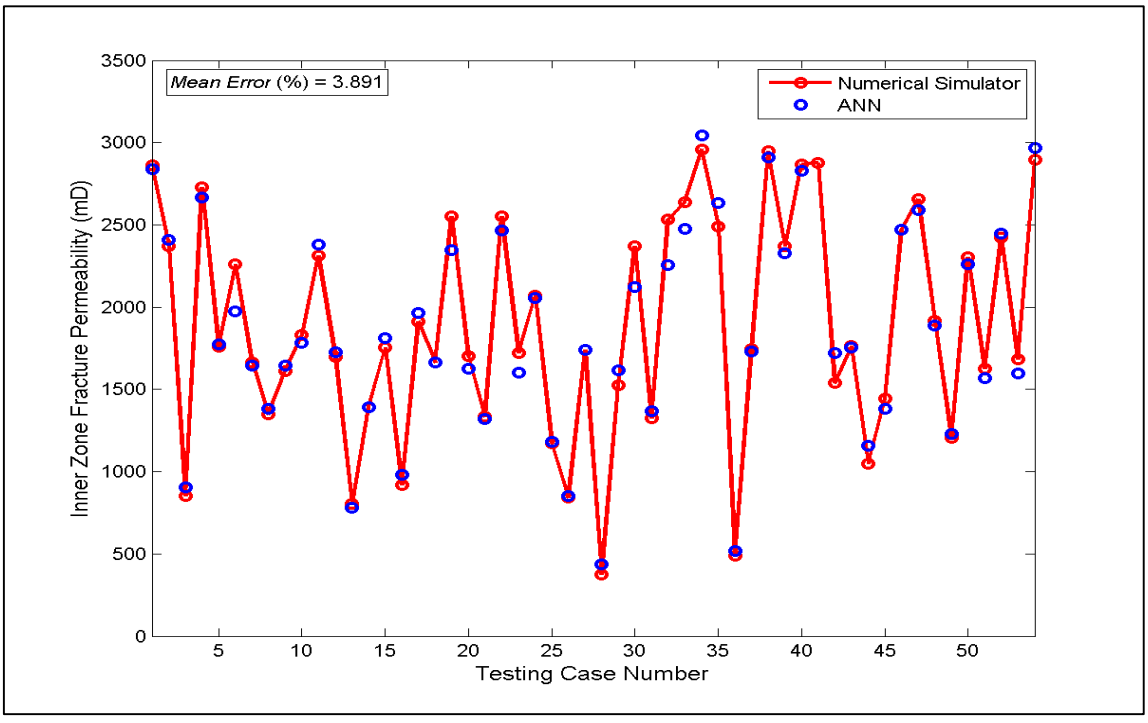

Figure 5.40 Comparison of simulator and predicted inner zone fracture permeability for Inverse ANN-1A

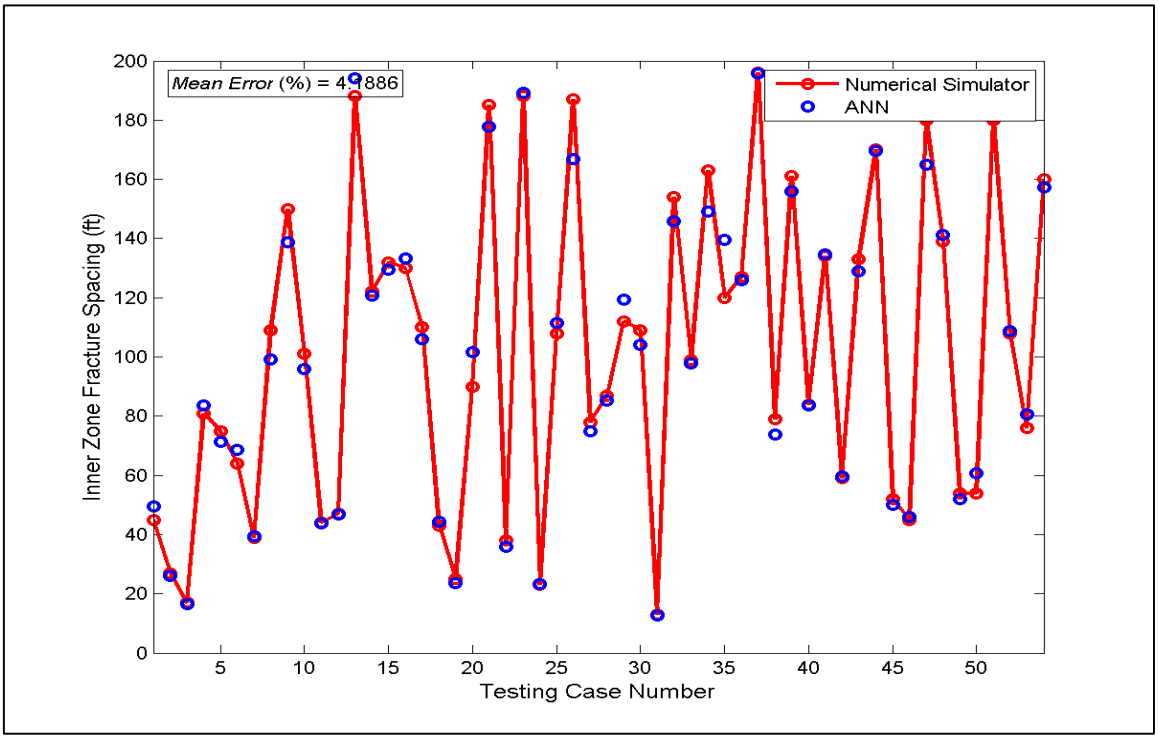

Figure 5.41 Comparison of simulator and predicted inner zone fracture spacing for Inverse ANN-1A

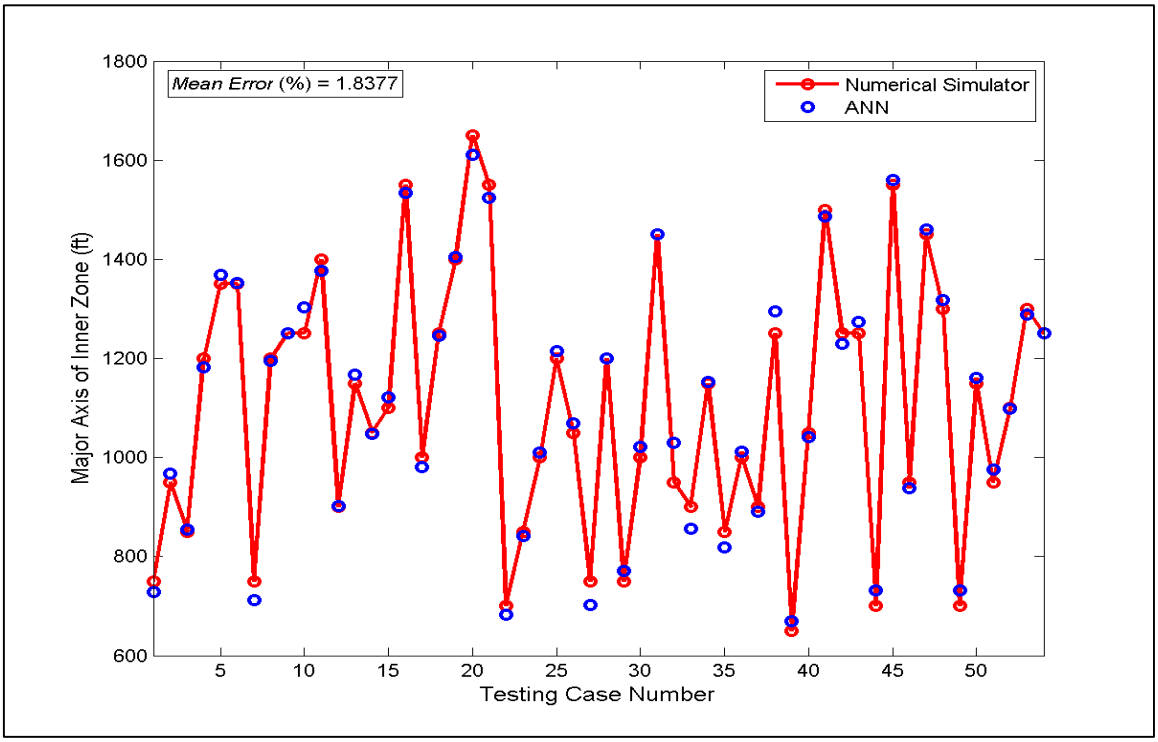

Figure 5.42 Comparison of simulator and predicted major axis of inner zone for Inverse ANN-1A

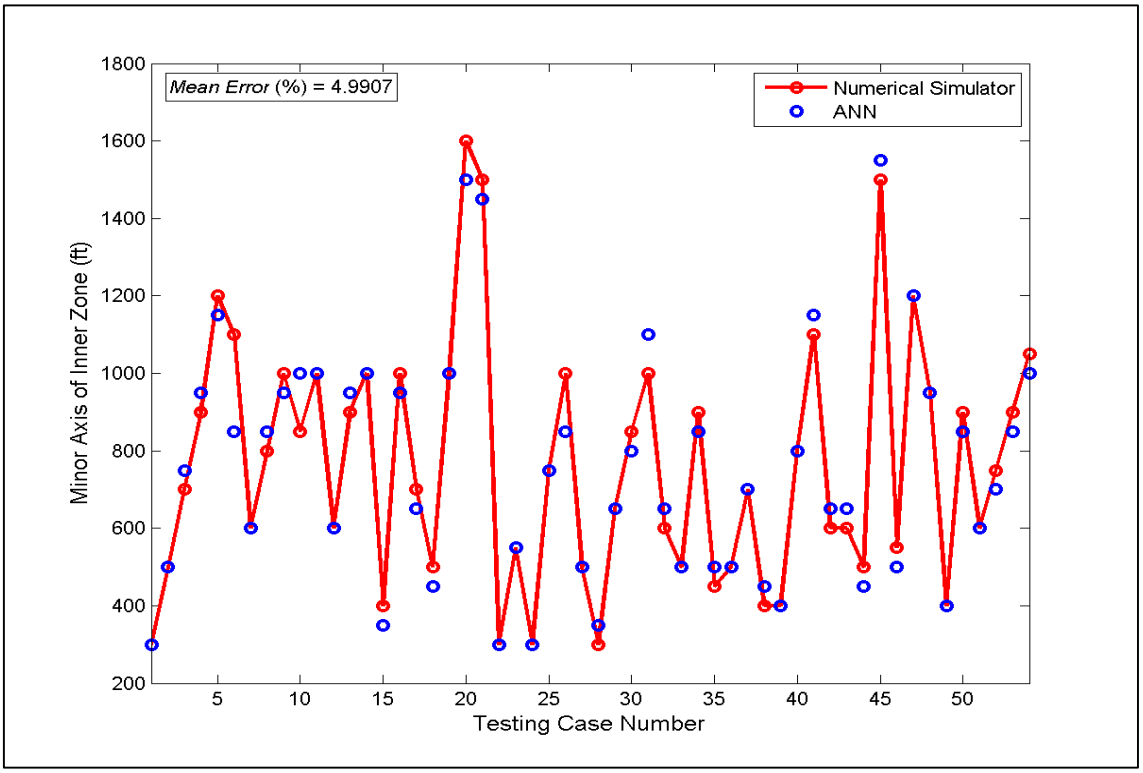

Figure 5.43 Comparison of simulator and predicted minor axis of inner zone for Inverse ANN-1A

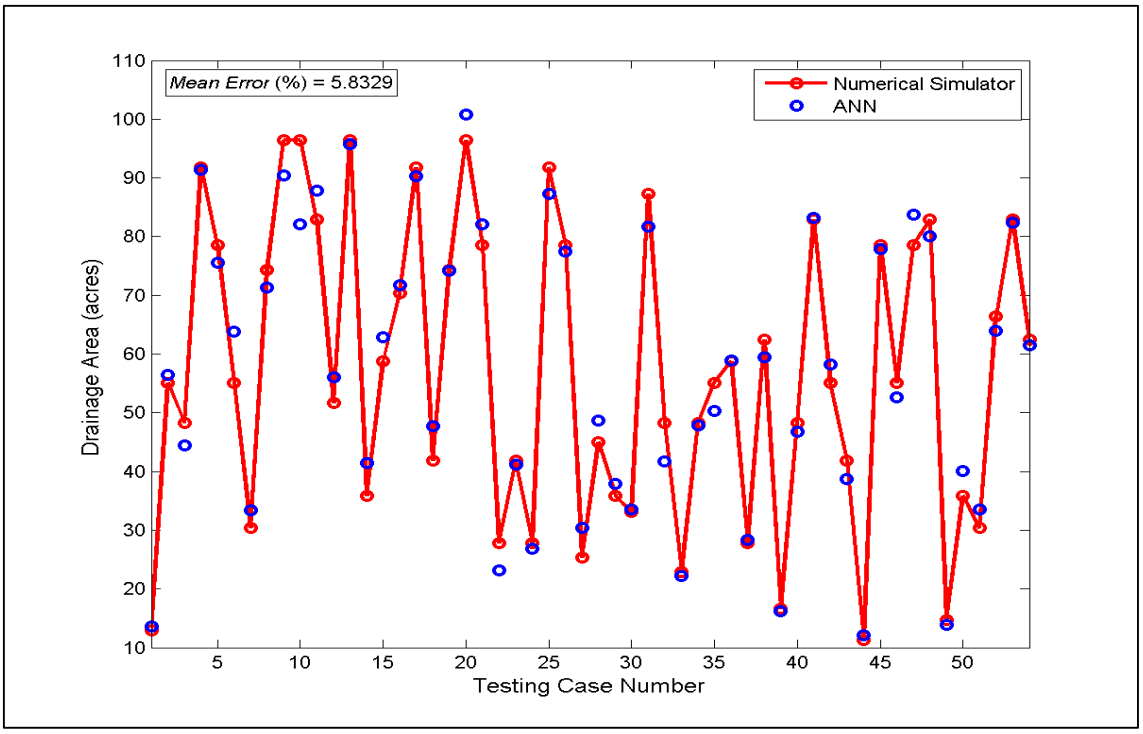

Figure 5.44 Comparison of simulator and predicted drainage area for Inverse ANN-1A

Even if it is possible to see average errors of each predicted parameters on the top of the associated figures, they are summarized in Table 5.5.

Table 5.5. Errors (%) for Inverse ANN-1A

Design Parameters	Average error (%)	Maximum error (%)	Minimum error (%)
Steam Quality	0.436	1.142	0.00024
Steam Temperature	0.602	2.091	0.0600
Soaking Period	2.832	8.734	0.0334
Injection Period	3.602	10.773	0.0392
Well Length	3.140	8.926	0.0208
Layer on Well Located	0.750	2.721	0.0119
Steam Injection Rate	5.027	14.215	0.0615
Inner Zone Fracture Porosity	1.253	3.428	0.0463
Inner Zone Fracture Permeability	3.890	16.253	0.0321
Inner Zone Fracture Spacing	4.188	16.221	0.0580
Major Axis of Inner Zone	1.837	8.3815	0.0364
Minor Axis of Inner Zone	4.990	22.727	0.95
Drainage Area	5.832	20.114	0.228

Interpretation of the network performance is done based on not only errors of the predicted outputs but also errors of each testing cases that is calculated by taking arithmetic average of all outputs errors. Although maximum error percentage of some parameters such as fracture porosity, fracture permeability and minor axis of inner zone are higher than desired tolerance, average error of the testing data sets for most of the parameters are lower than %5. The data set # 28 (Table 5.6) which have higher error percentage is examined in detailed by representing its properties as inputs to the constructed forward ANN tools. In addition, performance indicators are extracted from the simulator by using predicted design parameters. Then, simulator results of actual parameters, forward ANN results obtained from predicted design parameters and simulator results updated by predicted design parameters are compared from Figure 5.45 through Figure 5.47. From these figure, it is observed that performance indicators are in good agreements with actual results even if used data set has design parameters predicted with high error percentages in inverse ANN-1A.

Table 5.6. Comparison of simulator and ANN results of worst predicted data set in Inverse ANN-1A

Testing Sample # 28	Predicted (ANN)	Simulator (CMG)	Error (%)
Steam Quality	0.970	0.97663	0.677
Steam Temperature	696.372	698.6772	0.329
Soaking Period	46.810	48	2.477
Injection Period	25.039	28	10.575
Well Length	906	950	4.631
Layer on Well Located	3.0203	3	0.677
Steam Injection Rate	1410.726	1494	5.573
Inner Zone Fracture Porosity	0.0498	0.0501	0.497
Inner Zone Fracture Permeability	434.663	374	16.253
Inner Zone Fracture Spacing	85.167	87	2.106
Major Axis of Inner Zone	1199.562	1200	0.0364
Minor Axis of Inner Zone	361.9	300	20.642
Drainage Area	48.707	45	8.250

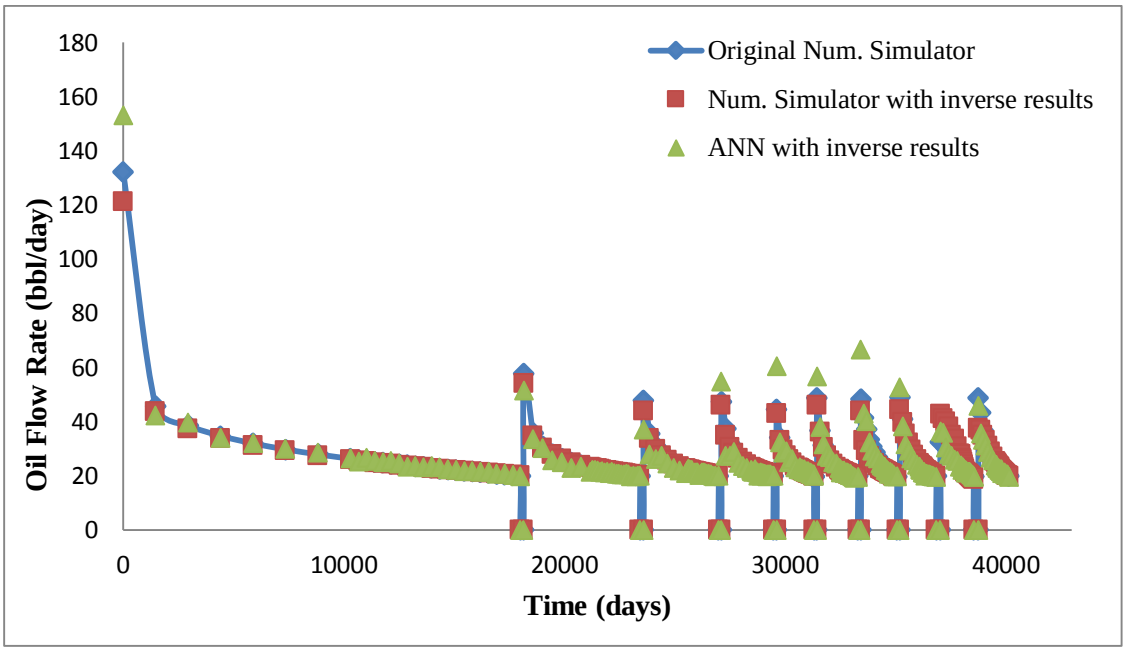

Figure 5.45 Oil flow rate comparison betwen simulator and ANN results of worst predicted data set

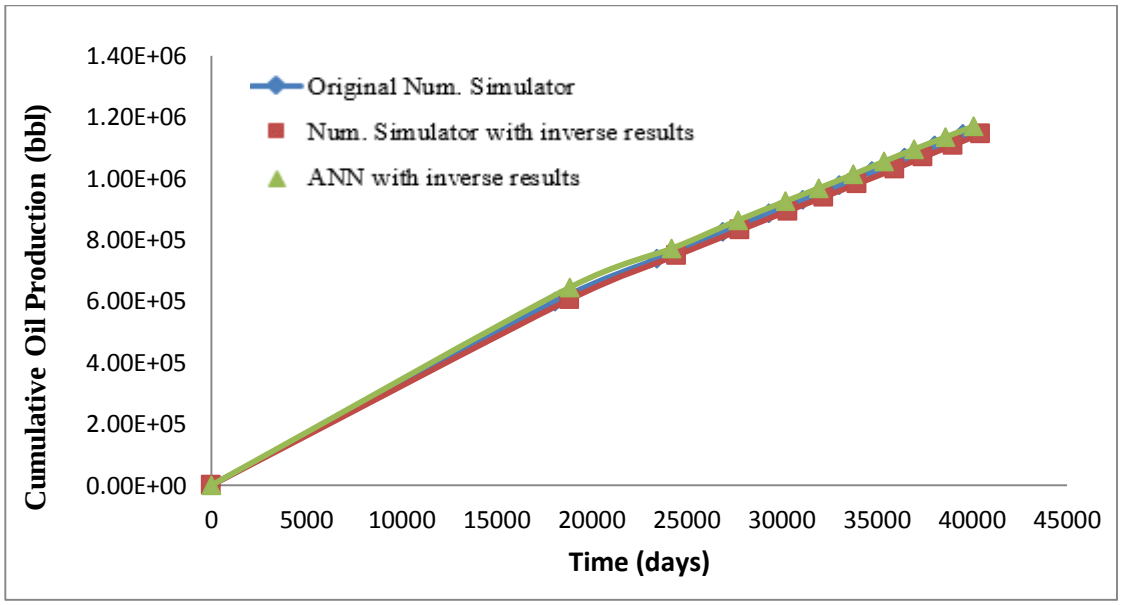

Figure 5.46 Cumulative oil production comparison betwen simulator and ANN results ofworstpredicted data set

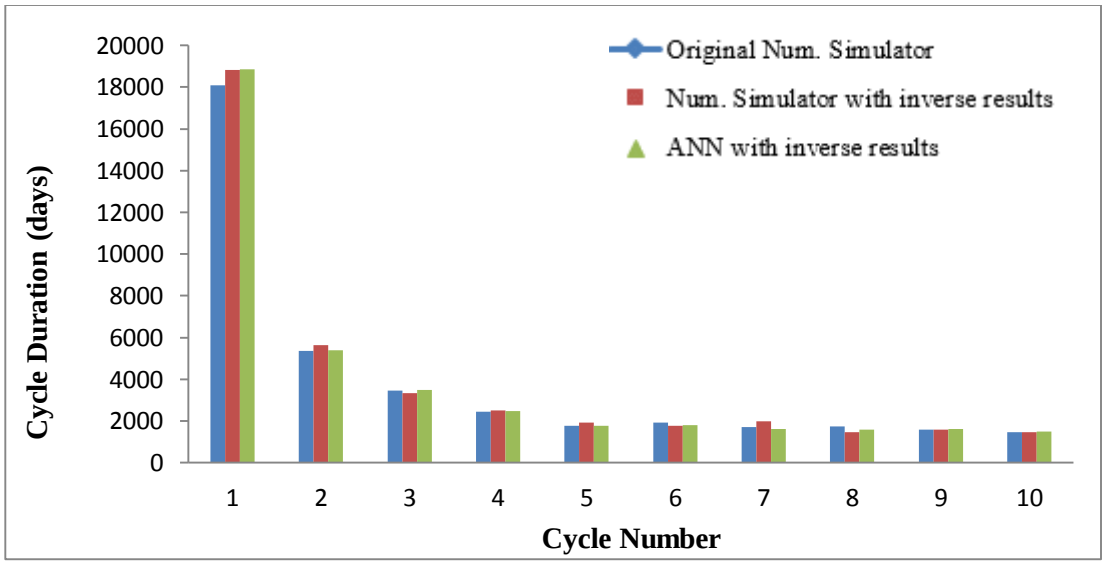

Figure 5.47 Cycle duration comparison betwen simulator and ANN results ofworstpredicted data set

The average errors of the oil flow rate, cumulative oil productions and duration of each cycles between actual and updated simulator results are 4.75 %, 2.85 %, 3.23 %, respectively.

5.2.2 Inverse ANN-1B

The Inverse ANN-1B tool was developed to provide predictions of cyclic steam stimulation design parameters when the reservoir properties, performance indicators, and fractured inner zone design parameters are given. This tool is expected to predict more accurately than Inverse ANN-1A by focusing on only design parameters of cyclic steam injection. In this ANN tool, 555 datasets were used and 82 %, 9 %, and 9 % of them were chosen randomly, for training, validation, and testing of network, respectively. The developed artificial neural network has a single hidden layer using tan-sigmoid *(tansig)* activation function. The scaled conjugate gradient *(trainscg)* training function was used in the output layer. The optimum structure that provides accurate estimations contains 37 neurons in the hidden layer. The network structure is illustrated in the Figure 5.48.

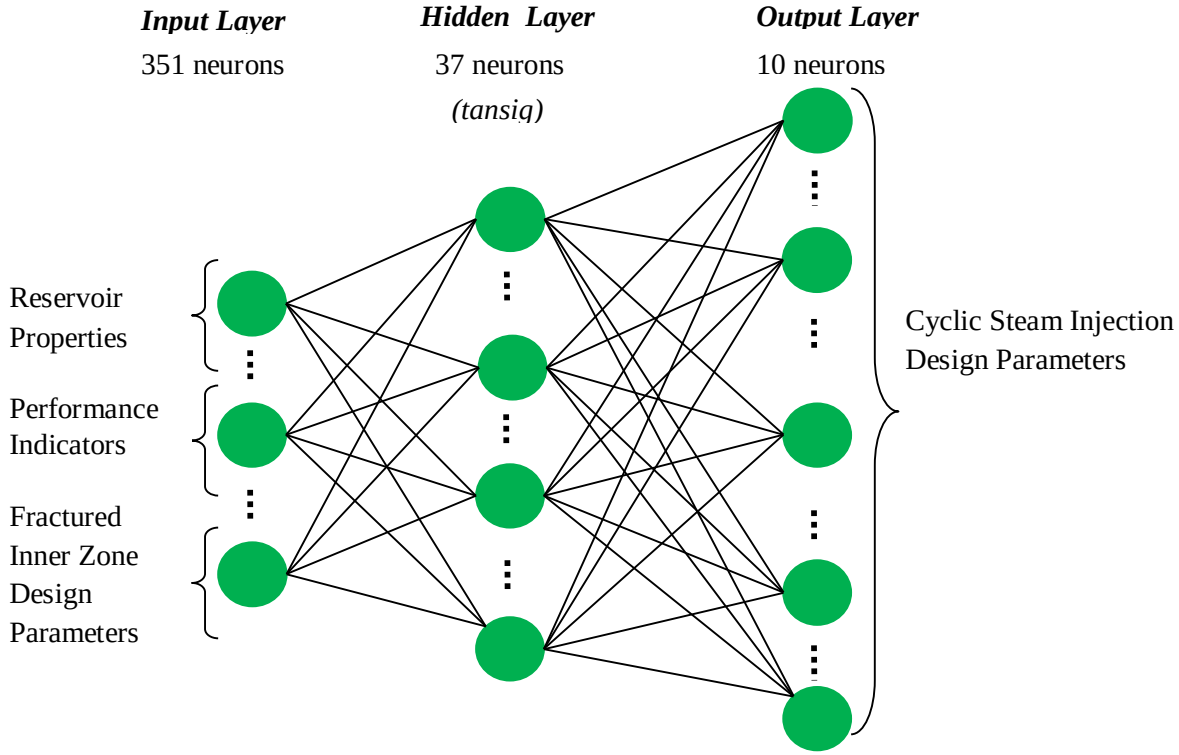

Figure 5.48 Network structure for the inverse ANN-1B

There are 351 neurons in the input layer and 10, 6 and 312 of them belong to reservoir properties, fractured inner zone design parameters and performance indicators, respectively. A number of 23 functional links listed in Table 5.8 were added to the input layer. Output layer has 10 neurons; 7 of them are cyclic steam injection design parameters and 3 of them are functional links. Input and output components used in the training of this ANN model are summarized in Table 5.7. An improvement of the network performance was achieved by logarithmic form of some output and input neurons.

Table 5.7. Input and output layer components of Inverse ANN-1B

INPUT	**Reservoir Properties**	Thickness Matrix Porosity Fracture Porosity Matrix Permeability Fracture Permeability Fracture Spacing Initial Pressure Initial Oil Saturation Depth Initial Reservoir Temperature
	Performance Indicators	Oil Flow Rate (290) Number of Cycle (1) Project Cumulative Oil Production (1) Cumulative Oil Production (10) Production Period (10)
	Fractured Inner Zone Design Parameters	Inner Zone Fracture Porosity Inner Zone Fracture Permeability Inner Zone Fracture Spacing Major Axis of Inner Zone Minor Axis of Inner Zone Drainage Area
OUTPUT	**Cyclic Steam Injection Design Parameters**	Steam Quality Steam Temperature Soaking Period Injection Period Steam Injection Rate Well Length Layer on Well Located

Additions of different functional links were tried in order to find the optimum structure that predicts accurately. Same steps, followed in the first inverse-looking ANN tool, were considered. It was decided to keep the functional links used in the input layer of the inverse ANN-1A. However, in this inverse network, fractured inner zone design parameters were moved to the input layer and an addition of 6 more functional links corresponding to these parameters were decided. Furthermore, 3 functional links are assigned for the output layer. All used functional links are listed in Table 5.8.

Table 5.8. Functional links of Inverse ANN-1B

Input Functional Links	Output Functional Links
log((Matrix Porosity)*100)	(Soaking Period + Injection Period)
log((Fracture Porosity)*100)	(Soaking Period / Injection Period)
log((Matrix Porosity + Fracture Porosity)*100)	(Injection Period * Injection Rate)
$(\text{Matrix Porosity})^{0.5}$	
$(\text{Fracture Porosity})^{0.5}$	
$(\text{Matrix Porosity + Fracture Porosity})^{0.5}$	
(Matrix Porosity - Fracture Porosity)	
(Matrix Porosity) / (Fracture Porosity)	
$(\text{Matrix Permeability})^{0.5}$	
$(\text{Fracture Permeability})^{0.5}$	
(Matrix Permeability)-(Fracture Permeability)	
(Matrix Permeability)/(Fracture Permeability)	
$(\text{Fracture Spacing})^{0.5}$	
$(\text{Initial Pressure})^{0.5}$	
$(\text{Depth})^{0.5}$	
$(\text{Initial Reservoir Temperature})^{0.5}$	
(Oil saturation)*100	
log((Inner Zone Fracture Porosity)*100)	
$(\text{Inner Zone Fracture Permeability})^{0.5}$	
$(\text{Inner Zone Fracture Spacing})^{0.5}$	
$(\text{Major Axis of Inner Zone})^{0.5}$	
$(\text{Minor Axis of Inner Zone})^{0.5}$	
$(\text{Drainage Area})^{0.5}$	

Performance of the network is evaluated based on the error percentages of predicted design parameters. They are tried to be lower than desired tolerance (5 %) and in this purpose, error percentages of the output functional links are evaluated, too. For example, if accurate predictions of soaking periods are achieved, injection period can be calculated from the first or second functional link of the output layer. Results of injection periods obtained from the network predictions and functional links are compared. One of them that have the lowest error can be used for calculation of the injection rate. Therefore, accurate predictions can be achieved for these 3 important design parameters. The comparison between the predicted values of design parameters *(ANN)* and results of numerical simulator for the testing data sets are illustrated from the Figure 5.49 through Figure 5.55.

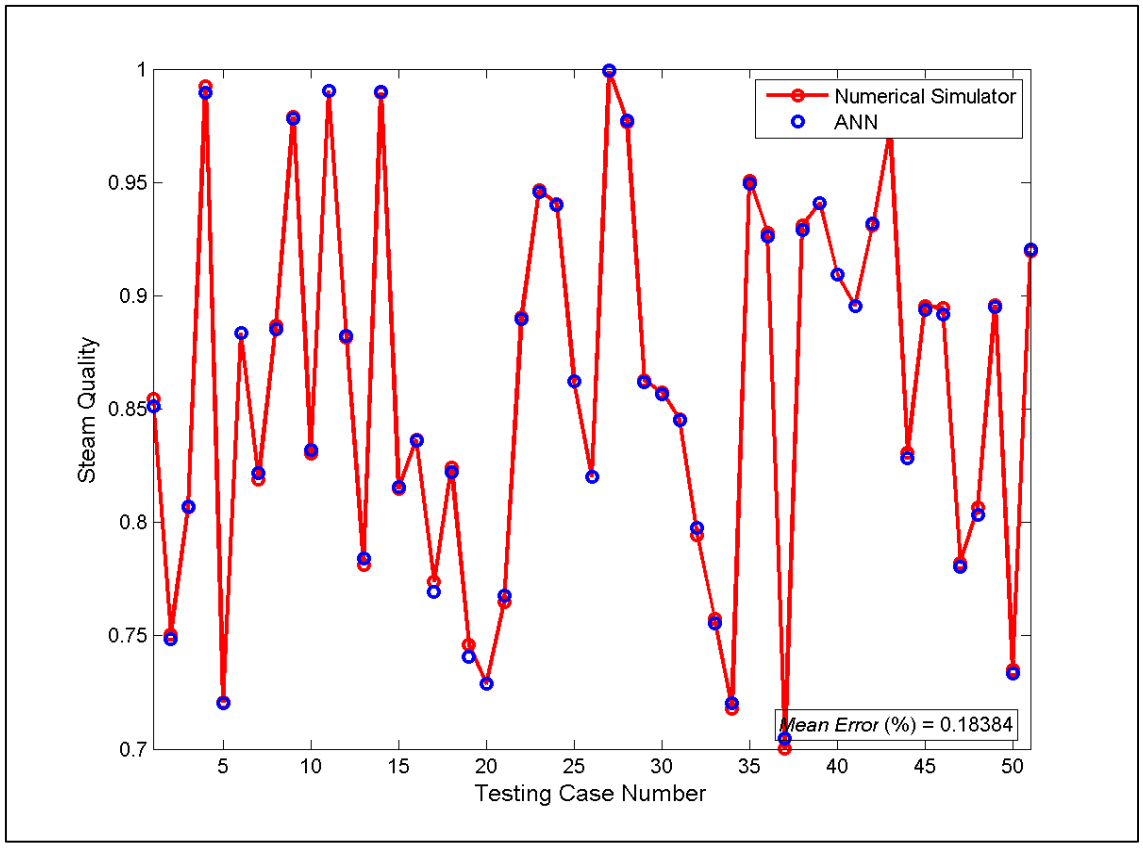

Figure 5.49 Comparison of simulator and predicted steam quality for Inverse ANN-1B

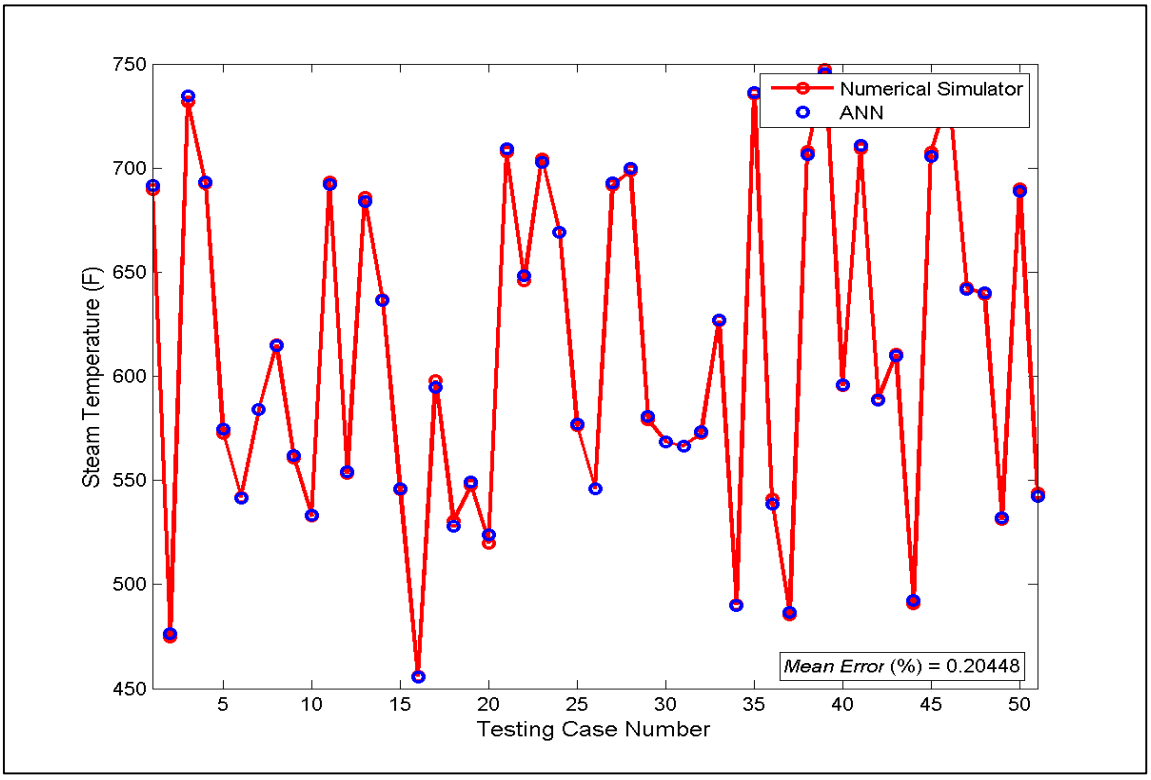

Figure 5.50 Comparison of simulator and predicted steam temperature for Inverse ANN-1B

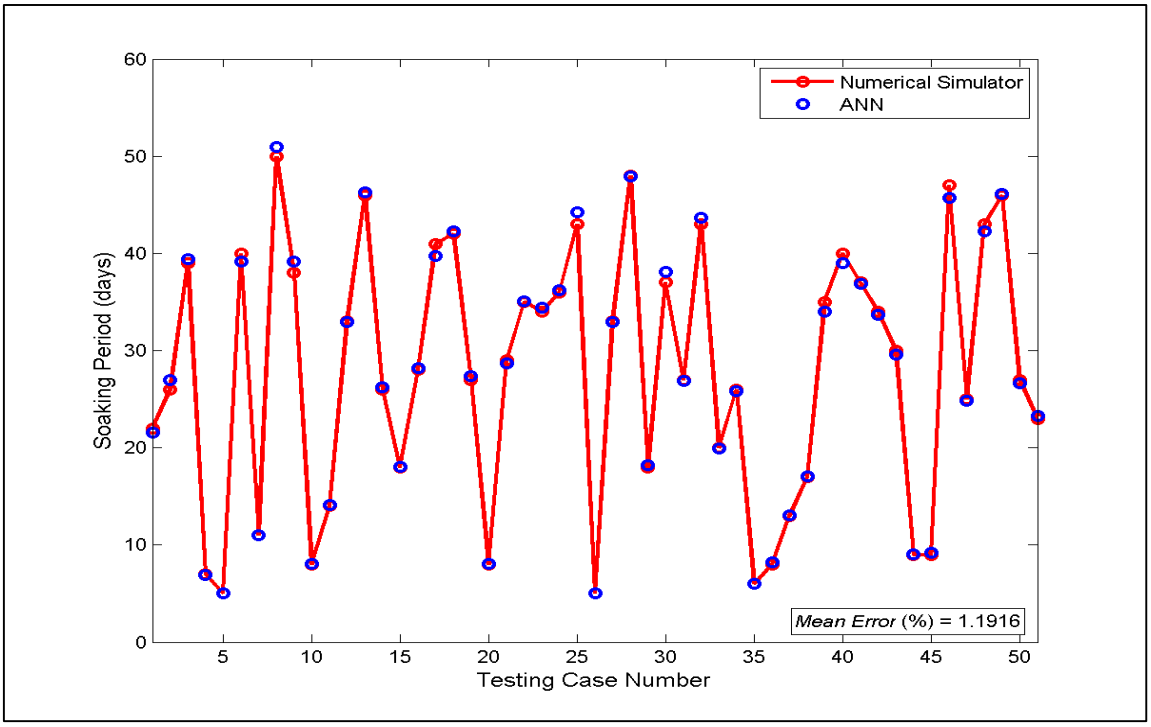

Figure 5.51 Comparison of simulator and predicted soaking period for Inverse ANN-1B

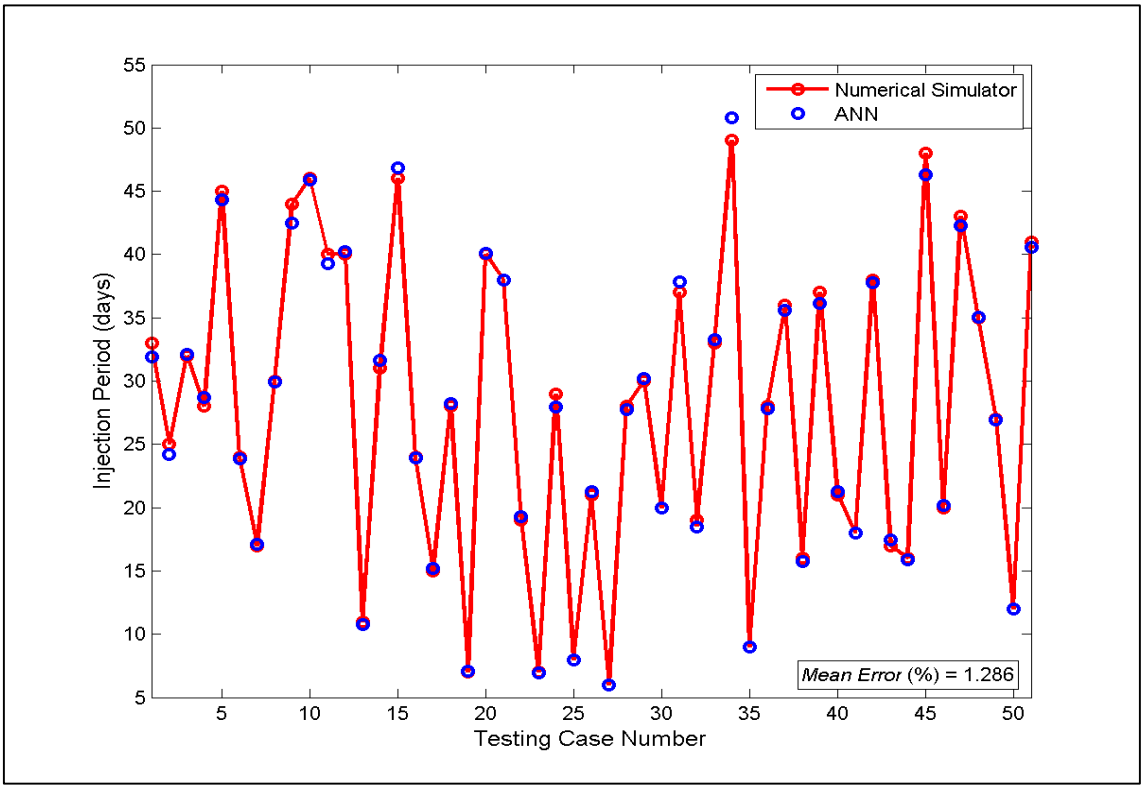

Figure 5.52 Comparison of simulator and predicted injection period for Inverse ANN-1B

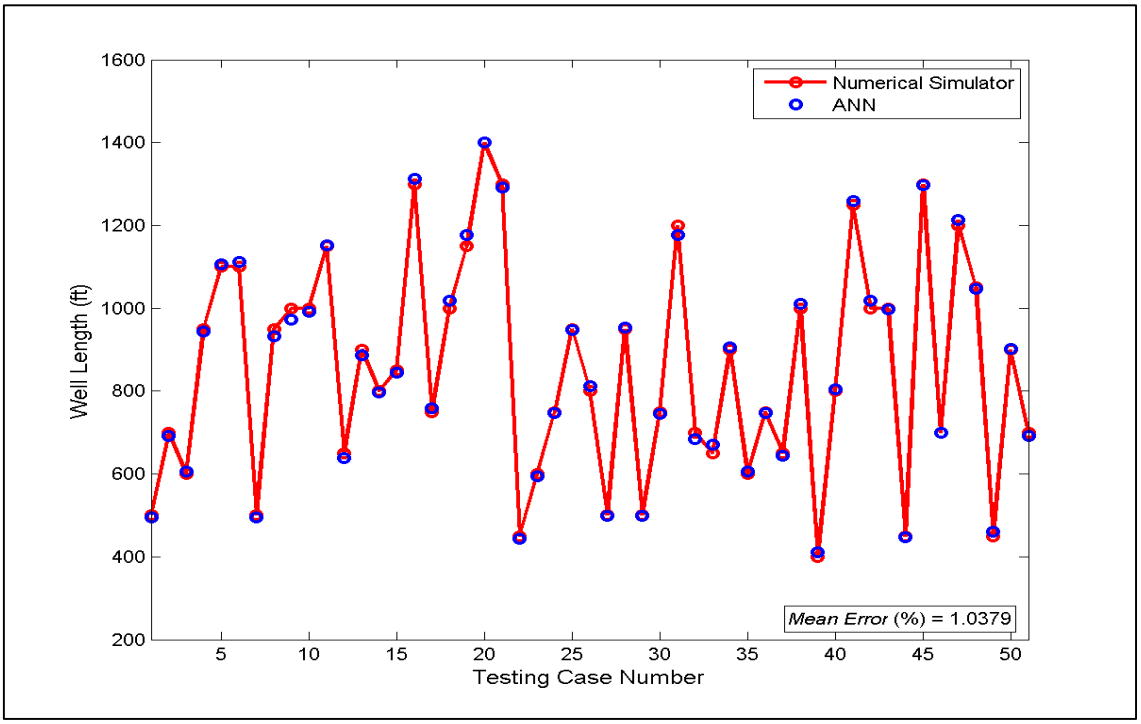

Figure 5.53 Comparison of simulator and predicted well length for Inverse ANN-1B

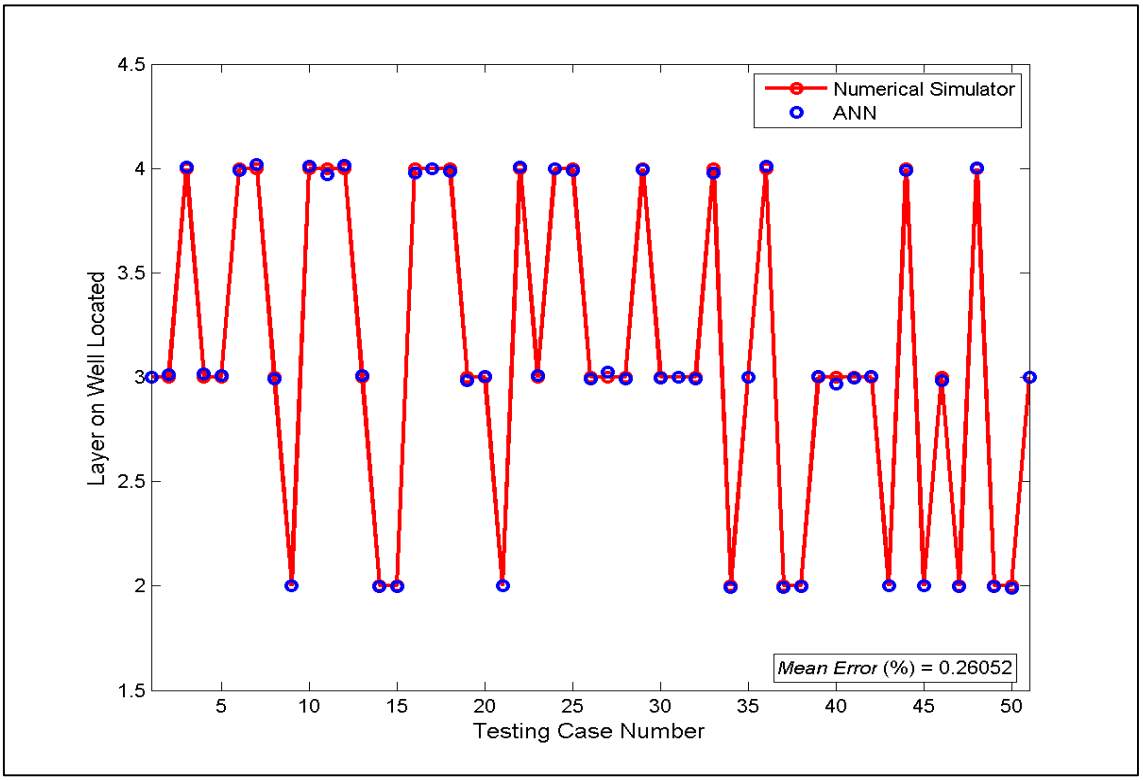

Figure 5.54 Comparison of simulator and predicted layer on well located for Inverse ANN-1B

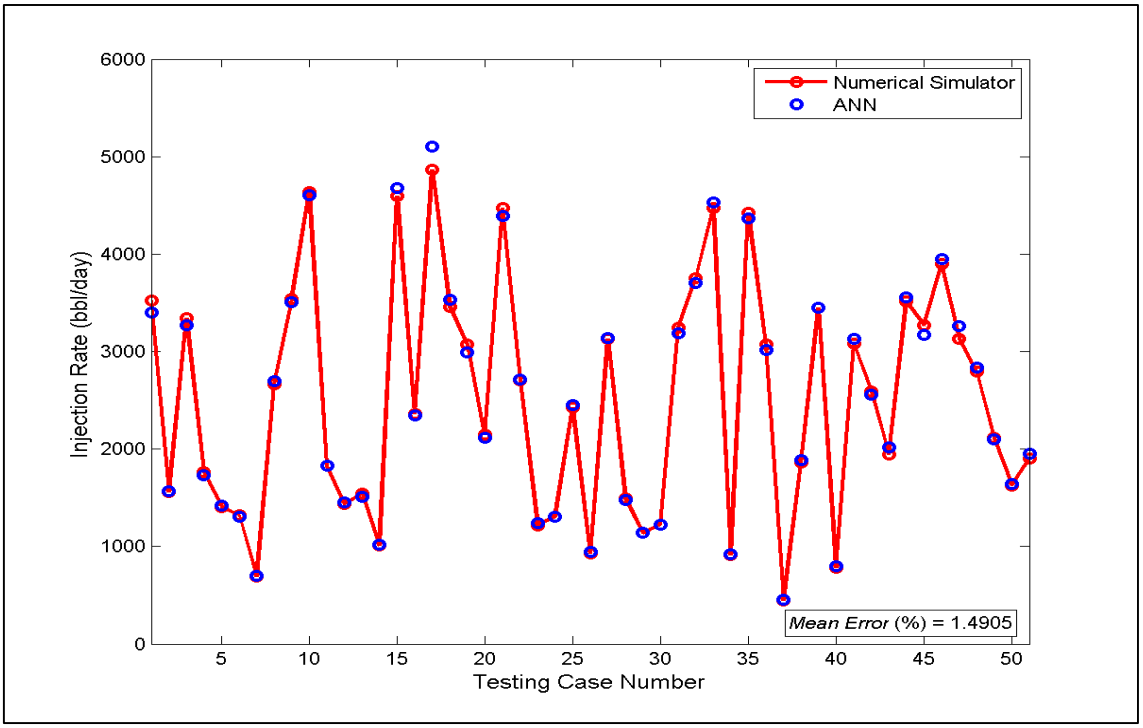

Figure 5.55 Comparison of simulator and predicted injection rate for Inverse ANN-1B

Even if it is possible to see average errors of each predicted parameters on the top of corresponding figures, they are summarized in Table 5.9.

Table 5.9. Errors (%) for Inverse ANN-1B

Design Parameters	Average error (%)	Maximum error (%)	Minimum error (%)
Steam Quality	0.184	0.683	0.0027
Steam Temperature	0.204	0.761	0.0076
Soaking Period	1.192	3.740	0.0383
Injection Period	1.286	3.663	0.0108
Well Length	1.038	3.139	0.0099
Layer on Well Located	0.260	1.039	0.0107
Steam Injection Rate	1.490	4.937	0.0167

Interpretation of the network performance is done based on not only errors of the predicted outputs but also errors of each testing cases that is calculated by taking arithmetic average of all outputs errors. It is seen in above error table that not only average error but also maximum error of predicted outputs are less than 5 %. It can be concluded by saying that developing a separate ANN tool for only cyclic steam injection and adding functional links to both input and output layer provide high-level accuracy. Achieved improvement can be evaluated by comparing average error percentages of Inverse ANN-1A and Inverse ANN-1B in Table 5.10.

Table 5.10. Comparison of error (%) between Inverse ANN-1A and Inverse ANN-1B

CSI Design Parameters	Inverse ANN-1A Error (%)	Inverse ANN-1B Error (%)
Steam Quality	0.436	0.184
Steam Temperature	0.602	0.204
Soaking Period	2.832	1.192
Injection Period	3.602	1.286
Well Length	3.140	1.038
Layer on Well Located	0.750	0.260
Steam Injection Rate	5.027	1.490

5.2.3 Inverse ANN-2A

The Inverse ANN-2A tool is a predictor of the reservoir properties and the fractured inner zone design parameters by using existent performance indicators with cyclic steam stimulation design parameters. In this ANN tool, 82 %, 9 %, and 9 % of 555 generated data sets were used for training, validation, and testing of the network, respectively. The division of data sets was done by using *dividerand* function of MATLAB. The developed artificial neural network contains a single hidden layer with 200 neurons. Tan-sigmoid *(tansig)* activation function was used in the hidden layer while the scaled conjugate gradient *(trainscg)* training function was applied in the output layer. The network structure is illustrated in the Figure 5.56.

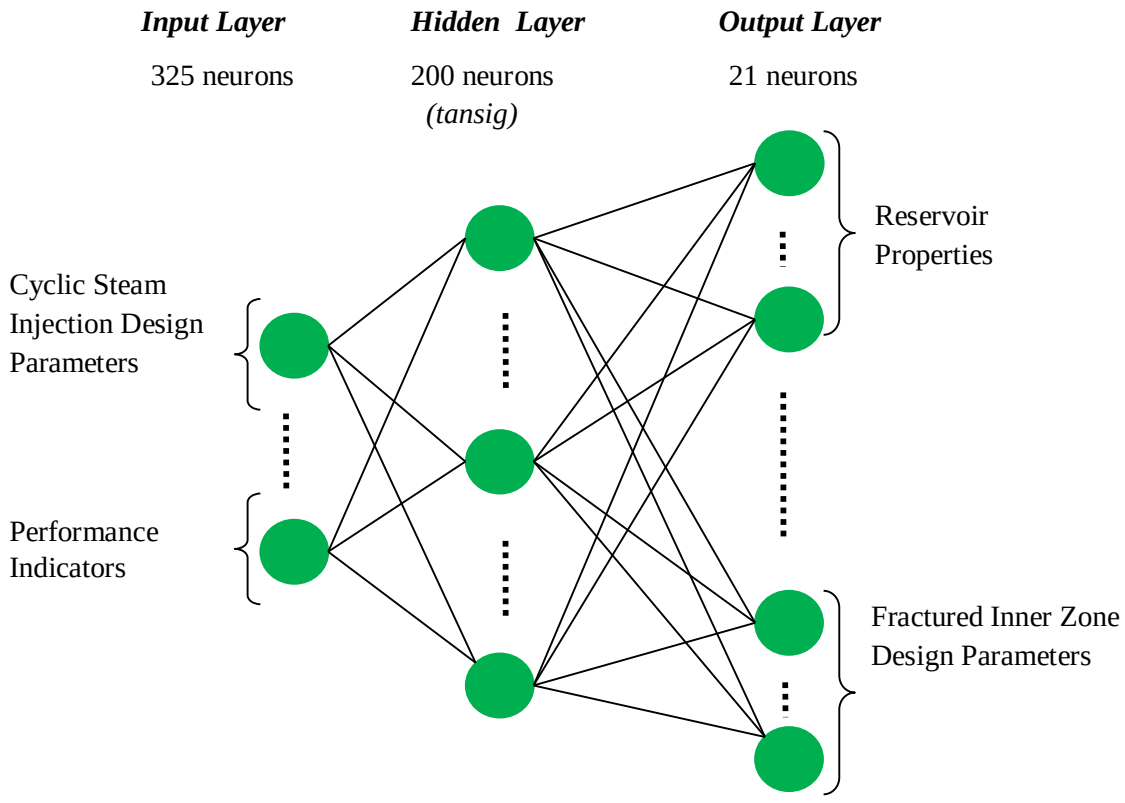

Figure 5.56 Network structure for the inverse ANN-2A

Input layer includes a total of 325 neurons; 7 of them are cyclic steam injection design parameters, 312 of them belong to performance indictors while 6 of them are functional links listed in Table 5.12. Output layer has 21 neurons; 10 of them are reservoir properties, 6 of them are fractured inner zone design parameters and 5 of them are functional links. Input and output components used in the training of this ANN model are summarized in Table 5.11. Logarithmic transformations of some input and output parameters improve the prediction performance of this network, too.

Table 5.11. Input and output layer components of Inverse ANN-2A

INPUT	**Cyclic Steam Injection Design Parameters**	Steam Quality Steam Temperature Soaking Period Injection Period Steam Injection Rate Well Length Layer on Well Located
	Performance Indicators	Oil Flow Rate (290) Number of Cycle (1) Project Cumulative Oil Production (1) Cumulative Oil Production (10) Production Period (10)
OUTPUT	**Reservoir Properties**	Thickness Matrix Porosity Fracture Porosity Matrix Permeability Fracture Permeability Fracture Spacing Initial Pressure Initial Oil Saturation Depth Initial Reservoir Temperature
	Fractured Inner Zone Design Parameters	Inner Zone Fracture Porosity Inner Zone Fracture Permeability Inner Zone Fracture Spacing Major Axis of Inner Zone Minor Axis of Inner Zone Drainage Area

Effectiveness of different functional link combinations was tested whether they improve the network performance, or not. Addition of these links to the input layer is more effective, thus; the relations of cyclic steam injection design parameters were focused. For example, injection volume that provides a relationship between the injection period and injection rate was added as a function. In this network structure, 6 functional links corresponding to cyclic steam stimulation design parameters and 5 functional links corresponding to reservoir properties were used in the input layer and output layer, respectively. All used functional links are listed in Table 5.12.

Table 5.12. Functional links of Inverse ANN-2A

Input Functional Links	Output Functional Links
log((Steam Quality)*100)	(Matrix Porosity / Fracture Porosity)
(Steam Temperature)$^{0.5}$	(Fracture Permeability / Matrix Permeability)
(Well Length)$^{0.5}$	(Inner Zone Fracture Porosity / Fracture Porosity)
(Injection Period)$^{0.5}$	Inner Zone Fracture Permeability / Fracture Permeability
(Steam Injection Rate)$^{0.5}$	(Major Axis / Minor Axis of Inner Zone)
(Steam Injection Rate)*(Injection Period)	

Performance of the network is evaluated depending on error percentages of predicted outputs and functional links. If lower error percentages are achieved for functional links, value of reservoir properties can be calculated by using them. For example, when accurate prediction of matrix porosity is obtained, fracture porosity can be calculated from their ratios. Results of the fracture porosity that are obtained from the network predictions and functional links are compared. One of them that has the most accurate value can be used for calculation of inner zone fracture porosity. Therefore, predictions that are more accurate can be provided for those 3 important outputs. Same procedure can be applied for other outputs by using all functional links. The comparisons between the predicted values of reservoir properties *(ANN)* and results of numerical simulator for the testing datasets are shown from the Figure 5.57 through Figure 5.72.

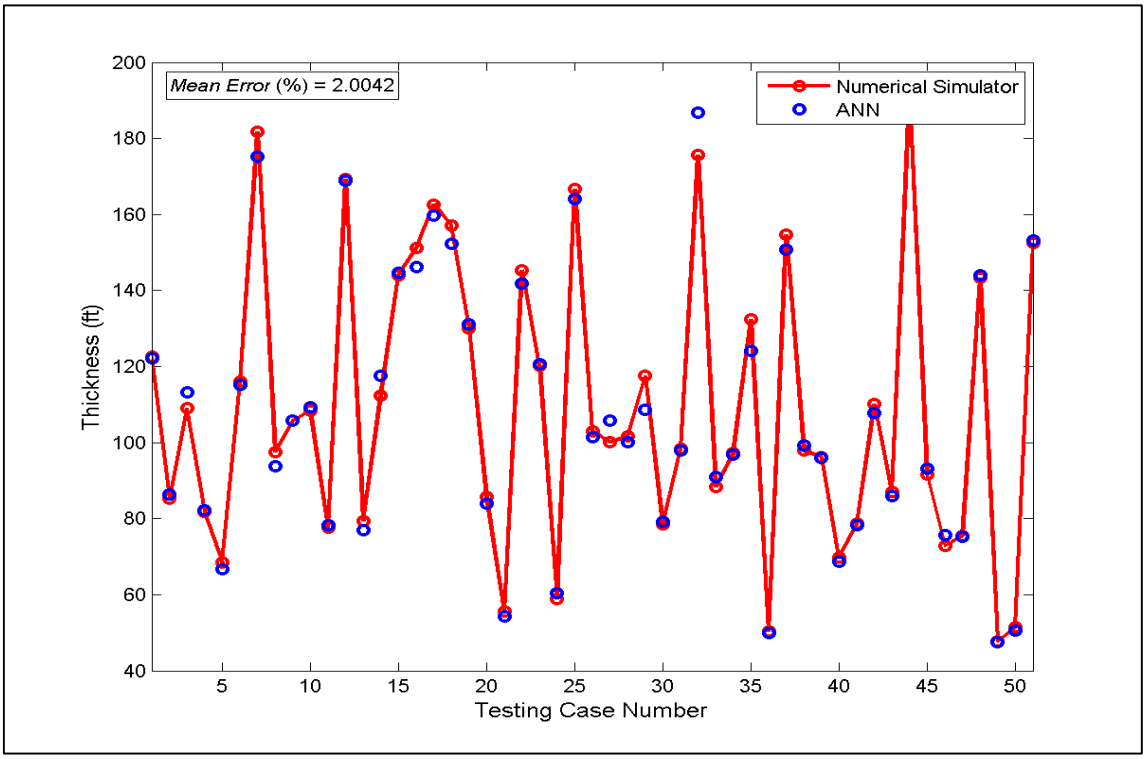

Figure 5.57 Comparison of simulator and predicted thickness for Inverse ANN-2A

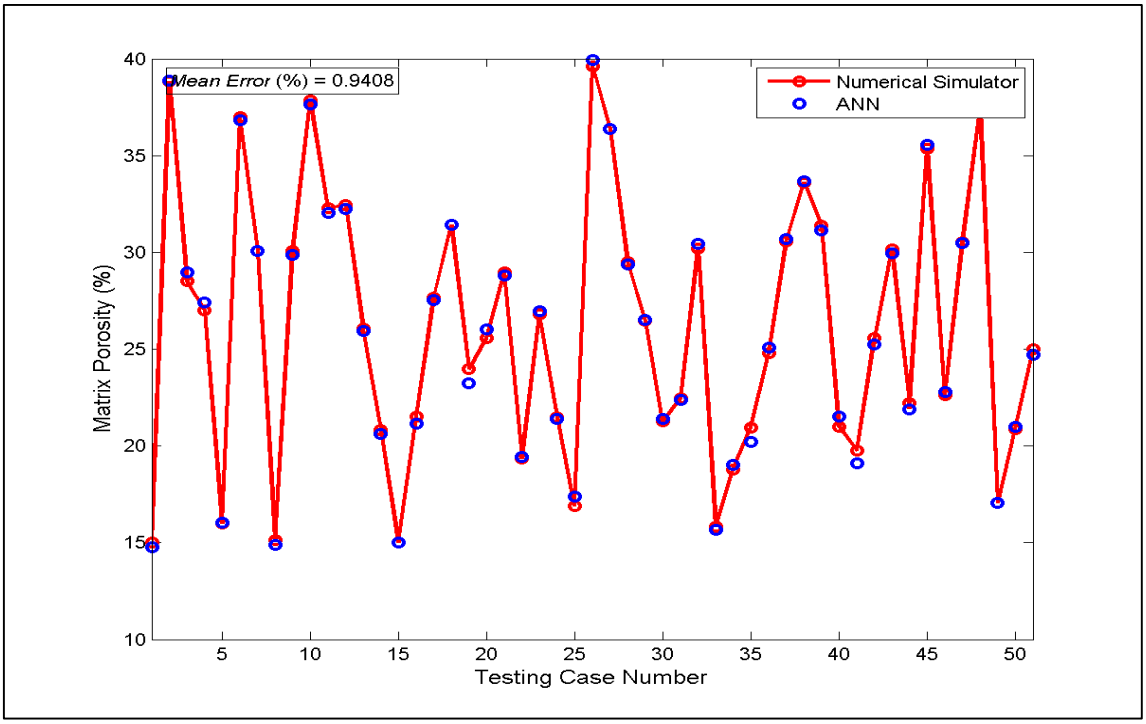

Figure 5.58 Comparison of simulator and predicted matrix porosity for Inverse ANN-2A

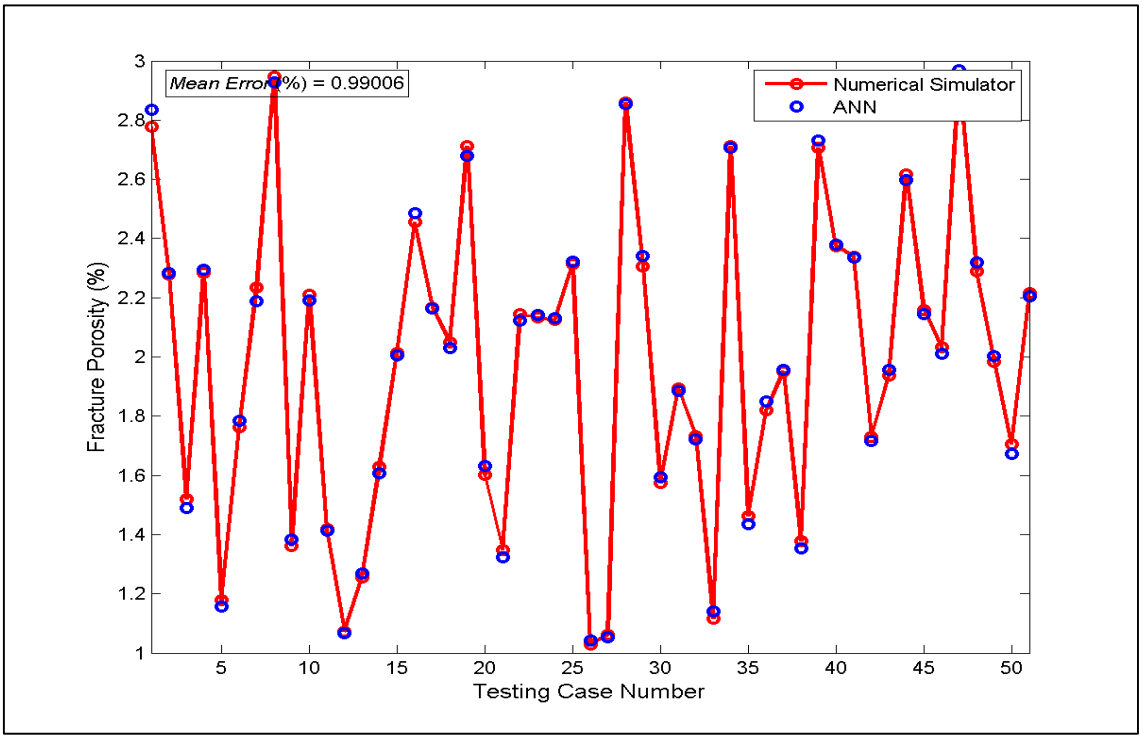

Figure 5.59 Comparison of simulator and predicted fracture porosity for Inverse ANN-2A

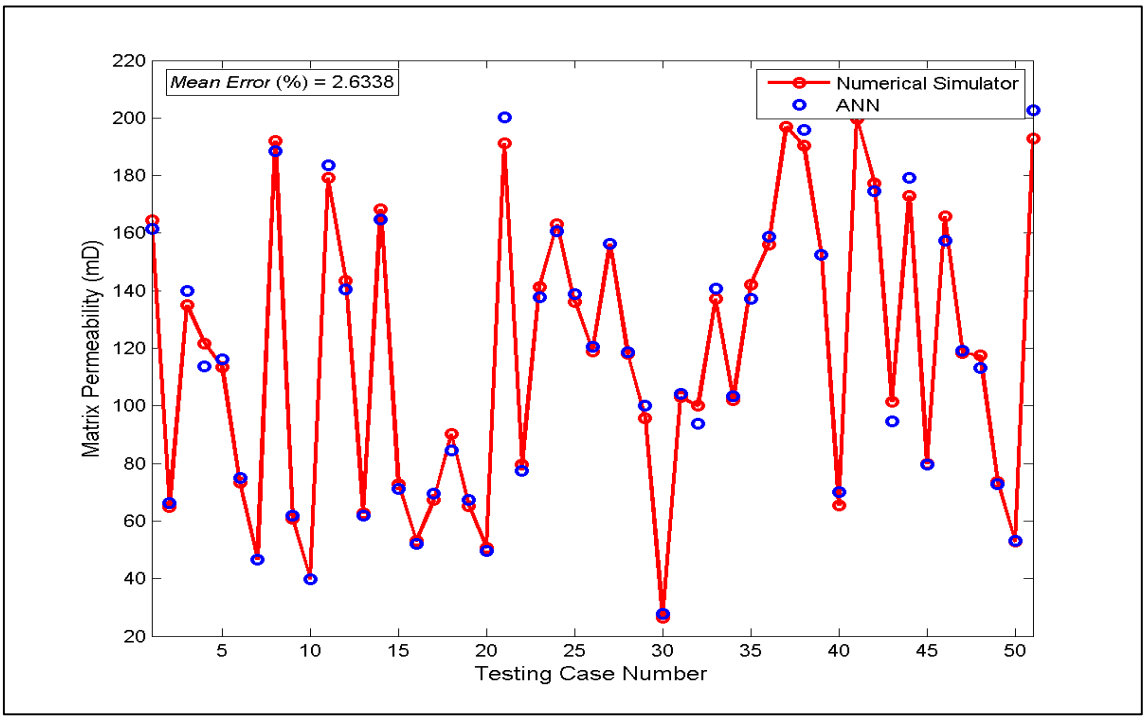

Figure 5.60 Comparison of simulator and predicted matrix permeability for Inverse ANN-2A

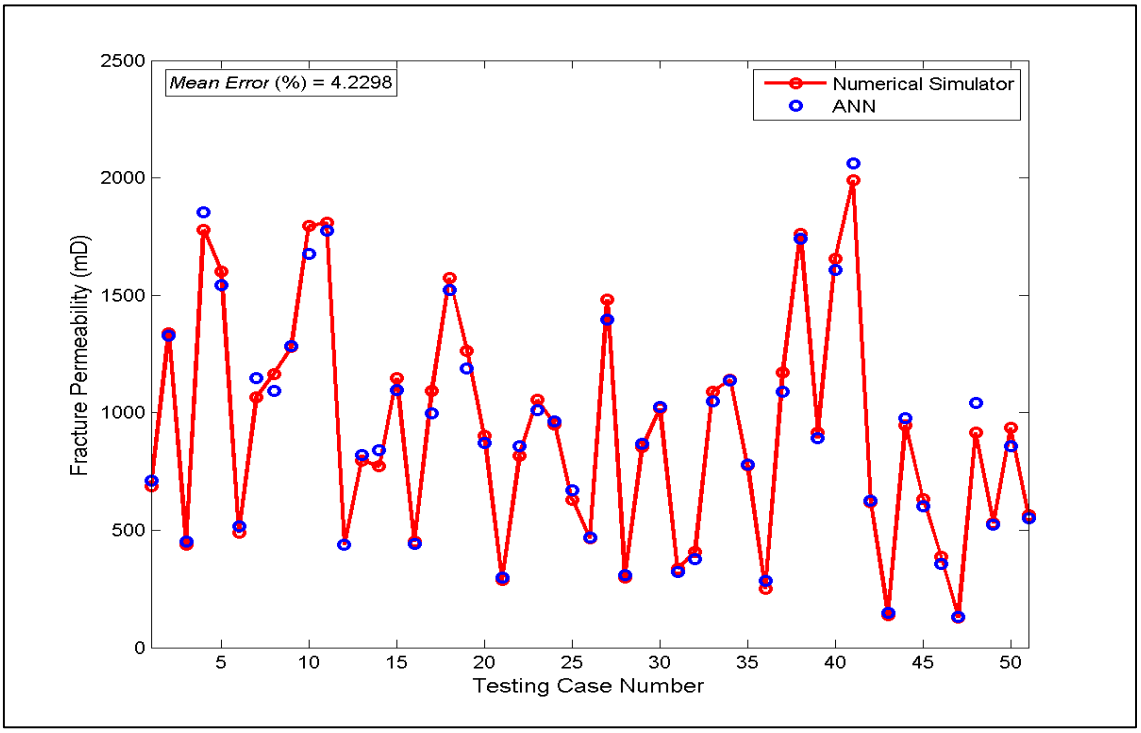

Figure 5.61 Comparison of simulator and predicted fracture permeability for Inverse ANN-2A

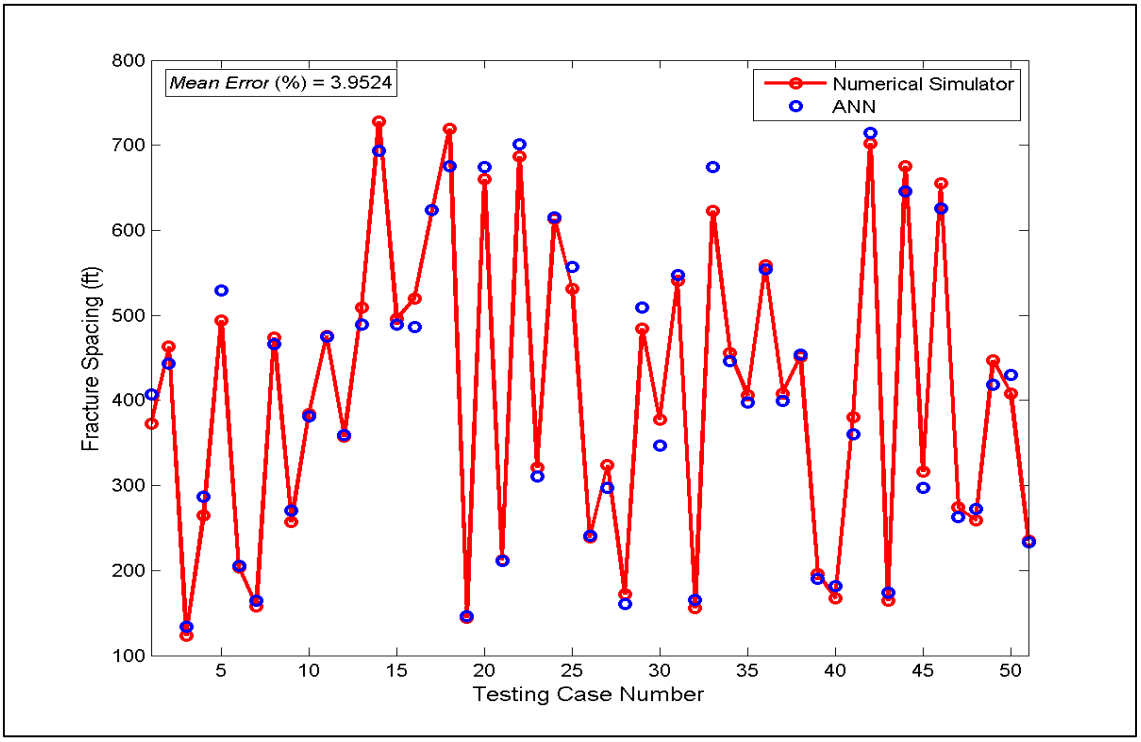

Figure 5.62 Comparison of simulator and predicted fracture spacing for Inverse ANN-2A

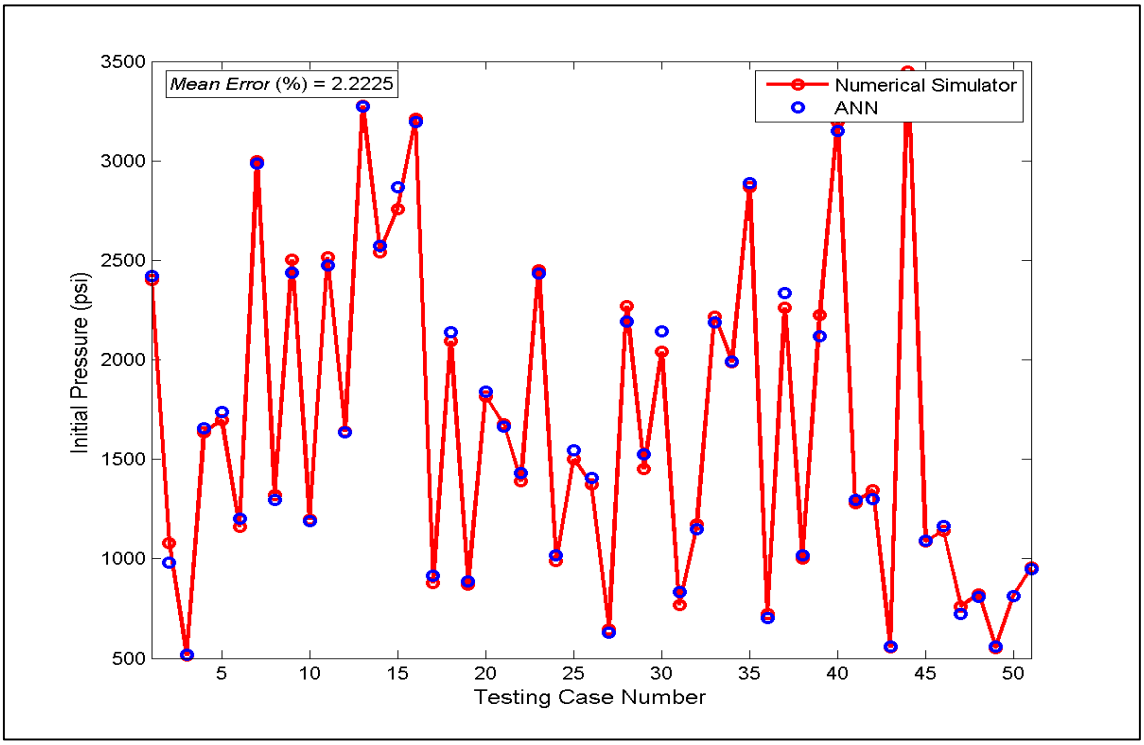

Figure 5.63 Comparison of simulator and predicted initial pressure for Inverse ANN-2A

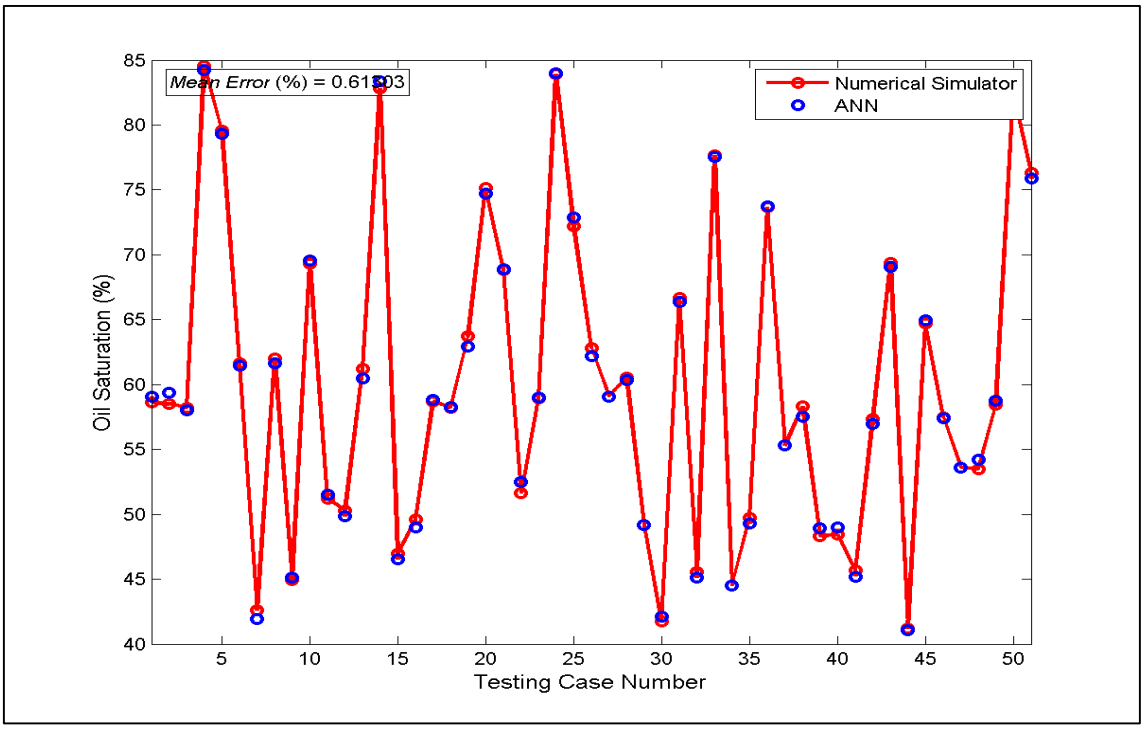

Figure 5.64 Comparison of simulator and predicted oil saturation for Inverse ANN-2A

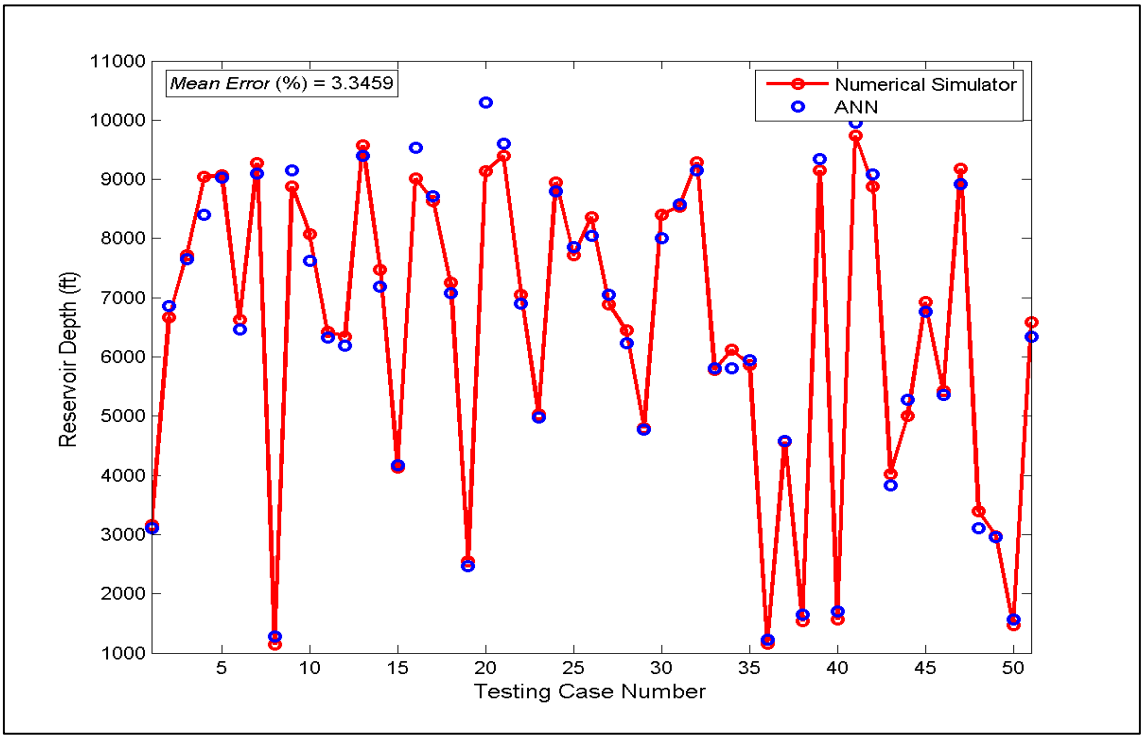

Figure 5.65 Comparison of simulator and predicted reservoir depth for Inverse ANN-2A

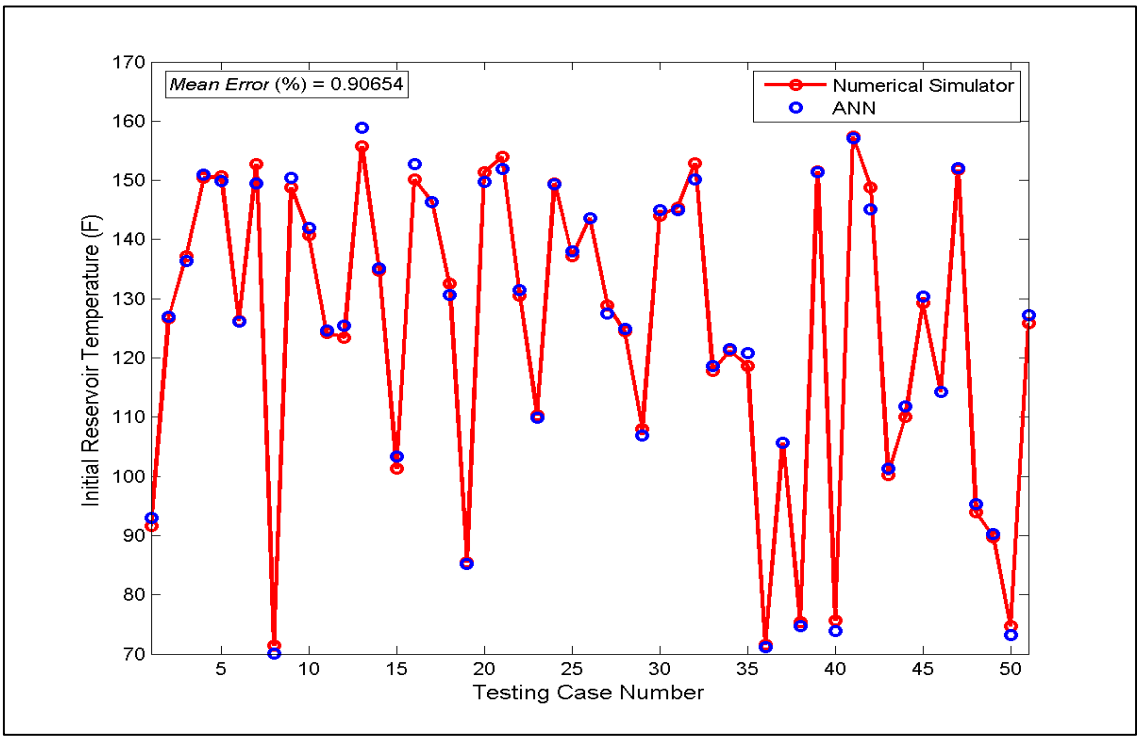

Figure 5.66 Comparison of simulator and predicted initial reservoir temperature for Inverse ANN-2A

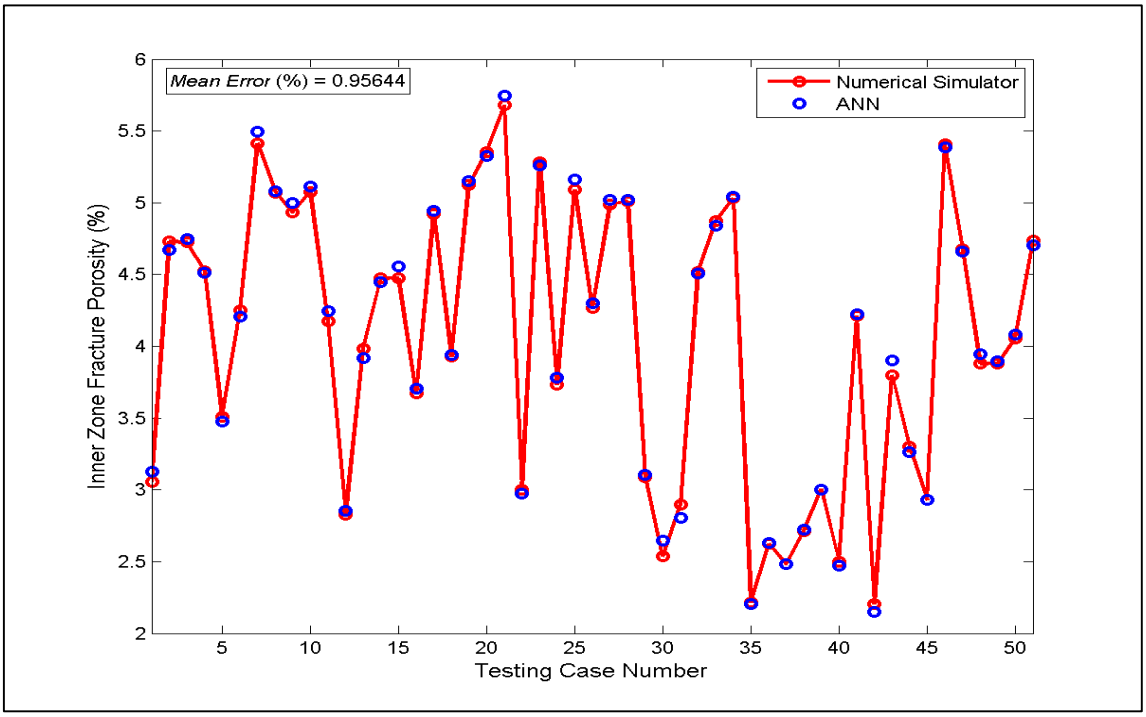

Figure 5.67 Comparison of simulator and predicted inner zone fracture porosity for Inverse ANN-2A

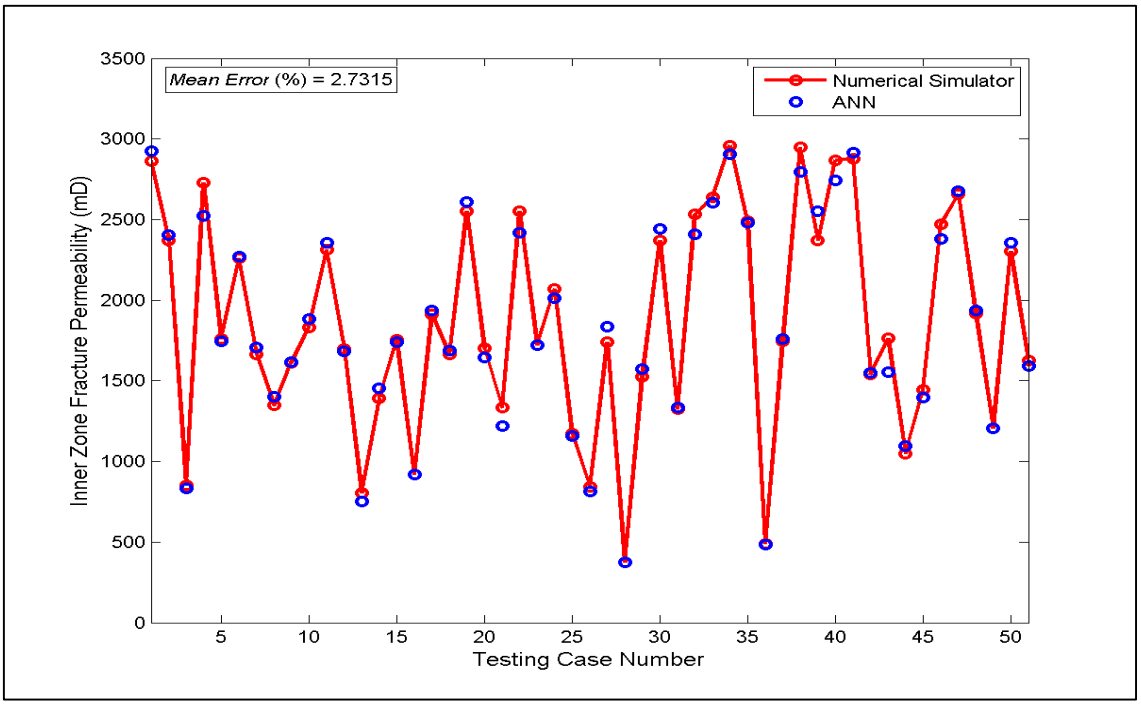

Figure 5.68 Comparison of simulator and predicted inner zone fracture permeability for Inverse ANN-2A

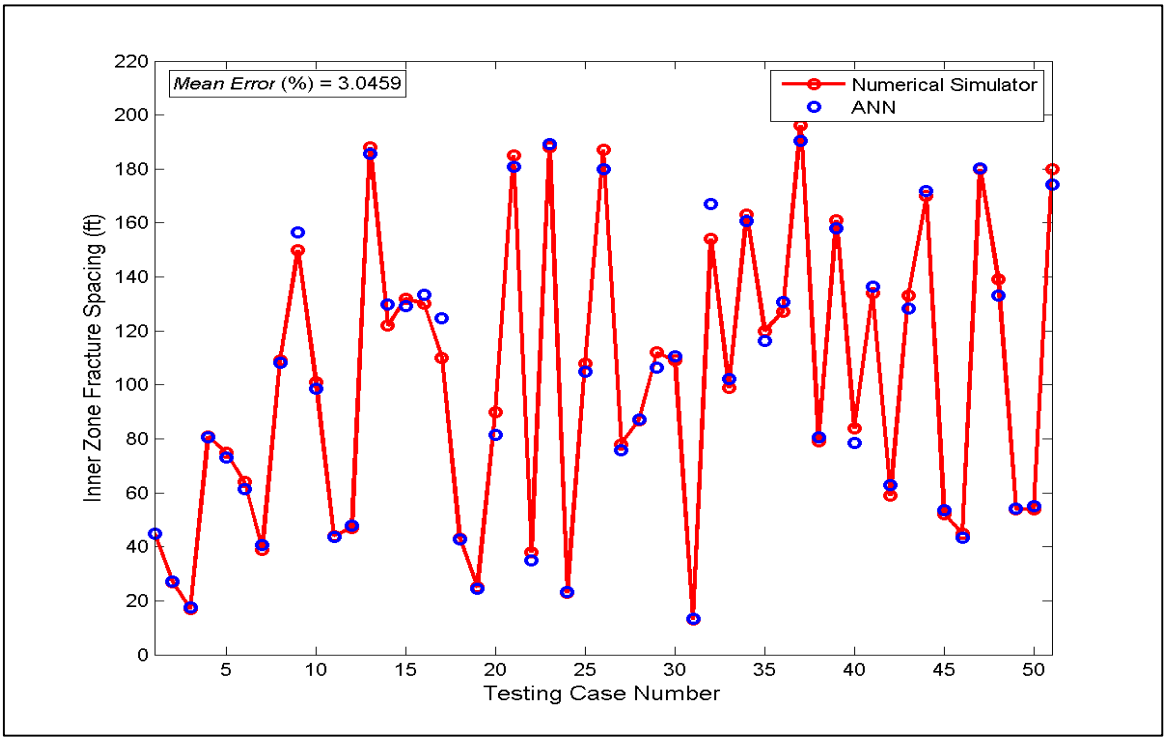

Figure 5.69 Comparison of simulator and predicted inner zone fracture spacing for Inverse ANN-2A

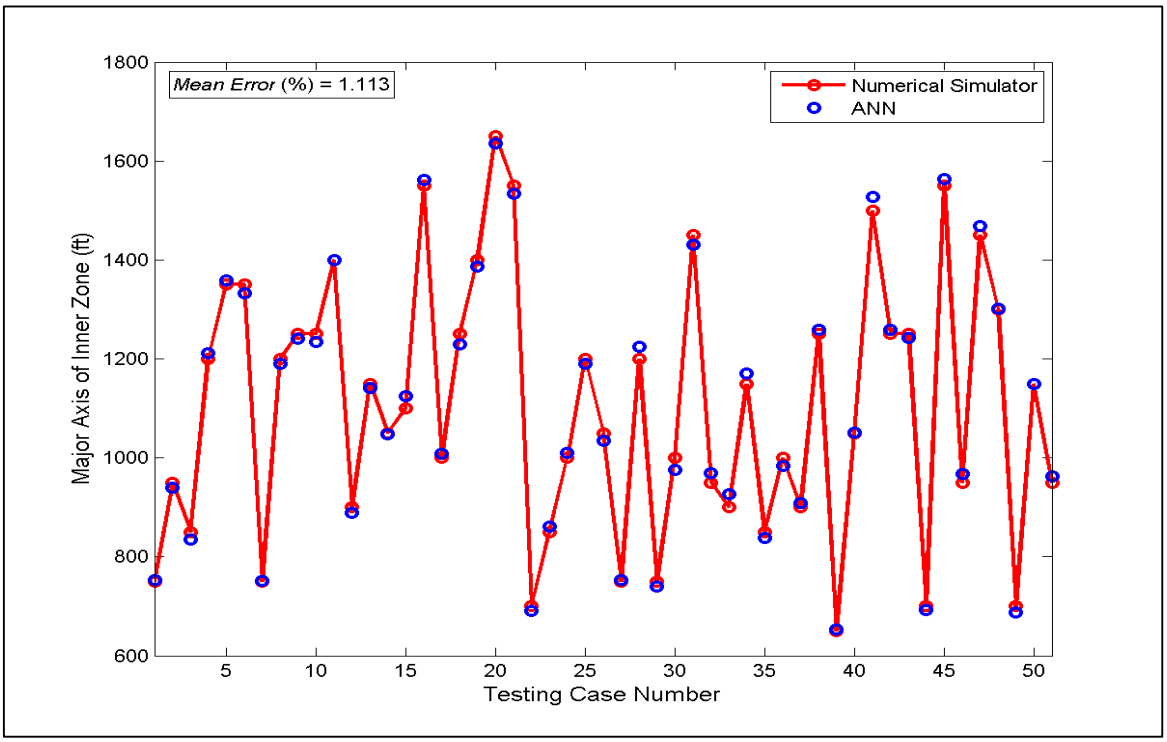

Figure 5.70 Comparison of simulator and predicted major axis of inner zone for Inverse ANN-2A

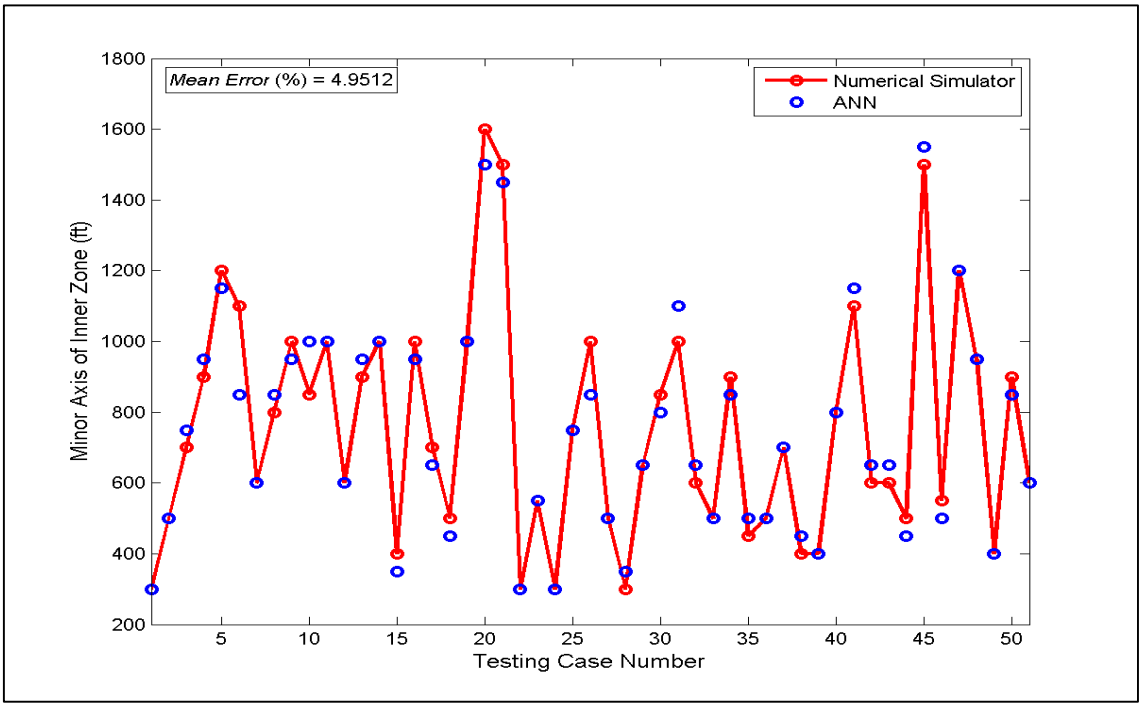

Figure 5.71 Comparison of simulator and predicted minor axis of inner zone for Inverse ANN-2A

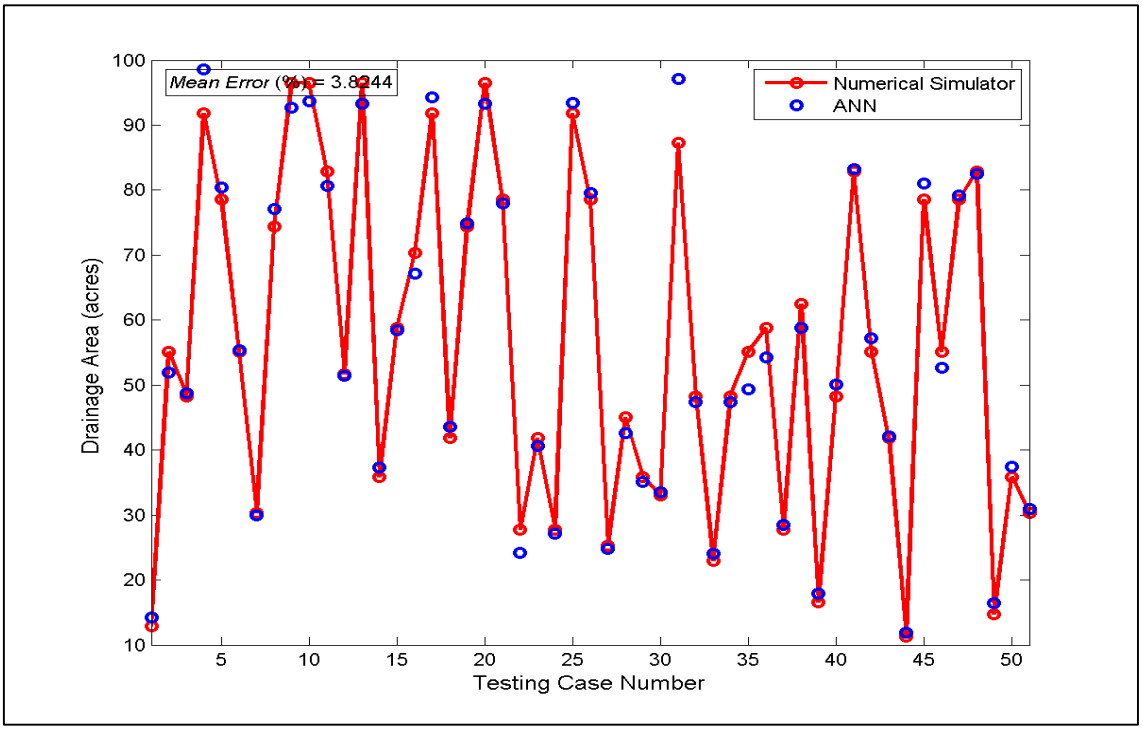

Figure 5.72 Comparison of simulator and predicted drainage area for Inverse ANN-2A

Even if it is possible to see average errors of each predicted properties on the top of corresponding figures, they are summarized in Table 5.13, also.

Table 5.13. Errors (%) for Inverse ANN-2A

Predicted Properties	Average error (%)	Maximum error (%)	Minimum error (%)
Thickness	2.004	7.583	0.081
Matrix Porosity	0.940	3.670	0.017
Fracture Porosity	0.990	2.0613	0.067
Matrix Permeability	2.633	7.126	0.002
Fracture Permeability	4.229	13.899	0.092
Fracture Spacing	3.952	9.206	0.073
Initial Pressure	2.222	9.025	0.017
Initial Oil Saturation	0.613	1.650	0.002
Depth	3.345	12.704	0.028
Initial Reservoir Temperature	0.906	2.459	0.003
Inner Zone Fracture Porosity	0.956	4.335	0.015
Inner Zone Fracture Permeability	2.731	11.848	0.056
Inner Zone Fracture Spacing	3.046	13.356	0.080
Major Axis of Inner Zone	1.113	2.989	0.053
Minor Axis of Inner Zone	4.951	12.115	0.305
Drainage Area	3.824	12.902	0.329

Interpretation of the network performance is done based on both the errors of predicted outputs and the average errors of each testing cases that is calculated by taking arithmetic average of all outputs errors. Even if maximum error percentages of some properties exceed the desired tolerance, the network provides accurate predictions. It is seen in the second column of the above error table that average errors of all predicted parameters are less than 5 %. However, it is considered to get more accurate results for especially fractured inner zone design parameters. Therefore, developing of Inverse ANN-2B tool that has lower error percentages is considered. Structure and performance of this network are discussed in the next section.

5.2.4 Inverse ANN-2B

The Inverse ANN-2B tool is a predictor of the fractured inner zone design parameters by using performance indicators and cyclic steam stimulation design parameters with corresponding reservoir properties. In this ANN tool, 555 data sets were used and they were divided randomly as 82 %, 9 %, and 9 % for training, validation, and testing, respectively. A single hidden with 44 neurons provides high-level accuracy on predictions. Tan-sigmoid *(tansig)* activation function and the scaled conjugate gradient *(trainscg)* training function were used in the hidden layer and output layer, respectively. The network structure is illustrated in the Figure 5.73.

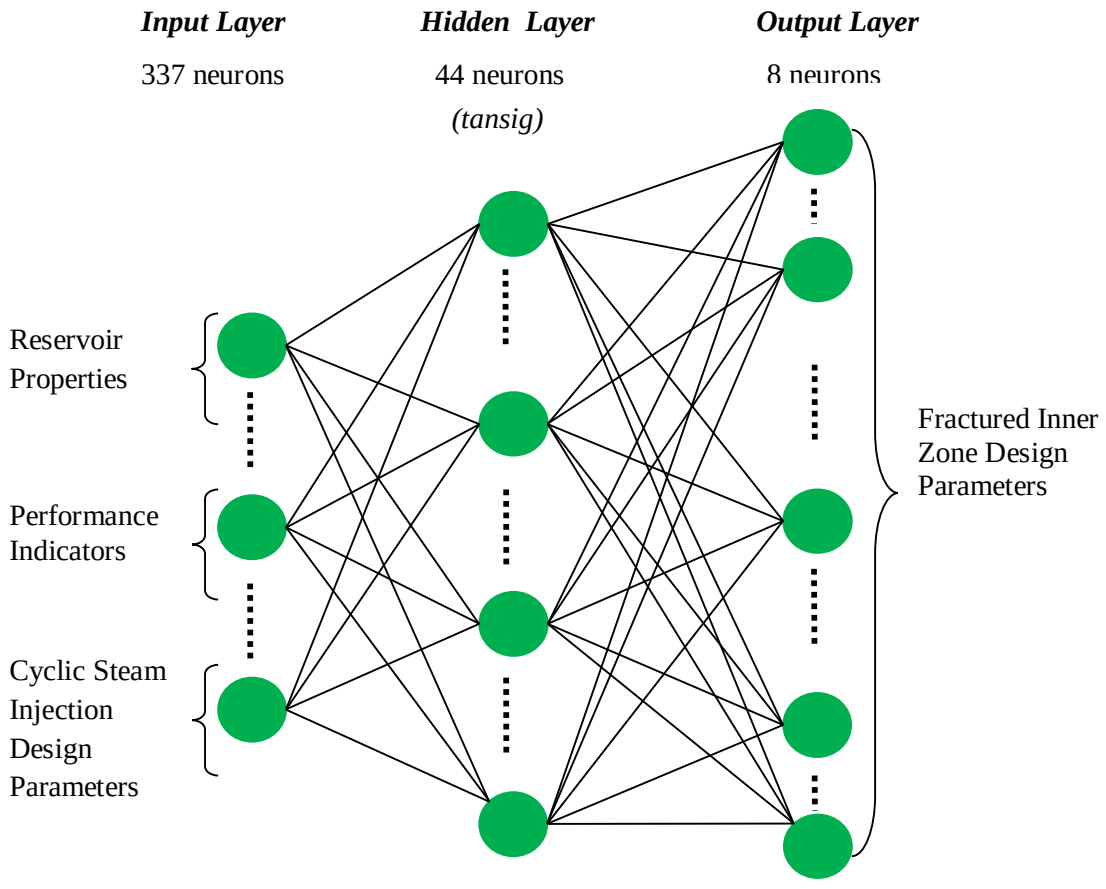

Figure 5.73 Network structure for the inverse ANN-2B

There are 337 input neurons as it is seen from the network structure figure and 10 of them are reservoir properties, 312 of them are performance indicators while 7 of them belong to cyclic steam injection design parameters. Same 6 functional links are kept from the previous network and 2 more functional links are added for the reservoir properties to the input layer. Output layer has just 8 neurons; 6 of them are fractured inner zone design parameters and 2 of them are functional links. Input and output components that were used in the training of this ANN model are summarized in Table 5.14. Logarithm of some input and output parameters were taken.

Table 5.14. Input and output layer components of Inverse ANN-2B

INPUT	**Reservoir Properties**	Thickness Matrix Porosity Fracture Porosity Matrix Permeability Fracture Permeability Fracture Spacing Initial Pressure Initial Oil Saturation Depth Initial Reservoir Temperature
	Performance Indicators	Oil Flow Rate (290) Number of Cycle (1) Project Cumulative Oil Production (1) Cumulative Oil Production (10) Production Period (10)
	Cyclic Steam Injection Design Parameters	Steam Quality Steam Temperature Soaking Period Injection Period Steam Injection Rate Well Length Layer on Well Located
OUTPUT	**Fractured Inner Zone Design Parameters**	Inner Zone Fracture Porosity Inner Zone Fracture Permeability Inner Zone Fracture Spacing Major Axis of Inner Zone Minor Axis of Inner Zone Drainage Area

Effectiveness of using different functional links was observed whether they improve the network performance, or not. All functional links used in the input layer of Inverse ANN-2A and some of the functional links used in the input layer of Inverse ANN-1B are combined for the input layer of this network. Only 2 functional links corresponding to fractured inner zone design parameters are assigned for the output layer and they are listed in Table 5.15.

Table 5.15. Functional links of Inverse ANN-2B

Input Functional Links	Output Functional Links
log((Steam Quality)*100) (Steam Temperature)$^{0.5}$ (Well Length)$^{0.5}$ (Injection Period)$^{0.5}$ (Steam Injection Rate)$^{0.5}$ (Steam Injection Rate)*(Injection Period) (Matrix Porosity / Fracture Porosity) (Fracture Permeability / Matrix Permeability)	(Major Axis - Minor Axis of Inner Zone) (Major Axis / Minor Axis of Inner Zone)

Accuracy of the network is controlled by error percentages of the predicted design parameters and functional links of the output layer. In case the lower error percentages are achieved for functional links, value of fractured inner zone design parameters can be calculated by using them. For example, when accurate predictions of major axis inner area are obtained, minor axis of it can be calculated by using two functional links. Therefore, the most accurate prediction of minor axis can be determined by comparing results that are obtained from predictions and functional links. The comparison between the predicted values of reservoir properties *(ANN)* and results of numerical simulator for the testing data sets are shown from the Figure 5.74 through Figure 5.79.

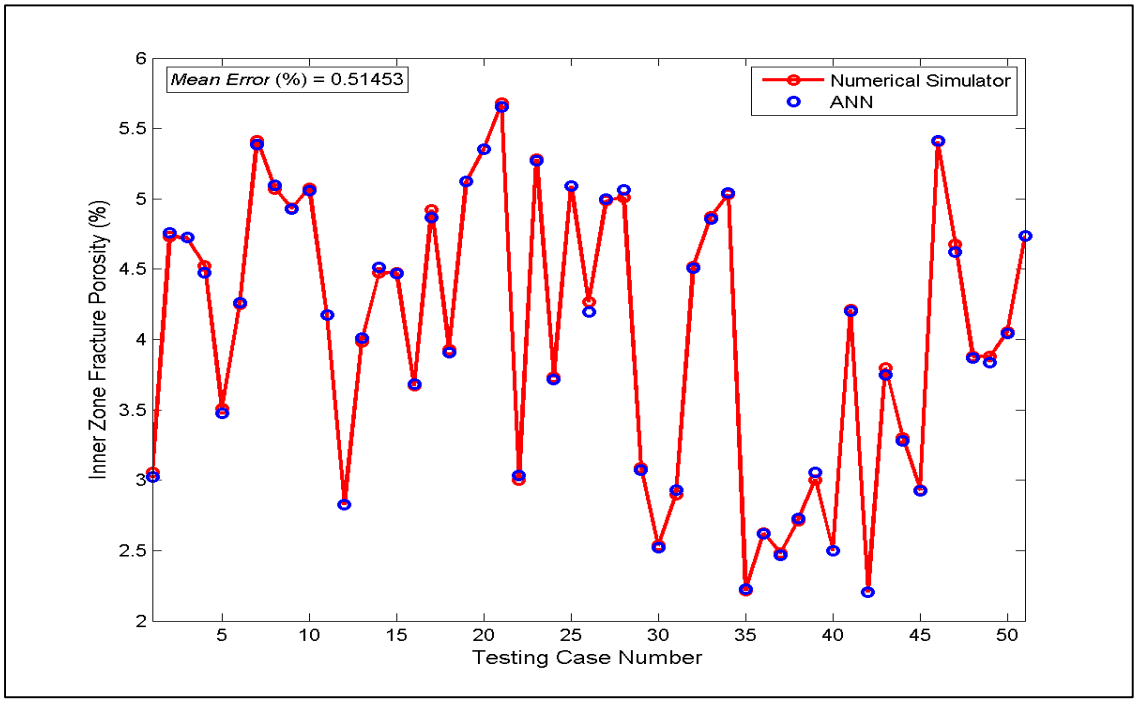

Figure 5.74 Comparison of simulator and predicted inner zone fracture porosity for Inverse ANN-2B

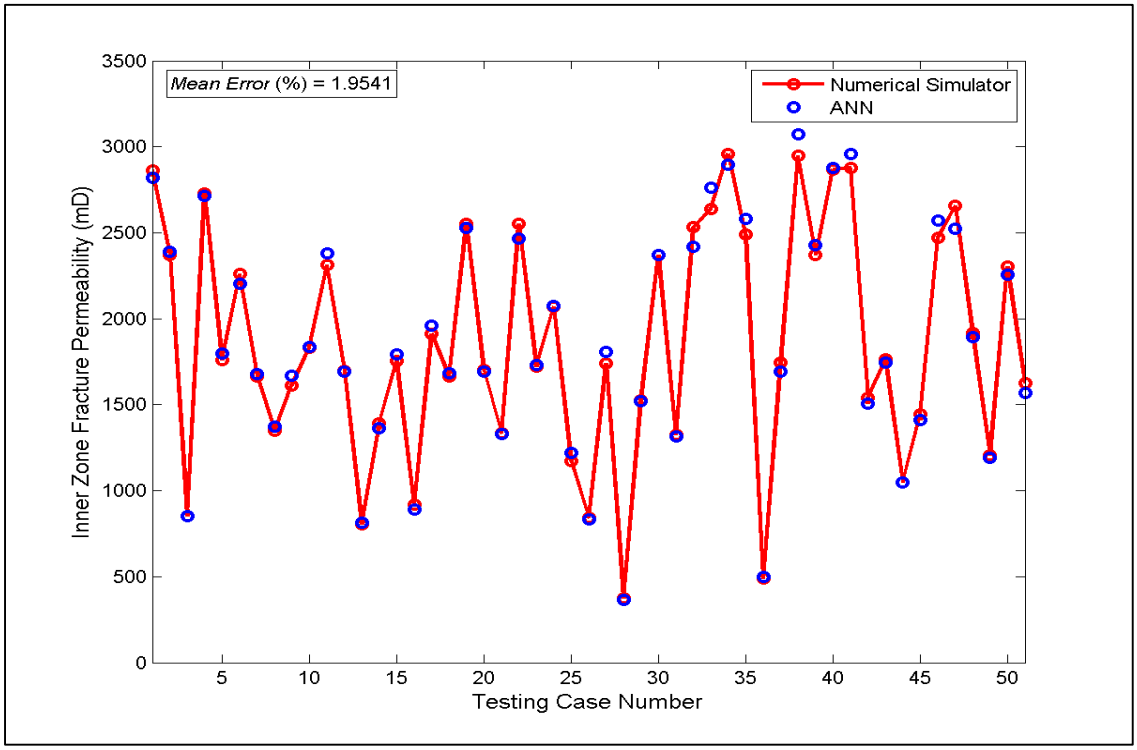

Figure 5.75 Comparison of simulator and predicted inner zone fracture permeability for Inverse ANN-2B

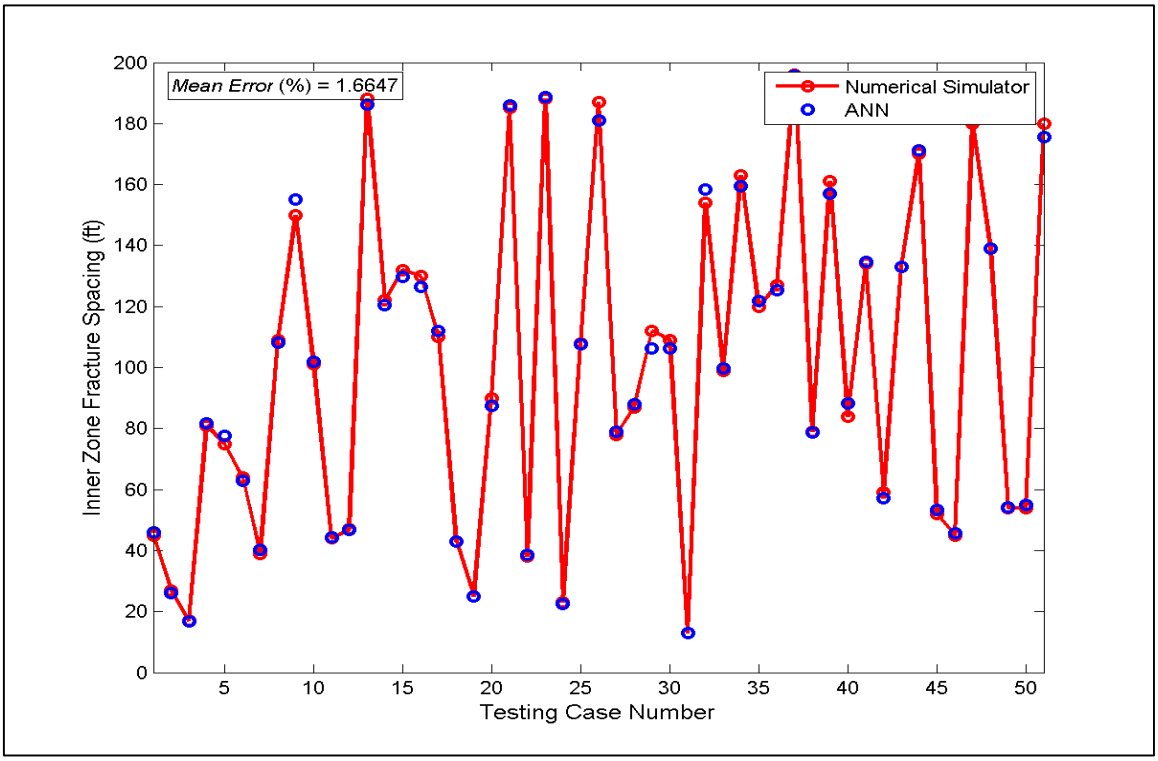

Figure 5.76 Comparison of simulator and predicted inner zone fracture spacing for Inverse ANN-2B

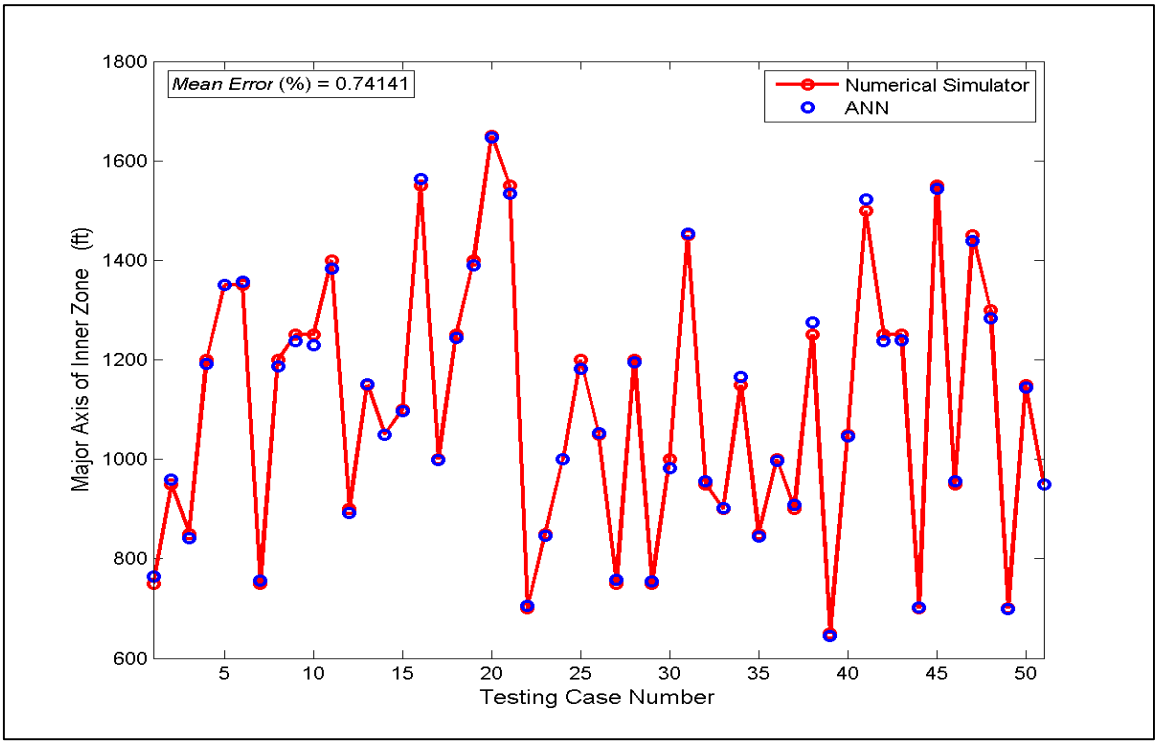

Figure 5.77 Comparison of simulator and predicted major axis of inner zone for Inverse ANN-2B

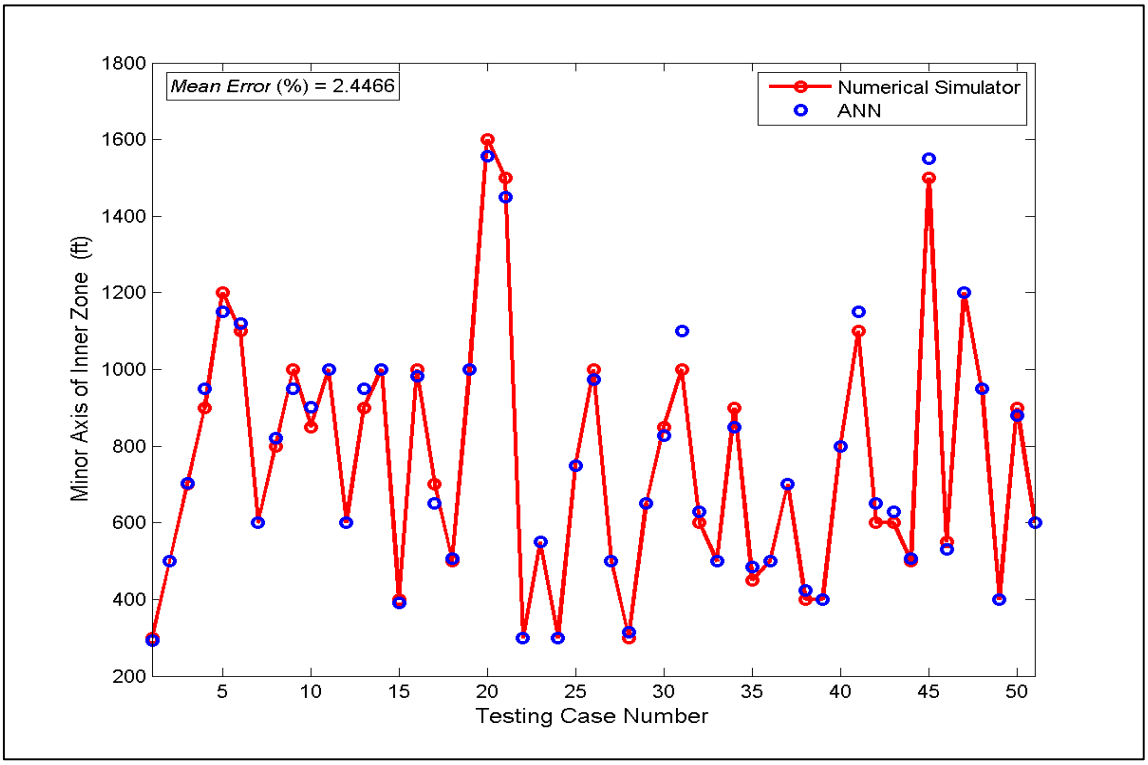

Figure 5.78 Comparison of simulator and predicted minor axis of inner zone for Inverse ANN-2B

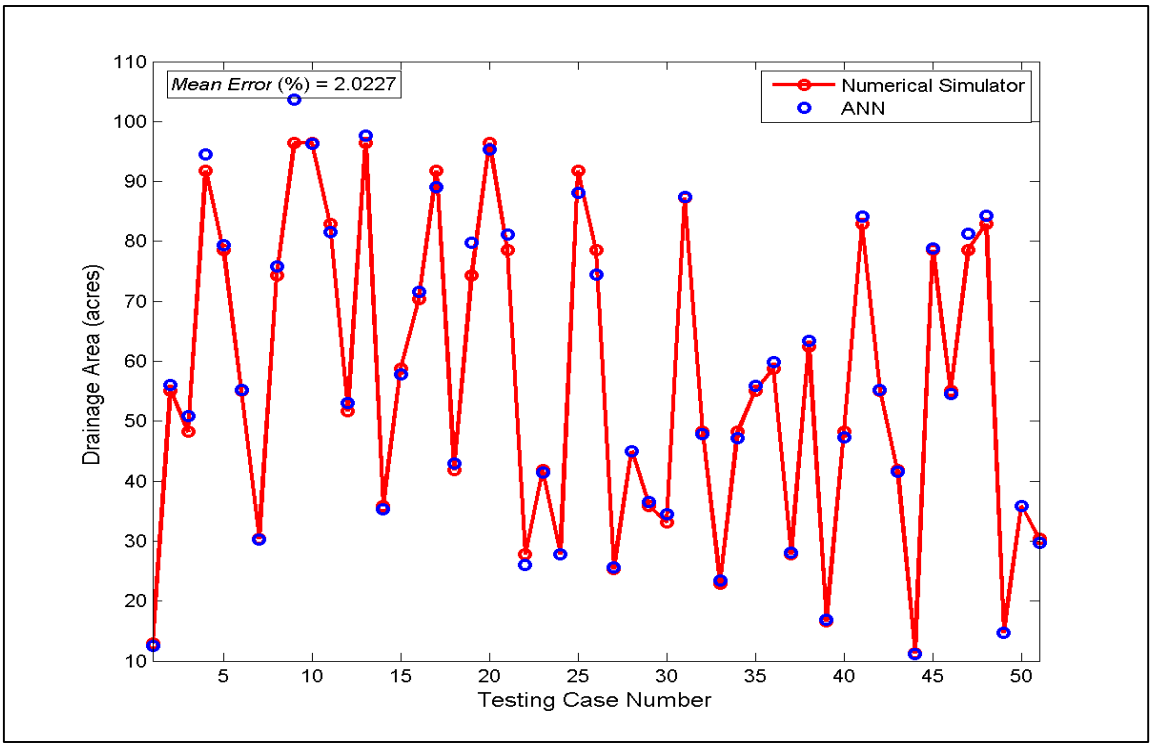

Figure 5.79 Comparison of simulator and predicted drainage area for Inverse ANN-2B

Even if it is possible to see average errors of each predicted properties on the top of corresponding figures, they are summarized in Table 5.16.

Table 5.16. Errors (%) for Inverse ANN-2B

Predicted Design Parameters	Average error (%)	Maximum error (%)	Minimum error (%)
Inner Zone Fracture Porosity	0.514	1.717	0.0049
Inner Zone Fracture Permeability	1.954	4.996	0.0339
Inner Zone Fracture Spacing	1.664	5.229	0.0461
Major Axis of Inner Zone	0.741	1.973	0.0034
Minor Axis of Inner Zone	2.446	9.349	0.0096
Drainage Area	2.022	7.390	0.0388

It is seen in the error table that only 2 design parameters have maximum error percentages which are higher than desired tolerance. The average errors of each parameter are less than 5 %. Moreover, significant progress is accomplished by developing a distinct ANN tool for fractured inner zone design parameters. Average error percentages of Inverse ANN-2A and Inverse ANN-2B are compared in Table 5.17 in order to see the improvement clearly.

Table 5.17. Comparison of errors (%) between Inverse ANN-2A and Inverse ANN-2B

Fractured Inner Zone Design Parameters	Inverse ANN-2A Error (%)	Inverse ANN-2B Error (%)
Inner Zone Fracture Porosity	0.956	0.514
Inner Zone Fracture Permeability	2.731	1.954
Inner Zone Fracture Spacing	3.046	1.664
Major Axis of Inner Zone	1.113	0.741
Minor Axis of Inner Zone	4.951	2.446
Drainage Area	3.824	2.022

Chapter 6

Graphical User Interface

A total of 6 neural network based proxy models were developed. Two of them were designed for forward-looking while four of them were assigned to inverse-looking problems. However, these networks are incorporated into a single screening toolbox by creating a graphical user interface (GUI) in order to provide an ease of use of the developed ANN tools. It is the most important point for user that this interface was developed by using tool of MATLAB R2009b. Instruction of the GUI is explained by screenshots in this section.

The main panel of the GUI which have 5 different tools corresponding to all developed networks is seen in Figure 6.1. The user has an option to select a predictor that he wants to study. The key point of this panel that forward ANN-1 and forward ANN-2 were incorporated into Tool-1 to provide an integrity for an evaluation of the production profile.

If the user selects the Tool-1, a new panel is opened which is designed for prediction of the perfromance indicators. Figure 6.2 displays the screenshot of GUI after Tool-1 is chosen. The user needs to enter valid input values for both reservoir properties and design parameters which are within the specified ranges. Then, it is required to click the simulation button. This tool is able to provide cumulative oil productions of each cycle with corresponding time in the " Network-I Outputs" section. In addition, number of cycle, peak oil flow rates and their corresponding time are given in the " Network-II Outputs" section. In addtion, cumulative oil production and oil flow rate are graphed as a function of time, seperately. Screenshot of simulated Tool-1 is shown in Figure 6.3.

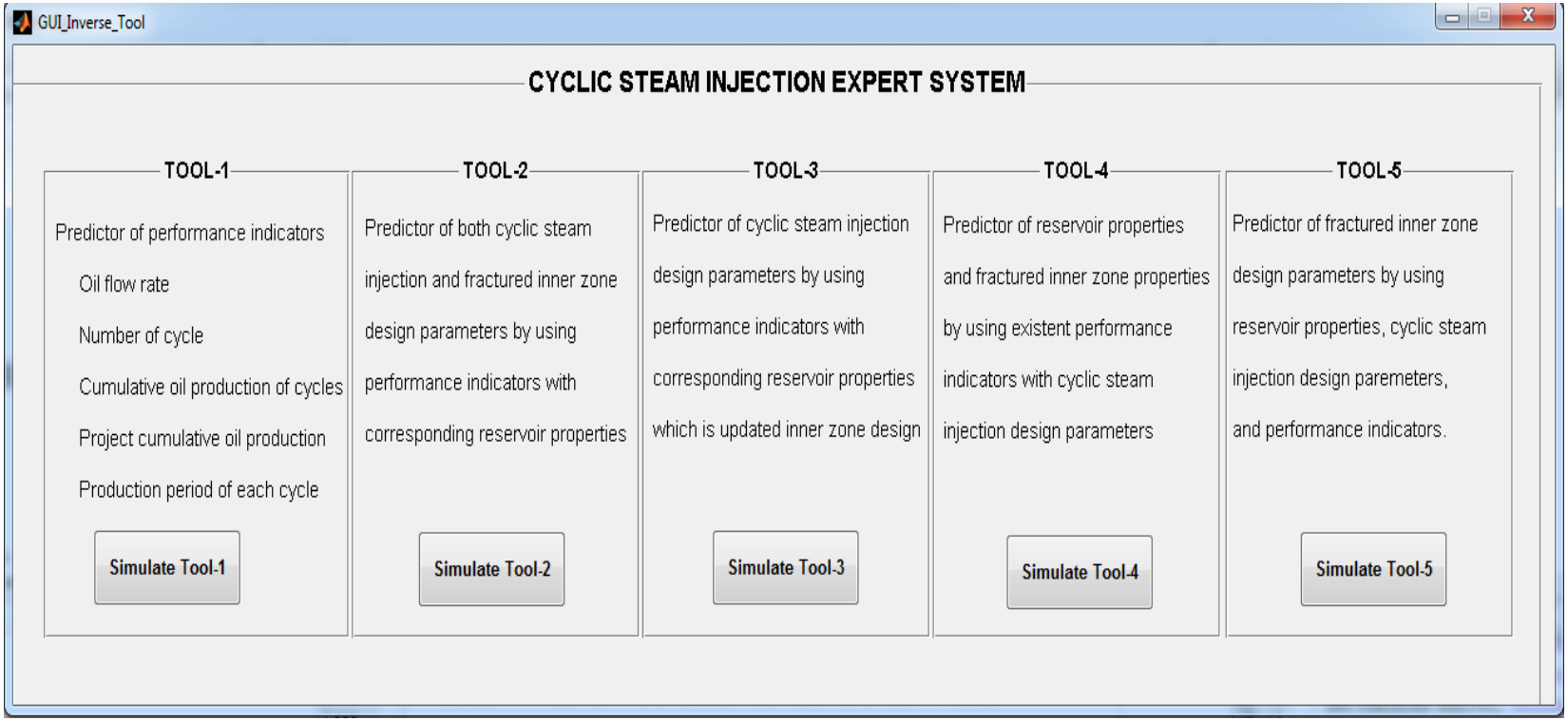

Figure 6.1 Main panel of graphical user interface

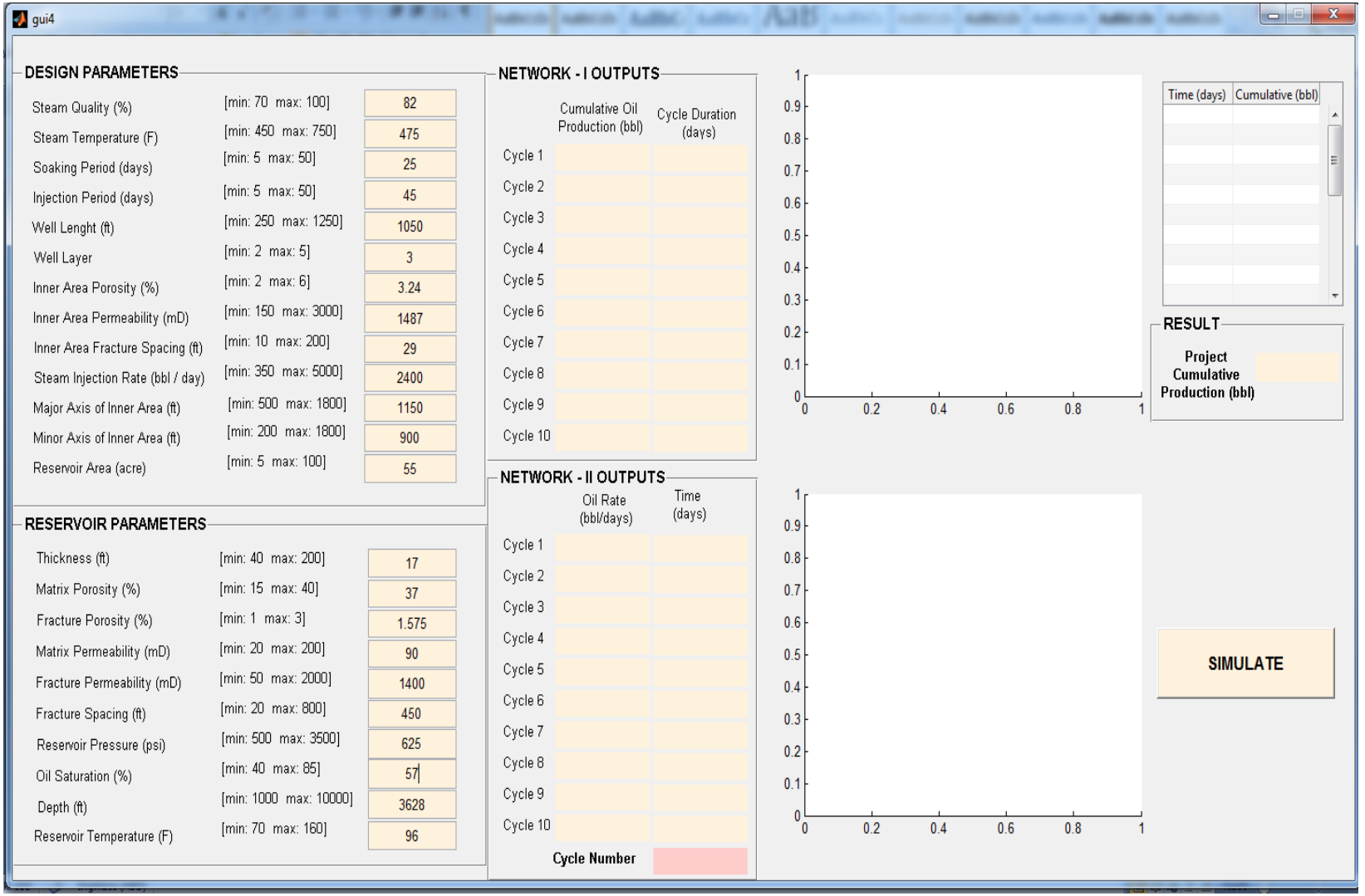

Figure 6.2 Graphical user interface for forward looking tool

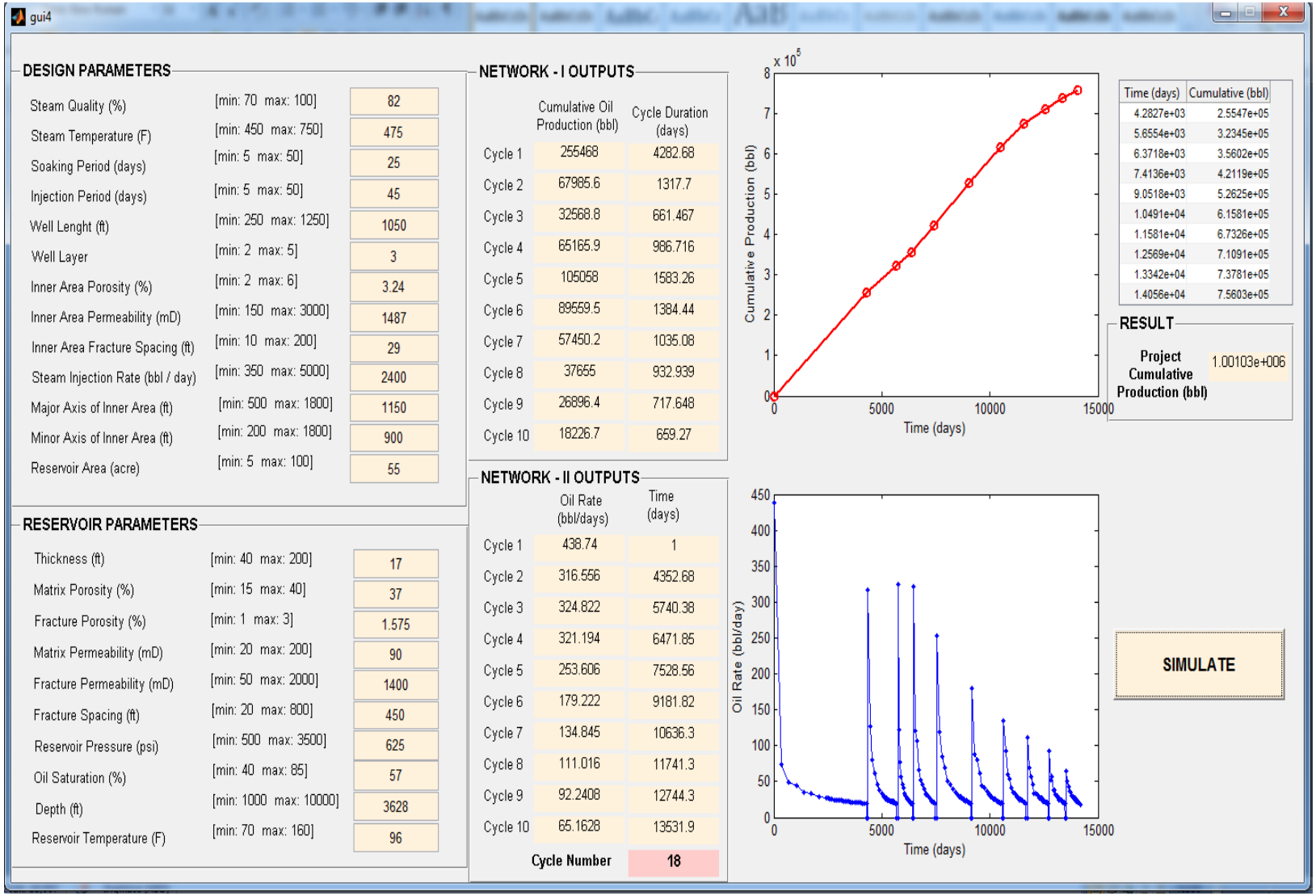

Figure 6.3 Graphical user interfaces for forward looking tool after simulation

When the user selects the Tool-2, a new panel is opened which is designed for the prediction of cyclic steam injection and fractured inner zone design parameters by using perfromance indicators with corresponding reservoir properties. Figure 6.4 shows the screenshot of GUI after Tool- 2 is chosen. First, the user is asked to enter cumulative oil production of ecah cycle with corresponding cycle duration. Second, the user needs to click the "Production Time" button which calcutes the time from cycle duration that user enteres in order to prepare data in the format of developed network. Third, the user wanted to upload oil flow rate data for calculated time by clicking "Load Oil Rate " button. Explained three steps are shown in Figure 6.5, Figure 6.6, and Figure 6.7, respectively. Finally, reservoir properties should be given with in the specified ranges as it is seen in Figure 6.8. This tool has an option to simulate design parameters seperately by two distinct pushbuttons. First pushbutton is assigned for prediction of cyclic steam injection parameters while second button is designed for estimation of fracture inner zone design parameters. Figure 6.9 shows the snapshot after simulation of Tool-2 is completed. Each step is shown in red circle in the figures.

Tool-3, Tool-4, and Tool-5 are created for an ease use of Inverse ANN-1B, Inverse ANN-2A and Inverse ANN-2B, respectively. They are designed by following steps which were explained deeply for Tool-2. Figure 6.10, Figure 6.11, and Figure 6.12 display the screenshots after simulation of these tools.

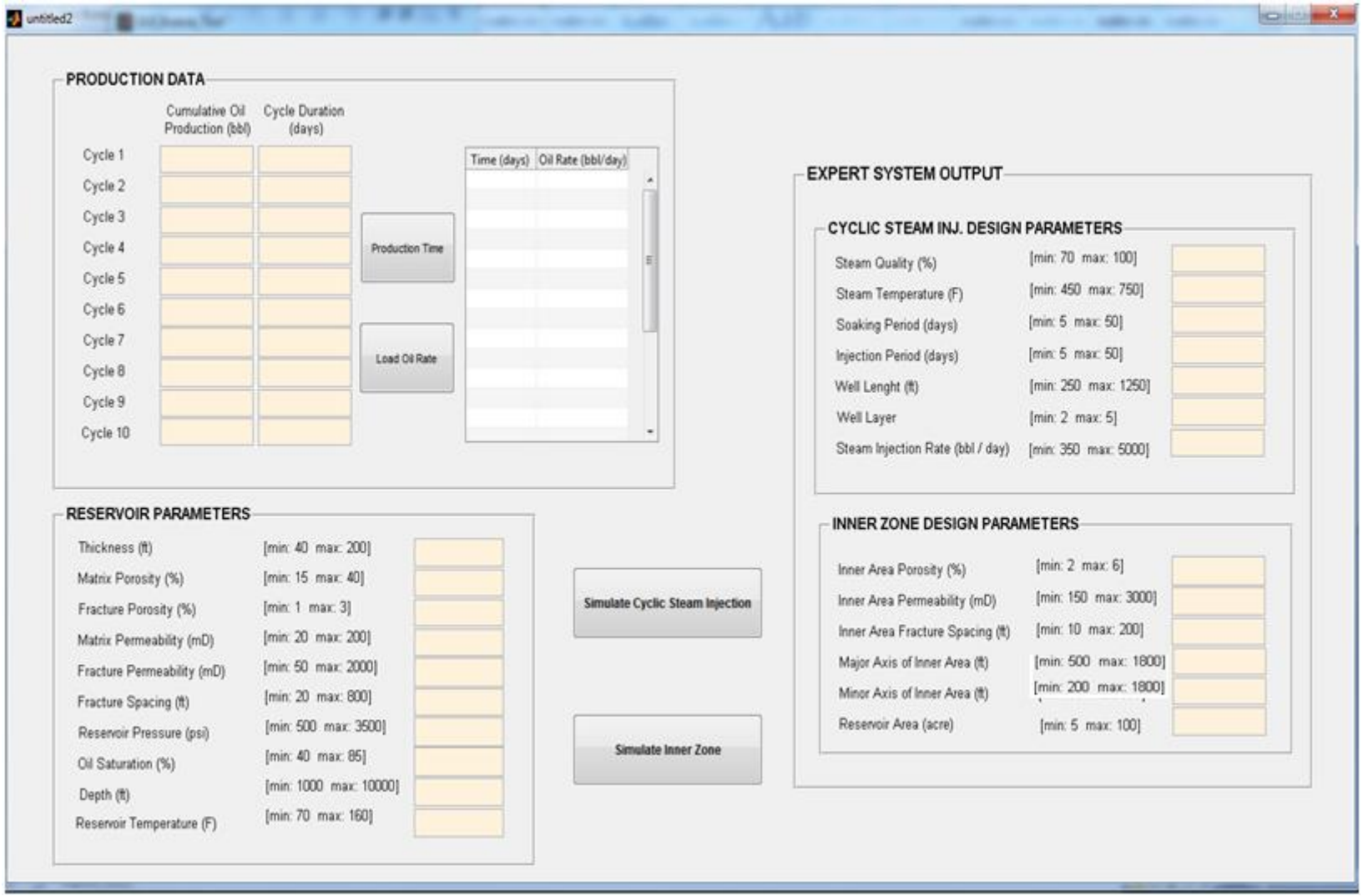

Figure 6.4 Graphical user interface for Inverse ANN-1A tool

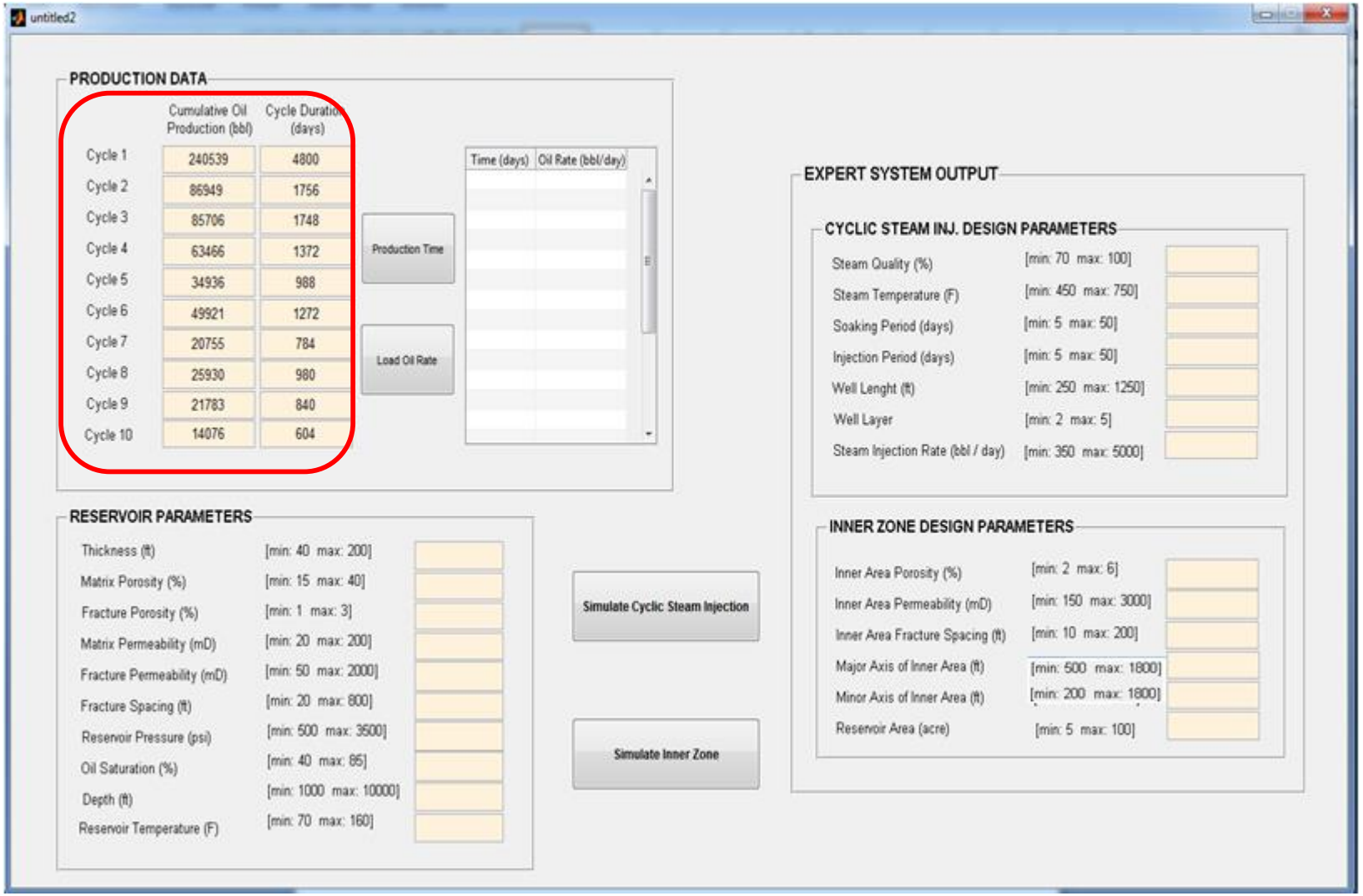

Figure 6.5 Step-1 of graphical user interface for Inverse ANN-1A tool

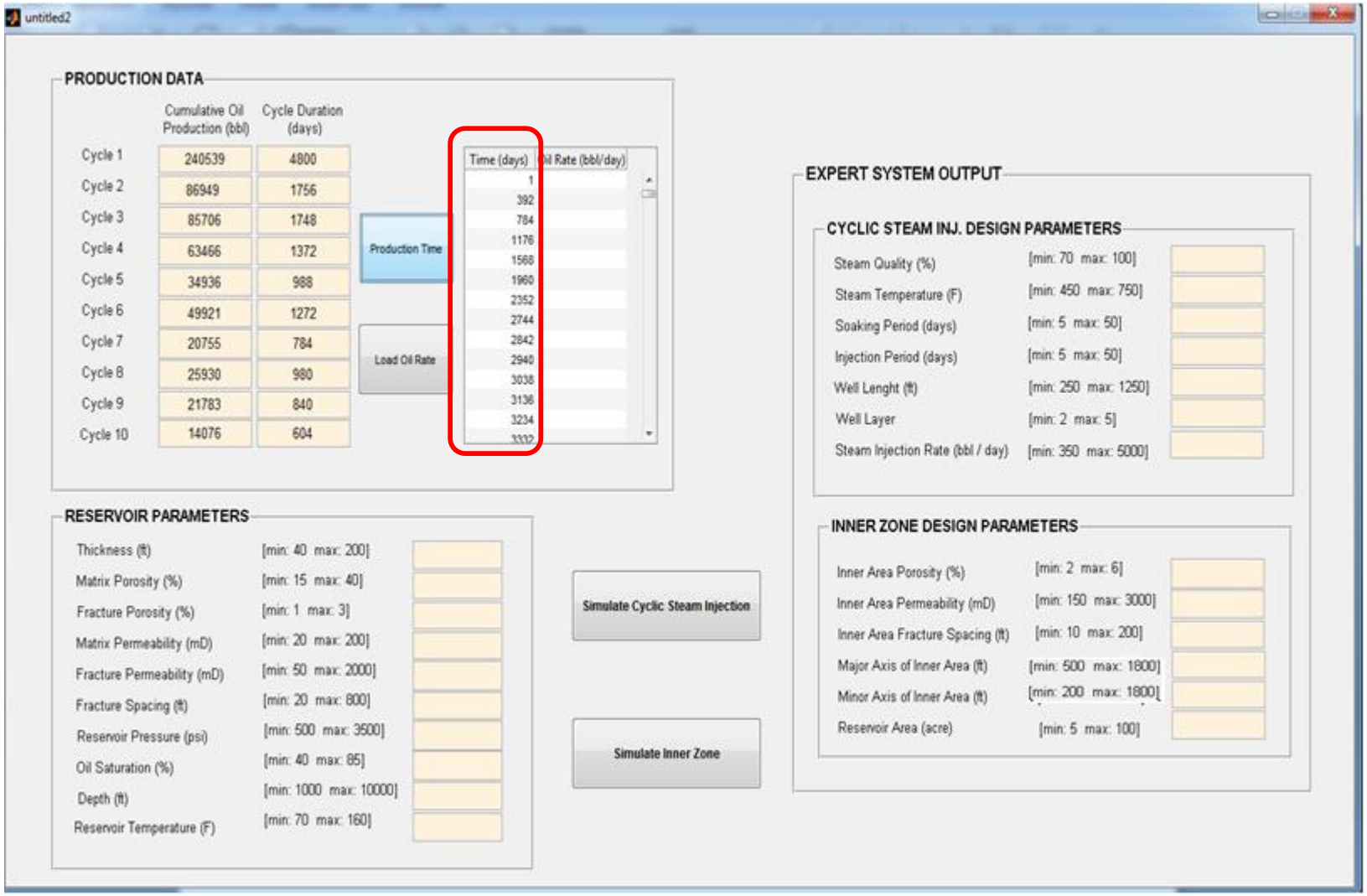

Figure 6.6 Step-2 of graphical user interface for Inverse ANN-1A tool

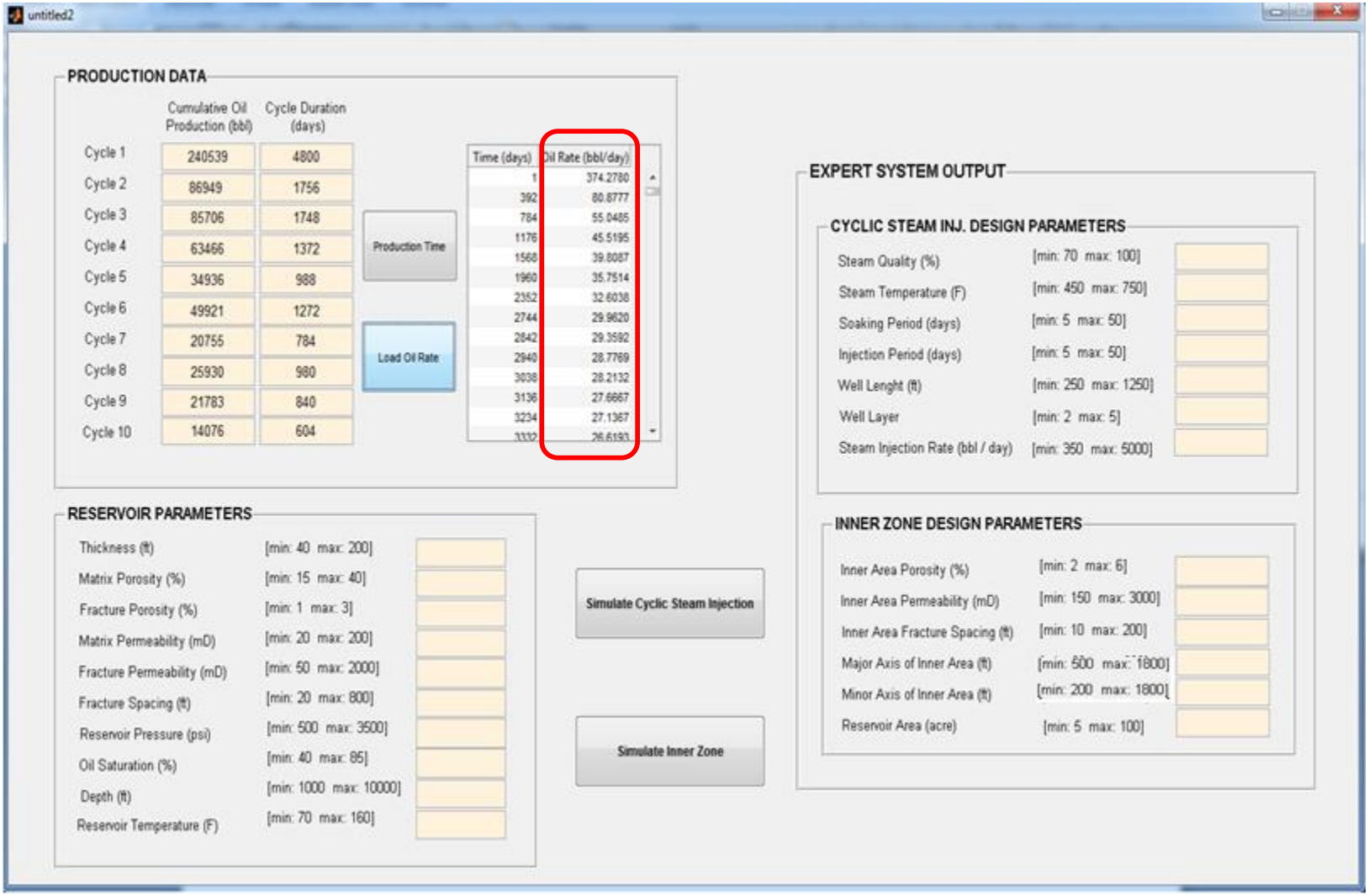

Figure 6.7 Step-3 of graphical user interface for Inverse ANN-1A tool

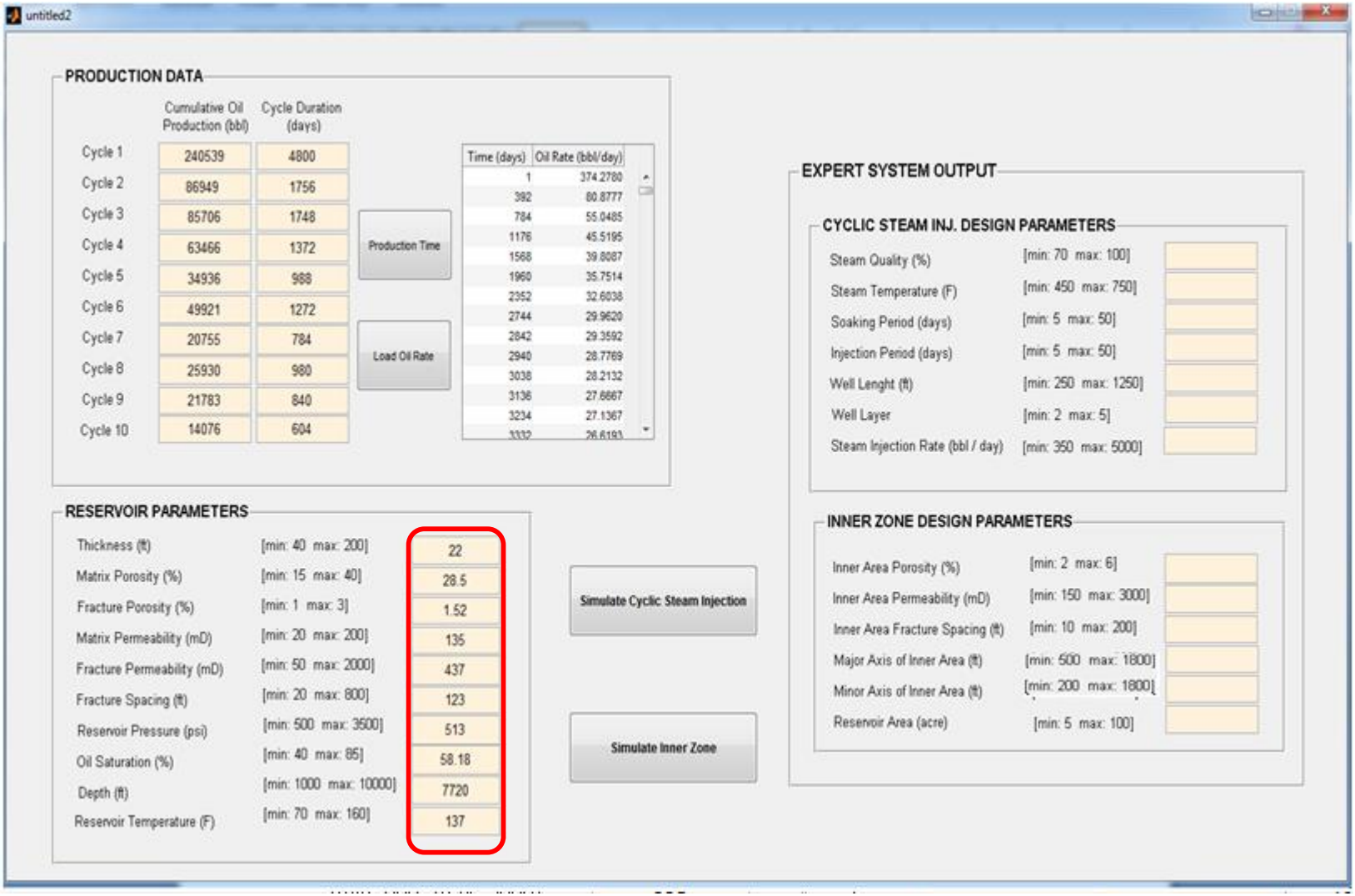

Figure 6.8 Step-4 of graphical user interface for Inverse ANN-1A tool

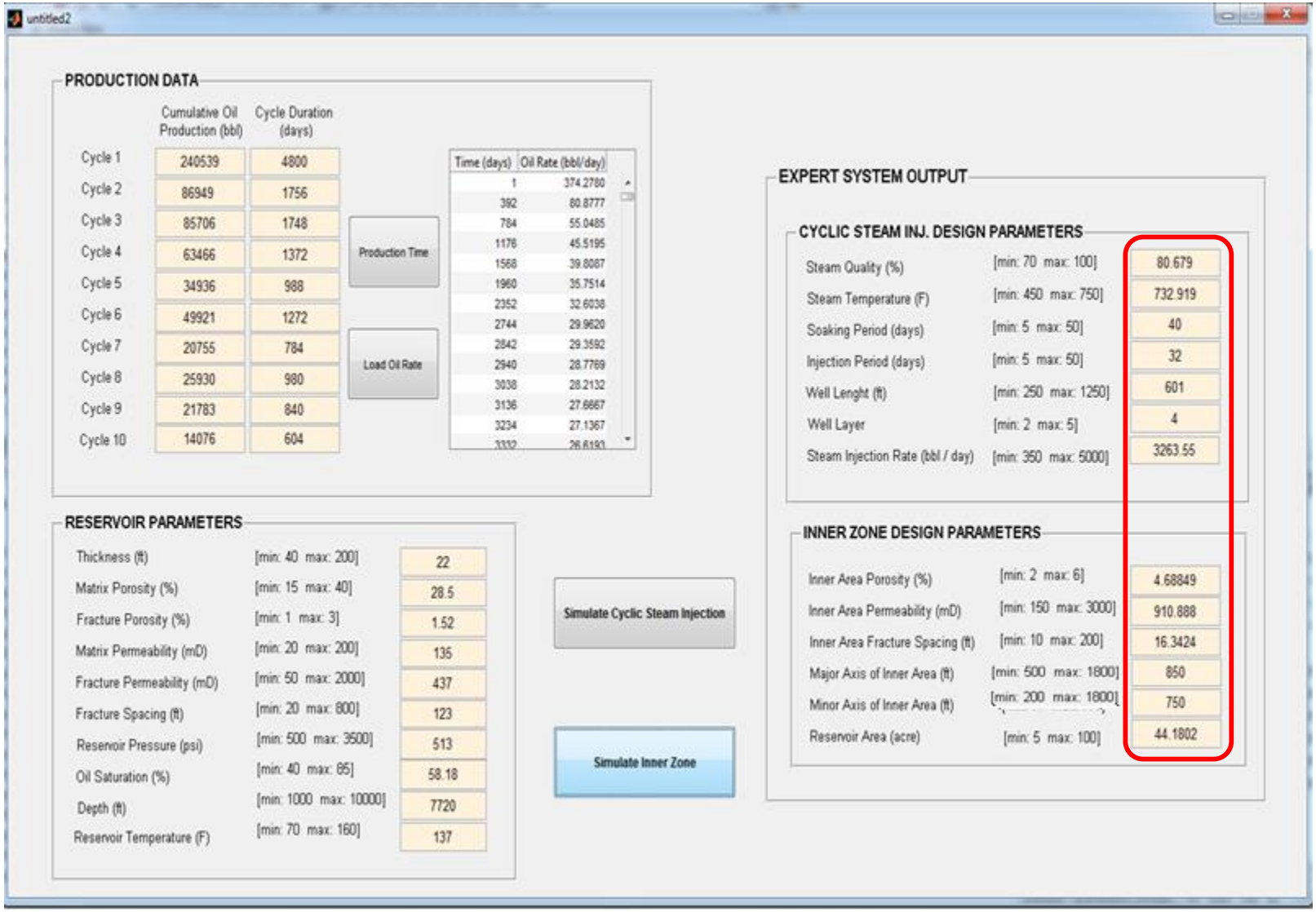

Figure 6.9 Graphical user interface for Inverse ANN-1A tool after simulation

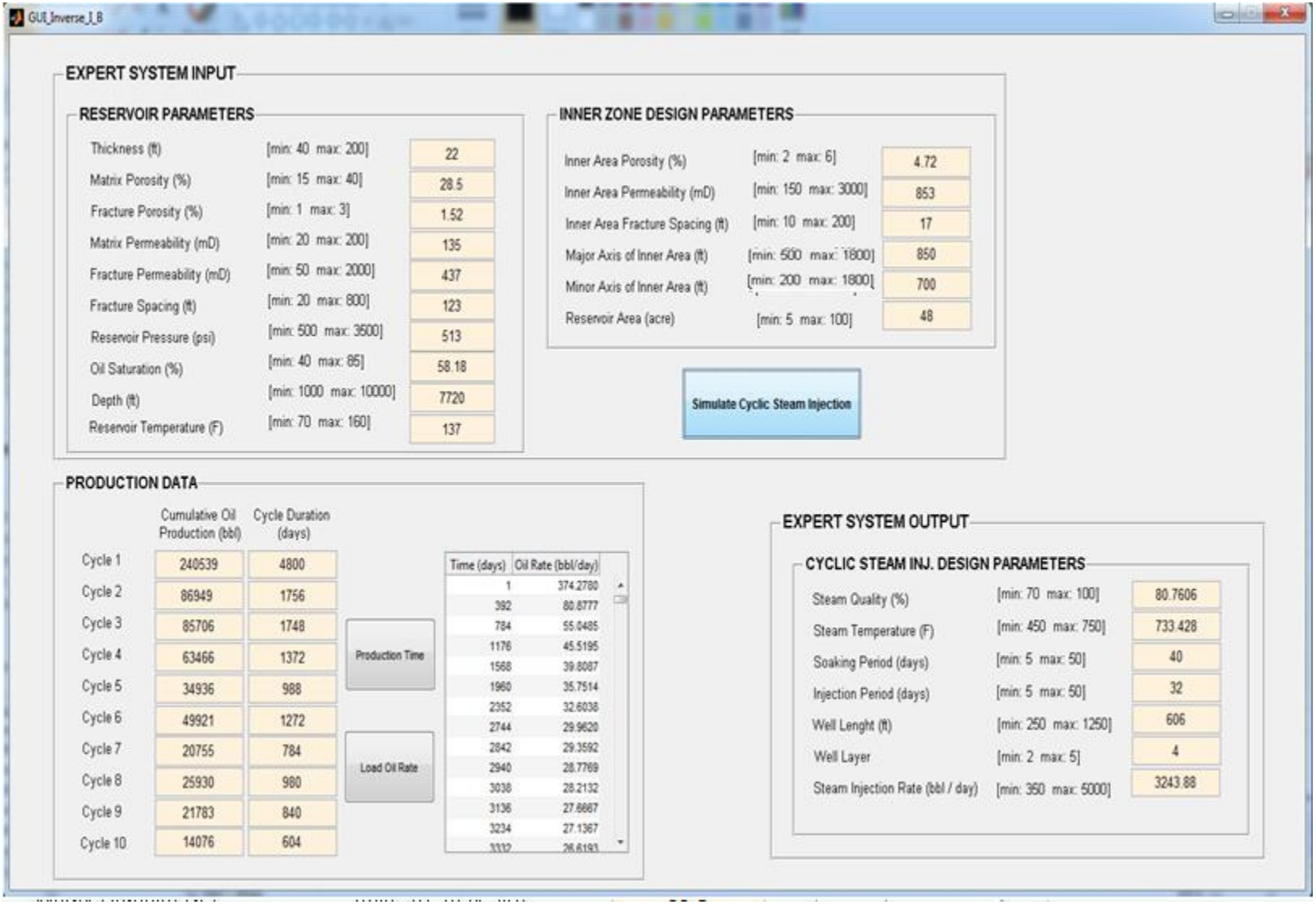

Figure 6.10 Graphical user interface for Inverse ANN-1B tool after simulation

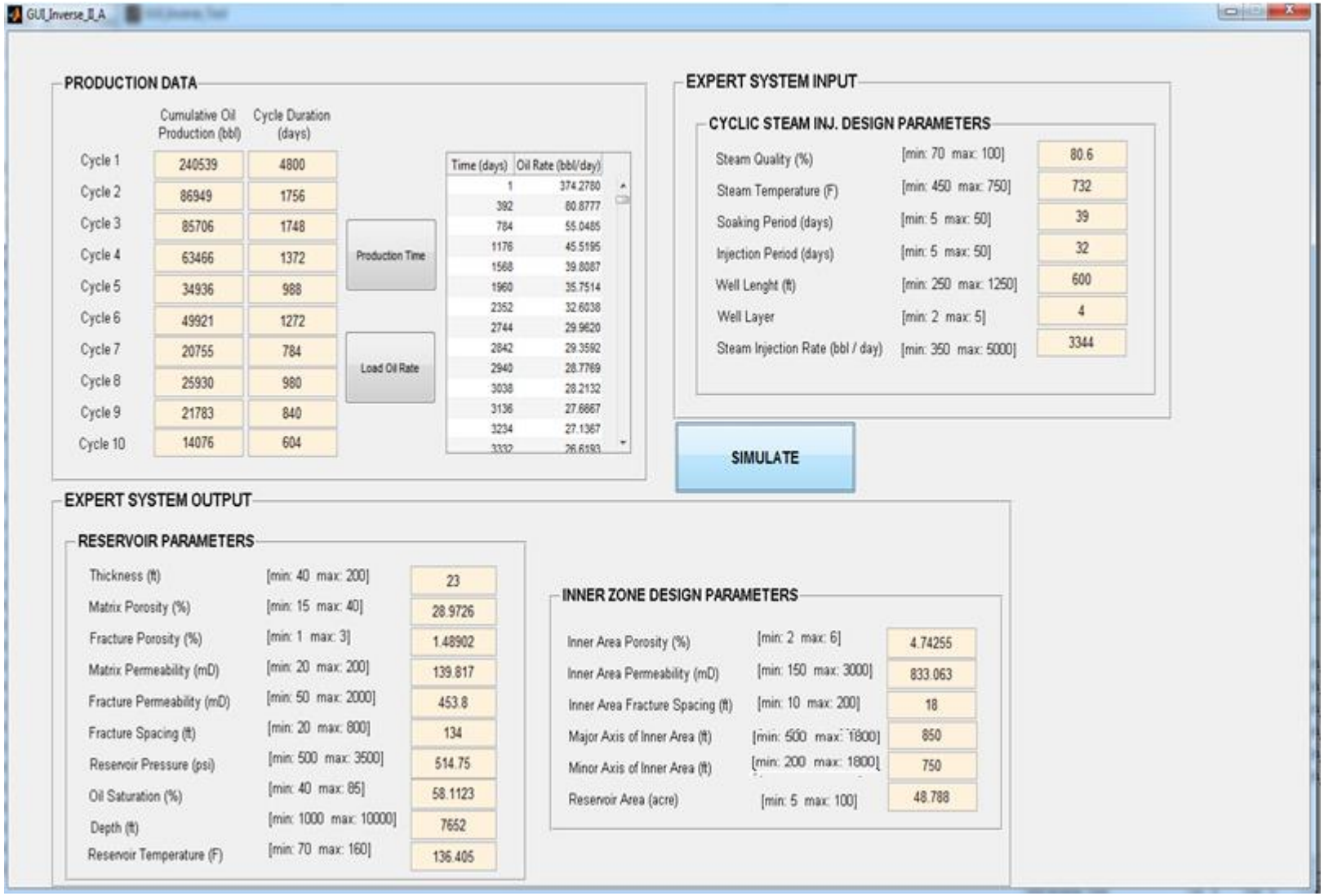

Figure 6.11 Graphical user interface for Inverse ANN-2A tool after simulation

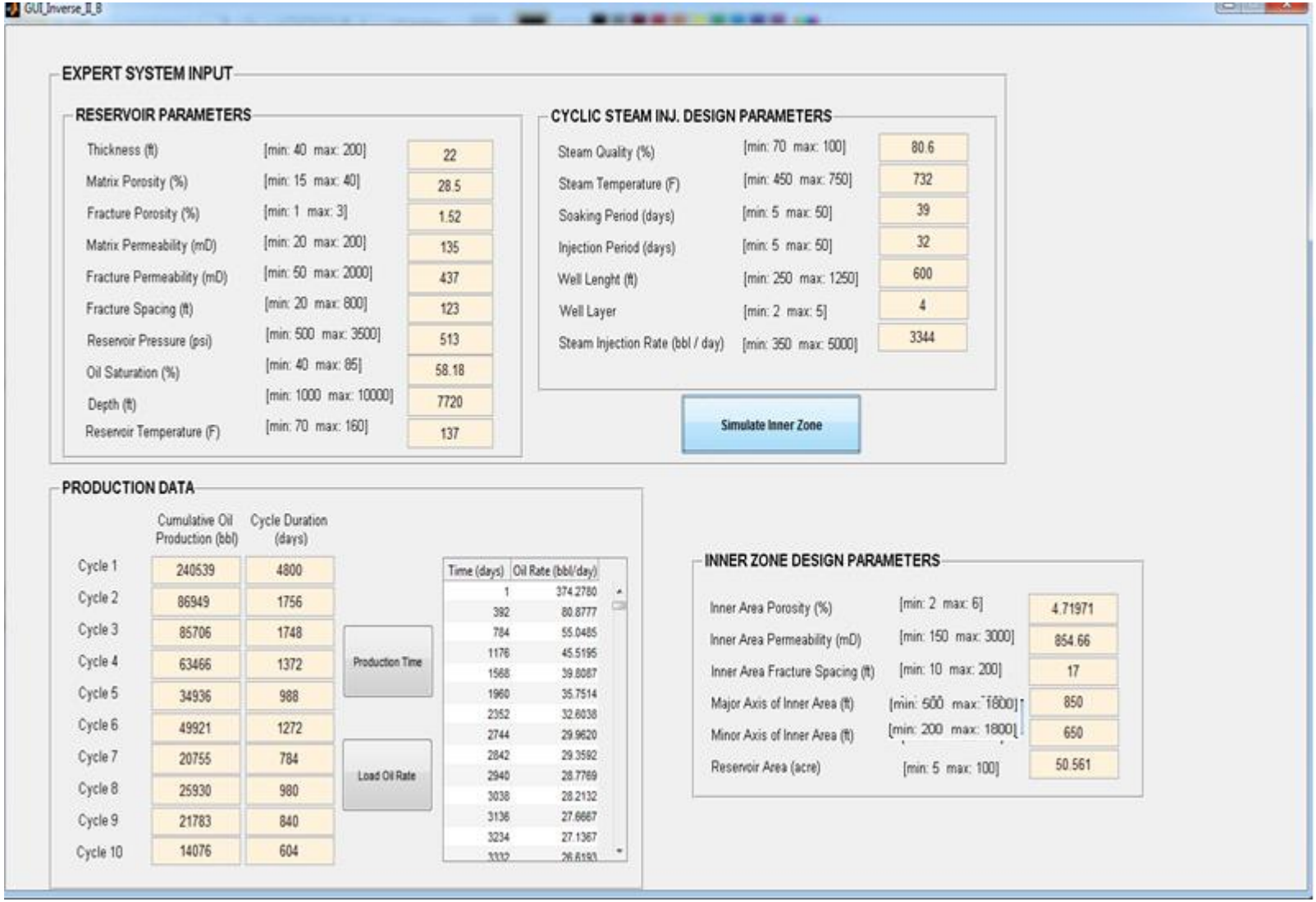

Figure 6.12 Graphical user interface for Inverse ANN-2B tool after simulation

Chapter 7

Summary and Conclusions

Cyclic steam injection is an effective thermal EOR method to enhance the oil displacement in naturally fractured reservoirs. More intensely fractured inner zone is created in elliptical-shape around the wellbore based on fracture porosity, fracture permeability and fracture spacing. Reservoir properties are taken into consideration during design of inner zone. The reservoirs are stimulated by cyclic steam injection after primary production is completed. The aim of this study is to develop ANN models for cyclic steam injection implementation on naturally fractured reservoir and decrease the computing time of reservoir simulations. In order to have a better performance for the most possible scenarios, network is trained by parameters that are uniformly distributed within the specified ranges. Actual performances of the generated reservoir samples are obtained by CMG-STARS. Six different artificial neural networks are developed as follows:

First ANN model is looking for forward problem and named as Forward ANN-1. It is able to estimate the oil flow rate and total number of cycles for reservoirs in where cyclic steam injection is implemented.

Second ANN model called as Forward ANN-2 is created for the prediction of production profile. However, it estimates the cumulative oil production and production period of each cycle and cumulative production at the end of whole project.

Third network, Inverse ANN-1A, is designed for determination of necessary CSI and fractured zone design parameters in order to achieve desired production performance of specified reservoirs.

Fourth ANN model called as Inverse ANN-1B is developed to improve the ability of design parameters prediction by focusing on only cyclic steam injection design parameters.

Fifth network is Inverse ANN-2A and it is employed for estimation of reservoir properties after fractured inner zone was created. Data of production profile and CSI design parameters should be provided to the network as inputs.

Sixth and the last ANN model named as Inverse ANN-2B is applied for only fractured inner zone properties. Reservoir properties used in the output layer of the previous model, transferred to the input layer of the last ANN.

In this research, single hidden layer with *tansig* transfer function is optimized for all networks with 275, 175, 42, 37, 200 and 44 neurons, respectively. The desired tolerance for evaluating the efficiency of the networks is specified as 10 % for the first ANN model and 5 % for the rest five ANN models. All developed expert systems are able to predict accurately.

The major conclusions of this study are listed as follows:

1. Scaled conjugate gradient *(trainscg)* back propagation algorithm function was found more efficient when it was used with tan-sigmoid *(tansig)* activation function in the hidden layer.
2. The complexity level of the network structure can be overcome by changing the number of hidden layer neurons, adding functional links and taking the logarithm of input and output components.
3. Eiegen values used as functional links are not always effective for getting accurate prediction. It was worked for the forward models whereas they did not help to improvement of the inverse models. Usually, implementation of the functional links into the input layer is more helpful.

4. Division of two separate forward models increased the performance of the network to estimate cumulative oil production and cycle duration of each cycle. However, prediction capability of Forward ANN-1 still has difficulty to estimate the peak rate of each cycle.
5. Development of Inverse ANN-1B in addition to Inverse ANN-1A enhanced the accuracy of the cyclic steam injection design parameters' prediction by decreasing the complexity of the problem. Furthermore, lower error percentages were observed in Inverse ANN-2B than Inverse ANN-2A by simplifying the problem.
6. Graphical user interface provides an easy access to all six networks by integrating them.

Chapter 8

Recommendations

This current research can be further improved by implementing following,

1. Simulation of a total of 555 data sets can be repeated for six different abandonment oil flow rates of primary production such as of 10, 20, 30, 40 and 50 bbl/day. In addition, ANN model that incorporates all six distinct designs can be developed.
2. Termination oil flow rate at the end of each cycle can be considered as one of the design parameters to create more expert system.
3. Number of oil flow rate data points can be increased at the beginning of each cycle.
4. Initial rate of every cycle and their corresponding time can be taken as additional performance indicators to increase the capability of network during prediction of peak rates.
5. Reservoir without inner zone can be simulated and compared with the current model to observe the contribution of intensely fractured inner zone to cyclic steam injection.
6. Data sets that are out of specified ranges may be tested in the developed ANN models to examine the ability of them for all possible scenarios.

References

Al-Hadrami, H., Rajtar, J. M., Hazlett, W. G. (1997). Optimization of Horizontal Well Performance in a Mature Cyclic-Steam Project. In *SPE Fifth Latin American and Caribbean Conference Proceedings.* SPE 39081. 30 August – 3 September. Rio de Janeiro, Brazil.

Alvarez, J., Han, S. (2013). Current Overview of Cyclic Steam Injection Process. *Journal of Petroleum Science Research Vol.*, **2**, 116-127.

Artun, E. (2008). *Optimized Design of Cyclic Pressure Pulsing in Naturally Fractured Reservoirs Using Neural-Network Based Proxy Models*. Ph.D. Thesis, The Pennsylvania State University, University Park, Pennsylvania.

Aziz, K., Ramesh, A.B., Woo, P.T. (1987). Fourth SPE Comparative Solution Project: Comparison of Steam Injection Simulators. *J. Pet. Tech.*, **39**, 1576-1584.

Bahrami, H., Siavoshi, J., Parvizi, H., Esmaili, S., Karimi, M. H. (2008). Characterization of Fracture Dynamic Parameters to Simulate Naturally Fractured Reservoirs. In *International Petroleum Technology Conference Proceedings.* IPTC 11971. 3-5 December. Kuala, Lumpur, Malaysia.

Fausett, L. (1994). Fundamentals of Neural Networks: Architectures, Algorithms, and Applications. Prentice-Hall, Englewood Cliffs, New Jersey.

Karsoliya, S. (2012). Approximating Number of Hidden Layer Neurons in Multiple Hidden Layer BPNN Architecture. International Journal of Engineering Trends and Tech. Volume 3. 714-717, June. ISSN 2231-5381.

Kazemi, H. (1969). Pressure Transient Analysis of Naturally Fractured Reservoirs with Uniform Fracture Distribution. In *SPE 43rd Annual Fall Meeting Proceedings.* SPE 2156A. 29 September – 2 October. Houston, Texas.

Kriesel, D. (2011). A Brief Introduction to Neural Networks. In University of Bonn Seminar Proceeding. 8-12, Germany.

Kulga, I. B. (2010). *Development of an Artificial Neural Network for hydraulically fractured horizontal wells in tight gas sands.* Master's thesis, The Pennsylvania State University.

Maren, A., Harston, C., Pap, R. (1990). Handbook of Neural Computing Applications. Academic Press, Inc., San Diego. ISBN 0-12-546090-2.

Mohaghegh, S. (2000). Virtual Intelligence Applications in Petroleum Engineering: Part 1 - Artificial Neural Networks. *J. Pet. Tech.*, **53**(9):64–73. SPE 58046.

Mohammadi, H., Manshad, A.K., Montazeri, G. H. (2012). A Reservoir Simulation Approach for Modeling of Naturally Fractured Reservoirs. *Egyptian Journal of Petroleum.***21**, 125-133.

Parada, C. (2008). *An Artificial Neural Network Based Tool-Box for Screening and Designing Improved Oil Recovery Methods.* Ph.D. Thesis, The Pennsylvania State University, University Park, Pennsylvania.

Patterson, D., W. (1196). Artificial Neural Network, Theory and Applications. Prentice-Hall, INC., Singapore. ISBN 0-1-295353-6.

Razavi, S. D., Kharrat, R. (2009). Application of Cyclic Steam Stimulation by Horizontal Well in Iranian Heavy Oil Reservoirs. *Sharif University of Technology*, **16**(2): 125-139.

Rodriguez, E., barrios, W., Sandoval, R., Santos, N., Cortes, I. (2008). Numerical Simulation for Cyclic Steam Injection at Santa Clara Field. *CT&F- Ciencia, Technology Futuro,* **3**(4):107-127.

STARS Advanced Process and Thermal Reservoir Simulator, Version 2007 User Guide. 2007. Calgary, Alberta Canada.

TOTAL Oil and Gas Corporation. (2012). France.

Appendix A

Parameter Distribution in the Search Space

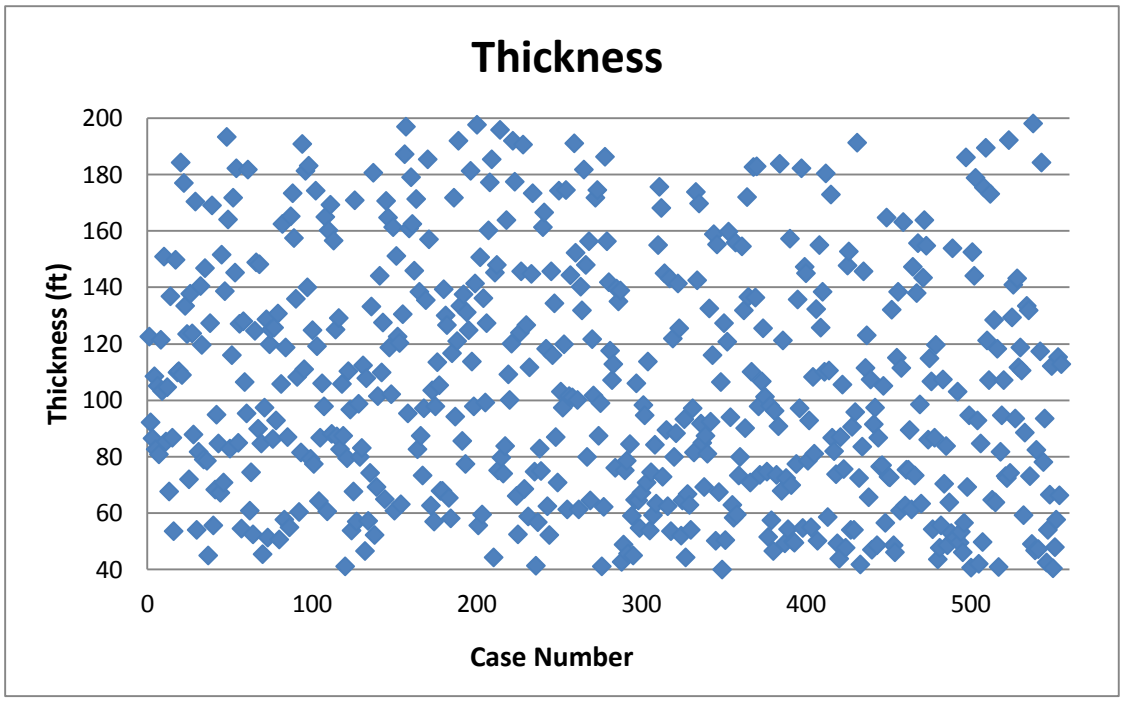

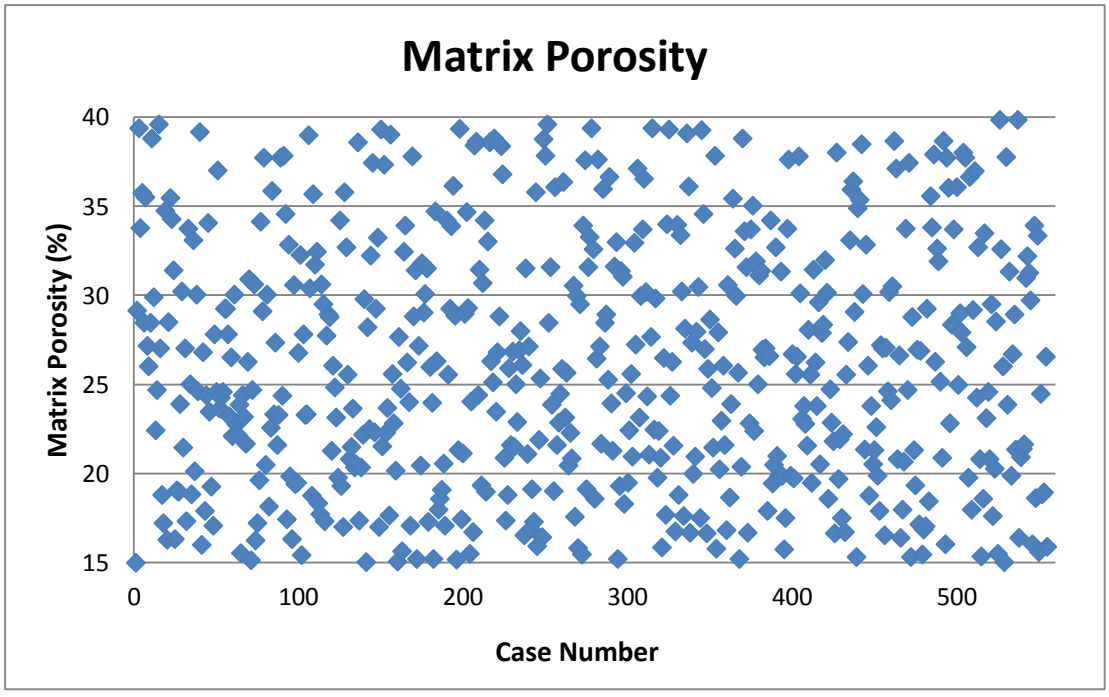

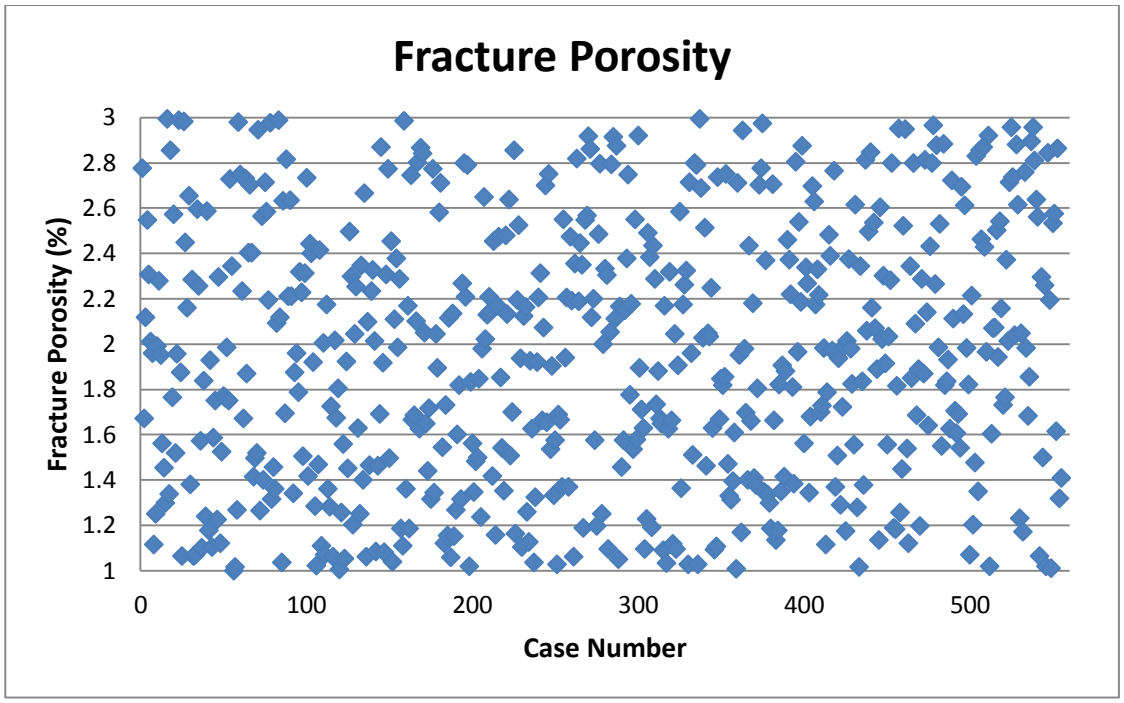
Fracture Porosity
Fracture Porosity (%)
3
2.8
2.6
2.4
2.2
2
1.8
1.6
1.4
1.2
1
0
100
200
300
400
500
Case Number

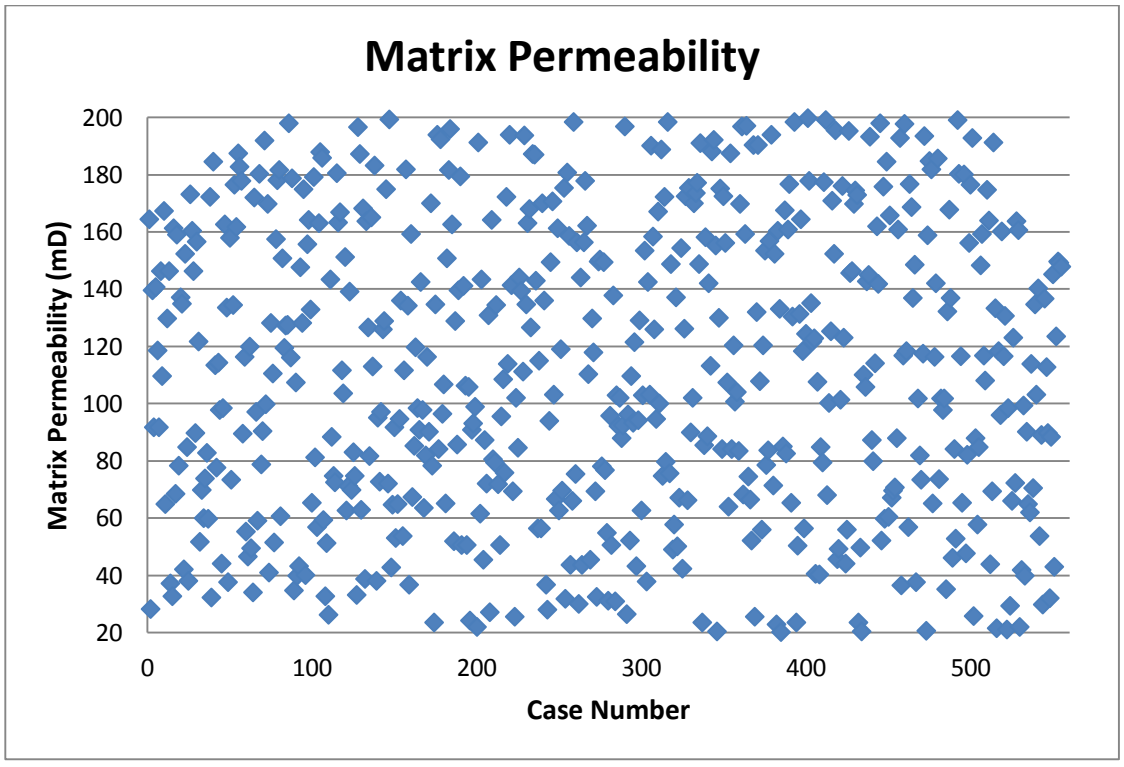
Matrix Permeability
Matrix Permeability (mD)
200
180
160
140
120
100
80
60
40
20
0
100
200
300
400
500
Case Number

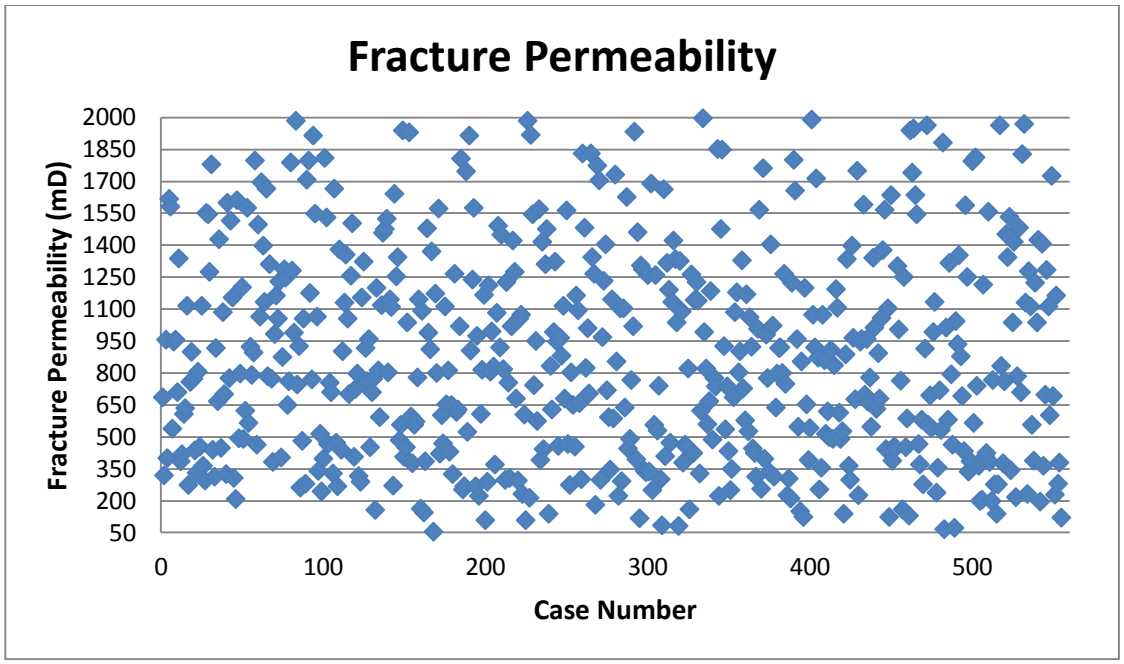
Fracture Permeability
Fracture Permeability (mD)
2000
1850
1700
1550
1400
1250
1100
950
800
650
500
350
200
50
0
100
200
300
400
500
Case Number

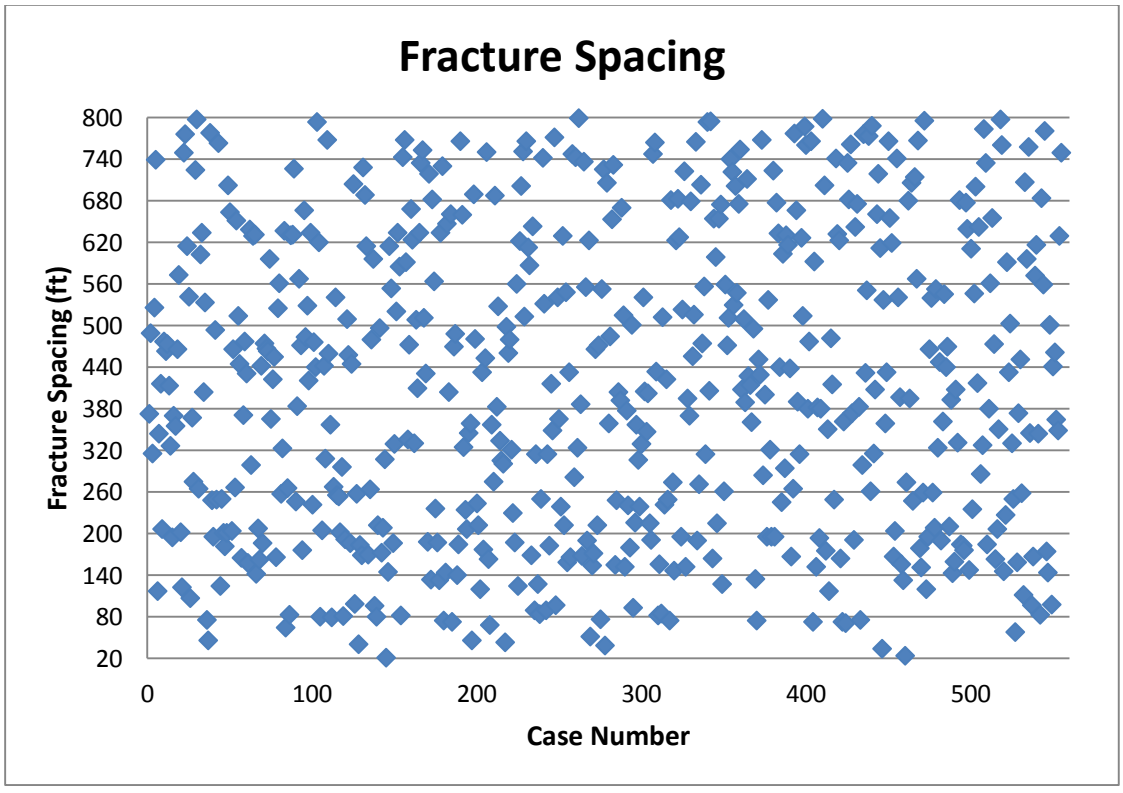
Fracture Spacing
Fracture Spacing (ft)
800
740
680
620
560
500
440
380
320
260
200
140
80
20
0
100
200
300
400
500
Case Number

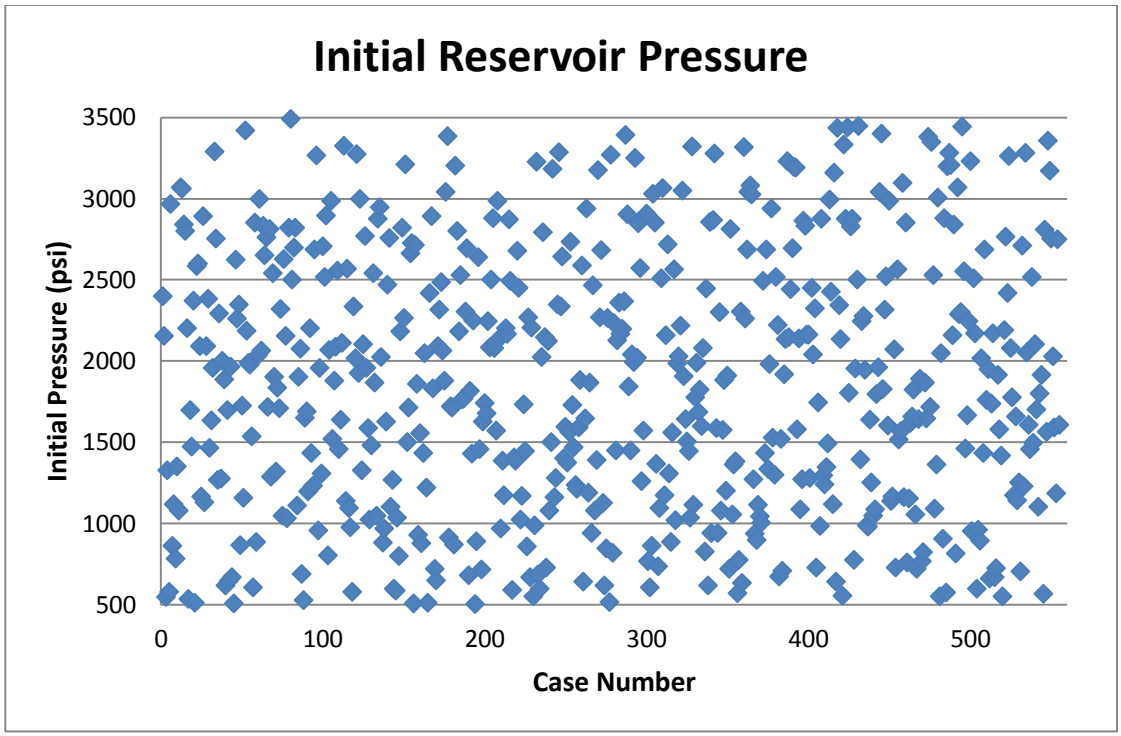
Initial Reservoir Pressure
Initial Pressure (psi)
3500
3000
2500
2000
1500
1000
500
0
100
200
300
400
500
Case Number

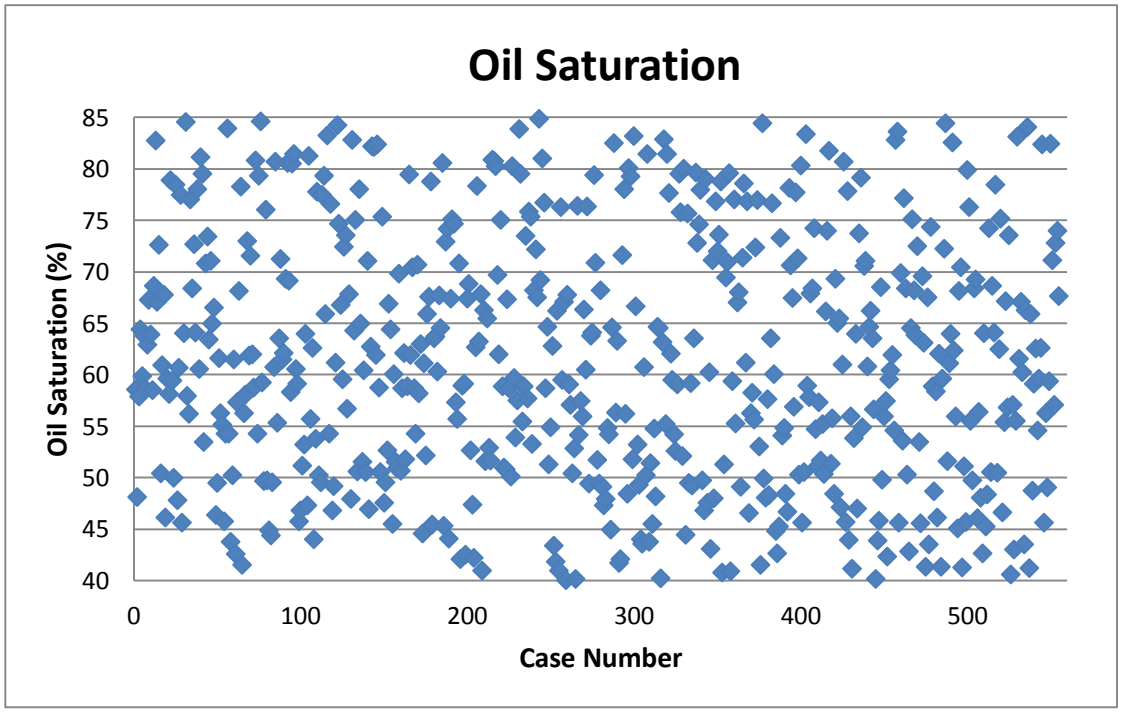
Oil Saturation
Oil Saturation (%)
85
80
75
70
65
60
55
50
45
40
0
100
200
300
400
500
Case Number

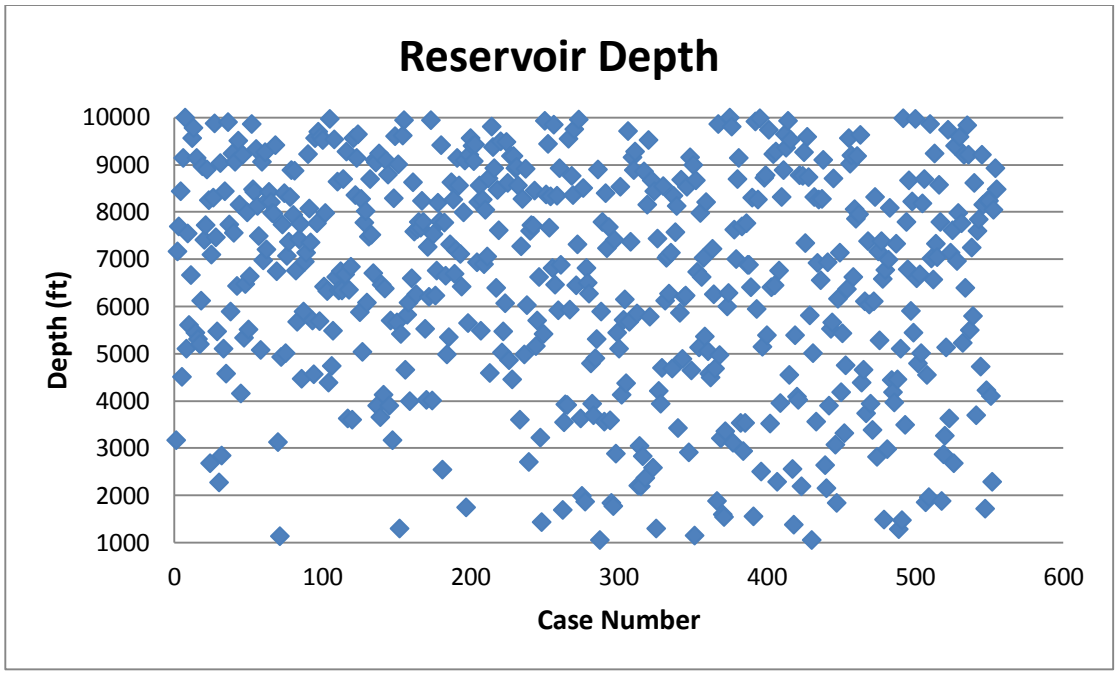
Reservoir Depth
Depth (ft)
10000
9000
8000
7000
6000
5000
4000
3000
2000
1000
0
100
200
300
400
500
600
Case Number

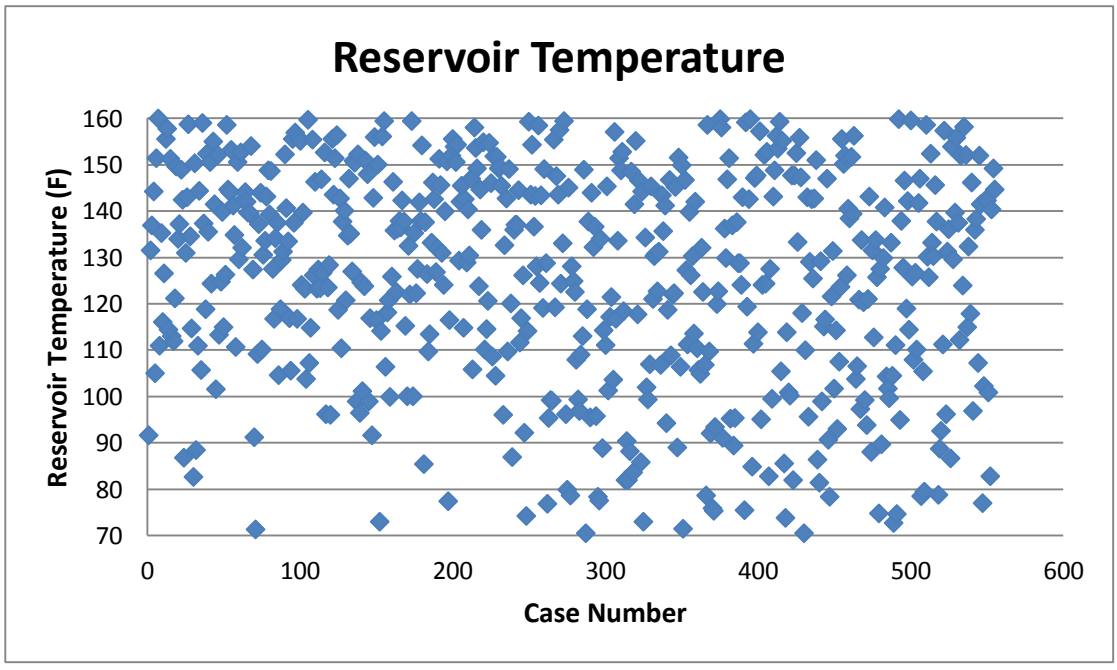
Reservoir Temperature
Reservoir Temperature (F)
160
150
140
130
120
110
100
90
80
70
0
100
200
300
400
500
600
Case Number

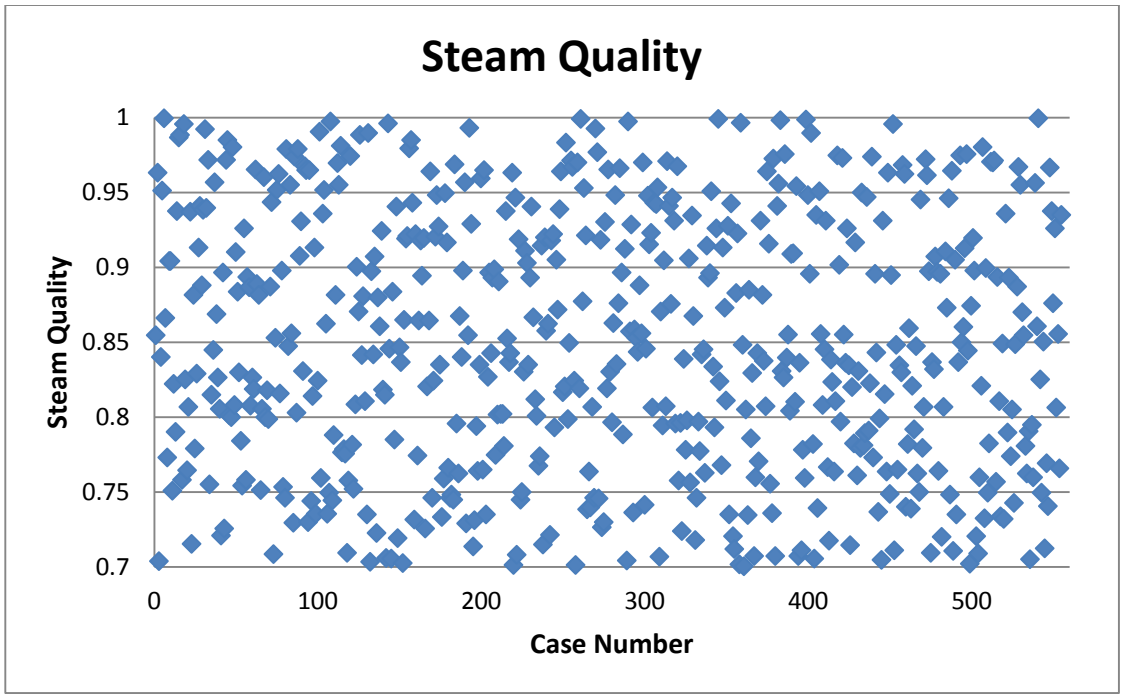
Steam Quality
Steam Quality
1
0.95
0.9
0.85
0.8
0.75
0.7
0
100
200
300
400
500
Case Number

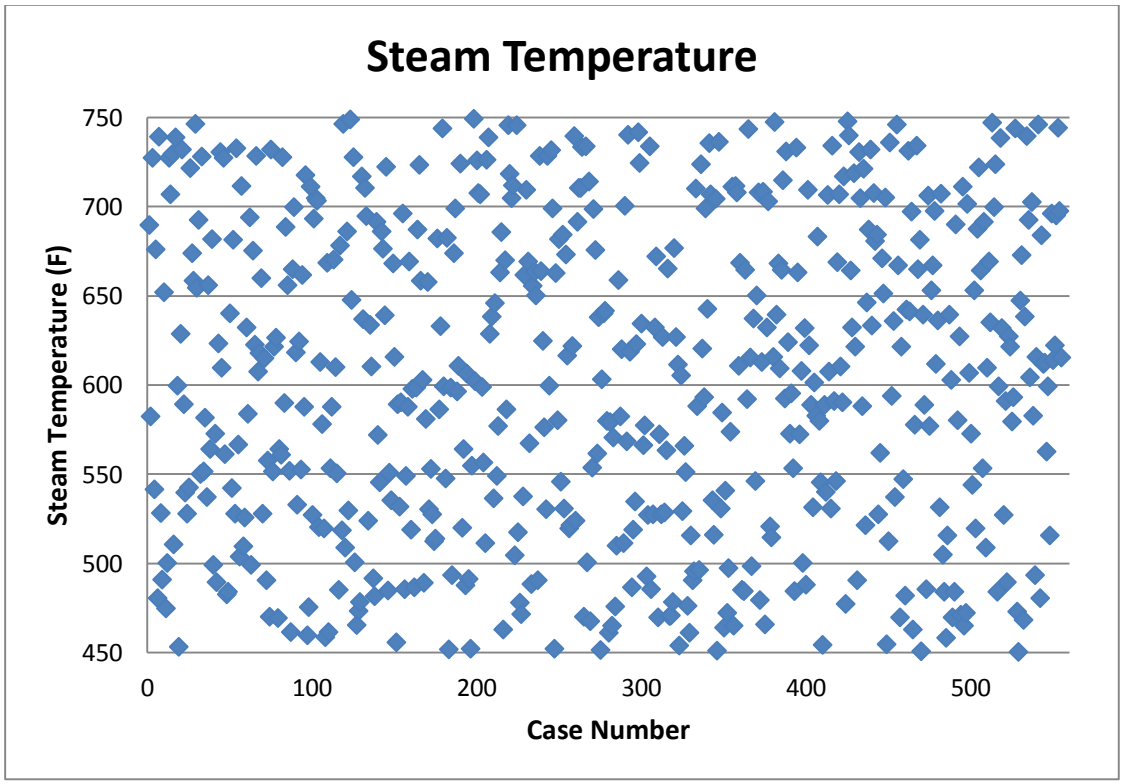
Steam Temperature
Steam Temperature (F)
750
700
650
600
550
500
450
0
100
200
300
400
500
Case Number

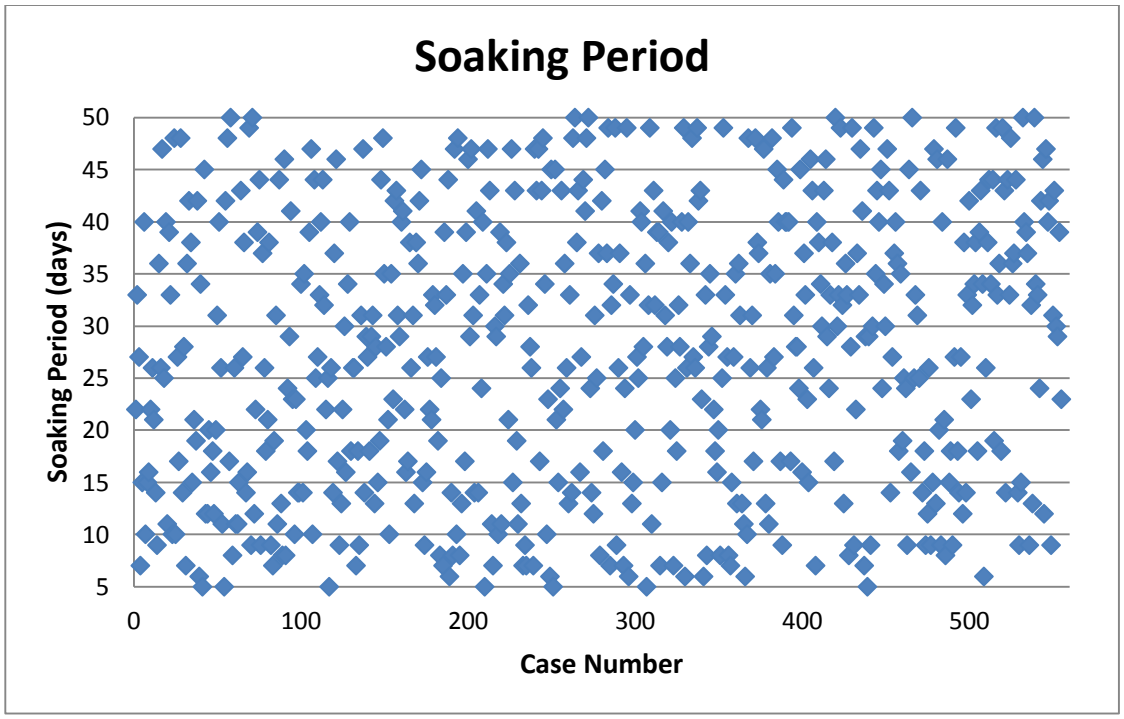
Soaking Period
Soaking Period (days)
50
45
40
35
30
25
20
15
10
5
0
100
200
300
400
500
Case Number

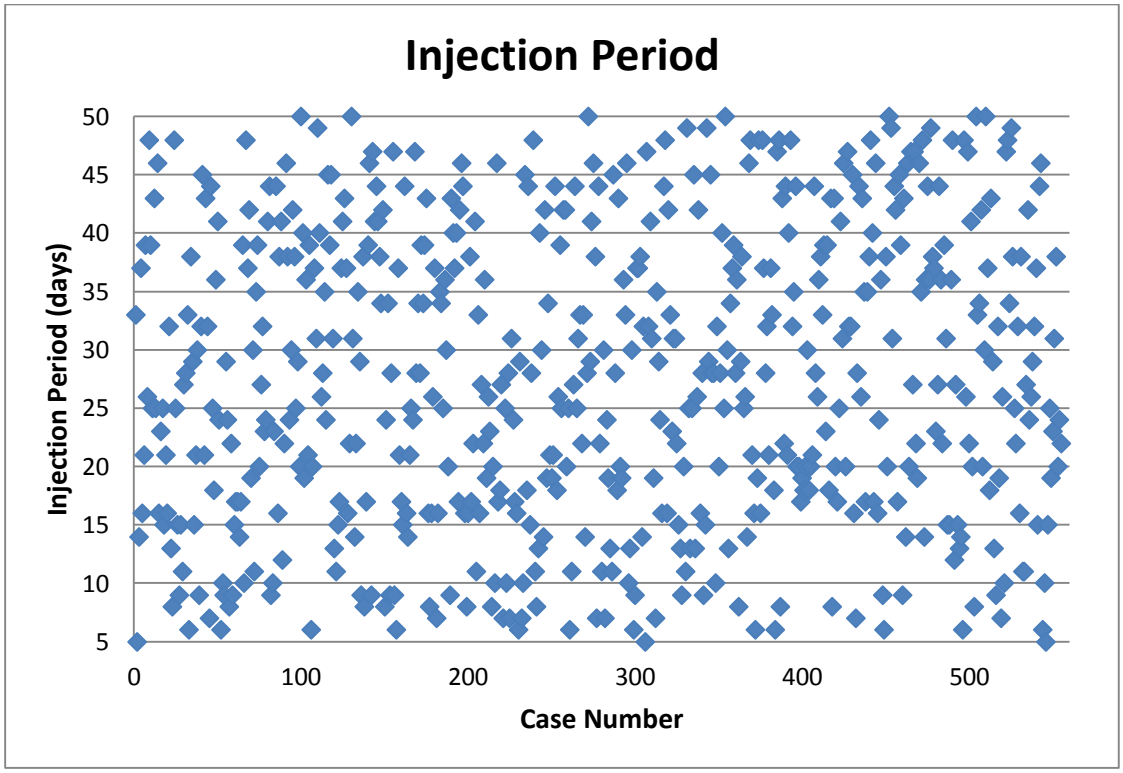
Injection Period
Injection Period (days)
50
45
40
35
30
25
20
15
10
5
0
100
200
300
400
500
Case Number

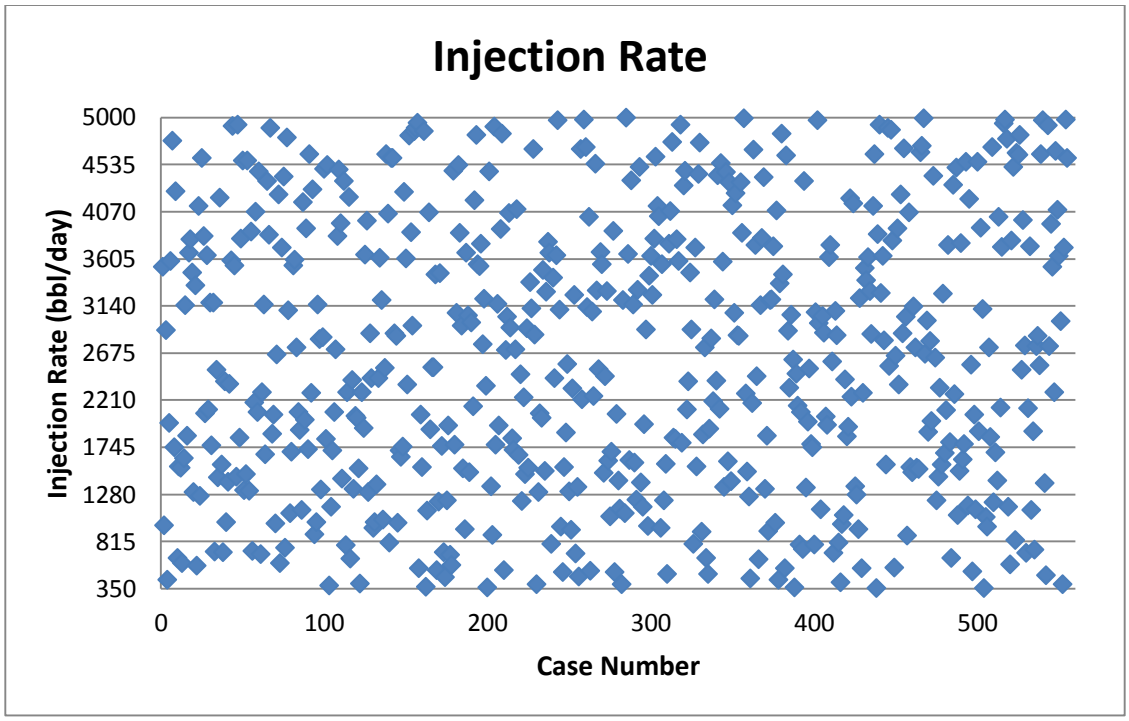
Injection Rate
Injection Rate (bbl/day)
5000
4535
4070
3605
3140
2675
2210
1745
1280
815
350
0
100
200
300
400
500
Case Number

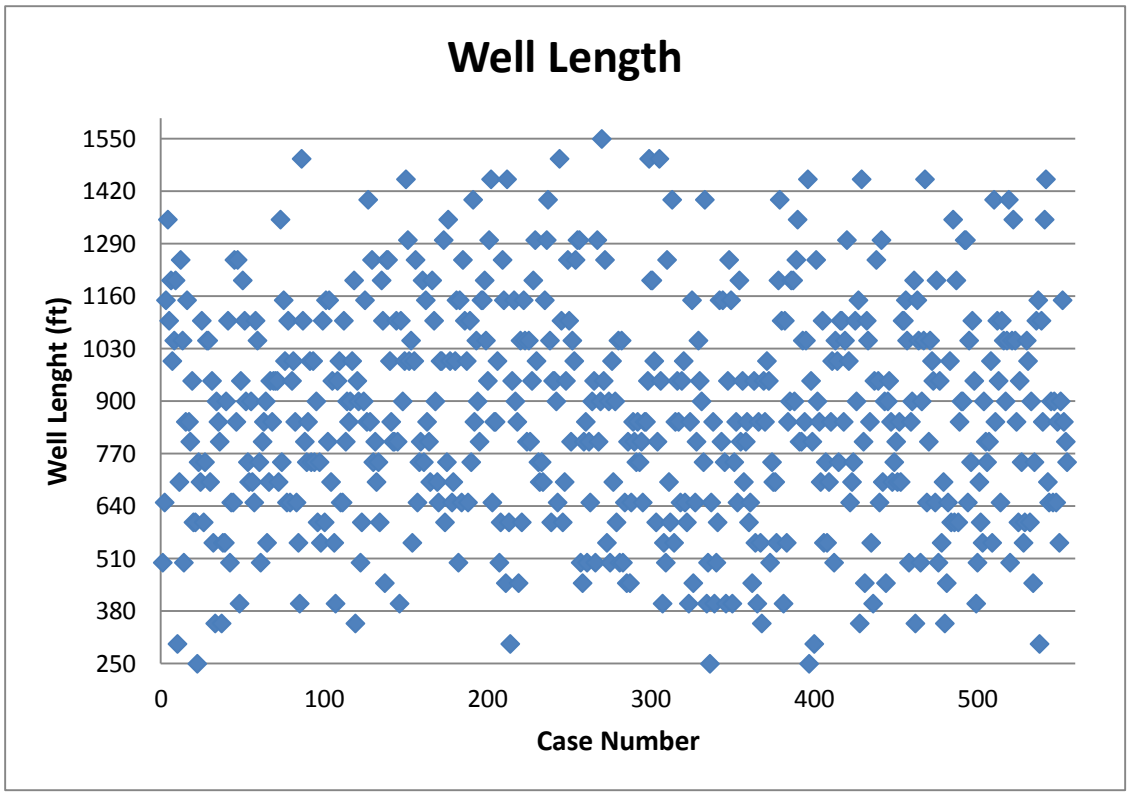
Well Length
Well Lenght (ft)
1550
1420
1290
1160
1030
900
770
640
510
380
250
0
100
200
300
400
500
Case Number

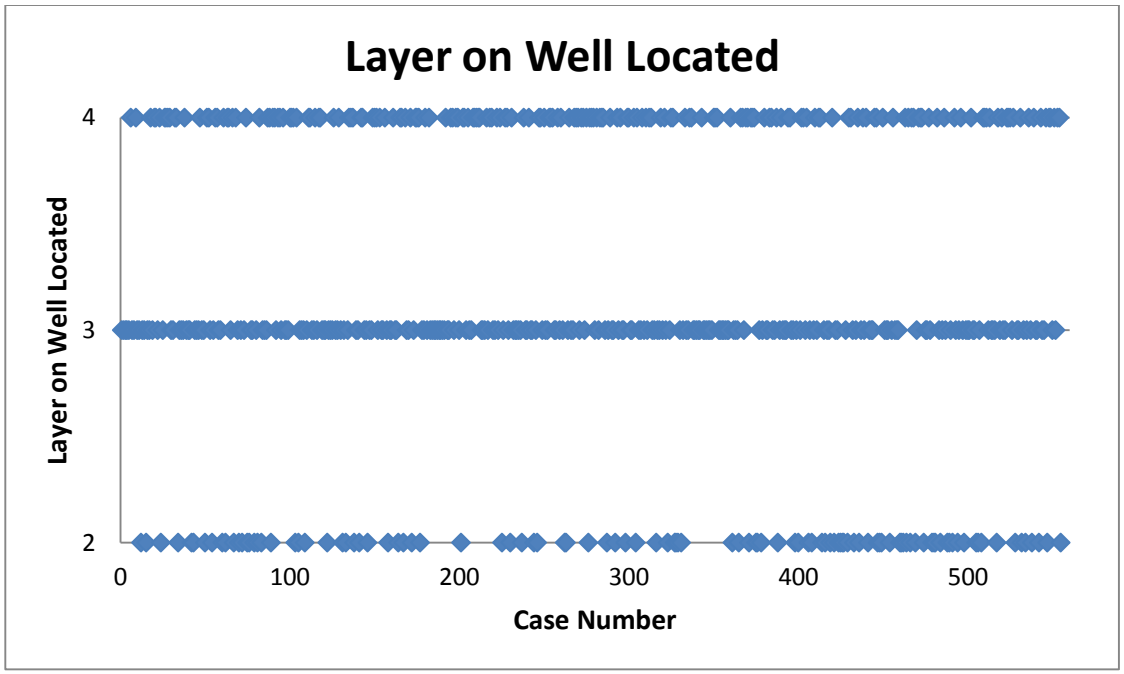
Layer on Well Located
Layer on Well Located
4
3
2
0
100
200
300
400
500
Case Number

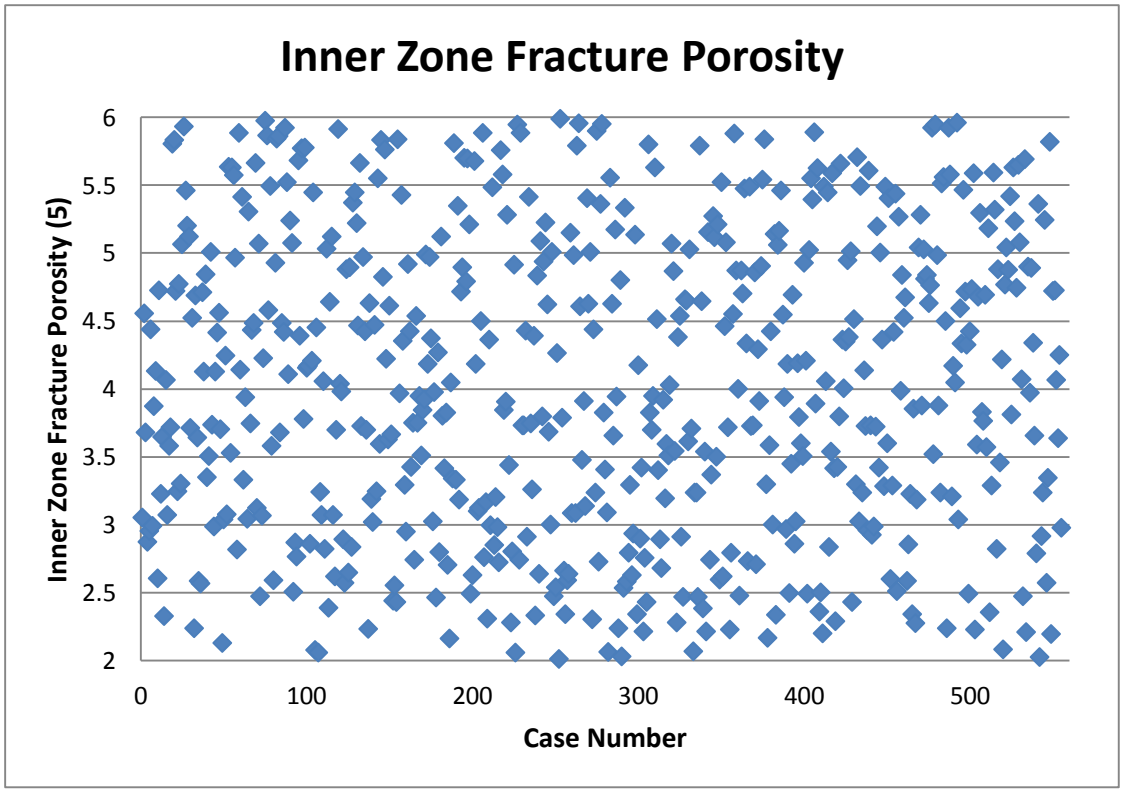
Inner Zone Fracture Porosity
Inner Zone Fracture Porosity (5)
6
5.5
5
4.5
4
3.5
3
2.5
2
0
100
200
300
400
500
Case Number

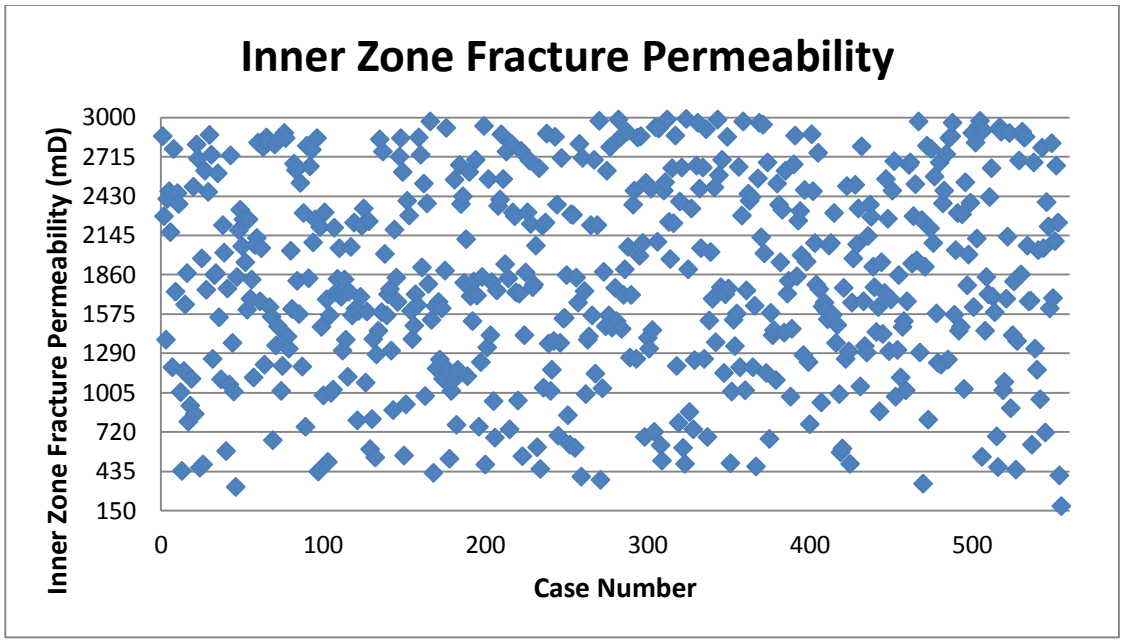
Inner Zone Fracture Permeability
Inner Zone Fracture Permeability (mD)
3000
2715
2430
2145
1860
1575
1290
1005
720
435
150
0
100
200
300
400
500
Case Number

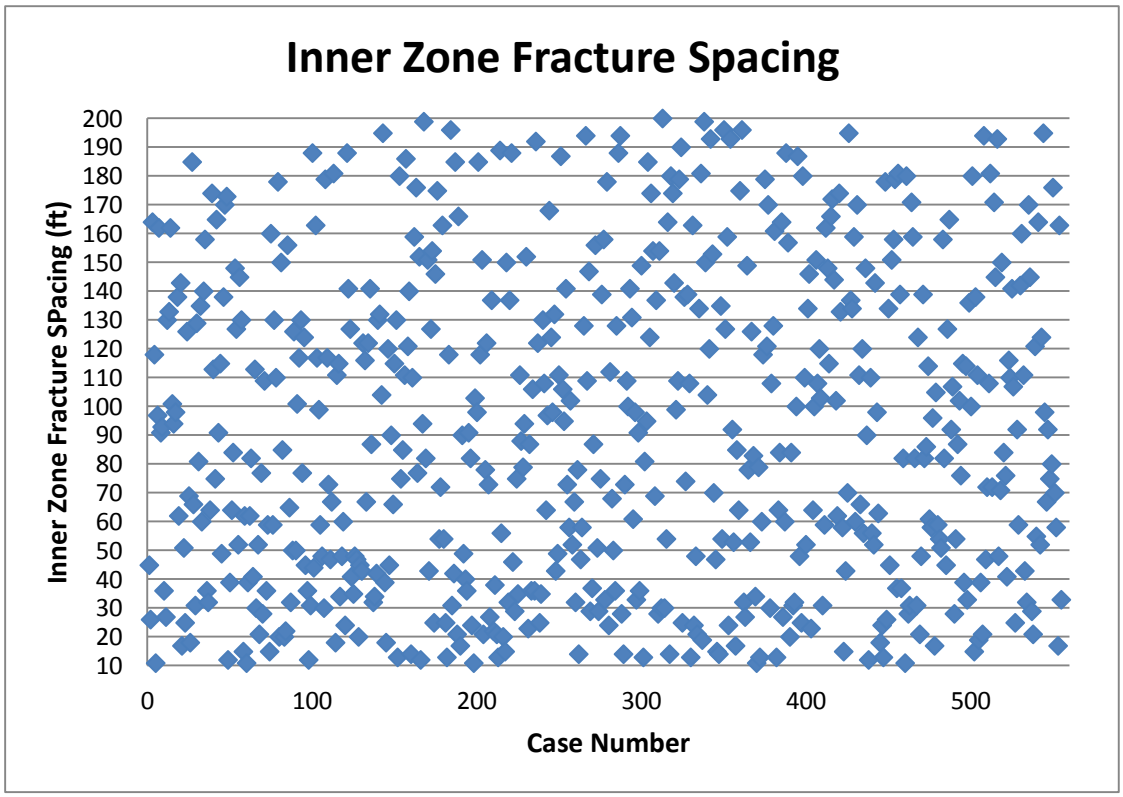
Inner Zone Fracture Spacing
Inner Zone Fracture SPacing (ft)
200
190
180
170
160
150
140
130
120
110
100
90
80
70
60
50
40
30
20
10
0
100
200
300
400
500
Case Number

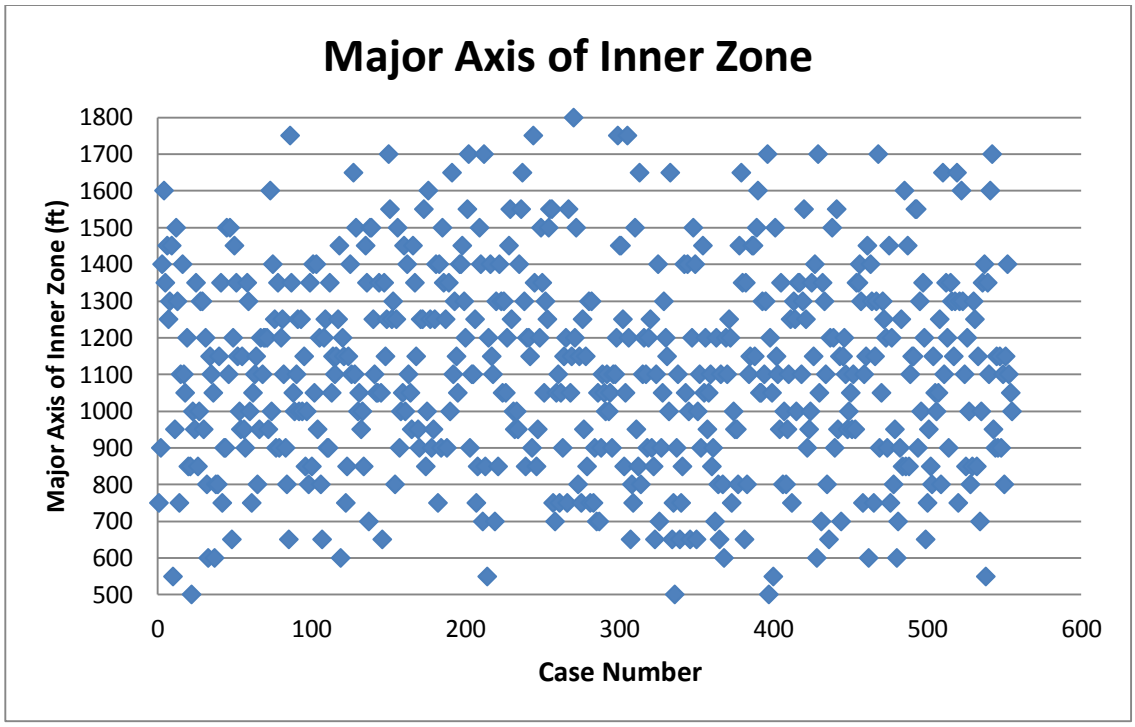
Major Axis of Inner Zone
Major Axis of Inner Zone (ft)
1800
1700
1600
1500
1400
1300
1200
1100
1000
900
800
700
600
500
0
100
200
300
400
500
600
Case Number

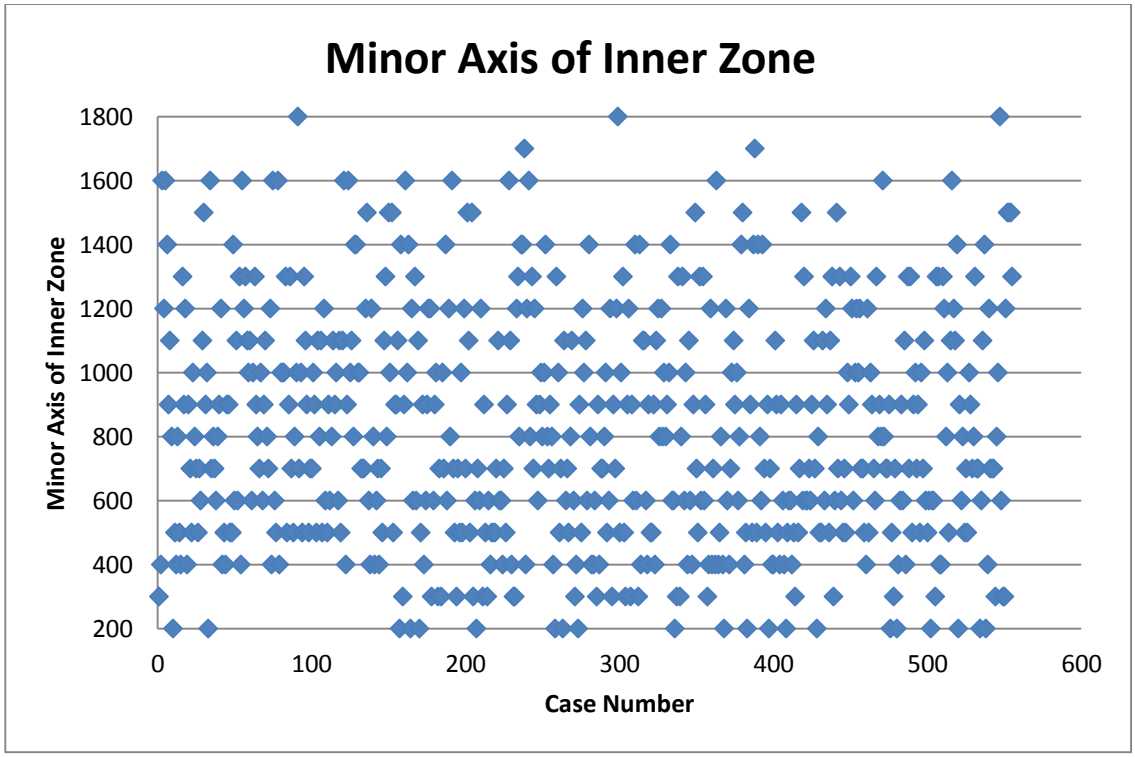
Minor Axis of Inner Zone
Minor Axis of Inner Zone
1800
1600
1400
1200
1000
800
600
400
200
0
100
200
300
400
500
600
Case Number

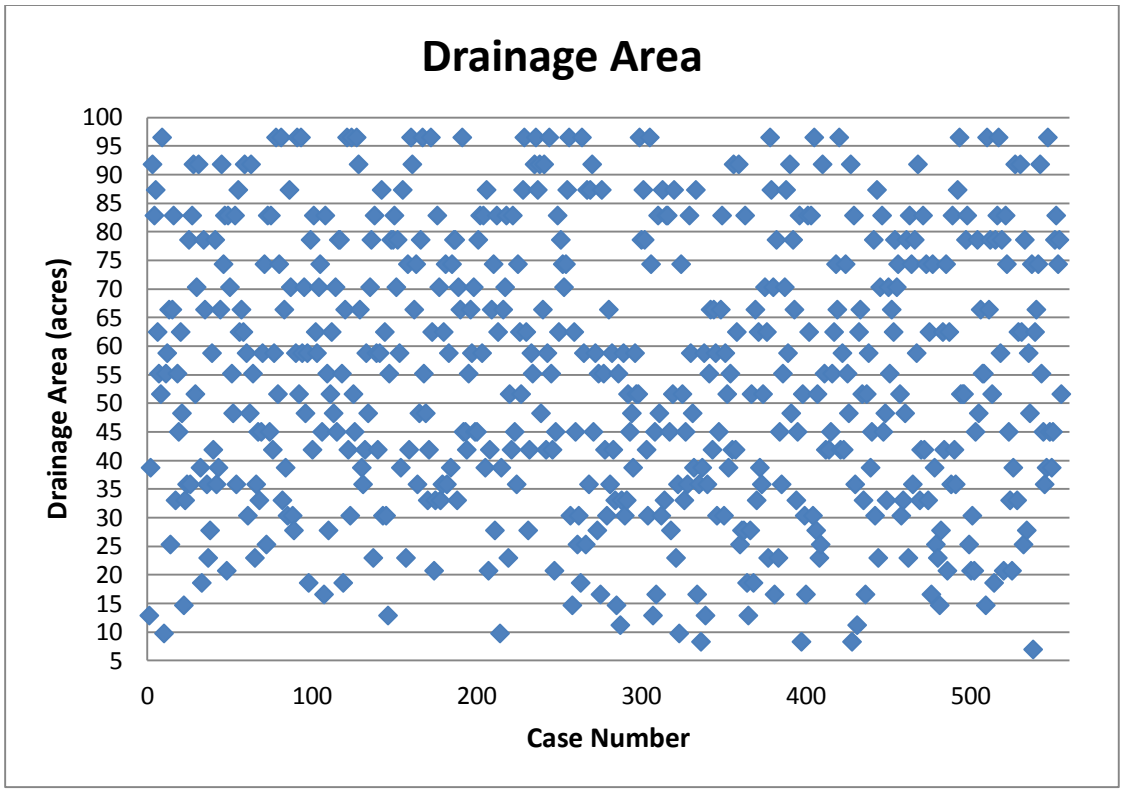
Drainage Area
Drainage Area (acres)
100
95
90
85
80
75
70
65
60
55
50
45
40
35
30
25
20
15
10
5
0
100
200
300
400
500
Case Number

Appendix B

Example of Simulator Input File for CSI

**Parameters for this run:
** 1) grid block number = 31
** 2) depth = 6630.73
** 3) layer thickness = 23.2113
** 4) matrix porosity = 0.370114
** 5) fracture porosity = 0.0176298
** 6) matrix permeability = 73.3811
** 7) fracture permeability = 490.184
** 8) fracture spacing= 204
** 9) reservoir temperature = 126.307
** 10) initial pressure = 1159.27
** 12) oil saturation = 0.61634
** 13) steam quality = 0.883673
** 14) steam temperature = 542.082
** 15) soaking period = 40
** 16) injection period= 24
** 19) layer on well-located = 4
** 24) first grid block number of well = 5
** 25) last grid block number of well = 27
** 26) number of grid block along the minor axis of inner zone = 22
** 27) inner zone fracture porosity= 0.0425011
** 28) inner zone fracture permeability= 2259.64
** 29) inner zone fracture spacing = 64
** 30) injection rate = 1321

RESULTS SIMULATOR STARS 201110
*interrupt *stop
*inunit *field

```
*outprn *grid pres sw so sg temp y x w solconc obhloss viso visg
*outprn *well *all
*wrst 200
*wprn *grid 200
*wprn *iter 200

OUTSRF GRID PRES SG SO TEMP
**$ Distance units: ft
RESULTS XOFFSET 0.0000
RESULTS YOFFSET 0.0000
RESULTS ROTATION 0.0000 **$ (DEGREES)
RESULTS AXES-DIRECTIONS 1.0 -1.0 1.0

**$ ************************************************************************
**$ Definition of fundamental Cartesian grid
**$ ************************************************************************

GRID VARI 31 31 5
KDIR UP
DI IVAR
31*50
DJ JVAR
31*50
DK ALL
4805*2.321134e+01
DTOP
961*6.630728e+03
DUALPOR
SHAPE GK
**$ Property: NULL Blocks Max: 1 Min: 1
**$ 0 = null block, 1 = active block
NULL MATRIX CON    1
NULL FRACTURE CON    1
```

```
**$ Fracture Spacing
DIFRAC CON 204.000000
 *MOD
 3:29   15:15   1:5  = 64
 4:28   14:14   1:5  = 64
 5:27   13:13   1:5  = 64
 6:26   12:12   1:5  = 64
 7:25   11:11   1:5  = 64
 8:24   10:10   1:5  = 64
 9:23     9:9   1:5  = 64
 10:22    8:8   1:5  = 64
 11:21    7:7   1:5  = 64
 12:20    6:6   1:5  = 64
 13:19    5:5   1:5  = 64
 3:29   17:17   1:5  = 64
 4:28   18:18   1:5  = 64
 5:27   19:19   1:5  = 64
 6:26   20:20   1:5  = 64
 7:25   21:21   1:5  = 64
 8:24   22:22   1:5  = 64
 9:23   23:23   1:5  = 64
 10:22 24:24   1:5  = 64
 11:21 25:25   1:5  = 64
 12:20 26:26   1:5  = 64
 13:19 27:27   1:5  = 64
 3:3    16:16   1:5  = 64
 4:4    16:16   1:5  = 64
 28:28 16:16   1:5  = 64
 29:29 16:16   1:5  = 64
```

DJFRAC CON 204.000000

*MOD

3:29 15:15 1:5 = 64

4:28 14:14 1:5 = 64

5:27 13:13 1:5 = 64

6:26 12:12 1:5 = 64

7:25 11:11 1:5 = 64

8:24 10:10 1:5 = 64

9:23 9:9 1:5 = 64

10:22 8:8 1:5 = 64

11:21 7:7 1:5 = 64

12:20 6:6 1:5 = 64

13:19 5:5 1:5 = 64

3:29 17:17 1:5 = 64

4:28 18:18 1:5 = 64

5:27 19:19 1:5 = 64

6:26 20:20 1:5 = 64

7:25 21:21 1:5 = 64

8:24 22:22 1:5 = 64

9:23 23:23 1:5 = 64

10:22 24:24 1:5 = 64

11:21 25:25 1:5 = 64

12:20 26:26 1:5 = 64

13:19 27:27 1:5 = 64

3:3 16:16 1:5 = 64

4:4 16:16 1:5 = 64

28:28 16:16 1:5 = 64

29:29 16:16 1:5 = 64

```
DKFRAC CON 204.000000
*MOD
3:29   15:15   1:5  = 64
4:28   14:14   1:5  = 64
5:27   13:13   1:5  = 64
6:26   12:12   1:5  = 64
7:25   11:11   1:5  = 64
8:24   10:10   1:5  = 64
9:23     9:9   1:5  = 64
10:22    8:8   1:5  = 64
11:21    7:7   1:5  = 64
12:20    6:6   1:5  = 64
13:19    5:5   1:5  = 64
3:29   17:17   1:5  = 64
4:28   18:18   1:5  = 64
5:27   19:19   1:5  = 64
6:26   20:20   1:5  = 64
7:25   21:21   1:5  = 64
8:24   22:22   1:5  = 64
9:23   23:23   1:5  = 64
10:22 24:24   1:5  = 64
11:21 25:25   1:5  = 64
12:20 26:26   1:5  = 64
13:19 27:27   1:5  = 64
3:3    16:16   1:5  = 64
4:4    16:16   1:5  = 64
28:28 16:16   1:5  = 64
29:29 16:16   1:5  = 64

**$ Property: Porosity  Max: 3.701142e-01 Min: 3.701142e-01
POR MATRIX CON 3.701142e-01
**$ Property: Porosity  Max: 1.762978e-02 Min: 1.762978e-02
POR FRACTURE CON 1.762978e-02
```

*MOD

3:29 15:15 1:5 = 4.250109e-02

4:28 14:14 1:5 = 4.250109e-02

5:27 13:13 1:5 = 4.250109e-02

6:26 12:12 1:5 = 4.250109e-02

7:25 11:11 1:5 = 4.250109e-02

8:24 10:10 1:5 = 4.250109e-02

9:23 9:9 1:5 = 4.250109e-02

10:22 8:8 1:5 = 4.250109e-02

11:21 7:7 1:5 = 4.250109e-02

12:20 6:6 1:5 = 4.250109e-02

13:19 5:5 1:5 = 4.250109e-02

3:29 17:17 1:5 = 4.250109e-02

4:28 18:18 1:5 = 4.250109e-02

5:27 19:19 1:5 = 4.250109e-02

6:26 20:20 1:5 = 4.250109e-02

7:25 21:21 1:5 = 4.250109e-02

8:24 22:22 1:5 = 4.250109e-02

9:23 23:23 1:5 = 4.250109e-02

10:22 24:24 1:5 = 4.250109e-02

11:21 25:25 1:5 = 4.250109e-02

12:20 26:26 1:5 = 4.250109e-02

13:19 27:27 1:5 = 4.250109e-02

3:3 16:16 1:5 = 4.250109e-02

4:4 16:16 1:5 = 4.250109e-02

28:28 16:16 1:5 = 4.250109e-02

29:29 16:16 1:5 = 4.250109e-02

**$ Property: Permeability I (md) Max: 4.901836e+02 Min: 4.901836e+02

PERMI FRACTURE CON 4.901836e+02

*MOD

3:29 15:15 1:5 = 2.259643e+03

4:28 14:14 1:5 = 2.259643e+03

5:27 13:13 1:5 = 2.259643e+03

6:26 12:12 1:5 = 2.259643e+03

7:25 11:11 1:5 = 2.259643e+03

8:24 10:10 1:5 = 2.259643e+03

9:23 9:9 1:5 = 2.259643e+03

10:22 8:8 1:5 = 2.259643e+03

11:21 7:7 1:5 = 2.259643e+03

12:20 6:6 1:5 = 2.259643e+03

13:19 5:5 1:5 = 2.259643e+03

3:29 17:17 1:5 = 2.259643e+03

4:28 18:18 1:5 = 2.259643e+03

5:27 19:19 1:5 = 2.259643e+03

6:26 20:20 1:5 = 2.259643e+03

7:25 21:21 1:5 = 2.259643e+03

8:24 22:22 1:5 = 2.259643e+03

9:23 23:23 1:5 = 2.259643e+03

10:22 24:24 1:5 = 2.259643e+03

11:21 25:25 1:5 = 2.259643e+03

12:20 26:26 1:5 = 2.259643e+03

13:19 27:27 1:5 = 2.259643e+03

3:3 16:16 1:5 = 2.259643e+03

4:4 16:16 1:5 = 2.259643e+03

28:28 16:16 1:5 = 2.259643e+03

29:29 16:16 1:5 = 2.259643e+03

```
**$ Property: Permeability I (md) Max: 7.338112e+01 Min: 7.338112e+01
PERMI MATRIX CON 7.338112e+01
PERMJ FRACTURE EQUALSI
PERMJ MATRIX EQUALSI
PERMK FRACTURE EQUALSI
PERMK MATRIX EQUALSI

**$ Property: Pinchout Array Max: 1 Min: 1
**$ 0 = pinched block, 1 = active block
PINCHOUTARRAY CON 1
*FRFRAC *CON 0.025
*FORMINFRAC *CON 0.2
*end-grid

ROCKTYPE 1
*CPOR 5e-4
*PRPOR 75
*ROCKCP 35
*THCONR 24
*THCONW 24
*THCONO 24
*THCONG 24
*HLOSSPROP  OVERBUR 35 24  UNDERBUR 35 24
**==============FLUID DEFINITIONS==================
**$ Model and number of components
MODEL 2 2 2 1
    **properties are defaulted (=0). Dead oil K values
    **are zero and no gas properties are needed.
*COMPNAME 'Water' 'OIL'
  *CMM         18.2        600
  *PCRIT     3206.2          0     **These fur properties
  *TCRIT      705.4          0     **are for the gas phase.
  *AVG          1.13e-5      0     **The dead oil component does
```

```
 *BVG        1.075        0     **not appear in the gas phase
 *MOLDEN     0            0.10113
 *CP         0            5.e-6
 *CT1        0            3.8e-4
 *CPL1       0            300

*VISCTABLE
 **$     Temp
   75     0    5780
  100     0    1380
  150     0     187
  200     0      47
  250     0     17.4
  300     0      8.5
  350     0      5.2
  500     0      2.5
  750     0      2.4

*PRSR 14.7
*TEMR 60
*PSURF 14.7
*TSURF 60

**==============ROCK-FLUID PROPERTIES==================
*ROCKFLUID
**Water-oil relative permeabilities
**$ Sw    Krw    Krow
 SWT
SMOOTHEND CUBIC
0.25   0.0       0.4
0.30   0.0002    0.3361
0.35   0.001134  0.2777
0.40   0.003125  0.225
```

0.45 0.00641 0.17777
0.50 0.01112 0.1361
0.55 0.01768 0.1
0.60 0.02598 0.0694
0.65 0.03628 0.0444
0.70 0.04871 0.025
0.75 0.06339 0.01111
0.80 0.08045 0.00277
0.85 0.1 0.0

**Liquid-gas relative permeabilities
**$ SL Krg Krog
SLT
SMOOTHEND LINEAR
0.25 0.2 0.0
0.35 0.15813 0.0
0.37 0.15016 0.000379
0.40 0.13846 0.002367
0.42 0.13084 0.004639
0.45 0.11968 0.009467
0.47 0.11243 0.013633
0.50 0.10184 0.021302
0.52 0.09498 0.027361
0.55 0.08498 0.037870
0.57 0.07853 0.045822
0.60 0.06917 0.05917
0.62 0.06316 0.06901
0.65 0.05449 0.08520
0.67 0.04895 0.09694
0.70 0.04102 0.11597
0.72 0.03600 0.12961
0.75 0.02889 0.15147
0.77 0.02445 0.16700

```
0.80   0.01827   0.19171
0.82   0.01450   0.20913
0.85   0.00942   0.23668
0.87   0.00646   0.25600
0.90   0.00279   0.28639
0.94   0.0   0.32956
1.00   0.0   0.4

*RPT 2 WATWET
**$ Sw    Krw    Krow
SWT
  0        0       1.0
  0.2      0.2     0.8
  0.4      0.4     0.6
  0.6      0.6     0.4
  0.8      0.8     0.2
  1.0      1.0     0.0
**$ SL    Krg    Krog
SLT
  0        1.0     0.0
  0.2      0.8     0.2
  0.4      0.6     0.4
  0.6      0.4     0.6
  0.8      0.2     0.8
  1.0      0.0     1.0

**==============INITIAL CONDITIONS==================
*INITIAL
**Automatic static vertical equilibrium
*VERTICAL *DEPTH_AVE
REFPRES 1.159266e+03
REFDEPTH 6689
TEMP MATRIX CON  1.263073e+02
```

```
 TEMP FRACTURE CON  1.263073e+02
 SW MATRIX CON  3.836596e-01
 SW FRACTURE CON  3.836596e-01

 **=================NUMERICAL CONTROL==================
 *NUMERICAL
 DTMAX 90
 DTMIN 0.0000001
 MAXSTEPS 9999999
 NEWTONCYC 30
 SORDER NATURAL
 NORTH 150
 SORDER NATURAL
 SDEGREE 2
 ITERMAX 200
 NCUTS 50
 *RUN

 **=================RECURRENT DATA==================
DATE 2013 1 20
DTWELL 0.02

WELL 'Injector'
 INJECTOR MOBWEIGHT IMPLICIT 'Injector'
 INCOMP  WATER  1.  0.
 TINJW  5.420817e+02
 QUAL  8.836732e-01
 OPERATE MAX STW 1321. CONT
 **$ perf geometric data: UBA, block entry(x,y,z) block exit(x,y,z), length
 **$ rad geofac wfrac skin
 GEOMETRY I 0.3 0.37 1 0
```

```
PERF GEO 'Injector'
**$ UBA ff Status Connection
5   16 4 1. OPEN FLOW-FROM 'SURFACE' REFLAYER
6   16 4 1. OPEN FLOW-FROM 1
7   16 4 1. OPEN FLOW-FROM 2
8   16 4 1. OPEN FLOW-FROM 3
9   16 4 1. OPEN FLOW-FROM 4
10 16 4 1. OPEN FLOW-FROM 5
11 16 4 1. OPEN FLOW-FROM 6
12 16 4 1. OPEN FLOW-FROM 7
13 16 4 1. OPEN FLOW-FROM 8
14 16 4 1. OPEN FLOW-FROM 9
15 16 4 1. OPEN FLOW-FROM 10
16 16 4 1. OPEN FLOW-FROM 11
17 16 4 1. OPEN FLOW-FROM 12
18 16 4 1. OPEN FLOW-FROM 13
19 16 4 1. OPEN FLOW-FROM 14
20 16 4 1. OPEN FLOW-FROM 15
21 16 4 1. OPEN FLOW-FROM 16
22 16 4 1. OPEN FLOW-FROM 17
23 16 4 1. OPEN FLOW-FROM 18
24 16 4 1. OPEN FLOW-FROM 19
25 16 4 1. OPEN FLOW-FROM 20
26 16 4 1. OPEN FLOW-FROM 21
27 16 4 1. OPEN FLOW-FROM 22

**$
WELL 'Producer'
PRODUCER 'Producer '
OPERATE  MAX  STO  5e+006  CONT
**$ rad geofac wfrac skin
GEOMETRY I 0.3 0.37 1 0
```

```
PERF GEO 'Producer'
 **$ UBA ff Status Connection
 5   16 4 1. OPEN FLOW-TO 'SURFACE' REFLAYER
 6   16 4 1. OPEN FLOW-TO 1
 7   16 4 1. OPEN FLOW-TO 2
 8   16 4 1. OPEN FLOW-TO 3
 9   16 4 1. OPEN FLOW-TO 4
 10 16 4 1. OPEN FLOW-TO 5
 11 16 4 1. OPEN FLOW-TO 6
 12 16 4 1. OPEN FLOW-TO 7
 13 16 4 1. OPEN FLOW-TO 8
 14 16 4 1. OPEN FLOW-TO 9
 15 16 4 1. OPEN FLOW-TO 10
 16 16 4 1. OPEN FLOW-TO 11
 17 16 4 1. OPEN FLOW-TO 12
 18 16 4 1. OPEN FLOW-TO 13
 19 16 4 1. OPEN FLOW-TO 14
 20 16 4 1. OPEN FLOW-TO 15
 21 16 4 1. OPEN FLOW-TO 16
 22 16 4 1. OPEN FLOW-TO 17
 23 16 4 1. OPEN FLOW-TO 18
 24 16 4 1. OPEN FLOW-TO 19
 25 16 4 1. OPEN FLOW-TO 20
 26 16 4 1. OPEN FLOW-TO 21
 27 16 4 1. OPEN FLOW-TO 22

 SHUTIN 'Injector'
 OPEN 'Producer'
 TRIGGER 'Production'
 ON_WELL 'Producer' STO-RP < 30
   *SHUTIN 'Producer'
   *OPEN 'Injector'
 END_TRIGGER
```

```
TRIGGER 'Prod_to_Inject'
ON_ELAPSED 'TIME' TRELTD > 1.
  TRIGGER 'Injection'
  ON_WELL 'Injector' STW-CI > 31704.
  APPLY_TIMES 30 INCREMENT 31704.
   *SHUTIN 'Injector'
    TRIGGER 'Soaking'
    ON_ELAPSED 'TIME' TRELTD > 40.
     *OPEN 'Producer'
      TRIGGER 'Oil_Rate_Limit'
      ON_WELL 'Producer' STO-RP > 20.
       TRIGGER 'Oil_Rate_Limit_Time'
       ON_ELAPSED 'TIME' TRELTD > 1.
        TRIGGER 'Oil_Rate_Termination'
        ON_WELL 'Producer' STO-RP < 20.
         *SHUTIN 'Producer'
         *OPEN 'Injector'
        END_TRIGGER
       END_TRIGGER
      END_TRIGGER
    END_TRIGGER
  END_TRIGGER
END_TRIGGER
DATE 2300 12 20
*stop
```

Appendix C

MATLAB Code for Training of Forward ANN-1

```
%*************************************************************************
% Forward ANN-1 for prediction of oil flow rate and number of cycles
% Developed by Buket ARPACI
%*************************************************************************

format long
clear
clc
close all

% Input data set for training
data=xlsread('INPUT.xlsx');

% Output (target) data set for training
oilrate=xlsread('oilrate.xlsx');

% Preparation of input parameters for training
input=[log(data(1,:));log(data(2,:));(data(3,:));(data(4,:));log(data(5,:));...
      log(data(6,:));log(data(7,:));log(data(8,:));data(9,:);(data(10,:));...
      log(data(11,:));log((data(12,:)));log((data(13,:)));log(data(14,:));...
      log((data(15,:)));((data(16,:)));log(data(17,:));log(data(18,:));...
      log(data(19,:));(data(20,:));(data(21,:));log(data(22,:));log(data(23,:));];

% Definition of parameters used in the calculation of Eigen values

  A=data(1,:);       % Drainage Area
  h=data(2,:);       % Layer Thickness
  phi_m=data(3,:);   % Matrix Porosity
  phi_f=data(4,:);   % Fracture Porosity
  k_m=log(data(5,:)); % Matrix Permeability
  k_f=log(data(6,:)); % Fracture Permeability
  Fs=data(7,:);      % Fracture Spacing
  Pres=log(data(8,:));% Initial Pressure
  In_A=(((data(20,:)).*(data(21,:))*50*50*pi)/(4*43560)); % Inner zone area
  In_phi_f=data(16,:); % Inner zone fracture porosity
  In_k_f=log(data(17,:)); %Inner zone fracture permeability
  In_Fs=log(data(18,:));  %Inner zone fracture spacing
  STR=log(data(19,:));    %Injection rate

%% Functional Links (Eigen values)

%[km-lamda   phim]
%[kf  phif-lamda]
```

```
  for i=1:555
det1 =[ 1  (-1*(k_m(1,i)+phi_f(1,i))) ((k_m(1,i)*phi_f(1,i))-(phi_m(1,i)*k_f(1,i))) ];
x=roots(det1);
lamda1(1,i)=x(1,1);
lamda2(1,i)=x(2,1);
  end

%*************************************************************************
%[A-lamda   In_A]
%[Fs  In_Fs-lamda]

  for i=1:555
det2 =[ 1  (-1*(A(1,i)+In_Fs(1,i))) ((A(1,i)*In_Fs(1,i))-(In_A(1,i)*Fs(1,i))) ];
y=roots(det2);
lamda3(1,i)=y(1,1);
lamda4(1,i)=y(2,1);
  end

 %*************************************************************************
 %[A-lamda   In_A]
 %[k_f  In_k_f]

  for i=1:555
det3 =[ 1  (-1*(A(1,i)+In_k_f(1,i))) ((A(1,i)*In_k_f(1,i))-(In_A(1,i)*k_f(1,i))) ];
z=roots(det3);
lamda5(1,i)=z(1,1);
lamda6(1,i)=z(2,1);
  end

 %*************************************************************************
 %[A-lamda   h]
 %[Pres  STR]

  for i=1:555
det4 =[ 1  (-1*(A(1,i)+STR(1,i))) ((A(1,i)*STR(1,i))-(h(1,i)*Pres(1,i))) ];
u=roots(det4);
lamda7(1,i)=u(1,1);
lamda8(1,i)=u(2,1);
  end


P = [input;lamda1;lamda3;lamda5;lamda7];
T = [log(oilrate)];


%%
[mi,ni] = size(Pn); %size of input layer
[mo,no] = size(Tn); %size of output layer
```

```
N_in = mi;   %Number of inputs
N_out = mo;  %Number of outputs
Tot_in = ni; %Total number of simulations

% Normalization of data
[Pn,ps] = mapminmax(P,-1,1); %normalizing between -1 and 1
[Tn,ts] = mapminmax(T,-1,1); %normalizing between -1 and 1

% Division of data sets by dividerand function for training, testing and validation
[Pn_train,Pn_val,Pn_test,trainInd,valInd,testInd] = dividerand(Pn,0.79,0.14,0.07);

%Training sets
[Tn_train,Tn_val,Tn_test] = divideind(Tn,trainInd,valInd,testInd);

%Validation sets
val.T = Tn_val;
val.P = Pn_val;

%Training sets
test.T = Tn_test;
test.P = Pn_test;

% Initiating number of neurons for hidden layer
Nneuron = 275;

% Creating backpropagation algorithm
net = newcf(Pn,Tn,[Nneuron,mo],{'tansig','purelin'},'trainscg','learngdm','msereg');


% Adjustment of training parameters
net.trainParam.goal = 0.00005; %Accuracy check
net.trainParam.epochs = 15000; %Number of iterations check
net.trainParam.show = 1;
net.trainParam.max_fail = 10000; %Number of validation check
net.trainParam.mem_reduc = 60; %Reduction of memory requirements
net.trainParam.showWindow = true;

% Training of the network
[net,tr] = train(net,Pn_train,Tn_train,[],[],test,val);

% Simulation of the network with the tarining data
Tn_train_ann = sim(net,Pn_train);

% Simulation of the network with the testing data
Tn_test_ann = sim(net,Pn_test);

% Denormalization of the input layer
Pn_train = mapminmax('reverse',Pn_train,ps);
```

```
Pn_val = mapminmax('reverse',Pn_val,ps);
Pn_test = mapminmax('reverse',Pn_test,ps);

% Denormalization of the simulation for output layer
T_train = mapminmax('reverse',Tn_train,ts);
T_test = mapminmax('reverse',Tn_test,ts);
T_train_ann = mapminmax('reverse',Tn_train_ann,ts);
T_test_ann = mapminmax('reverse',Tn_test_ann,ts);



   for i=1:length(T_train(1,:));
      for j=1:length(T_train(:,1));

   Error_training_data(j,i) = abs(((exp(T_train(j,i))-
(exp(T_train_ann(j,i)))./(exp(T_train(j,i))))*100;

      end
   end


   for i=1:length(T_test(1,:));
      for j=1:length(T_test(:,1));

   Error_testing_data(j,i) = abs(((exp(T_test(j,i))-(exp(T_test_ann(j,i)))./(exp(T_test(j,i))))*100;

      end
   end


save result_forward_ann_1.mat
```